11th INTERNATIONAL 100% RENEWABLE ENERGY CONFERENCE

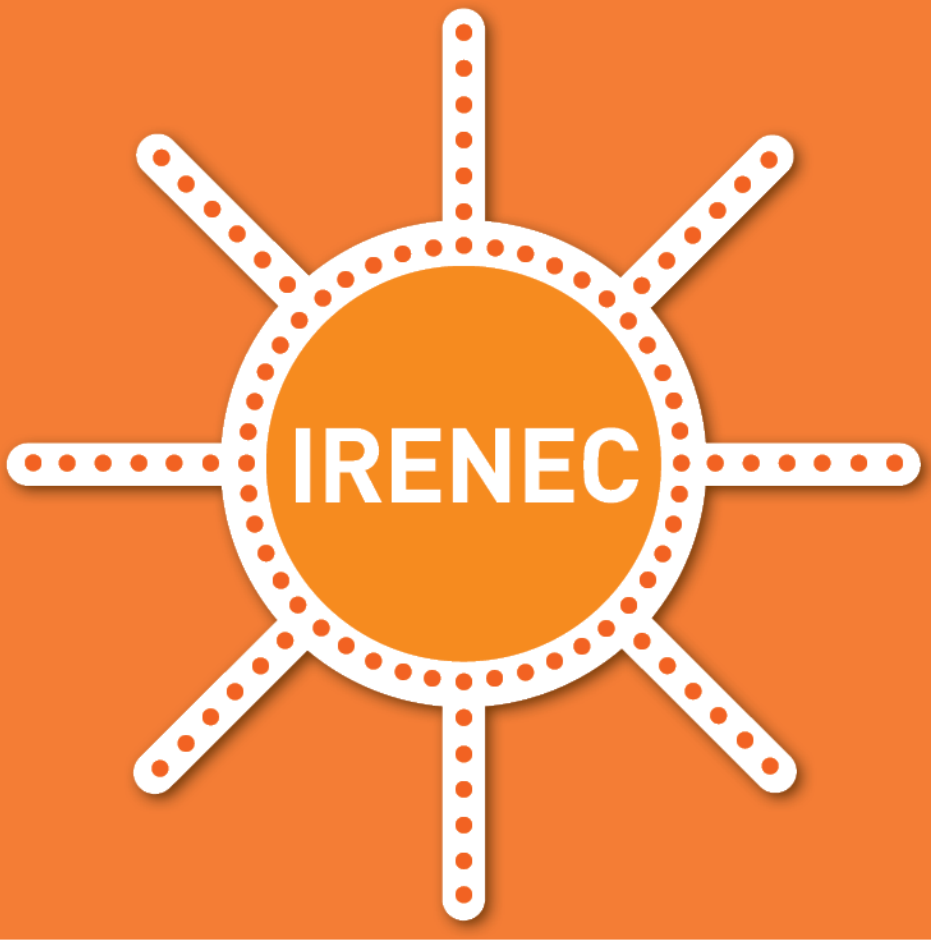

IRENEC 2021

PROCEEDINGS

20-23 MAY 2021

RENEWABLE ENERGY ASSOCIATION

EUROSOLAR Turkey

Editors

Tanay Sıdkı Uyar

Alper Saydam

Publishing Date 20 October 2021

ISBN 978-605-62511-7-7

Dear Participants,
In our journey of promoting 100% Renewable Energy, we have arrived the 11th stop where we shall again share our research results and other achievements.

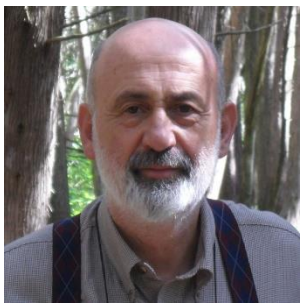

Tanay Sıdkı Uyar

Conference Chair,
IRENEC 2021

Every day we are discovering and practicing the good quality of renewable energies. The genie is out of the bottle. It is time to use the good quality of human beings to guide this opportunity effectively to the destination. The qualities of human beings can play its role if the individuals and countries talk together and define problems correctly and find solutions that can be implemented.

Renewable energy resources at each corner of the atmosphere are ready to be converted to electricity and process heat locally when needed. Kinetic energy of the moving air, chemical energy stored in biomass, heat and light of the sun and geothermal resources are available all over our planet earth free of charge. As the main energy source of living space on earth, sun and its derivatives were available before, are available today and will be available in the future.

Global support provided for the renewable energy made the market penetration of renewables possible. Today wind and solar energy became the cheapest way of producing electricity in many parts of the World.

Cities and countries who are trying to reach 100% renewable energy mix are working on preparing the infrastructure necessary to be able to supply more renewable energy for industry, transportation and buildings by smart grids and renewable energy storage systems.

Since renewable energy is available at every corner of our atmosphere, Community Power (the involvement of the local people individually or through their cooperatives and municipalities in the decision-making process and ownership of their energy production facilities) is becoming the most effective approach for transition to 100% renewable energy future.

During IRENEC 2021 we shall share and learn from the global experiences on difficulties, barriers, opportunities and solutions for transition to 100 % renewable energy societies and make our contribution to Global Transition to 100% Renewable Energy.

Best Regards,

Tanay Sıdkı Uyar

Conference Chair, IRENEC 2021

President, Renewable Energy Association of Turkey

(EUROSOLAR Turkey)

Organization

Organizing Committee

Conference Chair

Tanay Sıdkı Uyar	President, EUROSOLAR Turkey, TR

Conference Co-Chairs

İbrahim Dinçer	University of Ontario Institute of Technology, CA
Christian Rakos	President of World Bioenergy Association, AT
Wolfgang Palz	EU Commission Official (ret.)
Şener Oktik	ŞİŞECAM Chief Research & Technological Development Officer, TR
Hasan Heperkan	Professor in Mechanical Engineering, İstanbul Aydın University, TR

Local Organizing Committee (Administrative)

Başak Gündüz

Serdar Tan

Işıl Uyar

Local Organizing Committee (Academic)

Alper Saydam

Doğancan Beşikci

Tanay Sıdkı Uyar

Program Committee (Research Papers)

Kayadelen, Nilgün	Cukurova University, TR
Yücel, Uğur	Kocaeli University, TR
Işın, Hazal	Yildiz Technical University, TR
Ulusan, M. Emre	Yildiz Technical University, TR
Çınar, Mustafa Yüksel	Iskenderun Technical University, TR
Qurban Ali, Natasha	Istanbul Bilgi University, TR
Ünal, Gizem	Gazi University, TR
Bilto, Moaz	Beykent University, TR
Köker, Utku	Suleyman Demirel University, TR
Sarı, Alperen	Marmara University, TR
Leblebicioğlu, Emre	Marmara University, TR
Yıldız, Aleyna	Beykent University, TR
Topçu, Merve	Beykent University, TR
Erdem, Simay	Beykent University, TR
Baltacı, Özge	Dokuz Eylul University, TR
Çolakoğlu, Mert	Istanbul Technical University, TR
Yılgın, Büşra	Kocaeli University, TR
Akbulut, Levent	Capital University, TR
Sunusi, Nuraini	Cyprus International University, CY
Hammemi, Rania	National Engineering School of Tunis, TN

Scientific Advisory Committee

Dr. Arni Ragnarsson	University of Iceland and Reykjavik University
Assoc. Prof. Atakan Öngen	Istanbul University
Prof. Dr. Eberhard Waffenschmidt	Chairman of Society to Promote Solar Energy Germany
Assoc. Prof. Dr. Egemen Sulukan	Turkish Naval Academy of National Defence University
Prof. Dr. Emine Meşe	University of Durham
Monica Oliphant	University of South Australia
Prof. Dr. Yukio Tamura	Chongqing University

Contents

Full Research Papers

Assessment of Turkey's Wind Energy 3
A. Nilgün Kayadelen, Z. Figen Antmen, Hamza Erol

Wind Energy and Hydro Storage System Integration 11
Uğur Yücel, Samet Tükel, Soner Şahin

The Analysis of 40-Year Wind and Wave Characteristics 23
Hazal Işın, H. Anıl Arı Güner, Yalçın Yüksel

Determination of the Wave Energy Potential of Marmara Sea 31
M. Emre Ulusan, H. Anıl Arı Güner, Yalçın Yüksel

Energy Resilience in Turkey: A perspective and Application 40
Mustafa Yüksel Çınar, Suha Orçun Mert

Potential renewable energy resources of Istanbul and installation of a micro-grid system 50
Salah Masry, Natasha Qurban Ali, Füsun S. Tut Haklıdır

Evaluation of improvement studies of the use of green hydrogen production in industry – An economic perspective 59
Gizem Fırat, Ali Osman Fırat, Ahmet Taşkesen, Ahmet Emre Şahin

Renewable Energy Impact on Damascus City Transportation Sector 69
Moaz Bilto, Doğancan Beşikçi, Tanay Sıdkı Uyar

A Regional Energy Optimization for Afyonkarahisar, Turkey 95
Utku Köker, Halil İbrahim Koruca, Egemen Sulukan, Tanay Sıdkı Uyar

An On-board Energy and Environmental Analysis within the Framework of Green Deal 107
Alperen Sarı, Egemen Sulukan, Doğuş Özkan, Tanay Sıdkı Uyar, Levent Erişkin

An Energy System Simulation of Turkey with A Carbon-Neutral Scenario 122
Emre Leblebicioğlu, Egemen Sulukan, Tanay Sıdkı Uyar

Design and Analysis of Passive Buildings Using the Software Energy Plus and Open Studio 139
Merve Topçu, Doğancan Beşikçi, Tanay Sıdkı Uyar

Design And Analysis of Passive Buildings Using the Software Energy Plus and Open Studio 144
Simay Erdem, Tanay Sıdkı Uyar

Photovoltaic Energy Forecasting via Artificial Neural Networks and Support Vector Machine Approaches 161
Özge Baltacı, Zeki Kıral, Yüksel Çağrı Gürses

Energy, Exergy and Environmental Analysis and Multiobjective Optimization of a Solar Renewable Energy Multi-Generation System Considering the Summer Daytime Climatic Conditions of Mediterranean Region in Turkey 174
Mert Colakoglu, Ahmet Durmayaz

Use of Waste Heat Emitted from A Fuel Cell in Thermoelectric Module 185
Busra Yilgin, Anil Can Turkmen, Fatma Burcu Keles, Ismet Tikiz, Cenk Celik

Design of the Off-Grid PV Electricity Generation System for Residential Lighting and Income Generating Activities of Gediya Community, Sumaila Local Government, Kano State, Nigeria..... 190
Nuraini Sunusi Ma'aji, Tanay Sıdkı Uyar

Exergoeconomic Analysis and Multi Objective Optimization of a Solar Combined System (ORC - Ejector Refrigeration System)..... 202
Rania Hammemi, Mouna Elakhdar, Ezzedine Nehdi

Design of A Hybrid Solar Collector and The Numerical Analysis of Air Performance 219
Levent Akbulut, Özgür Erol

Assessment of Turkey's Wind Energy

A. Nilgün Kayadelen[1] [0000-0002-5442-893X], Z. Figen Antmen[0000-0001-8475-1300] and Hamza Erol[2][0000-0001-8983-4797]

[1] Cukurova University, Adana, Turkey
[2] Mersin University, Mersin, Turkey

Abstract. Technological developments and industrialization as well as the rate at which the world population grows increase the demand for energy. Energy is the main input for production and is an essential element for increasing the welfare of societies. It is used in almost every field in daily life. Energy sources are divided into renewable and non-renewable sources depending on their use. While fossil resources and nuclear energy constitute non-renewable energy sources, solar energy, wind energy, hydroelectric energy and geothermal energy are renewable resources. Determining the presence of energy resources available in the world and in Turkey is key for a greater use of renewable energy sources and the planned utilization of energy resources. There have been two major, energy-related developments in Turkey recently. Right after the discovery of 320 billion cubic meters of natural gas reserves in the Black Sea, the all-time electric power generation record was broken on September 3, 2020. Turkey gradually depends more on its own energy resources. This study adopts a statistical approach to assess the wind energy potential for Turkey based on the wind data for 2012-2016 by General Directorate of State Meteorological Services of Turkey. To that end, Mixture Weibull Distribution was used to estimate the average wind power density, which is an important parameter in the assessment of wind energy potential. The study offers a projection for Turkey's wind energy potential.

Keywords: Wind Power Potential, Mixture Weibull Distribution, Average Power Density.

1 Introduction

Every system in the universe needs energy to survive. Energy is considered a strategic element that affects not only the internal dynamics of countries, but also international relations including political and military conflicts. While energy consumption in the world is increasing day by day, limited and unsustainable fossil fuels mostly meet the energy needs. The use of fossil fuels is not only environmentally but also economically unsustainable. Therefore, transition to alternative renewable energy sources emerges as a requirement[1]. Considering their environmental factors, renewable energy resources play an important role among all energy sources as they provide sustainable economic development [2]. Wind energy can be considered as one of the most com-

mon and useful renewable energy resources. As it is an environmentally-friendly energy source for the future, wind energy has been used in irrigation, wheat milling and ships among many other sectors. The use of wind energy in electric power generation has increased considerably in the last two decades. Wind energy has been used as an important renewable energy resource in electricity generation in many developed countries [3].

Wind power generation plays an important role in meeting a large portion of the global energy demand in the transition from fossil fuels to renewable energy. In addition, wind power systems have made a significant contribution to daily life in some developing countries[4]. According to the preliminary wind energy statistics published by the World Wind Energy Association, a new world record was broken in wind power installations with the addition of new wind turbines with an installed capacity of 93 GW in 2020. Global wind power generation capacity stands at 744 GW and corresponds to 7% of the global demand in electric power. The importance attached to renewable energy resources in Turkey is increasing each day. The Ministry of Energy and Natural Resources set the national target for wind power at 20 GW by 2023. Moreover, many regions of Turkey have not been analyzed in terms of their wind energy potential.

Assessment of the wind energy potential in a region may cover different dimensions. Meteorological wind energy potential measures the energy content of the wind in a given area according to the wind speed. Wind speed is generally modeled using theoretical wind speed distributions, considering its multidimensional variation [5]. Wind power density is an important indicator for determining the potential of wind sources and defining the amount of wind energy at various wind speed values at a particular location. Wind power density is calculated with a suitable distribution function according to the data of the wind speed measured. Various probability distribution functions are used for wind power density in the literature [6]. Weibull distributions have frequently been used in the literature as an approach that has proven successful in terms of the probability distributions of wind speeds. However, in some cases, multiple different wind speeds with a high probability distribution may occur, particularly in the long-time wind data. In such cases, the use of unimodal distribution may not be suitable for obtaining sufficient accuracy in calculations. Instead, it would be more appropriate to use mixture probability distributions that can express multimodal probability distributions. Therefore, the study has used wind data from 2012-2016 to assess Turkey's wind energy potential via Mixture Weibull Distribution Models. For 2012-2016, an analysis of the distribution of installed capacity in electric power generation showed that 2.3% of our installed capacity was based on wind power as of the end of 2012, which increased to 5.8% in 2016 (see Table 1). As of the end of September 2019, this rate increased to 8.1% [7].

Table 1. The scatter installed power of Turkey according to resources.

Sources	Installed Power (MW)					
	2012	**2013**	**2014**	**2015**	**2016**	**Average**
Naturel Gas	17.164	20.255	21.476	21.261	22.217	20.475
Coal	12.530	171.812	200.417	179.366	184.889	149.803
Geothermal	162.200	310.8	404.9	623.9	820.9	464.540
Wind	2.261	2.76	3.63	4.503	5.751	3.781
Hydraulic	19.620	59.42	40.645	67.146	67.268	50.820
Others	5.335	5.83	5.555	5.159	4.878	5.351
Total	219.110	570.877	676.623	901.335	1105.9	

1.1 Wind Power Density

Wind power density is a key factor in determining the potential of generating electricity from wind power. The basic data used in calculating this factor is wind speed data. Parameters and variables used in the calculation of power density for the Mixture Weibull Distribution model are as follows:

ρ: air density (kg/m3), P: air pressure measured simultaneously with wind speed (Pa), R: Ideal gas constant (287 kJ/kg.K), T: air temperature measured simultaneously with wind speed (0C) as seen in the equation in (1) [8].

$$\rho = \frac{P}{R * T} \tag{1}$$

The annual average wind power density is estimated using the equation in (2), which employs the Mixture Weibull Distribution with ρ: air density (kg/m3), wi: mix ratio, ci: Weibull Distribution scale parameter and ki: Weibull Distribution shape parameter.

$$\overline{\mathrm{WPD}} = 0.5 * \rho * \left(\sum_{i=1}^{n} wi * c_i^3 * \Gamma\left(\frac{k_i+3}{k_i}\right)\right) \tag{2}$$

The annual average wind speed is estimated using the equation in (3), which employs the Mixture Weibull Distribution with wi: mix ratio, ci: Weibull Distribution scale parameter and ki: Weibull Distribution shape parameter. Here, Γ indicated the Gamma function.

$$\overline{\mathrm{V}} = \sum_{i=1}^{n} wi * c_i^3 * \Gamma\left(\frac{k_i+1}{k_i}\right) \tag{3}$$

1.2 Wind Energy Potential with Mixture Weibull Distribution

Mixture distributions are distributions expressed by the inclusion of multiple probability density functions at different rates. Considering the proven success of Weibull distribution in expressing the probability distributions of wind speeds, this study has been found eligible for the use of Mixture Weibull distribution. To that end, Mixture Weibull Distribution Models were established for the geographical regions of Turkey, and the average wind power density ($\overline{WPD}$) and average wind speed values ($\overline{V}$) were estimated via these distribution models (see Table 2).

Table 2. Wind Energy Potential Prediction of Regions by Mixture Weibull Distribution.

Region	2012		2013		2014		2015		2016		Average	
	$\overline{V}$	$\overline{WPD}$	$\overline{V}$	$\overline{WPD}$	$\overline{V}$	$\overline{WPD}$	$\overline{V}$	$\overline{WPD}$	$\overline{V}$	$\overline{WPD}$	$\overline{\overline{V}}$	$\overline{\overline{WPI}}$
Marmara	2.98	31.90	2.66	24.39	3.06	44.09	2.77	22.75	3.35	57.27	2.96	36.08
Aegean	2.95	25.39	2.51	16.13	2.66	18.54	2.37	12.74	2.66	18.13	2.63	18.19
Mediterranean	2.65	30.91	2.66	26.51	2.79	29.29	2.53	21.18	2.65	25.31	2.66	26.64
Middle Anatolia	3.07	39.29	2.96	30.94	3.30	47.97	2.93	29.73	3.23	41.75	3.10	37.94
Black Sea	2.64	37.77	2.57	33.34	2.75	35.44	2.59	44.60	2.72	37.19	2.65	37.67
Eastern Anatolia	2.07	36.52	2.00	21.87	2.22	24.50	2.31	19.16	2.23	18.54	2.17	24.12
South-Eastern Anatolia	3.37	75.14	2.65	28.95	2.64	25.13	2.62	25.70	2.93	51.52	2.84	41.29

In the model created by regions, the cities in each region constitute the components of the mixture model. Accordingly, Mixture Weibull Distribution Models were created with 11 components for the Marmara Region, 8 components for the Aegean Region, 8 components for the Mediterranean Region, 14 components for the Central Anatolia Region, 16 components for the Black Sea Region, 14 components for the Eastern Anatolia Region and 9 components for the Southeastern Anatolia Region.

The results estimated that the region with the highest annual average power density was the Southeastern Anatolia Region with 41.29 W/m^2. Higher power density values reinforce the possibility of generating electric power from wind resources in the region the wind power potential of which is estimated. The Aegean Region was the region with the lowest annual average power density with 18.19 W/m^2.

Electric Power Resources Survey and Development Administration (EIE) initiated a study in 1983 in order to continue R&D projects in the field of wind energy. As a first step, as part of the efforts to determine the potential, 10-year data for monthly wind speed and direction between 1970 and 1980 acquired from stations of the General Directorate of State Meteorological Services were analyzed to calculate the average wind power densities and wind speeds of Turkey's geographical regions. Accordingly, the region where power density is highest is Marmara with 51.91 W/m^2 while it is lowest in the Eastern Anatolia region with 13.19 W/m^2 (see Table 3).

Table 3. Wind Energy Potential of Regions.

Region	Average Wind Power Density (W/m²)	Average Wind Speed (m/sn)
Marmara	51.91	3.29
Aegean	23.47	2.65
Mediterranean	21.36	2.45
Middle Anatolia	20.14	2.46
Black Sea	21.31	2.38
Eastern Anatolia	29.33	2.69
South-Eastern Anatolia	13.19	2.12
Average	**25.82**	**2.58**

The table shows that the power density value of the Southeastern Anatolia Region is second only to the Marmara Region. Using the Mixture Weibull Distribution based on wind data for the years 2012-2016, the highest power density value was estimated for

the Southeastern Anatolia Region. These results indicate that the Southeastern Region may have a strong wind energy potential which should be analyzed thoroughly.

In 2006, General Directorate of Renewable Energy in Turkey used the medium-scale digital weather forecasting model and the micro-scale wind flow model to generate wind source information, which were subsequently integrated into the Wind Energy Potential Atlas (REPA). The REPA study calculated the technical potential for Turkey. The results of this study showed that the total capacity of Turkey for wind energy potential was 47,849.44 MW, comprising of 37,836 MW on-shore capacity and 10,013 MW off-shore capacity (see Table 4).

Table 4. Turkey's Wind Energy Potential.

Wind Class	Wind Power (W/m^2)	Annually Average Wind Speed (m/s)	Total Capacity (MW)
4	400-500	7,0 - 7,5	29.259,36
5	500-600	7,5 - 8,0	12.994,32
6	600-800	8,0 - 9,0	5.399,92
7	> 800	> 9,0	195,84
			47.849,44
Total Capacity			Onshore:37.836
			Offshore: 10.013

Wind Power Generation Projection Values. In this section, the power density values estimated by the Mixture Weibull Distribution were used to calculate the annual electric power generation projection values. Power generation values were calculated according to the formula in (4). Some assumptions were employed while making these calculations. Accordingly, it is assumed that a wind turbine with a rotor diameter of 54 m and a capacity of 1 MW (technical standard) will be installed on a land of 10 hectares, that is, 100,000 m2. The REPA study calculated not only the technical potential but also the total windswept area in Turkey in general. While calculating this area, locations where a Wind Power Plant (WPP) cannot be built such as residential areas, lakes, rivers, wetlands, roads, railways and airways, marine ports, transformer centers, energy transmission lines, power plants, earthquake fault lines, land use, forests, environmental protection areas and bird migration routes were determined and excluded from the calculation. The calculated area corresponds to approximately

1.30% of the surface area of Turkey. Accordingly, how many turbines of 1 MW capacity can be erected per each 100,000 m2 in the windswept area in the 7 geographical regions were determined, and the result was used in calculating the projection values. No matter how ideal the system is in turbine systems, the power to be obtained from the wind has a certain limit. The capacity factor called the Betz Limit can be a maximum of 59%. While creating the REPA, it was assumed that a capacity factor of 35% and above was required for an economic WPP investment, so the power coefficient Cp was considered as 0.35 in the calculation of power.

$$\text{Power} = Cp * \overline{WPD} * \left(\frac{\prod}{4} * r^2\right) * 8760 \text{ h/year} * \frac{1kw}{1000MW} \quad (4)$$

Table 4 provides the wind power generation projection values for 5 years (2012-2016).

The highest value of power was calculated in 2016 according to the wind power generation projection values. Turkey's electric power generation stood at 261.7 million MWh and 274.7 million MWh in 2015 and 2016 respectively. Current data by the Ministry of Energy of the Republic of Turkey shows that 304.8 million MWh of electric power was generated in 2018. Accordingly, the projected energy values are above the current values.

Conclusion. This study assesses Turkey's potential for wind energy. 5-year wind data from 2012-2016 by the General Directorate of State Meteorological Services were used to estimate the power density values, which are a key factor in assessing the wind energy potential. Since long-time wind data were used to estimate the power density values for Turkey's geographical regions, Mixture Weibull Distribution was preferred over pure distributions such as Weibull and Gamma. As a result, the Southeastern Anatolia Region was found to be the region with the highest annual average power density value. Having the lowest installed capacity for wind energy with 27.5 MW, the Southeastern Anatolia Region has vast rural areas, and the establishment of wind power systems in this region will provide economic benefits for the entire region. The study offers a prospective projection for Turkey's wind energy based on the calculated 5-year wind power generation projection values.

Consequently, it is possible to speak of a strong wind power potential for Turkey, which ranks 11th in the world and 7th among the 38 European countries led by Germany in terms of total installed capacity for wind power. In the near future, following the increase in the use of wind power from renewable energy resources and the discovery of new reserves of non-renewable energy resources, Turkey will be able to survive with no dependence on foreign energy.

Last but not least, it is concluded that an up-to-date, comprehensive and new study is needed as it has been a long time since 2006, when the latest study on Turkey's wind power potential was conducted by the Turkish General Directorate of Renewable Energy.

References

1. Bagci K., Arslan T., Celik H.E: Inverted Kumarswamy distribution for modeling the wind speed data: Lake Van, Turkey. Renewable and Sustainable Energy Reviews 135, 1–11 (2021).
2. Li M., Li X.,: Investigation of wind characteristics and assessment of wind energy potential for Waterloo region, Canada. Energy Conversion and Management 46 (18-19), 3014-3033 (2005).
3. Ouammi A., Dagdougui H., Sacile R., Mimet A.: Monthly and seasonal assessment of wind energy characteristics at four monitored locations in Liguria region (Italy). Renewable and Sustainable Energy Reviews 14, 1959-1968 (2010).
4. Ouammi A., Sacile R., Mimet A.: Wind energy potential in Liguria region. Renewable and Sustainable Energy Reviews 14, 289-300 (2010).
5. Grau L., Jung C., Schindler D.: Sounding out the repowering potential of wind energy e A scenario based assessment from Germany. Journal of Cleaner Production 293, 1-11 (2021).
6. Arslan H., Baltaci H., Akkoyunlu B.O., Karanfil S., Tayanç M.: Wind speed variability and wind power potential over Turkey: Case studies for Çanakkale and Istanbul. Renewable Energy 145, 1020-1032 (2020).
7. Republic of Turkey Ministry of Energy and Natural Sciences Homepage https://enerji.gov.tr/bilgi-merkezi-enerji-elektrik, last accessed 2021 /04/ 29.
8. WPP Technical Assessment Regulations Appendix-1, Official Gazette of the Republic of Turkey, 2015.

Wind Energy and Hydro Storage System Integration

Uğur Yücel [1][0000-0003-1201-4672], Samet Tükel [2][0000-0001-8154-3557], Soner Şahin[3][0000-0002-2523-1978]

[1] Hereke Asım Kocabıyık Vocational School, Kocaeli University 41800 Kocaeli Turkey
[2,3] Gürçelik Makina A.Ş. 41400 Gebze, Kocaeli, Turkey
uyucel@kocaeli.edu.tr, stukel@gurcelikmakina.com, ssahin@gurcelikmakina.com

Abstract. The installed wind power capacity worldwide is increasing by approximately 30% per year. Due to the stochastic nature of wind, the electrical energy generated by wind turbines is highly irregular. This irregularity of wind energy negatively affects both the energy quality and the planning of the power systems. The uncertain nature of wind power plants in power generation can be regulated by using fast and efficient distributable sources such as natural gas turbines or hydro generators. However, using dispersible resources in a short time to correct the variability of wind power can increase the cost of large-scale wind energy integration. To fix this, the incorporation of a large-scale hydro energy storage system in wind farm production can be used to increase the predictability of wind power, reduce the need for tracking loads, and regulate hydro or fossil fuel reserve generation. Energy Storage Systems (ESS) control the wind power plant output and allow greater penetration of wind power into the system. Pumped Hydroelectric Energy Storage (PHES) systems stand out as the most used EES technology today. With more effective control and coordination of energy storage systems, predictability of wind farm outputs can be increased and integration costs associated with reserve requirements can be reduced.

Keywords: Wind Energy, Hydroelectric Storage, Energy Efficiency.

1 Introduction

Wind energy use is one of the fastest growing sources of electricity today. As a matter of fact, while the installed power of wind energy was 24,332 MW all over the world in 2001, it reached 650,758 MW in 2019 [1]. The world supplied 5.2% of its electrical energy needs from wind turbines in 2019 [2]. So much so that the share of wind energy in total electricity generation in Denmark is 48% [3]. The electrical energy generated by wind turbines is extremely irregular, therefore wind energy penetration in power systems can cause problems with the operation of the system and planning of the power systems [4]. Wind power plants must have special control systems for output power and voltage in accordance with the network structure, and must withstand interruptions and by-passes in the network for specified periods [5]. ESSs controls the wind power plant output and supply the grid power demands. Thus, it plays an important role in wind energy applications by enabling the wind energy to affect the system more. ESSs are designed to energize or denergize the system in less than a minute [6-7-8].

It is necessary to use appropriate energy storages to use wind energy as a clean electricity generation source, to minimize wind energy waste and to keep investors' interest alive. Electric grids generally have 8-10% extra capacity for emergency power requirements [9]. Providing Pumped Hydroelectric Energy Storage (PHES) in isolated networks such as in the islands is an appropriate option to for high cost of electricity generation and the constantly increasing power demand encountered in these areas [10-11-12]. Positive and realistic way to introduce pumped storage in island systems is based on the coordinated PHES concept of wind farms and storage facilities [13-14-15]. Caralis at al. researched the Greek energy system's ability to use renewable power and the necessity of pumped storage systems. Their work has shown that pumped storage is necessary for the variable outputs of Renewable Energy Sources (RES) to become regular [16]. Energy storage systems, which can recover economic losses due to instability in wind power plants, are widely applied and maximum benefit is obtained from wind energy [17-18-19].

2 Pumped Hydroelectric Energy Storage (PHES) Structure

PHES stores gravitational potential energy by raising water. The charging process converts electrical energy into mechanical energy and ultimately gravitational potential energy by pumping water from a lower reservoir to a higher reservoir. In this type of system, low-cost electrical power generated during low-energy hours is used to run the pumps in order to raise the water from the lower reservoir to the upper reservoir. In the unloading process, by allowing the water to flow from the higher reservoir to the lower reservoir, gravitational potential energy is transformed first into mechanical energy and then into electrical energy. Turbine / generator groups can act as pumps or turbines when necessary. This technique is currently the most cost-effective way to store large amounts of electrical energy. The design of the PHES power plant depends mostly on site characteristics.

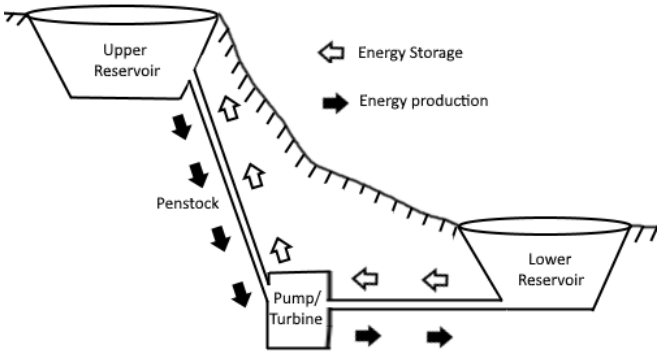

Fig. 1. PHES storage and energy extraction [21]

The Pumped Hydroelectric Energy Storage System is the first generation energy storage system. In Figure 1, the storage capacity of PHES depends on the difference in gravity height between the upper and lower reservoirs combined with the volume of the reservoir and the capacity of the water to be pumped (see Fig. 1). Currently PHES is the largest, most efficient and commercially sustainable ESS in the world. 65-85% energy conversion efficiency can be achieved by using PHES [20].

In many countries, the economy and sustainability of this technology has been proven. Recently, another system has been developed that allows for wind energy integration forming the hybrid energy storage system known as Wind-Hydro-Pumped storage System (WHPSS) (see Fig. 2) [22].

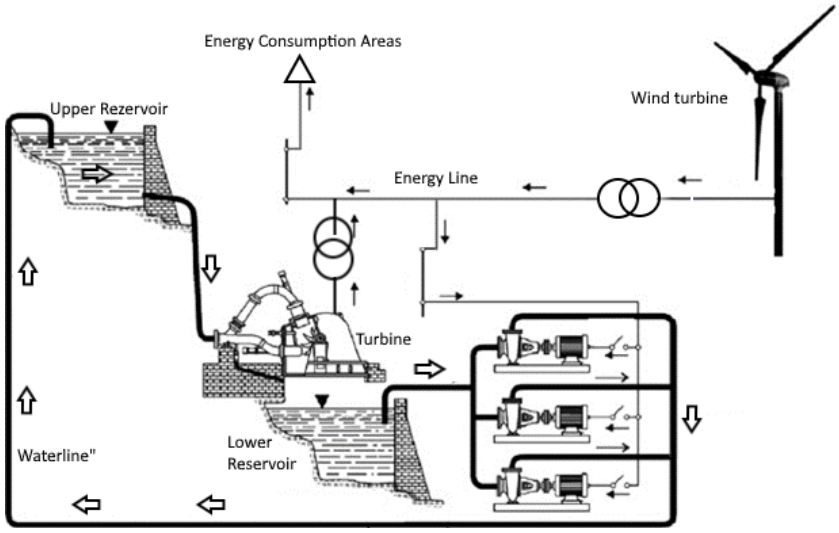

Fig. 2. Model of wind-hydro pump storage systems

Generally, the life of PHES installations is approximately 65-75 years. Cost depreciation periods are around 30-50 years [23]. Fast response time is less than 1 minute, despite the large power volumes and energy management in PHES installations [24].

Such a power system integration can be used to balance electricity demand and supply in the area where wind and hydroelectric power sources could potentially coexist.

- Despite the growing nature of PHES technology, there are some disadvantages:
- Huge fund requirement.
- Finding suitable structured areas.
- The necessity to use some of the energy generated for the system to work.
- Proper planning is required to pump water to the base reservoir during low energy demand and to use water in energy production during high energy demand.

3 Technical Specifications of PHES

Table 1 shows the specifications of a typical PHES facility. PHES can be installed between 10 and 4,000 MW power. Charging time at nominal power varies between 1 and 24 hours. There is a loss of 20-25% during the energy conversion.

Table 1. Technical Specifications of PHES [25-26-27]

Power	10–4000 MW
Discharge time at nominal power	1–24 + hours
Round-trip efficiency	%70-85
Reaction time	Minimum 1 min
Power/fund cost	2.000–4.300 $ / kW
Lifetime	40-60 + years

The installed power values of some of the countries with PHES capacity are shown in Table 2. According to 2014 data, the countries with the most installed storage power in the world stand out as Japan, China and the United States.

Pumped storage systems currently provide the most commercially important tools of large-scale grid energy storage and improve the daily capacity factor of the generation system.

Table 2. Installed PHES Capacity by Country [28-29]

Country	**Installed Capacity (GW)**	**The Under Construction (GW)**	**PHES/ Installed Power Capacity (%)**
Japan	24.5	3.3	8.5
China	22.6	11.6	1.8
USA	20.5	-	1.9
Italy	7.1	-	5.7
Spain	6.8	-	6.6
Germany	6.3	-	3.5
France	5.8	-	4.4
India	5.0	1.7	2.2
Austria	4.8	0.2	21
Great Britain	2.7	-	3.0
Switzerland	2.5	2.1	12
Portugal	1.1	1.5	6.1

4 Why Pumped Hydroelectric Energy Storage (PHES) Facilities?

Wind, sun, wave, tide, biomass etc. renewable and clean energy sources are intermittent by nature and therefore cannot generate energy continuously. Wind energy also shows hourly, daily, weekly, monthly and yearly changes according to the meteorological situation [30]. Although solar radiation is a more stable energy source than wind, it is only possible to produce energy during the daytime. In this case, relatively smaller energy storage systems can be beneficial to provide continuous and quality power. According to Hino and Lejeune [31], pumped hydropower storage facilities have the advantages of flexible start / stop and fast response speed, tracking load changes and adapting to drastic load changes. It can modulate the frequency and keep the voltage stability. Although the cost of PHES systems seems to be a disadvantage; being a renewable energy source and providing peak power efficiency has increased its applicability [32-33-34]. Clean and renewable energy sources are promoted and used in the modern world. Considering these increasing trends to use intermittent energy sources, there is a greater need for flexibility in modern energy transmission and distribution systems. With regard to the integration of wind power into the electricity grid, a number of issues need to be addressed [35-36]:

- The grid capacity and voltage profile should not exceed specified limits.
- Network congestion.
- The effect of Variable Energy Sources (VER) on collective power transmission due to wind integration.
- Controlling harmonics created by adding wind to the network
- Determination of the system's transient stability performance for normal and unexpected conditions and power transfer levels restricted by a stability constraint due to the addition of VER interconnections.
- Addressing changes in impedances to the grid due to their effects on wind farm connection to the grid and subsequent remote control signals.
- Protection problems of grid protection equipment in the grid due to the addition of wind energy to the grid.
- Stability problems may occur in networks due to the dynamic behavior of wind farms connected to the grids.
- A capital investment assessment may be required to mitigate any adverse system impacts, including equipment, transmission lines, and dedicated / high speed protection system.

All these problems can be addressed using bulk energy storage systems including mechanical systems (pumped hydro, compressed air energy storage-CAES-, flywheels), electrical systems (capacitors and ultra capacitors, superconducting magnetic energy storage-SMES-), and chemical / electrochemical systems(metal air, flow batteries, Li-ion battery, NaS battery, hydrogen energy storage)[37].

Weisser at al. stated that there should not be a technical problem for instantaneous wind penetrations of up to 20% in a power grid [38]. However, Jacob stated that a

maximum wind penetration of 25-50% is possible in the electricity sector and also reported that the feasibility of very high wind penetrations significantly decreased when the size of the electricity grid increased from 100 kW to 10 MW. While 80% wind penetration is possible for a 100 kW grid, only 20% wind penetration is possible for a 10 MW grid. The author concluded that the primary reason for this dramatic reduction in applicable wind penetrations was the lack of energy storage in the grid [39]. Bakos concluded that a storage capacity is required for the energy required for 1-3 days to achieve over 90% wind penetration [40]. PHES is the largest and most mature form of energy storage available, and therefore it is likely that PHES will become more important in energy systems as penetrations of renewable energy increase. The efficiency of pumped hydroelectric power plants is between 70% and 80% [41]. While the establishment cost of a storage reservoir is 600-1000 $ / kW depending on the geographical structure, the energy cost varies between 1 and 20 $ / kW [42]. Although the benefits of PHES are known, places available to build the facilities are running out [43].

PHES systems require low energy density, a very large body of water or a big height change. According to the Electric Power Research Institute (EPRI), PHES accounts for over 99% of global bulk storage capacity of around 127 GW [44]. In 2009, the global PHES capacity was around 100 GW. The energy efficiency of PHES in practice ranges from 70% to 80% [45] with some researchers reporting an efficiency of 87% [46].

5 PHES Location Criteria and Methodologies

Choosing a technical, commercially and socially acceptable site is a critical issue for PHES. It is necessary to develop simple and economical methods in determining the correct application areas. As time passes, the availability of technically and economically viable areas decreases. Therefore, new methods should be developed [47]. Connolly at al. have developed a computer program that can scan the terrain and determine whether it is suitable for the PHES installation. This program has proven to be helpful in identifying suitable sites for PHES [48].

6 Storage Systems Lifetime

The lifetime of the storage systems is shown in Table 3. PHES systems are the longest-lasting system compared to other storage methods and at the same time there is no cycle problem. Cycle durability of batteries is generally not high. Lead-acid batteries have a lifetime of 2,000 cycles in the case of 1 hour charge and 1 hour discharge. The NaS battery has been tested to determine its lifespan and has operated over 4,500 cycles for about 4.5 years. It was found to be extremely reliable for 2,250 cycles or 15 years of life according to the findings [49]. In the lifetime test of the Zn / Br battery, it has been determined that it works stable even in more than 1500 cycles [50]. The vanadium redox flow battery with a 20 kW cell stack has a 13, 342 cycles record in a 2-year accelerated test.

Table 3. Life of electrical energy storage systems [51]

Storage System	Year	Cycle
Pumped hydro	> 40	-
CAES (Compressed Air)	> 20	-
Lead-acid battery	13	2000
Na/S (Sodium sulfide) battery	15	2250
Zn/Br (Zinc Bromine) battery	10	1500
Redox flow battery	-	13342
Volan	> 15	> 21.000
Double layer capacitor	-	> 50.000
Redox super capacitor	> 5	Small Effect

7 PHES Approaches in the World

Currently the largest PHES investments are China, India, Switzerland and Japan. All of these countries have partially liberalized electricity markets with PHES transmission and distribution infrastructure. The Swiss market resembles the competitive markets of the USA and the EU, but is also exceptional in that it is highly interconnected with the liberalized markets of Germany, France, Italy and Austria. Therefore, European wholesale electricity prices had a negative impact on the Swiss market and two new large-pump storage plans were suspended in the early stages of construction [52].

PHES investments are constantly increasing in India and China, two countries where peak-time electricity supply is insufficient [53]. In these regions, there is no excess electricity generation capacity required for power generation or load tracking flexibility. PHES facilities in these countries are developed as an integrated public service by states that have both generation and transmission assets [54-55].

Although existing PHES facilities in the US continue to operate, little investment has been made since 1990. Demand for PHES in the liberalized electricity market is low, although there is a potential market and suitable fields [56].

8 Integrating Wind Energy and Hydro Storage

A mathematical programming model is used to allocate electricity generation between generators / power plants in a way that minimizes total generation costs. It enables the power grid operator to know about generation costs and capacities, technical constraints, current wind power, river flows and future electricity demand [57].

The wind park profit of the wind-hydro system in operation should be at the highest level. Numerous techniques have been developed to provide current wind energy estimates for short and medium-term time periods [58]. These approaches are important for defining optimal strategies to be followed in system operation. Wind fore-

casts, wind energy curve characteristic and availability of wind generators, projected current electric wind energy curve can be obtained [59].

Even if the current wind power is low, the energy stored in the upper water tank may be sufficient to cover the required demand. In order to achieve this, the minimum demand curve must be defined.

Due to some network operating conditions mainly arising from the boundaries in the system branches, all the power generated by the wind parks cannot penetrate the system. Then a curve of the maximum allowable power variation with the system must also be defined, this models the limitations in wind power penetration into the grid.

To solve this problem, 24 hour transactions should be defined. The following information should be foreseen in the work schedule envisaged for each time period;

1. Total power to be supplied to the grid
2. The power expected to be generated by both wind and hydro generators
3. Power consumed in the pump unit
4. Upper reservoir water level.

An increase in wind penetration creates instability in the system, so backup capacity can be increased with a gas or diesel generator operating only during short peak load hours during the year. Additional investment costs correspond to approximately 15% to 30% of the investment costs of a wind farm. It also increases the costs of reducing greenhouse gas emissions as the peak-load generator consumes fossil fuels [60].

9 Conclusion

When the focus is on reducing CO2 emissions and hydraulic storage, we must ignore fossil fuel power generation during peak times. The additional system cost associated with wind may be less than the cost of meeting the same growth with a new fossil fuel power plant. However, the variability of the wind requires more wind power to be installed.

If hydraulic storage is available, the costs of wind penetration are lower, Electric grids that are more compatible with hydroelectric energy ensure that intermittent wind and other power sources are better integrated into the grid. It may be necessary to increase the size of existing reservoirs or add a storage system to store water for energy generation purposes. However, energy storage areas are likely to compete with agriculture, wildlife, industrial, commercial and residential users for water. In addition, many environmental groups are against building more dams due to their devastating impact on fish and other wildlife environments.

Advanced forecasting tools predict highly accurate wind, precipitation and energy demand. Electric energy providers strive to increase the availability and security of the energy supply. Conditional changes in energy consumption level depending on the variability in energy supply sources and time, the use of energy storage systems will maintain its importance in terms of reliability.

References

1. Global Wind Energy Council Website, https://gwec.net/global-wind-report-2019/#:~:text=Offshore%20wind%20is%20playing%20an,per%20cent%20of%20new%20installations, last accessed 2021/02/10.
2. International Energy Agency Website, https://www.iea.org/reports/global-energy-review-2019/renewables#abstract, last accessed 2021/02/13.
3. US Department of Energy, https://emp.lbl.gov/sites/default/files/2020_wind_energy_technology_data_update.xlsx, last accessed 2021/02/13.
4. Georgilakis P.S., Technical challenges associated with the integration of wind power into power systems. Renewable and Sustainable Energy Reviews 12(3), 852–863, (2008).
5. Tsili M., Papathanassiou S., A review of grid code technical requirements for wind farms. IET Renewable Power Generation 3(3), 308–332 (2009).
6. Beaudin M., Zareipour H., Schellenberglabe A., Rosehart W., Energy storage for mitigating the variability of renewable electricity sources: an updated review. Energy for Sustainable Development 14(4), 302–314 (2010).
7. Ibrahim H., Ilinca A., Perron J., Energy storage systems—characteristics and comparisons. Renewable and Sustainable Energy Reviews 12, 1221–1250 (2008).
8. Pickard W.F., Shen Q.A., Hansing N.J., Parking the power: Strategies and physical limitations for bulk energy storage in supply-demand matching on a grid whose input power is provided by intermittent sources. Renewable and Sustainable Energy Reviews 13, 1934–1945 (2009).
9. Ridgway S.L., Dooley J.L., Hammond R.P., Large energy storage systems for utilities. Applied Energy 6, 133–142 (1980)
10. RAPOR Denholm P., Ela E., Kirby B., Milligan M., The role of energy storage with renewable electricity generation. (Tech. Rep.;January). National Renewable Energy Laboratory; 2010(NREL/TP-6A2-47187).
11. Electrical Energy Storage, https://basecamp.iec.ch/download/iec-white-paper-electrical-energy-storage/?wpdmdl=411&ind=1540545738591, last accessed 2021/03/13.
12. Kaldellis J.K., Kapsali M., Kavadias K.A., Energy balance analysis of wind-based pumped hydro storage systems in remote island electrical networks. Applied Energy 87(8), 2427–2437 (2010).
13. Papaefthimiou S., Karamanou E., Papathanassiou S., Papadopoulos M., Operating policies forwind-pumped storage hybrid power stations in island grids. IET Renewable Power Gener 3(3), 293–307 (2009).
14. Papaefthymiou S.V., Karamanou E.G., Papathanassiou S.A., Papadopoulos M.P., A wind-hydro-pumped storage station leading to high RES penetration in the autonomous island system of Ikaria. IEEE Process on Sustainable Energy 1(3), 163–72 (2010).
15. KİTAP Papaefthymiou S.V., Papathanassiou S.A., Karamanou E.G., Application of pumped storage to increase renewable energy penetration in autonomous island systems. Wind energy conversion systems: technology and trends. London: Springer-Verlag 295–335 (2012).
16. Caralis G., Papantonis D., Zervos A., The role of pumped storage systems towards the large scale wind integration in the Greek power supply system. Renewable and Sustainable Energy Reviews 16(5), 2558–2565 (2012).
17. Kaldellis J.K., Zafirakis D., Kavadias K.A., Techno-economic comparison of energy storage systems for island autonomous electrical networks. Renewable and Sustainable Energy Reviews 13(2), 378–392 (2009)

18. Salgi G., Lund H., System behavior of compressed-air energy-storagein Denmark with a high penetration of renewable energy sources. Applied Energy 85(4),182–189 (2008).
19. Ibrahim H., Younès R., Ilinca A., Dimitrova M., Perron J., Study and design of a hybrid wind–diesel-compressed air energy storage system for remote areas. Applied Energy 87(5), 1749–1762 (2010).
20. Ibrahim H., Ilinca A., Perron J., Energy storage systems—characteristics and comparisons. Renewable and Sustainable Energy Reviews, 12, 1221–1250 (2008).
21. Deane J.P., O'Gallachoir B.P., Mc Keogh E.J., Techno-economic review of existing and new pumped hydro energy storage plant. Renewable and Sustainable Energy Reviews 14(4), 1293–1302 (2010).
22. Dursun B., Alboyaci B., The contribution of wind-hydro pumped storage systems in meeting Turkey's electric energy demand. Renewable and Sustainable Energy Reviews 14(7), 1979–1988 (2010).
23. Kaldellis J.K., Zafirakis D., Optimum energy storage techniques for the improvement of renewable energy sources-based electricity generation economic efficiency. Energy 32(12), 2295–2305 (2007).
24. First Hydro Company Website, http://www.fhc.co.uk/pumped storage.htm, last accessed 2021/02/10.
25. Beaudin M., Zareipour H., Schellenberglabe A., Rosehart W., Energy storage for mitigating the variability of renewable electricity sources: an updated review Energy for Sustainable Development 14(4), 302–314 (2010).
26. Luo X.,Wang J., Dooner M., Clarke J., Overview of current development in electrical energy storage technologies and the application potential in power system operation. Applied Energy 137, 511–36 (2015).
27. Chen H.S., Cong T.N.,Yang W.,Tan C.Q., Li Y.L., Ding Y.L., Progress in electrical energy storage system: acritical review. Progress in Natural Science 19(3), 291–312 (2009).
28. Yang C., Jackson R.B., Opportunities and barrier stopumped-hydro energy storage in the United States. Renewable and Sustainable Energy Reviews 15(1), 839–844 (2011).
29. Deane J.P., Gallachóir B.P.Ó., Mc Keogh E. J., Techno-economic review of existing and new pumped hydro energy storage plant. Renewable and Sustainable Energy Reviews 14(4), 1293-1302 (2010).
30. Alam M.M., Rehman S., Meyer J., Al-Hadhrami L.M., Extraction of the inherent nature of wind using wavelets. Proceedings of the 10th International Conference on Heat Transfer, Fluid Mechanics and Thermodynamics pp. 37-47. Orlando, Florida (2014).
31. Hino T., Lejeune A., Pumped storage hydro power developments. Compre Renewable Energy 6, 405–434 (2012).
32. Mitteregger A., Penninger G. Austrian pumped storage power stations supply peak demands. World Pumps 16(18), 20-31 (2008).
33. Nazari M.E., Ardehali M.M., Jafari S., Pumped storage unit commitment with considerations for energy demand, economics and environmental constraints. Energy 35(10), 4092-4101 (2010).
34. Kear G., Chapman R., Reserv ingjudgement: perceptions of pumped hydro and utility-scale batteries for electricity storage and reserve generation in New Zealand. Renewable Energy 57(C), 249-261 (2013).
35. Bousseau P., Fesquet F., Belhomme G., Nguefeu S., Thai T.C., Solutions for the grid integration of wind forms - a survey. Wind Energy 9(1-2), 13-25 (2006).
36. Estanqueiro A.I., De Jesus J.M.F., Ricardo J., Dos Santos A., Lopes J.A.P., Barriers to very high wind penetration in power systems. In Proceedings of the 2007 IEEE power engineering society general meeting, pp. 2103–2109. Florida, USA (2007).

37. Rahman F., Rehman S., Abdul Majeed M.A., Overview of energy storage systems for storing electricity from renewable energy sources in Saudi Arabia. Renewable and Sustainable Energy Reviews 16(1), 274-283 (2012).
38. Weisser D., Garcia R.S., Instant an eous wind energy penetration in isolated electricity grids: concepts and review. Renewable Energy 30(8), 1299-1308 (2005).
39. Kocaman A.S., Optimization of hybrid energy systems with pumped hydro storage- A case study for Turkey. Journal of the Faculty of Engineering and Architecture of Gazi University 34(1), 53-67 (2019).
40. Bakos G.C., Feasibility study of a hybrid wind/hydropower-system for low-cost electricity production. Applied Energy 72(3-4), 599-608 (2002).
41. Rehman S., Al-Hadhrami L.M., Alam M.D., Pumped hydro energy storage system: A technological review, Renewable and Sustainable Energy Reviews 44, 586-598 (2002).
42. Schoenung S., Hassenzahl W., Long-vs. short-term energy storage technology analysis—a life-cycle cost study. Sandia National Laboratories, USA, (2003).
43. Kaldellis J.K., Kavadias K.A., Optimal wind-hydro solution for Aegean Sea islands' electricity-demand fulfilment. Applied Energy 70(4), 333-354 (2001).
44. The Economist, Energy storage packing some power, https://www.economist.com/technology-quarterly/2012/03/03/packing-some-power, last accessed 2021/01/05
45. Levine J.G., Pumped hydroelectric energy storage and spatial diversity of wind resources as methods of improving utilization of renewable energy sources, Master Thesis, University of Colorado (2007).
46. Energy Storage Hawaiian Electric Company, https://www.hawaiianelectric.com/about-us/innovation/energy-storage, last accessed 2021/01/04.
47. Blaabjerg F., Consoli A., Ferreira J., Van Wyk J., The future of electronic power processing and conversion. IEEE Trans Power Electron 20(3), 715–720 (2005).
48. Connolly D., Mac Laughlin S., Leahy M., Development of a computer program to locate potential sites for pumped hydro electric energy storage. Energy 35, 375-381 (2010).
49. Ma T., Yang H., Lin L., Peng J., Pumped storage-based standalone photovoltaic power generation system: Modeling and techno-economic optimization. Applied Energy 137, 649-659 (2015).
50. Tateyama Y., First-principles Calculation Study on Solid Electrolyte Interphase (SEI) in Lithium Ion Battery. Journal of computer chemistry 18(1), 18-28 (2019)
51. Kondoh J., Ishii I., Yamaguchi E., Murata A., Otani K., Sakuta K., Higuchi N., Electrical energy storage systems for energy networks. Energy Conversion and management 41(17), 1863-1874 (2000).
52. Reuters, http://www.reuters.com/article/2014/08/31/utilities-swiss-pumpedstorage-idUSL5N0QV3FK20140831, last accessed 2021/01/05.
53. US Energy Information Administration, https://www.eia.gov/international/overview/country/IND, last accessed 2021/02/13.
54. Ming Z., Kun Z., Daoxin L., Overall review of pumped-hydro energy storage in China: status quo, operation mechanism and policy barriers. Renewable and Sustainable Energy Reviews 17 (C), 35-43 (2013).
55. Sivakumar N., Das D., Padhy N.P., Senthil K.R., Bisoyi N., Status of pumped hydro-storage scheme sand its future in India. Renewable and Sustainable Energy Reviews 19, 208-213 (2013).
56. Yang C., Jackson R.B., Opportunities and barrier stopumped-hydro energy storage in the United States. Renewable and Sustainable Energy Reviews 15(1), 839-844 (2011).

57. Benitez L.E., Benitez P.C., Kooten G.C.V., The economics of wind power with energy storage, Energy Economics 30, 1973-1989 (2008).
58. Korpas M., Hildrum R., Holen A.T., Operation and sizing of energy storage for wind power plants in a market system. International Journal of Electrical Power & Energy Systems 25(8) 599-606, (2003)
59. Project Anemos, https://www.osti.gov/etdeweb/servlets/purl/20675341, last accessed 2021/02/13.
60. Castronuovo E.D., Pec J.A., Optimal operation and hydro storage sizing of a wind–hydro power plant, International Journal of Electrical Power & Energy Systems 26(10), 771-778 (2004).

The Analysis of 40-Year Wind and Wave Characteristics

HazalIşın[1], H. Anıl Arı Güner[1], Yalçın Yüksel[1]

[1] Civil Engineering Department/ Yıldız Technical University
34220 Esenler, Istanbul, Turkey
hazal_isin@hotmail.com, anilariguner@gmail.com,
yalcinyksl@gmail.com

Abstract. The energy potential of renewable energy sources like sea and ocean can be calculated directional and regional with wind and wave characteristics. Long-term wind and wave parameters can be examined for suitable coordinates of energy production. Besides, variations in long-term wind and wave parameters can determine the effects of climate change over the years. In this study, the wave climate over the Sea of Marmara was investigated by providing extensive datasets covering the last 40 years (1979-2018). Wave simulations were generated from the MIKE 21 Spectral Wave (SW) model forced with European Centre for Medium-Range Weather Forecasts (ECMWF) ERA-Interim wind datasets. The MIKE 21 SW model was calibrated and validated with directional buoy measurements at Silivri offshore location. Based on the ultimate model, dominant wind and wave directions were determined at various locations along the Sea of Marmara. In addition, the temporal variations of wind and wave characteristics were investigated according to the monthly and annual basis. The trends of 40-year average changes in wind speed (Ws) and significant wave height (H_s) were examined. The potential effect of the long-term variability on Ws and H_s was discussed in the context of climate change.

Keywords: Wave modeling, Long-term changes, MIKE 21 SW.

1 Introduction

Recently, more energy sources are needed because of the increasing energy consumption. Ocean and sea energy sources are among the clean and renewable energy generation types. For this, the potentials of wind and wave energy generation systems have been investigated in Turkey's coastal and deep water. In this study, 40 years long-term wind and wave characteristics in the Sea of Marmara were examined. The reference coordinates selected from different directions along the Sea of Marmara were used. Besides, the monthly and annual changes of the 40-year wind and wave parameters were analyzed.

Long-term wave measurements of a region are required to find the wave climate of that region. Long-term wind data measurements are usually available. However, measuring long-term wave data is inconvenient and expensive. In the absence of long-term wave data, wave prediction can be made with long-term wind data by using nu-

merical models. In this study, the long-term wave characteristics in the Sea of Marmara were investigated by using the 3rd generation numerical wave model MIKE 21 SW [1].

There are few studies evaluated the wind and wave climate in the Sea of Marmara so far. The first attempt to assess wave climate in the Sea of Marmara was performed by Özhan et. al. (1999) [2]. They studied 68 locations over the Sea of Marmara, and prepared a wind and wave atlas. At the end of the study, they presented wind and wave roses at these locations. In addition, they gave significant wave height and mean wave period relationship, long-term extreme values, and the probability of wave exceeding.

Saraçoğlu (2011) examined the wind and wave climate of the Sea of Marmara by using MIKE 21 SW [3]. Three months of wave data measurements in Ambarlı were used in the calibration of the numerical wave model. At the end of the study, results were compared with the Wave Atlas [2].

Kutupoğlu et al. (2018) performed the SWAN model for wind-wave hindcast in the Sea of Marmara [4]. They used 4 years of Silivri wave measurements for the calibration and validation of the numerical wave model. In their study, they compared two different wind data sources which are Climate Forecast System Reanalysis (CFSR) and Era-Interim and concluded CFSR based wind data obtain better results.

Akpınar et al. (2021) analyzed wind and wave climate over the Sea of Marmara using the SWAN numerical model [5]. For this, wind and wave characteristics were determined for 40 years (1979–2018). They found that the center of the Sea of Marmara and shores of Kapıdağ Peninsula and Marmara Island have the highest maximum significant wave heights.

Yüksel et al. (2021) evaluated wind and wave characteristics over the Sea of Marmara for the 40 years (1979–2018) [6]. SWAN model was forced with CFSR and ERA-Interim wind data for generation of wave parameters. At the end of the study, they compared the results of two wind datasets for long-term wind and wave characteristics. Also, they concluded that the northern side has stronger wind and wave climate than the southern side at the Sea of Marmara.

2 Area of Interest and Availability of Data

The study location is the Sea of Marmara between 40°- 41.25° North and 26°- 30° East. The Sea of Marmara which has an area of 11500 km^2 connects the Black Sea and the Mediterranean Sea.

The wave climate study is performed on the same coordinates at 68 study locations in the Wave Atlas [2]. Figure 1 which is adopted from Wave Atlas illustrates the area and study locations. Moreover, the long-term variations of Ws and H_s are examined at 7 reference locations selected from each direction over the Sea of Marmara. The blue pins represent these reference locations, and the red pin displays the Silivri measurement station, shown in Figure 2. The directional wave record at this station was used for calibration and verification of the wave model.

The ERA-Interim dataset obtained from ECMWF was used as input wind data. This dataset covering the 40-year from 1979 to 2018 has 6-h wind fields with a spatial resolution of 0.25° in longitude and 0.25° in latitude.

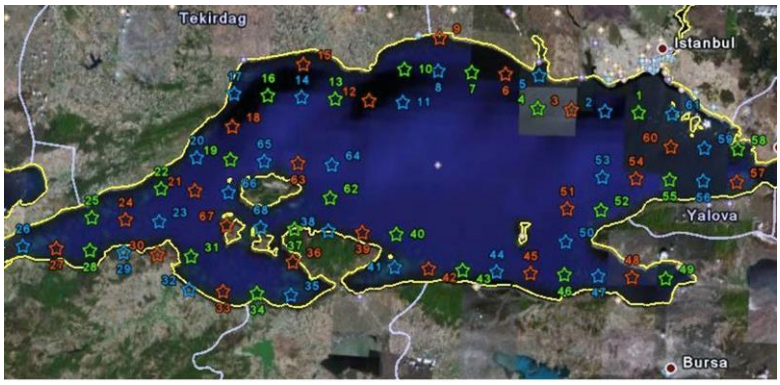

Fig. 1. The study locations of wave climate over the Sea of Marmara [2]

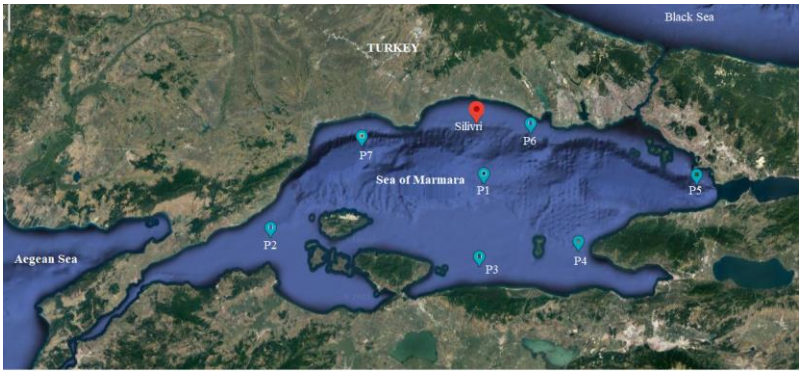

Fig. 2. The Silivri measurement station and reference locations

3 Set-Up and Calibration of the Wave Model

The MIKE 21 SW model comprises an unstructured and flexible mesh system. The resolution of the areas can be adjusted with triangular elements. For more precise results, a fine mesh structure can be created in the coastal. In this study, the mesh system has 2141 nodes and 3372 triangular elements.

The calibration of the numerical model was performed with different scenarios. By altering the parameters' values, their effects on significant height (H_s) and mean period (T_m) were determined. The following values gave the best result: Cdis=2.5 and δ=1 for white capping, γ=0.8 and α=1 for wave breaking and f_w=0.0212 for bottom friction. The model results and Silivri measurements were compared by coefficient of determination (R^2), root mean square error (RMSE), and scatter index (SI). Table 1

shows statistical error measures of the accepted wave model against the measurements at the Silivri station. Finally, the hindcast dataset was generated along the Sea of Marmara for a period between 1979 and 2018.

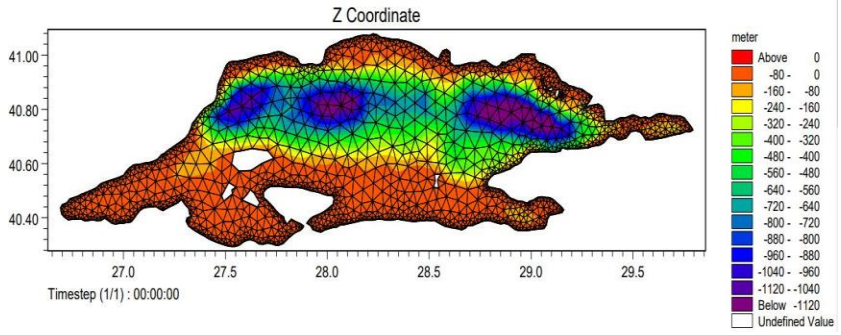

Fig. 3. The mesh network of the Sea of Marmara

Table 1. The statistical error measures for January 2015, and the years between 2013 and 2018

Month / Year	RMSE		SI		R^2	
	H_s	T_m	H_s	T_m	H_s	T_m
January 2015	0.272	1.125	0.508	0.335	0.628	0.310
2013	0.200	1.233	0.545	0.396	0.465	0.015
2014	0.204	1.185	0.614	0.385	0.431	0.024
2015	0.218	1.229	0.540	0.390	0.576	0.059
2016	0.232	1.056	0.544	0.334	0.534	0.137
2017	0.163	8.145	0.564	0.973	0.492	0.049
2018	0.165	7.128	0.544	0.985	0.547	0.066

4 Results

4.1 Wind and Wave Roses

Wind and wave roses are created at 68 study locations as indicated in the Figure 1 based on 40 years data. A few examples of roses from these locations are presented in Figure 4 and Figure 5. As seen in both figures, locations in the first row are P1, P12, P18, P24, and in the second row are P33, P43, P54, P65.

Wind speed less than 5 m/s is accepted as calm period for wind roses. The dominant wind direction is north-east, and the secondary is south-west for all locations as seen in Figure 4.

Significant wave height less than 0.5 m is attributed as calm in wave roses. When the wave roses are examined, it is understood that the dominant directions of the locations in the same aspect over the Sea of Marmara are similar. As seen in Figure 5, the points of P12, P18, P24, and P65 which are in the north-west direction of the sea possess the east-north-east dominant wave direction. The points of P33 and P43 located at the south of the sea have the north-east dominant wave direction.

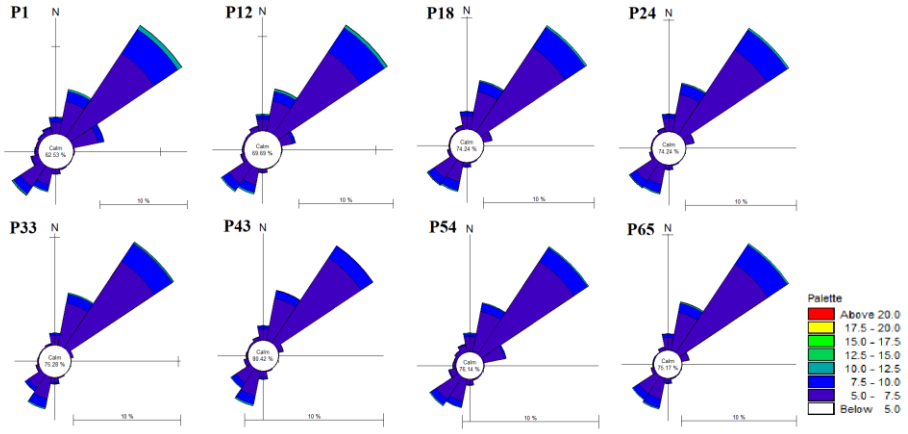

Fig. 4. Wind roses at the study locations for the reference points of P1, P12, P18, P24, P33, P43, P54, and P65

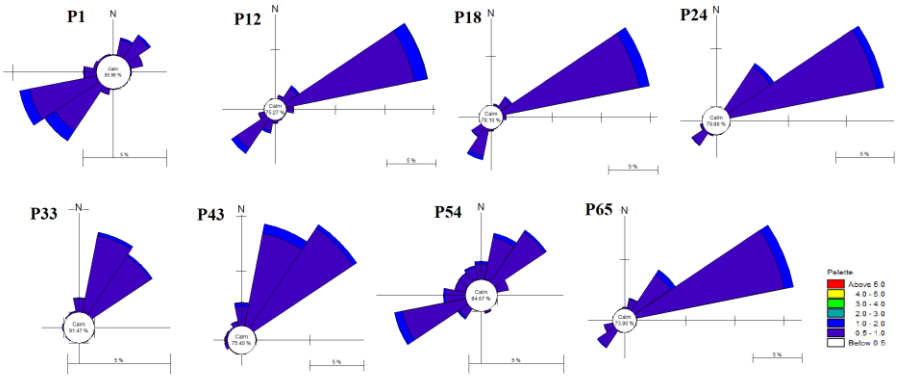

Fig. 5. Wave roses at the study locations for the points of P1, P12, P18, P24, P33, P43, P54, and P65

4.2 Long-term Variation of Wind Speed and Significant Wave Height

Mean wind speed and significant wave height values were computed with the 40-year dataset for 7 reference locations which are shown in Figure 2. The monthly and annual changes of the Ws and H_s are shown in the graphs below. As seen in Figure 6, the

mean wind speed has the lowest value in June and the highest value in December for all reference locations. The significant wave height for all locations except location 5 reaches the highest value in the winter months. The significant wave height of location 5 shows incompatibility with others in terms of months because of the different proximity to the shore. As can be seen in Figure 8 and Figure 9, Ws and H_s variations over the years are similar. For 40 years, the highest values are determined in 1982, while the lowest results are examined in 2014. When variations of Ws and H_s at all reference locations are examined, the most changes over 40 years are determined in location 1. The trends of Ws and H_s for location 1 are given in the figures. Figure 10 and Figure 11 show that there is a decrease of 0.25 cm/s/year for Ws and 0.04 cm/year for H_s, respectively.

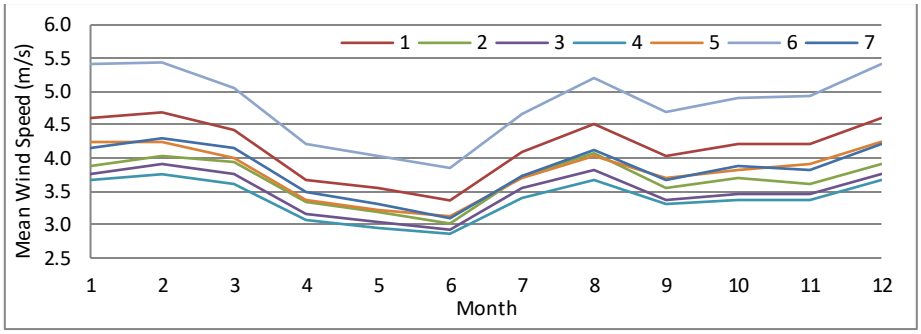

Fig. 6. Monthly variations of the mean wind speeds at the reference locations

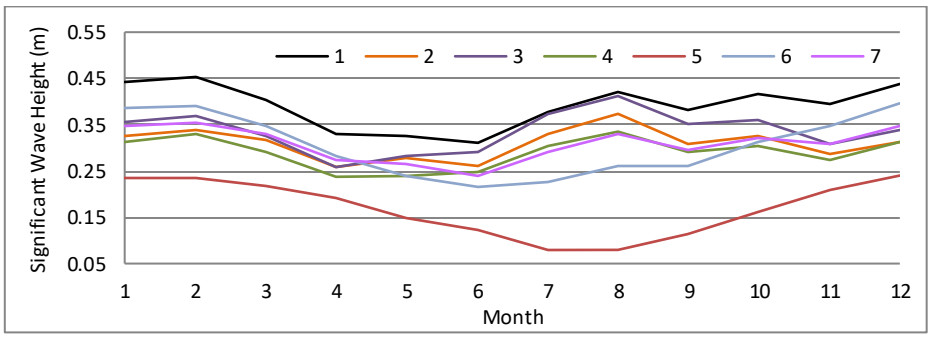

Fig. 7. Monthly variations of the significant wave heights at the reference locations

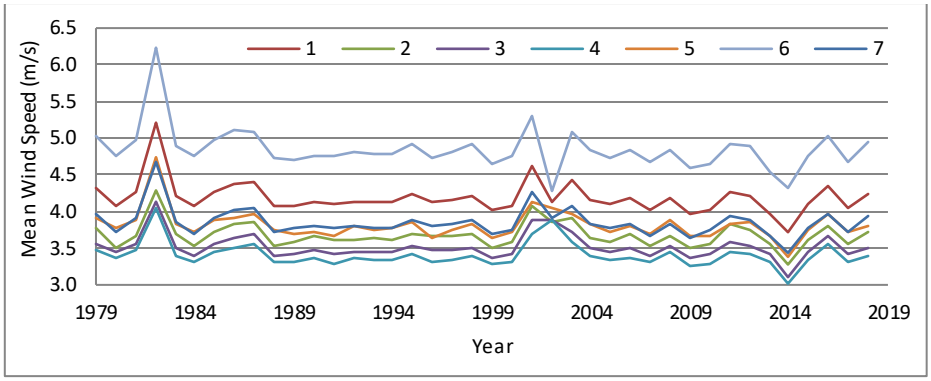

Fig. 8. Yearly variations of the mean wind speeds at the reference locations

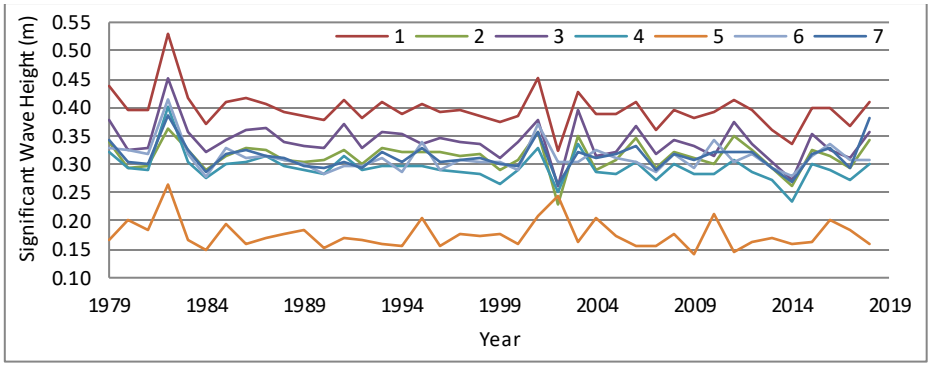

Fig. 9. Yearly variations of the significant wave heights at the reference locations

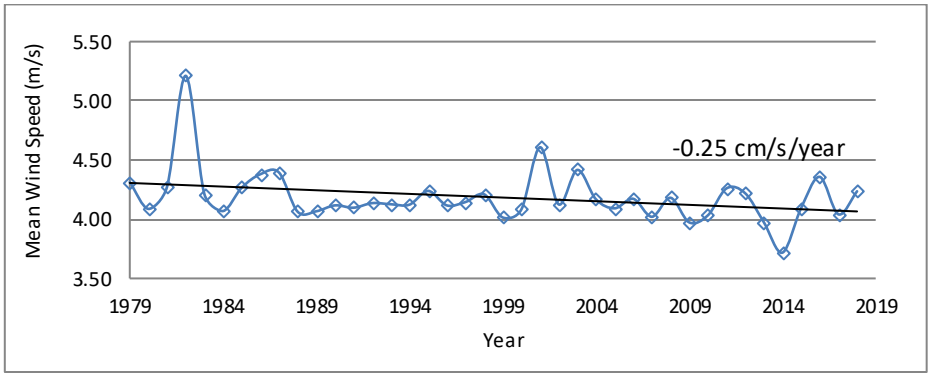

Fig. 10. The trend-line for location 1 during the period of 1979–2018

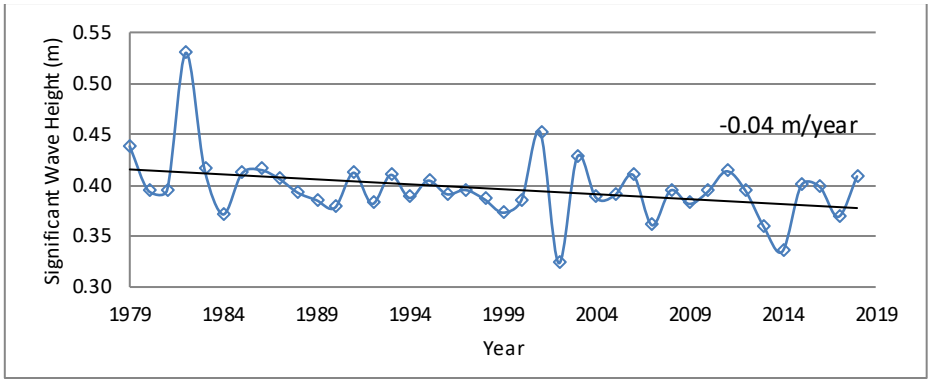

Fig. 11. The trend-line for location 1 during the period of 1979–2018

5 Conclusion

In this study, the 40-year wind and wave characteristics over the Sea of Marmara are determined by using MIKE 21 SW. The numerical wave model was forced with Era-Interim wind data between the years of 1979-2018. Wave measurements obtained from directional buoy at the Silivri station were used for calibration and verification. The white capping parameter was found the most major parameter for the calibration of the model and the values of Cds=2.5 and δ=1 give the lowest statistical error measures. After the calibrated model run, few reference locations were examined. The dominant and secondary wind directions were determined as the north-east and the south-west, respectively. Ws and H_s variations over the years and months were figured. The 40-year decreasing trends at location 1 were depicted for Ws and H_s.

References

1. DHI: MIKE 21 Spectral Waves FM-User Guide, DHI Water and Environment, Denmark (2017).
2. Özhan, E., and Abdalla, S.: Turkish Coast Wind and Deep Water Wave Atlas. Applied Project Report, Middle East Technical University, Civil Engineering Dept., Ocean Eng. Research Center, Ankara (1999).
3. Saraçoğlu, K. E.: The wave modelling and analysis of the Black Sea and the Sea of Marmara, Master Thesis, Yildiz Technical University, Institute of Science, Istanbul (2011).
4. Kutupoğlu, V., Çakmak, R. E., Akpınar, A., & Vledder, G. P.: Setup and evaluation of a SWAN wind wave model for the Sea of Marmara. Ocean Engineering 165, 450-464 (2018).
5. Akpınar, A., Kutupoğlu, V., Bingölbali, B., & Çalışır, E.: Spatial characteristics of wind and wave parameters over the Sea of Marmara. Ocean Engineering 222, 108640 (2021).
6. Yuksel, Y., Yuksel, Z.T., Islek, F., Sahin, C. and Guner, H.A.A.: Spatiotemporal long-term trends of wind and wave climate and extreme characteristics over the Sea of Marmara. Ocean Engineering 228, 108946 (2021).

Determination of the Wave Energy Potential of Marmara Sea

M. Emre Ulusan [1][0000-0001-8359-0007], H. Anıl Arı Güner [1][0000-0002-8603-9576], Yalçın Yüksel [1][0000-0001-6949-5345]

[1] Hydraulic and Coastal Engineering Laboratory, Department of Civil Engineering, Yildiz Technical University, Istanbul, Turkey
m.emreulusan@gmail.com, anilariguner@gmail.com, yalcinyksl@gmail.com

Abstract. This study aims to determine the wave energy potential of Marmara Sea. For this purpose, wave parameters were simulated by using the 3rd generation Spectral Wave Model (MIKE 21 SW) of Danish Hydraulic Institute. The model was run by using ERA-Interim wind data from the European Center for Medium-Range Weather Forecasts (ECMWF) between the years of 1979 and 2018. Calculated wave parameters were compared against wave measurements obtained from the buoy located at Silivri, Istanbul between the years of 2013 and 2018. Processes of sensitivity analysis, calibration and verification of wave characteristics were performed by using calibration parameters in MIKE 21 SW and statistical error parameters. The wave energy potential was analyzed in terms of the spatial and temporal variations. In 40-year average spatial distribution, the highest mean wave power value reaches up to 0.40 kW/m in the offshore. In addition, in the nearshore areas, the highest mean wave power value reaches up to 0.28 kW/m in the west coast, 0.30 kW/m in the north-north-west coast and 0.34 kW/m in the south coast. This study is important in terms of the long-term study for a period of 40 years and wave modeling analysis in a semi-enclosed sea like the Marmara Sea. The data concerning the wave power and wave energy obtained as a result of the study provides detailed information about the wave energy potential of Marmara Sea.

Keywords: Renewable Energy, Wave Energy, Marmara Sea.

1 Introduction

Energy resources are divided into two groups according to their renewability status as renewable energy resources and non-renewable energy resources. Non-renewable energy resources are widely used around the world, including fossil fuels (oil, coal and natural gas) and nuclear energy resources. However, when the uses of energy resources are examined, renewable energy resources have become widespread in recent years due to the limited amount of fossil fuels and the increasing energy need day by day. Renewable energy resources are defined as being able to renew themselves at an equal rate to the energy taken from the energy source or faster than the depletion

rate of the resource. Energy resources such as solar, wind, hydroelectric, geothermal, biomass, hydrogen and wave energy are the leading renewable energy resources. The wave energy is derived from wave motion in oceans and seas. The wave energy contains potential energy due to the height difference of the wave with the water surface and kinetic energy due to the movement of fluid particles. Various types of wave energy converters are used to convert wave energy into electrical energy. Studies on wave energy started after the oil crisis in the 1970s and have reached today.

The studies on estimation of the wave parameters and the wave energy have been carried out by several researchers in the Turkish seas and in many different regions of the world, however the studies performed on the Marmara Sea are less in number compared to the other regions.

Ozhan and Abdalla (1999) conducted a study on analyzing wave and wind parameters on all Turkish coasts. They examined the wave and wind parameters at 68 points on the Marmara Sea in their study.

Yuksel et al. (2011) analyzed the relationship between the significant wave height and mean wave period of all Turkish seas. They made an examination of the wave climate of 68 points on the Marmara Sea. As a result of the study, the relationship for Marmara Sea was given as $T_m = 3.521 H_s^{0.3327}$.

Saracoglu et al. (2014) determined the wave energy potential of Marmara Sea. They stated that the wave energy distributions were the highest as a percentage, below 0.75 m for the significant wave height and 2.50-3.50 s for the wave energy period and the average wave power value of the Marmara Sea was lower than 2.50 kW/m.

Kutupoglu (2017) conducted a comparison study on two different models on the Marmara Sea between 1979 and 2009. The highest value of the 31-year average significant wave heights were estimated to be around 0.4 m in the central regions of the Marmara Sea and the highest values of the 31-year average wave energy periods were estimated as 2.5 seconds on the southern coast of Tekirdag.

Abdollahzadehmoradi (2018) examined the wave energy potential of Marmara Sea in macro and micro scale. It was stated that the highest value in the mean wave power of 20 years was 0.47 kW/m and was in the central regions of the Marmara Sea.

Akpinar et al. (2021) determined the long-term spatial variability of wind and wave characteristics of Marmara Sea. The highest value of the mean significant wave heights were estimated to be around 0.4 m in the central regions of the Marmara Sea and the maximum values of significant wave height were estimates as 4.70 m.

Yuksel et al. (2021) analyzed the long-term trends of wind and wave climate on the Marmara Sea. Researchers determined that there are high waves reaching up to 2.5 m in the northern parts of the Marmara Sea and the mean values of significant wave height reaching up to 0.4 m. They stated that the maximum values of significant wave height tend to increase, the mean values of significant wave height and mean wave period tend to decrease.

Previous studies except Akpinar et al. (2021) and Yuksel et al. (2021) are limited in terms of the wind data and the measurement data. This study was carried out with longer wind data and measurement data compared to the other studies.

2 Methodology

In order to calculate the wave energy value at a specific time, the relationship between the wave power value and the time value is used.

$$E = P \times t \tag{1}$$

where E is the wave energy, P is the wave power and t is the time. Equation (2) is used to determine the wave power value.

$$P = \frac{\rho g^2}{64\pi} H_s{}^2 T_e \approx (0.491) H_s{}^2 T_e \tag{2}$$

where P is the wave power, g is the gravitational acceleration, ρ is the density of Marmara Sea (~1025 kg/m^3), H_s is the significant wave height and T_e is the wave energy period.

There are two methods for obtaining wave parameters, direct measurement with wave recorders and estimation with wind data. Direct measurement is made by pressure sensor, wave measurement masts, directional wave buoy, wave recording system, near coastal wave climate monitor and remote sensing methods. Although direct measurement records are available in recent years, data for previous years may not be available. In this case, previous years are estimated by generating a numerical model with various software with the help of existing measurement records and wind data.

In this study, wave parameters were simulated by using the 3rd generation Spectral Wave Model (MIKE 21 SW) of Danish Hydraulic Institute. Spectral Wave Model is used to simulate the growth, decay and transformation of wind-generated waves and swell in offshore and coastal areas [3].

The spectral moments used in the calculation of spectral wave parameters are obtained by equation (3).

$$m_i = \int_0^{2\pi} \int_0^{\infty} E(f,\theta) f^i df d\theta \tag{3}$$

where $E(f,\theta)$ is the directional wave spectrum that depends on the wave frequency (f) and the wave direction (θ). Parameters such as significant wave height (H_s), wave energy period (T_e) and mean wave period (T_m) are calculated using equations (4), (5) and (6).

$$H_s\ (H_{m0}) = 4\sqrt{m_0} \tag{4}$$

$$T_e\ (T_{m-1,0}) = m_{-1}/m_0 \tag{5}$$

$$T_m(T_{01}) = m_0/m_1 \tag{6}$$

3 The Study Area and Materials

The Marmara Sea is located between the coordinates 26°14'00" E - 30°10'00" E and 40°00'00" N - 41°41'00" N inside Turkey. The Marmara Sea is a very important

closed basin surrounded by the coastlines of Istanbul, Kocaeli, Yalova, Bursa, Balıkesir, Canakkale and Tekirdag provinces, and also a transition between Asia and Europe. It connects the Black Sea and the Aegean Sea via the Bosphorus and the Dardanelles straits. The Marmara Sea is a semi-enclosed inland sea with an area of 11352 km^2 and has a coastline of 1089 km, with limited water exchange. There are three pits with a depth of approximately 1238, 1390 and 1112 meters, respectively from left to right in the Marmara Sea.

Fig. 12. Study area, wave measurement station (yellow pin) and the selected points (red pins).

In this study, ERA-Interim wind fields from ECMWF between the years of 1979 and 2018 were used as the input wind data. The ERA-Interim wind fields have wind velocity data with 0.25°x0.25° spatial resolution and 6-hour temporal resolution with four data per day at 00, 06, 12, 18 Universal Time Coordinated. The u and v wind components in latitudinal and longitudinal directions at 10 m height in the data correspond to the wind velocity 10 meters above the sea surface.

4 Model Description

The model area was formed to include the entire Marmara Sea between 26.69° E - 29.79° E longitudes and 40.29° N - 41.08° N latitudes, and the Bosphorus and the Dardanelles straits connections were disconnected. A mesh with 2141 nodes and 3372 triangular elements was generated by fining the resolution from the offshore to the nearshore. The model was simulated for a period of 40 years, covering the years of 1979 and 2018.

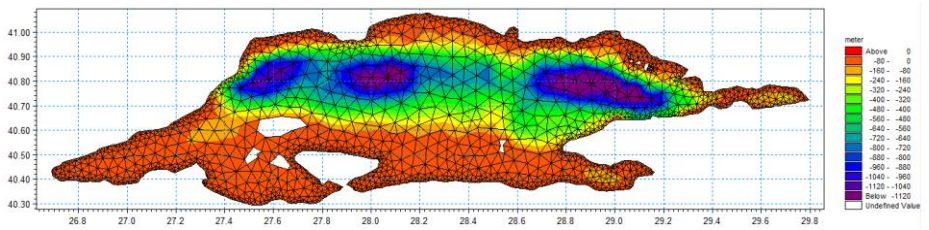

Fig. 2. Marmara Sea computational mesh.

Calculated wave parameters were compared against wave measurements obtained from the buoy located at Silivri, Istanbul between the years of 2013 and 2018. The Silivri measurement station is located at the coordinates of 40.9742° N and 28.2487° E, at a depth of 70 m and at a distance of about 10 km from the coast. The model was simulated with default values between the years of 2013 and 2018. The processes of sensitivity analysis, calibration and verification of wave parameters were performed by using calibration parameters such as bottom friction, breaking, white capping and Charnock parameter in MIKE 21 SW and statistical error parameters such as Root Mean Square Error (RMSE), Bias, Scatter Index (SI) and Coefficient of Determination (R^2).

Since it was known that the most effective parameter on the model from the previous studies was white capping dissipation coefficient (C_{ds}), this parameter was varied between the values of 0.5-4.0 and the model was simulated for the year of 2015, which has the highest number of measurement data. By examining the statistical parameters, measurement and model comparisons, the best agreement between the modeled and measured wave parameters was obtained for C_{ds} = 2.5.

From the sensitivity analysis and calibration studies it was determined that while the breaking and bottom friction had no effect on the model, the white capping dissipation coefficients (C_{ds} and δ) and Charnock parameter were significantly effective on the model. The best agreement between the modeled and measured wave parameters was obtained for C_{ds} = 2.5, δ = 1, γ = 0.8, α = 1, f_w = 0.0212 and Charnock parameter = 0.00525.

Table 1. Statistical results for the modeled H_s against to the measured H_s.

Year	Measured Mean (m)	Modeled Mean (m)	RMSE (m)	Bias (m)	SI	R^2
2013-2018	0.351	0.280	0.197	-0.072	0.561	0.507

5 Evaluation of the Wave Energy Potential

5.1 Spatial Distributions

Mean annual and seasonal spatial distributions were obtained for detailed analysis of the wave energy potential. Fig. 3 shows the spatial distributions of the 40–year average wave power values. In 40-year average spatial distribution, the highest mean wave power value reaches up to 0.40 kW/m in the offshore. In addition, in the nearshore areas, the highest mean wave power value reaches up to 0.28 kW/m in the west coast, 0.30 kW/m in the north-north-west coast and 0.34 kW/m in the south coast.

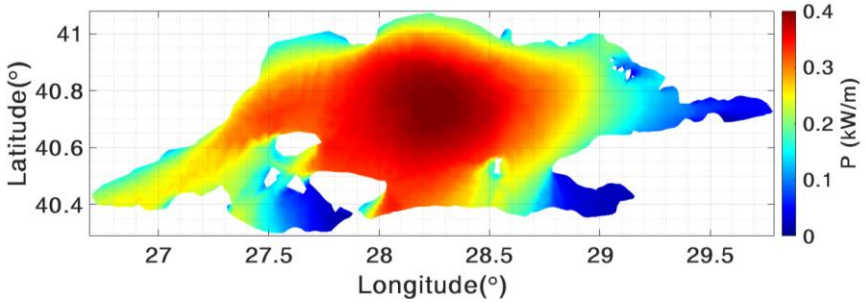

Fig. 3. Spatial distribution of the 40-year average wave power.

Fig. 4 shows the spatial distributions of the seasonal mean wave power values. Seasonally, the highest wave energy potential in the Marmara Sea is in winter. In the seasonal spatial distribution, the highest mean wave power value reaches up to 0.60 kW/m in the offshore in winter season. In addition, in the nearshore areas, the highest mean wave power value reaches up to 0.35 kW/m in the west coast, 0.38 kW/m in the north coast, 0.43 kW/m in the north-north-west coast and 0.46 kW/m in the south coast. In the other seasons, the mean wave power value decreases to 0.40 kW/m in autumn, 0.33 kW/m in spring and 0.31 kW/m in summer in the offshore.

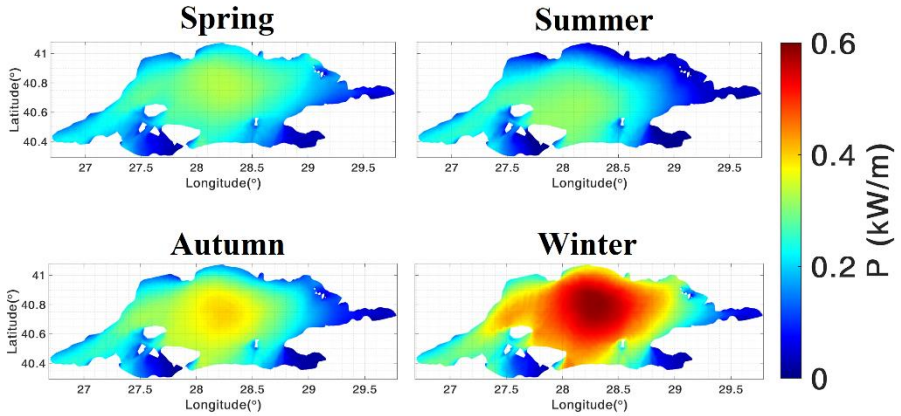

Fig. 4. Spatial distributions of the seasonal mean wave power values.

5.2 Local Analyses

Seven points were selected to represent the whole Marmara Sea shown in Fig. 1. The characteristics of these points are presented in Table 2.

Table 2. Characteristics of the selected points.

Points	Longitude (°)	Latitude (°)	H_s	T_e	Variability
P1	28.28	40.76	Higher	Long	Lower
P2	27.29	40.57	Moderate	Medium	High
P3	28.26	40.47	High	Longer	Moderate
P4	28.72	40.52	Low	Medium	Low
P5	29.27	40.75	Lower	Shorter	Higher
P6	28.50	40.94	Moderate	Short	High
P7	27.71	40.89	Moderate	Medium	Moderate

By using equation (1), yearly wave energy values were derived from the average wave power values at the selected points. The highest total wave energy value that can be obtained in 1 year from a selected location (P1) in the Marmara Sea is 3.47 MWh/m.

Table 3. The average wave power and yearly wave energies at the selected points.

Points	Wave power (kW/m)	Wave energy (MWh/m)
P1	0.40	3.47
P2	0.26	2.31
P3	0.32	2.78
P4	0.22	1.90
P5	0.12	1.02
P6	0.26	2.31
P7	0.26	2.29

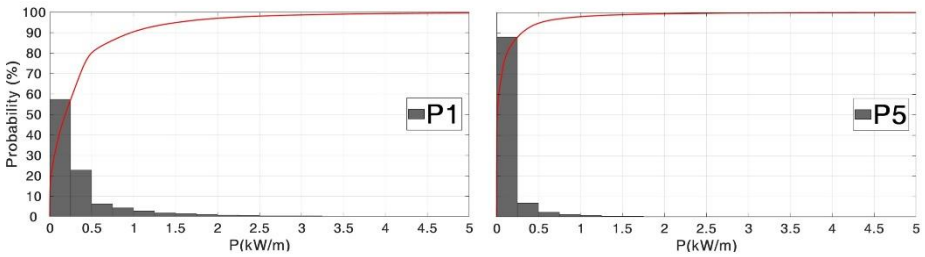

Fig. 5. Probability of occurrence (pdf) (gray bars) and cumulative distribution function (cdf) (red line) of the wave power at P1 and P5.

The probability of occurrence (pdf) and the cumulative distribution function (cdf) of the wave power values are presented in Fig. 5 for P1 and P5. Since these values were mostly below 5 kW/m, the x-axis was limited to this value. The maximum wave power values for these points increase up to the values of 22.5 kW/m and 19.1 kW/m,

respectively. Fig. 5 shows that the selected points mostly have wave power values in the range of 0−0.25 kW/m. The probability of occurrence of wave power values in the range of 0-0.25 kW/m at P1, which represents higher significant wave height and long wave energy period, is 57%, while this probability is 88% at P5, which represents lower significant wave height and shorter wave energy period.

Trend analysis was conducted by linear regression method to determine whether the variability of the data has an increasing or decreasing trend. The results of the trend analysis are presented in Table 4. According to the results, the mean wave power value tends to decrease in the Marmara Sea between the years of 1979 and 2018. P5 and P6, which have increasing trends, are the points with high variability compared to the other points.

Table 4. The long-terms trends of the wave power in 40 years at the selected points.

Points	%	kW/m
P1	- 7.22	- 0.030
P2	- 2.92	- 0.008
P3	- 9.63	- 0.032
P4	- 7.73	- 0.017
P5	+ 6.55	+ 0.007
P6	+ 5.62	+ 0.014
P7	- 0.31	- 0.001

6 Conclusions

The wave energy potential of Marmara Sea was investigated for a period of 40 years, covering the years of 1979 and 2018. Wave modeling analysis in a semi-enclosed and with not far boundaries sea like the Marmara Sea was carried out. The study results were presented as spatial and temporal distributions.

The results show that in the Marmara Sea, the highest average wave power was found in offshore as 0.40 kW/m and the highest total wave energy value that can be obtained in 1 year is 3.47 MWh/m. When the coastal regions are examined, the south, north-north-west and west coasts have the highest average wave power with values of 0.34 kW/m, 0.30 kW/m and 0.28 kW/m, respectively. The long-term study for a period of 40 years also provides information in order to observe the effects of climate change.

The data obtained as a result of the study provides detailed information about the wave energy potential of Marmara Sea. The data presented in this study can be used in wave energy conversion systems applications and will contribute to renewable energy studies.

References

1. Ozhan, E., Abdalla, S.: Turkish Coast Wind and Deep-Water Wave Atlas, Applied Project Report. Middle East Technical University, Civil Engineering Department Ocean Engineering Research Center, Ankara, Turkey (1999).
2. Artüz, M.L.: Bilimsel Açıdan Marmara Denizi. Türkiye Barolar Birliği, Ankara (2007).
3. DHI, MIKE 21 Spectral Waves FM Module User Guide, Danish Hydraulic Institute (2008).
4. DHI, MIKE 21 Spectral Wave Module Scientific Documentation, Danish Hydraulic Institute (2008).
5. Yüksel, Y., Çevik E., Aydoğan, B., Arı, A., Saraçoğlu, K.E., Alpli, R., Bekar, B.: Türkiye Denizleri Dalga İklim Modeli ve Uzun Dönem Dalga İklim Analizi. 7. Kıyı Mühendisliği Sempozyumu, pp. 411-420. Trabzon, Türkiye (2011).
6. Saraçoğlu, K.E., Yüksel, Y., Aydoğan, B., Ayat Aydoğan, B.: Marmara Denizi Dalga Enerji Potansiyelinin Belirlenmesi. 8. Kıyı Mühendisliği Sempozyumu, pp. 825-839. İstanbul, Türkiye (2014).
7. DHI, MIKE 21 Spectral Waves FM Module User Guide, Danish Hydraulic Institute (2017).
8. DHI, MIKE 21 Spectral Wave Module Scientific Documentation, Danish Hydraulic Institute (2017).
9. Kutupoğlu, V.: Marmara Denizi'nde CFSR ve ERA Interim Rüzgarları ile Çalıştırılan SWAN Model Performansları ve Model Sonuçlarının Uzun Dönemli Farklılıkları. Yüksek Lisans Tezi, Uludağ Üniversitesi, Fen Bilimleri Enstitüsü, Bursa (2017).
10. Abdollahzadehmoradi, Y.: Dalga Enerjisi Potansiyelinin Makro ve Mikro Ölçekte Çıkarılması. Doktora Tezi, İstanbul Teknik Üniversitesi, Fen Bilimleri Enstitüsü, İstanbul (2018).
11. Akpınar, A., Kutupoğlu, V., Bingölbali, B., Çalışır, E.: Spatial characteristics of wind and wave parameters over the Sea of Marmara. Ocean Engineering 222, 108640 (2021).
12. Yuksel, Y., Yuksel, Z.T., Islek, F., Sahin, C., Ari Guner, H.A.: Spatiotemporal long-term trends of wind and wave climate and extreme characteristics over the Sea of Marmara. Ocean Engineering 228, 108946 (2021).

Energy Resilience in Turkey: A perspective and Application

Mustafa Yüksel Çınar[1,2] [0000-0001-7864-1201] and Suha Orçun Mert[3] [0000-0002-7721-1629]

[1] İskenderun Technical University, Energy Systems Eng., 31080, Iskenderun, TR
2 HCTEK Defense, 06120, Ankara, TR
[3] İskenderun Technical University, Petroleum and Natural Gas Eng., 31080, Iskenderun, TR
orcun.mert@iste.edu.tr

Abstract. Although resilience as a concept, it contains a deeper meaning in essence. It is used in many disciplines and many dimensions of resilience are discussed. In this study, Turkey's Energy resilience will be revealed in terms of renewable energy sources and a new and novel indicator is proposed that is Energy Resilience Index (ER_I). The ratio of sustaining the energy need of the urban areas -cities of Turkey are in the case in this study- from renewables (solar, wind, bio energies are considered in this study. Thus, if renewable resources vary due to seasonal, daily, global warming, etc. effects, to what extent our energy production dynamics will be affected, and survival opportunities will be revealed in the face of these changes is also revealed. The urge for sprawl in population and industry is seen from the results of the study with having 64% of the cities in Turkey has Energy Resilience of 1 to 3 whereas only 3.7% of the cities as level 7 of ER_I. Based on the current share of renewable energy variables as results of the integration challenges faced in Turkey the level of renewable dependency and resilience factor is at the second level in country-wide.

Keywords: Resilience, Renewable Energy, Solar Energy, Wind Energy

1 Introduction and Resilience

Various studies are carried out in countless areas related to solving potential problems foreseen as part of the future.

The concept of resilience first appeared in ecology-focused studies in the 1970s, specifically in the field of planning, as a response to the increase in the effects of climate change in urban areas. Resilience in this perspective can be defined as the ability to cope with all the hazardous situations that a city may encounter in the physical, environmental, social, and economic frameworks and whether a city has systems that will adapt and respond to these situations as rapidly as possible.

The concept of resilience is since then considered with regard to existing and future risks that are threats for many cities, and many policies are already being developed through scientific studies [1]. Socio-ecological systems have also been examined as part of such studies, revealing how the complexity caused by the mutual relationship between humans and nature is linked to the negativities experienced. In this context, both ecological systems and social systems were found to have important roles in determining the overall resilience of an urban location. The significance of sustainable designs and the current global discourse on climate change adaptation have also been taken into account in many studies [2,3].

Various basic practices and measures are discussed to integrate the idea of resilience into urban planning theory and practice [4]. Since resilience is emerging as a new focus of planning, application methods should be characterized and the differences in applying the concept compared to classical plans should be revealed. Achieving these objectives will help resilience methods further develop cities healthily.

Regarding energy security, the Asia Pacific Energy Research Center (APEAM) "energy security is the ability of an economy to ensure the availability of its energy supply is sustainable and timely at a level that does not adversely affect the performance of the economy." (Asia Pacific Energy Research Center (APEAM), 2007).

Only a few of these studies dealing with urban energy have discussed energy and resilience together. This is a rather limited study, although 60-80% of global energy is consumed in cities and urban areas are expected to remain the main location for global energy consumption in the future given the increasing rate of global urbanization. Increasing energy consumption in urban areas contributes to greater warming of the climate and can therefore be considered as the main driver of climate change. In turn, climate change and global warming can have negative effects on the energy sector by increasing energy demand and intensifying extreme events that threaten the security of generation, transmission and distribution infrastructure [5].

Disruptions in energy supply, which are a vital component of economic systems at different levels of economic activity, can have serious consequences and seriously harm the efficient functioning of the economy.

In this study, taking into account the utilization rates of renewable energy resources in the system, a critical level in terms of resilience has been determined. This study demonstrated the costs and benefits of technical options that can help increase the flexibility of the system and reduce the cost of wind and solar energy integration into the grid.

2 Renewable Energy in Turkey

The importance of the renewable energy has been in a increasing trend in Turkey as well as the counties in developed and developing world. With the increase in domes-

tic production opportunities in Turkey, the demand for renewable energy systems is increasing. The reduction in costs associated with this domestic production encourages investors and the State to invest in renewable energy systems.

Most renewable energy systems in the country are based on solar energy wind energy, but besides this, bioenergy, geothermal energy and other renewable energy systems have gained an increasing momentum.

Table 1 The renewable energy production and share for January 2021 [6]

Energy System	MWh	% share in total production
Wind	8.936,54	10
Geothermal	1.623,94	1,82
Biomass	1.061,57	1,19
Solar	445,85	0,5

Turkey's renewable energy capacity will grow by 49 percent by 2024. According to the report of the International Energy Agency, Turkey uses 3 percent of its potential in solar energy and 15 percent in wind [7].

3 Methodology and Case Study

The study is based on the potential of the renewable energies that are wind, solar and biogas in Turkey, as being the major branch of the renewables. The importance of the renewables and the concept of resilience are revealed with the analysis.

The analysis covers Turkey in cities basis that are 81 in number.

3.1 Methodology

The methodology of the study covers data collection, Resilience calculation main steps. The details of the method are given below;

- Data Collection
  - The electricity consumptions of cities are gathered [6]
  - The average Solar energy potential of cities are gathered [8]
  - The average wind energy potentials are gathered [9]
  - The total bioenergy potential of the cities are gathered [10]

- Resilience Calculation
  - Calculation of the renewable energy potentials
  - Calculation of the Resilience Value
  - Calculation of Resilience Index

3.2 Data Collection and Geographical Information System.

The visualization of the data regarding calculations are conducted with Microsoft Excel's Geographic Information System tool that is 3-B Map Tool. The values for

every city calculated separately and implemented in the tool regarding geographical presence.
The yearly electricity consumption of cities in Turkey is gathered from the recent data of Energy Market Regulatory Authority's report in January 2021 [6]. The report covers wide range of data regarding electricity usage in Turkey as well as production systems.

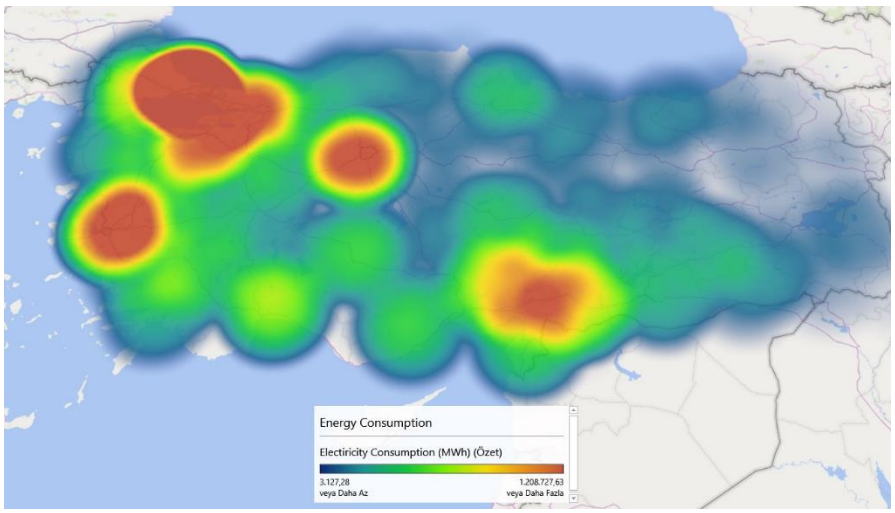

Figure 1 Energy Consumption (MWh) statistics for Turkey in cities bases.

Figure 2 Solar Energy Potential (MWh) statistics for cities in Turkey

Table 2. Energy Consumption and Renewable Energy Values of Cities

PostCode	Cities	Electiricity Consumption (MWh)	Solar Energy Potential (MWh)	Wind Energy Potential (MWh)	BioEnergy Potential (MWh)
1	Adana	612971	12787681	3236400	52721236
2	Adıyaman	105495	6930229	4309200	25246868
3	Afyonkarahisar	156228	11806195	3096000	88004763
4	Ağrı	39065	9681569	180000	53761039
5	Aksaray	65685	6975983	0	63365173
6	Amasya	53765	3802709	4320000	40417661
7	Ankara	1307822	19716150	288000	96568049
8	Antalya	612794	19999870	4212000	38399446
9	Ardahan	10580	3355436	32400	46544160
10	Artvin	35250	4425030	36000	10697305
11	Aydın	224333	7609768	9086400	99518981
12	Balıkesir	307958	11108594	49777200	121477966
13	Bartın	73856	1447131	223200	12649943
14	Batman	79239	4003434	28800	17538516
15	Bayburt	8681	2746973	0	15619363
16	Bilecik	187270	2860683	1112400	8945581
17	Bingöl	24787	6929300	219600	22890307
18	Bitlis	27733	7157324	144000	16008984
19	Bolu	94621	5670863	421200	27456579
20	Burdur	76362	6881026	208800	54483076
21	Bursa	1029908	7576442	13975200	52770767
22	Çanakkale	254969	7577988	46846800	51010323
23	Çankırı	46854	5430312	1134000	29096335
24	Çorum	72833	8856464	561600	49240112
25	Denizli	302557	11316705	860400	70992602
26	Diyarbakır	205478	11676172	2286000	95132347
27	Düzce	88148	1582185	0	10201297
28	Edirne	92654	4371975	12492000	35920803
29	Elazığ	101074	8430535	3700800	36066954
30	Erzincan	52816	9535237	1378800	23174588
31	Erzurum	71487	17444546	180000	127874792
32	Eskişehir	256808	10188254	320400	32067499
33	Gaziantep	727654	6410053	961200	54307973
34	Giresun	57057	4606960	576000	19093511
35	Gümüşhane	33025	4698940	3600	15794466
36	Hakkâri	28195	8014342	104400	6554838
37	Hatay	430688	5085827	12290400	33326005
38	Iğdır	18831	3376080	7200	28212799
39	Isparta	84128	8886205	5122800	30835850
40	Istanbul	3355375	5314875	15037200	19825314
41	İzmir	1337120	9377128	42674400	178827911
42	Kahramanmaraş	338741	12972331	7459200	43011063
43	Karabük	57640	2724059	262800	7600570
44	Karaman	49768	8663456	3362400	15405542
45	Kars	27045	7613078	144000	77841137

46	Kastamonu	97157	8531879	1854000	60098568
47	Kayseri	335361	15317448	6786000	68643715
48	Kırıkkale	47500	3704478	144000	12211489
49	Kırklareli	203051	4484597	11084400	0
50	Kırşehir	33748	5506323	604800	45872003
51	Kilis	47186	1323221	144000	2597937
52	Kocaeli	927008	2142635	482400	21063938
53	Konya	451556	38060885	6696000	207450562
54	Kütahya	153961	8871879	684000	42353905
55	Malatya	138537	11263390	5022000	33897356
56	Manisa	332937	11258756	19087200	50697092
57	Mardin	118402	8235517	1832400	19044328
58	Mersin	417810	15422126	12711600	23285160
59	Muğla	277146	12209794	18615600	59129574
60	Muş	33341	7393027	0	49800301
61	Nevşehir	50022	4778376	28800	19491503
62	Niğde	88868	6867381	223200	42220660
63	Ordu	110094	3456453	8193600	26724776
64	Osmaniye	374428	3050064	2584800	18036965
65	Rize	50853	2285639	0	4059800
66	Sakarya	339769	3053048	648000	32939524
67	Samsun	287522	6008475	18799200	64225688
68	Siirt	40482	5145454	54000	5639909
69	Sinop	33095	3564391	5367600	16542663
70	Sivas	113159	22983593	5911200	69208439
71	Şanlıurfa	279487	18512105	3600	53815453
72	Şırnak	53596	6742467	0	10020265
73	Tekirdağ	613105	4313467	16657200	36824569
74	Tokat	71808	7081586	10807200	55012569
75	Trabzon	113514	2750891	108000	23725010
76	Tunceli	11341	6503178	46800	5875007
77	Uşak	169168	4772671	205200	29948129
78	Van	99517	21220756	180000	29549090
79	Yalova	68635	519180	1918800	2673629
80	Yozgat	57709	10975005	3873600	50810106
81	Zonguldak	103593	2088710	432000	15904341

The Solar Energy potential of the cities in Turkey is given in Figure 2 in regarding a hybrid perspective. The values of this analysis is gathered from a report (GNS Solar 2021). Also the resulting map is compared with Ministry of Energies Solar Energy Atlas.

The values of the wind energy potential is taken from the report of [9]. The data is calculated for sustainable energy production with average wind conditions. The detailed results are given in Table 2.

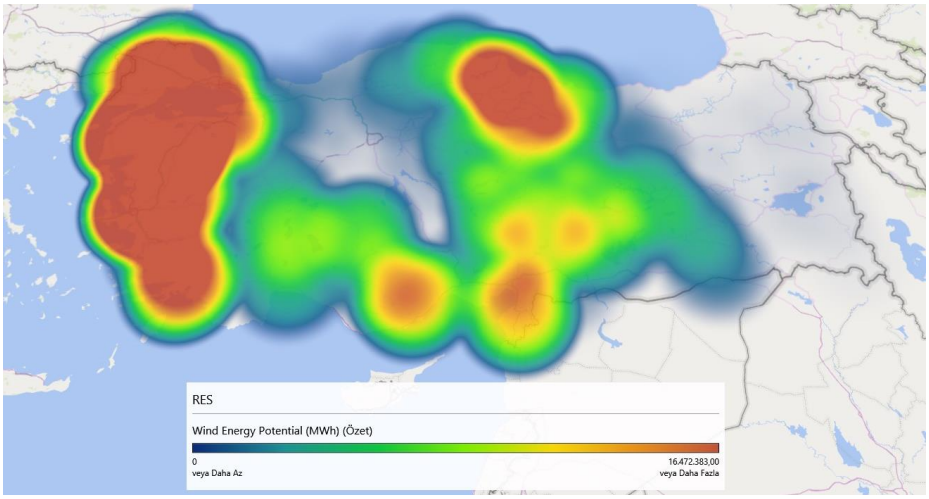

Figure 3 Wind Energy Potential (MWh) statistics for cities in Turkey

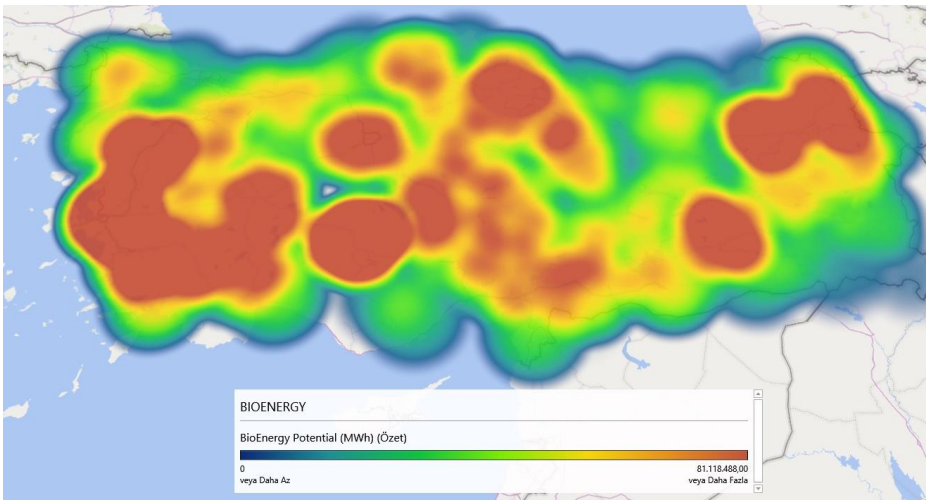

Figure 4 Bio-Energy Potential (MWh) statistics for cities in Turkey

3.3 Results and Resilience Index

Resilience values of the cities are calculated regarding the weighs of 40%,40% and 20% for individual coverage rates of each of renewable energy section that are solar, wind and bioenergy in percentage, respectively. The value represents the ratio of the potential of renewable energy for each individual city's consumption of electricity. Its an indication of freedom of electricity need from renewables point of view if all the potential can be turned into reality.

Resilience Index is the level of Energy resilience in a city. The levels (Table 3) are determined regarding the statistical values of the Resilience Values of the cities. The statistical data is given below for resilience values of the cities in Table 4

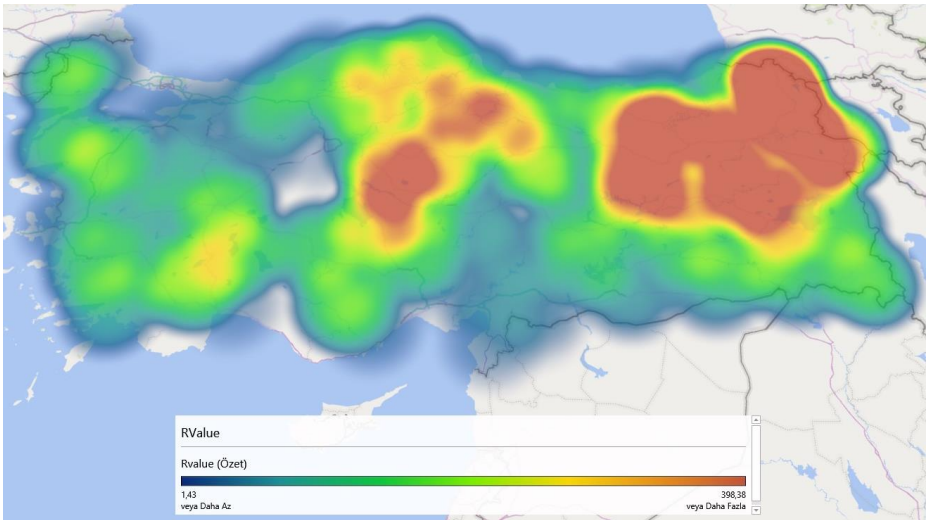

Figure 5 Calculated Resilience Values for cities in Turkey

Figure 5 gives us the change to investigate the Resilience through Turkey. Its seen that the north east parts of the country as much more higher values regarding the developed western parts. Also, there is a possibility in middle Anatolia.
This situation arises from the possible implementation of the biomass potential. These areas are the home of most of the livestock activities and when compared to the electricity consumption the amount of total renewable energy production is much higher than the other parts of the country. There for the resilience is much higher.

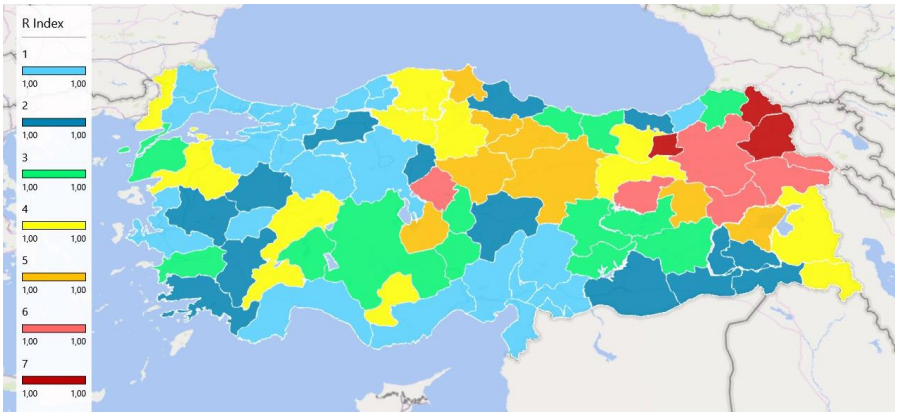

Figure 6 Calculated Energy Resilience Index for cities in Turkey (ER_I)

Such as Istanbul and Marmara region has minimum values of Energy Resilience. This depends on the low values of solar, wind and bioenergy potential as well as enormous

energy consumption. This region is not resilient at all. It depends on other parts of the country as from Energy side as most of other parameters such as food, agricultural needs, raw materials for most of the industry.

The Energy Resilience Index (ER_I) is the key result of the study. It's the indication of Resilience in a competitive manner with other cities in Turkey. It's a dynamic scaling and a unique and novel developed indicator for energy resilience. It's seen that there are 3 cities with high ER_I that is around 3.7% of the cities in Turkey. Where as majority of the cities are lies in the range of 1 to 3 ERI (Table 3).

Both from Figure 5 and Figure 6 it's seen that the potentials are high from renewable energy perspective but the reality is much different when the actual population density and energy consumption clumping is taken into account. The urge for sprawl in population and industry is seen from the figures also. A homogeneous distribution of industry and population through the country will increase the Energy Resilience as well as other positive effects.

Table 3 The limits and levels of Energy Resilience in Cities

Resilience Level	Lower Limit	Upper limit	# of Cities
1	0	50	25
2	51	90	14
3	91	140	13
4	141	200	12
5	201	330	8
6	331	480	6
7	481	1007	3

Table 4 The statistical data for Resilience Values.

Average	143,102117
High	1007,92584
Low	3,60791002
Stand. Dev.	158,535055

4 Conclusion

In this study, the utilization rates of renewable energy resources in the system, a critical level in terms of resilience has been determined. A novel and new indicator for this has been developed as Energy Resilience Index (ER_I).

Each cities electricity consumption and potential of renewable energy production is gathered and calculated and visualized in the GIS environment. Following the calculation of Energy Resilience values and ER_I. It's seen that the cities are mainly in the

lower three levels of energy resilience index and there is much more road to take in terms of Energy Resilience.

This study demonstrated the costs and benefits of technical options that can help increase the flexibility of the energy systems and reduce the cost of bio, wind and solar energy integration into the grid.

Also another important point is the urge for sprawl in population and industry is a need that is seen from the results of the study as must of the energy consumption and cities with low ER_I is gathered in western parts of the country. The distribution of these in country-wide will have a positive effect of Energy Resilience as well as various benefits.

Based on the current share of renewable energy variables as results of the integration challenges faced in Turkey the level of renewable dependency and resilience factor is at the second level in country-wide.

References

[1] S. Meerow, J.P. Newell, M. Stults, Defining urban resilience: A review, Landsc. Urban Plan. (2016). https://doi.org/10.1016/j.landurbplan.2015.11.011.

[2] S. Roostaie, N. Nawari, C.J. Kibert, Sustainability and resilience: A review of definitions, relationships, and their integration into a combined building assessment framework, Build. Environ. 154 (2019) 132–144. https://doi.org/10.1016/j.buildenv.2019.02.042.

[3] R. Emmanuel, E. Krüger, Urban heat island and its impact on climate change resilience in a shrinking city: The case of Glasgow, UK, Build. Environ. 53 (2012) 137–149. https://doi.org/10.1016/j.buildenv.2012.01.020.

[4] A. Sharifi, Resilient urban forms: A review of literature on streets and street networks, Build. Environ. 147 (2019) 171–187. https://doi.org/10.1016/j.buildenv.2018.09.040.

[5] B. Karabakan, GISP Yaklaşımı İle Van Edremit'in Dirençli Kent Olarak Değerlendirilmesi, Van Yuzuncu Yıl University, 2020.

[6] EPDK, Enerji Piyasası Ocak 2021 Sektör Raporu, 2021.

[7] International Renewable Energy Agency, World energy transitions outlook, 2021.

[8] GNS Solar, Türkiye Güneş Haritası, (2021). https://www.gnssolar.com/icerik/860/turkiye-gunes-haritasi.

[9] Enerji Atlası, Türkiye Rüzgar Enerjisi Potansiyeli Haritası, (2021). https://www.enerjiatlasi.com/ruzgar-enerjisi-haritasi/turkiye.

[10] TC Enerji ve Tabii Kaynaklar Bakanlığı, Türkiye Biyokütle Enerjisi Potansiyeli Haritası, (2021). Bepa.enerji.gov.tr.

Potential renewable energy resources of Istanbul and installation of a micro-grid system

Salah Masry[1], Natasha Qurban Ali[1], Füsun S. Tut Haklıdır[2]

[1]Electrical and Electronics Engineering, Istanbul Bilgi University, Istanbul, Turkey.
[2]Energy Systems Engineering, Istanbul Bilgi University, Istanbul, Turkey.

fusun.tut@bilgi.edu.tr

Abstract. There is a robust correlation between access to electricity and quality of life. Approximately 1.4 billion people around the world currently lack access to electricity. With momentous changes that the energy sector has been facing within the past decades, micro grids became a reality. A micro-grid concept expects a bunch of loads and smaller-scale sources, working as a solitary controllable system giving both power and warmth to its neighborhood. Micro grid can be used in decentralized mode providing full control for the energy of a specific area or as grid-connected mode to provide backup to the national grid.

Büyükada is the fourth largest and most populated island near Istanbul among the other islands and the energy is being supplied under the sea from the city. Related to this, it is possible to use micro grid systems on this island with the aim to apply renewable energy sources to Büyükada. Initial studies showed the potential of renewable sources on the island. Solar, wind, geothermal and biomass have been proved to have enough potential to handle the energy requirements.

The study aims to evolve renewable energy, design a Micro-grid and its control using a conventional control and machine learning for load forecasting for future works. Environmentalists are encouraging the integration of renewable energy due to global warming, increment in CO_2, green and sustainable energy. The micro-grid, provides one of the best solutions for powering islands such as Büyükada and extending the idea for the chain of micro-grids in the future.

Keywords: Micro-grid, solar, wind, green energy, Istanbul, Prince Island

1 Introduction

Problems of environmental protection, energy security, and economic development, mentioned as the "three E» (Environment, Energy, Economics), are interlinked global challenges of the current era. Nowadays, people are realizing that the challenges, which the energy sector is facing, are getting more serious. Power systems operation is becoming more labor-consuming, which will ultimately require more research for creating energy security, economic improvement, and efficiency, thereby creating the preconditions for a contemporary concept of "Smart Grid" (SG).

Sources of renewable energies delivered 16% of the overall demand for energy worldwide. Energy from biomass accounts for 10%, 3.4% accounts from hydroelectricity and 3% account for other renewable energy sources like hydro, modern biomass, solar, wind, biofuels, and geothermal. Sources of renewable energy that met the necessities of energy for domestic use have the potential in providing energy with almost zero emissions in terms of air pollutants as well as a greenhouse emission.

The solar photovoltaic (PV) technology and wind power systems are mainly widely used power generation systems around the world. PV adopted worldwide in order to satisfy the fundamental needs in terms of energy intended for rural areas, which not connected to the distribution network. Although using renewable energy sources increases year by year, there are some limitations of the system because of capacity factor effects. Batteries are used for storing the energy gained through the PV system. The operation characteristics of the PV module/array are investigated at a good range of operating conditions and physical parameters. In some places such as islands, using solar PV and wind turbine as hybrid energy systems will be beneficial with energy storage technologies.

In this study, using these technologies above in the Büyükada (Istanbul) are evaluated as micro-grid system.

2 Energy status of Turkey

Turkey is at the crossroads of Asia and Europe, with most of its territory located in South-western Asia and a small part in south-eastern Europe (Eastern Thrace).

Turkey's renewable energy potential is higher than fossil resources due to its perfect geographical position. Installed power capacity is around 97 GWe and it is noted around half of the capacity is based on the renewable energy sources as such hydro, wind, solar, geothermal and biomass by Turkish Ministry of Energy for April 2021. Technically evaluated potential is about half of this capacity. The installed hydropower capacity is around 31 GWe, while wind power generation is around 9 GWe and solar power generation is 7 GWe and installed geothermal power is 1.68 GWe in the country (EPİAŞ, 2021 March) [1]. The New Renewable Energy Support Mechanism

(YEKDEM) will also supports to new renewable energy investments till 2026 in Turkey (EMRA, 2021) [17].

Turkey has experienced impressive growth in renewables in the past decade (notably solar, wind and geothermal), driven by a favorable resource endowment, strong energy demand growth and supportive government policies. Turkey aims to continue to promote the expansion of renewable energy resources and will commission 10 GW each of solar and wind capacity in the period 2017-27 [2]. Reports claimed Turkey's effort to install new renewable energy power capacity to produce energy maximum possible from natural resources [9] [10]. Amid Covid-19 pandemic country's renewable energy investments reaches $7B in 2020 [11].

3 Micro-Grid Systems

Micro-grids provide efficient, low-cost, clean energy, enhance local resiliency, and improve the operation and stability of the regional electric grid. They provide dynamic responsiveness unprecedented for an energy resource [5].

Micro grid (MG) is a basic element and a key component of a shrewd grid and MGs are intended to boost energy efficiency, reliability of energy and power generation system and reduce CO2 emissions. A micro-grid is an aggregation of loads, through which, micro-sources operate like a stand-alone process generating both electricity and heat. Most of the micro sources must be electronically operated to form the vital flexibility and to assure operation like a stand-alone and fully integrated system. A MG is a connection between native distributed power loads and distributed energy sources including the micro turbine, wind turbine, photo-voltaic (PV), and storage devices in low-voltage (LV). With numerous micro sources connected through the distribution mechanism, some new issues like system stabilization, quality of generated power, and operational network, which need to be restrained by applying the developed control techniques on LV/MV.

3.1 A Brief Overview of Prince Islands (Adalar)

There are a total of 9 islands near the Anatolian part of Istanbul. 5 of them are operational for people to visit, live and explore. Büyükada is the largest of the Princes' Islands in the Sea of Marmara, near Istanbul, with an area of about 2 square miles (5 square kilometers). It is officially a neighborhood in the Adalar (Islands) district of Istanbul Province, Turkey. Total population of all the islands is around 16k. Currently energy is supplied from the Asian part to fulfill the energy requirements. Büyükada has an average sunshine duration of about 7.5 hours [8] and an average wind speed of 7.13m/s [7]. Both photovoltaic energy (PV Panels) and Wind Turbines are a good option for the energy production.

3.2 The Current power supply approach in Adalar

Büyükada as its name suggest being the largest one of all the islands receives electricity from the Anatolian Istanbul. The "ring topology" system with the cables lying directly on the ocean bed under the sea is responsible for all the electricity needs. 23 substations spread across 6 islands and 10 of them are installed on Büyükada. Total installed capacity of Adalar is 45.23 MWe with the peak load of about 20.30MWe (ref; AYEDAŞ, 2020). Fig. 1 demonstrates the idea of ring topology and the electricity distribution.

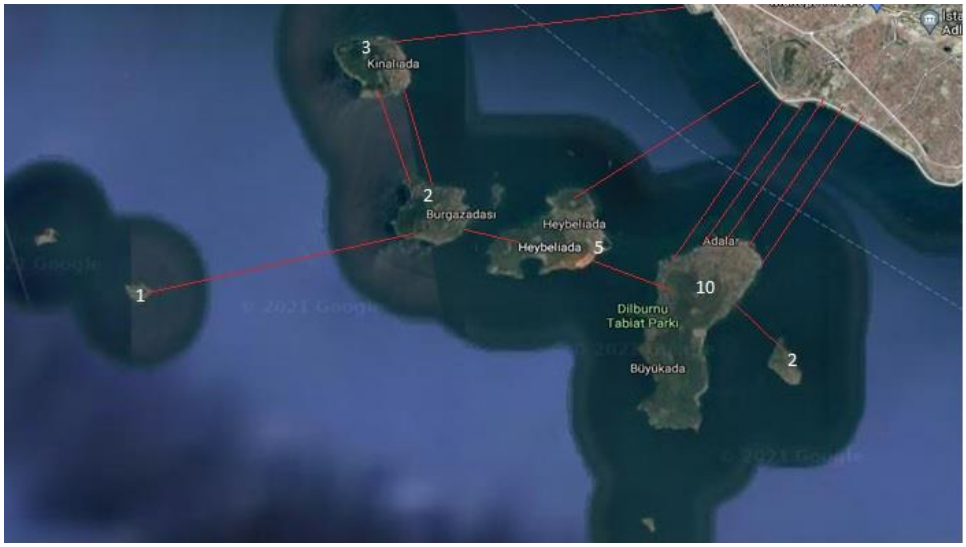

Fig. 1. No. of distribution station on the Islands (white) and ring topology network (red lines)

3.3 Concept of the study

Conventional energy resources provides most of our energy needs but they also pollute the environment and is one of the reason for climate change. For almost last two decades natural resource protection and restoration is vital. At current usage rate the oil reserve will run out in almost 50 years. We have natural gas for an almost of 70 years and coal has the life span of about 200 years more. Eventually we'll be out of our resources and the option left will be renewables [12].

Büyükada is a tourist and local favorite when it comes to explore the nature in a pleasant weather with a bicycle ride or horse ride. The island holds historical importance as well the current electric vehicles project made it a go to place. The idea of electric vehicles also supported in the favor of micro-grid with renewable energy resources. The best part about this installation will not only be clean energy to the

area but will also save a bunch of money that is currently being used on the infrastructure for providing the area with electricity under the sea from the Asian part of Istanbul.

The energy produced here will not only fulfill the local demand but the excess energy can be added to the national system in future studies to relieve the conventional energy load and working more and more with renewable energy.

3.4 Micro-grid system option for Büyükada

Out of many available softwares for designing a micro-grid, it is decided to use HOMER Pro as it has more subtle designing approach. HOMER provides a simulation model for all possible combinations for the equipment under consideration. Depending upon the variables HOMER can simulate hundreds even thousands of systems to get a best fit.in addition to that the simulation will be optimized, with sensitivity analysis [6]. Based on the data, HOMER proposed following results.

Fig. 2. Analysis based on input variables. (User can chose between "homer optimized results" or "overall possibility")

System Schematic and Architecture

As mentioned earlier HOMER software can simulate many results. It is up to the user to select from those the most suitable one. Considering all the factors we selected the following design. Schematic of system is shown in Fig. 3.

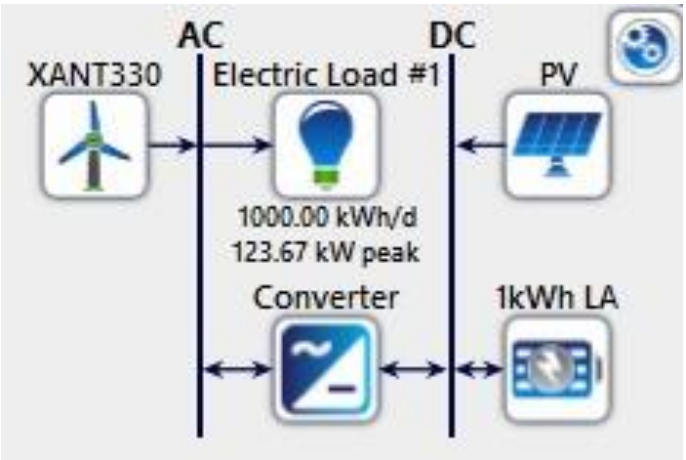

Fig. 3. The Micro-grid schematic using Homer Pro software

The suggested micro-grid is a hybrid micro-grid as it has both AC and DC bus bars. The advantage of such a system is the direct connectivity to the application. As it is known PV produces DC while wind turbine produces AC and the load also operates with AC so a hybrid system is capable of both operations simultaneously.

The huge amount of solar energy is available on the earth. Humans consume almost 15 TWe of solar energy [13]. Solar energy may sound easy to understand but is not easy to produce. There are many external factors that can affect the conversion of the Sun's energy to electrical energy. The uncertainty of solar irradiance affects the voltage profile and frequency response of the electric power system [14]. The effect of weather, movement of sun, position of panels all effects the efficiency of PV system. Fig. 4 shows the effect of natural conditions on solar panel output.

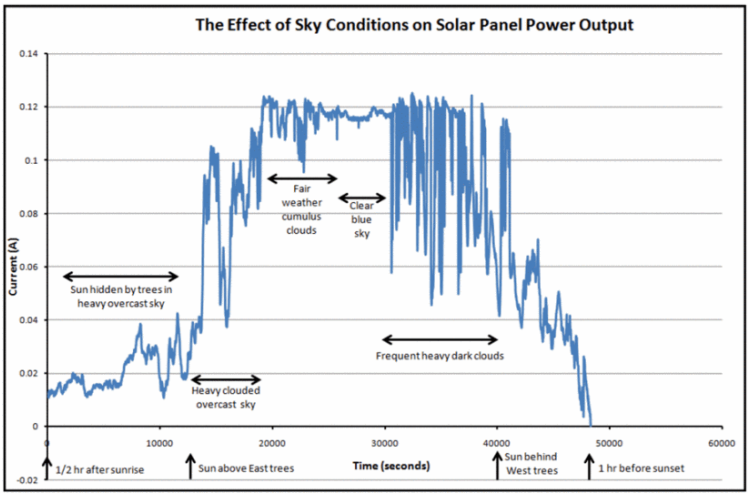

Fig. 4. Effect of sky conditions on solar panel [15].

Despite drawbacks solar energy is one of the widely used renewable resource because of its sustainability. The proposed system consists of a generic flat plate PV panel with max rating of 208 kW. PV panel has a uni-directional connection. The panel is connected to the DC bus bar and the produced energy is fed into the system. To overcome the natural pessimistic effects on PV output storage batteries are used. Battery has a bi-directional connection to the system. Battery system not only an optimal solution when it comes to solar as it can store the excess energy but also a wise back-up to use at night. Out of many options available like "Lithium ion batteries", "lead acid batteries", etc. it is opted for "lead acid battery" due to fair enough performance and easy availability and cost control over LiPo batteries.

The last connected component to DC bus is a converter (converting AC voltages to DC voltages) - inverter (DC voltages to AC voltages) box for the bi-directional conversion of energy. AC voltages from wind turbine are converted to DC for battery storage and later inverter can convert it back AC for utility use. The system is highly efficient to both ends but still results in loss of around 5818 kWh/yr.

Moving towards the AC bus bar which can be connected to a biomass, diesel or any other generator that produces AC. This bus bar can input the direct AC source (wind turbine) or the after the conversion of energy from DC to AC. In our case it is connected to wind turbine to fetch and inject the produced electricity into the system. 330kW wind turbine has a hub height of 50m and cut-in wind speed of 2.5m/s. The turbine can be installed onshore as the wind analysis of the island demonstrated the wind potential ranging between 4.81m/s to 8.26m/s [7].

Electrical load 1 represents all type of load. Since the island have both residential and commercial energy use so we considered our load to be community load.

3.5 Future work and Conclusion

Turkey joined the global effort for renewable energy production protecting the environment from carbon footprint. Increase in electric demand put the environment at great risk leaving green energy as the future of the planet. Renewable energy system may seem expensive and needs quite an investment to establish but its lifespan pays off.

Using micro-grid for Büyükada will not only make the island and its neighboring islands energy independent but will also pave a road for further studies in renewable sector. The island has made mode transportation smarter by the addition of electric vehicles [16] which can act as energy storage system for micro grid. The combined study will not only be an opportunity for the growth of renewables but will also provide better mode of transportation. The planned next frontier is to design the control and optimize the micro grid with short and medium term forecasting using machine learning. The idea is to create a hub of small micro grids for the neighboring islands as well and inject the excess energy into the national system, which not only will reduce the pressure of the conventional energy production but will also lead to economic stability in the country.

References:

1. https://www.epias.com.tr/#
2. https://www.iea.org/reports/turkey-2021
3. H. Gozde and M. Taplamacioglu, "Integration of renewable energy sources into turkey electric energy network general problems and solution proposals", *2018 5th International Conference on Electrical and Electronic Engineering (ICEEE)*, 2018. Available: 10.1109/iceee2.2018.8391348
4. S. Gok and R. Kavasoglu, "The renewable energy policy of Turkey", *4th International Conference on Power Engineering, Energy and Electrical Drives*, 2013. Available: 10.1109/powereng.2013.6635807
5. https://www.districtenergy.org/microgrids/about-microgrids97/features#:~:text=Microgrids%20provide%20efficient%2C%20low%2Dcost,unprecedented%20for%20an%20energy%20resource.
6. https://www.homerenergy.com/products/pro/index.html
7. https://globalwindatlas.info/
8. https://cati.ustasiyiz.org/istanbul/adalar/Büyükada/
9. https://balkangreenenergynews.com/renewables-make-up-99-6-of-new-power-capacity-in-turkey-this-year/
10. https://www.trtworld.com/turkey/turkey-aims-to-double-its-solar-energy-capacity-in-2021-compared-to-2020-43452
11. https://www.aa.com.tr/en/energy/renewable/turkeys-renewable-energy-investments-reach-7b-in-2020/31659
12. E. Irmak, M. Ayaz, S. Gok and A. Sahin, "A survey on public awareness towards renewable energy in Turkey", *2014 International Conference on Renewable Energy Research and Application (ICRERA)*, 2014. Available: 10.1109/icrera.2014.7016523.

13. N. Stodola and V. Modi, —"Penetration of solar power without storage," Energy Policy, vol. 37, no. 11, pp. 4730–4736, 2009.
14. E. M. Sandhu and D. T. Thakur, "Issues Challenges Causes Impacts and Utilization of Renewable Energy Sources-Grid Integration", *Int. J. of Engineering Research and Applications*, vol. 4, no. 3, pp. 636-643, 2014.
15. H. Gozde and M. Taplamacioglu, "Integration of renewable energy sources into turkey electric energy network general problems and solution proposals", *2018 5th International Conference on Electrical and Electronic Engineering (ICEEE)*, 2018. Available: 10.1109/iceee2.2018.8391348.
16. H. Gozde and M. Taplamacioglu, "Integration of renewable energy sources into turkey electric energy network general problems and solution proposals", *2018 5th International Conference on Electrical and Electronic Engineering (ICEEE)*, 2018. Available: 10.1109/iceee2.2018.8391348.
17. https://www.mondaq.com/turkey/oil-gas-electricity/1056798/turkey39s-energy-regulatory-authority-emra-announces-updated-fuel-ceiling-prices-applicable-in-turkey-from-9-april-2021

Evaluation of improvement studies of the use of green hydrogen production in industry – An economic perspective

Gizem Fırat [0000-0002-2279-5874], Ali Osman Fırat[2] [0000-0002-8498-0493], Ahmet Taşkesen [0000-0002-2479-1607], Ahmet Emre Şahin [0000-0002-6922-2344]

[1] Department of Industrial Design Engineering, Gazi University, Ankara 06560, Turkey
[2] Department of Aerospace Engineering, Middle East Technical University, Ankara 06800, Turkey
[3] Department of Industrial Design Engineering, Gazi University, Ankara 06560, Turkey
[4] Department of Mechanical Engineering, Kırıkkale University, Kırıkkale 71451, Turkey

Abstract. Technological developments are rapidly increasing the demand for energy.
Using of energy, which is vital from industry to transportation, consumes non-renewable energy sources. For this reason, the scientific world has turned to sustainable energy sources. The goal of decarbonizing our planet by 2050 has added importance to the production of green hydrogen. In this study, the economic effects of the use of green hydrogen in industry were examined. In the first part of the study, the costs of the production methods of hydrogen used in the industry and the costs of green hydrogen production methods were compared. In addition, the costs of green hydrogen production methods were compared among themselves. These differences have been analyzed. There are some studies designed to make green hydrogen production more economical. In the second part, the studies of cost improvements made in recent years have been emphasized. These studies include the impact of plant size on cost and their improvement. Another improvement study is green hydrogen production equipment. The power-to-gas system has been emphasized for improvements. This section continues with potential improvements in taxation, optimal designs for the plant. After the studies mentioned in the paper, green hydrogen costs can be reduced by up to 80% by 2050. As a result of the studies, it was inferenced that the use of green hydrogen in the industrial sector should be of a supportable project.

Keywords: Power to gas, Green hydrogen production, Economic analysis

1 Introduction

The need for energy is increasing day by day with increasing population and developing technology. Although mankind has changed the sources used for energy since the use of fire, energy use has remained the main phenomenon. Climate change caused by carbon dioxide emissions has huge and negative effects on living things. Especially during the covid-19 pandemic, the importance of carbon emissions was understood. Global efforts have begun to decarbonize our planet. With these studies, the World energy sector is focused on hydrogen energy. The fact that hydrogen does not create pollution, has many sources of raw materials, is used in many sectors, has a very high energy volume and has a higher efficiency compared to oil-derived energies has made hydrogen energy popular. Hydrogen production can be obtained from many energy sources. If the energy required for hydrogen production is provided from renewable sources, the hydrogen energy produced is green hydrogen. In these days when we go decarbonized, the hydrogen production methods already used are expected to be replaced by green hydrogen production methods. Hydrogen energy used in the industrial sector, which is responsible for a quarter of carbon emissions, should move to clean energy as soon as possible. Hydrogen energy, which is currently used in the industrial sector, is usually used in the production sector. The biggest obstacle to green hydrogen is its high cost. According to new research, the unit price of green hydrogen is 2-3 times the unit price of hydrogen produced from fossil sources used in industry (YEŞİL HİDROJEN RAPORU, 2020). This situation is a disadvantage for both manufacturers and customers and prevents the use of green hydrogen energy. When researchers consider carbon emissions data and the lifespan of fossil energy sources, they are focused on reducing the costs of green hydrogen energy. In addition to cost improvements in production, post-production transmission, logistics and storage also stand as an obstacle. Despite this, investment in green hydrogen energy is increasing with both researchers and government support. According to the new study, some major investments announced by the states are projected to strengthen the green hydrogen sector. Nikola Motor Company in the USA has supported the production of green hydrogen by ordering 85 megawatts of alkaline electrified. Air Products and ACWA Power said a facility planned to produce 237,000 tons of green hydrogen annually will be built in Saudi Arabia. NextEra Energy has announced it is closing its coal-fired plants for electricity generation then announced that it was investing in a green hydrogen plant in Florida. Another investment statement was announced Iberdrola and Fertiberia from Spain. According to this investment, they plan to install a hydrogen plant with 10MW PV, 20MWh lithium-ion battery and 20 MWh electrolyzer. The investment projects mentioned herein include only a few of the projects described. Especially countries that are producers and users of World hydrogen energy, such as China, plan to use hydrogen energy in every sector from passenger vehicles in the future. It makes investments in this direction. China plan to build 3,000 km of H_2 pipeline infrastructure to maintain hydrogen use. Currently in the industrial sector, hydrogen produced from fossil sources is used because it is highly efficient and the unit price is cheaper. The table below shows the costs of hydrogen production methods (Era of Hydrogen, 2020)

Table 1. Various Hydrogen production methods along with their advantages efficiency and cost (shiva kumar and himabindu,2019)

Hydrogen production method	Efficiency (%)	Cost($/kg]
Steam reforming	74-85	2.27
Partial oxidation	60-75	1.48
Auto thermal reforming	60-75	1.48
Bio photolysis	10-11	2.13
Photo fermentation	0.1	2.83
Dark fermentation	60-80	2.57
Gasification	30-40	1.77-2.05
Pyrolysis	35-50	1.59-1.70
Thermolysis	20-45	7.98-8.40
Photolysis	0 .06	8-10
Electrolysis	60-80	10.30

Steam reformation is the most advantageous method when unit price and efficiency are evaluated. The most common method currently used in the industrial sector is steam reformation. However, as a result of this process, high carbon emissions are released. There are two main headings on which the cost of green hydrogen is based. These are the cost of production and the cost of logistics. There are some steps that are foreseen that will be useful to implement to reduce these costs. Especially for the industrial sector, which is the main theme of this study, it is necessary to adapt industrial policy to green hydrogen. In the next parts of our study, the studies to reduce production and logistics costs will be examined. Then there is a new cost data generated as a result of these improvement studies.

2 Production Improvement Studies

The most popular form of green hydrogen production is the electrolysis of water. It is mainly based on the acquisition of hydrogen by separating water into ions using electrical energy. The electrical energy used during this process is also expected to be obtained from clean sources. Unit electricity prices and electrolysis equipment prices are two main cost situations. Some of the energy around the world is sourced from renewable energy sources. Especially developed countries make more careful choices about clean energy. According to the ROSATOM NEWSLETTER report, major investments have been made in renewable energy facilities by 2018. Especially countries that adopt decarbonization as a principle, such as Germany, have made huge investments for the continuity of renewable energy facilities. However, after 2018, these investments were stopped and the country turned to hydrogen energy. There are some reasons behind stopping investments. The current installed renewable energy capacity is 25% higher than the demand for stationary electricity. Studies on this

show that. As of July 3, 2020, total installed renewable capacity in Germany was 125.76GW (Gigawatt), while total consumption was usually 40GW, rising to 80-100GW during peak hours, according to the Energycharts.de. Another reason is that renewable energy production is unstable. Because electricity generation depends on the state of natural condition. There are also difficulties in finding suitable land for facilities established near natural resources. Renewable energy plants should be placed according to suitable of the natural resources so renewable energy in electricity from may be expensive to distribute all over the country, converting electric energy produced from renewable resources to the hydrogen is more efficient in such situations. These reasons supported the idea of switching from existing systems to a different system instead of generating electrical energy.

In research from Jovan and Dolanc (2020), they discussed a river hydroelectric power plant in Slovenia with 3 vertical units (an average of 16MW per unit). According to the data obtained from this facility, the plant provides only 160GWh of its full capacity of 45MW annual production capacity. This data shows that the plant is not operating highly efficiently. The study developed as a solution to this situation is to use this electrical energy to produce hydrogen energy and sell hydrogen instead of selling the electricity produced from the plant. Approximate price of hydrogen is 6.00 €/kg and approximate price of 1MWh electric energy can be bought from HPP is 5 €. HPP is able to convert 1MWh of electric energy to 20 kg hydrogen which can be sold 120.00 €. Costs of CapEx and OpEx equipment are approximately 27.20 € for 20 kg hydrogen. When 50.00 € is added to this cost, 77.20 € is the total cost of producing 20 kg
hydrogen from 1MWh electric energy. When the price of 20 kg hydrogen is considered, 42.80 € is profit also additional profit may be achieved if hydrogen is produced surplus of electric energy whose price is 0 €/MWh. Also producing hydrogen from surplus of electric energy may be the best way deal with waste of electric energy. Such use is based on the production of hydrogen from electrolysis, known as a power-to-gas system.
According to new research, in the Western Inner Mongolia region, a new electrolysis hydrogen production optimization has been developed in the study. With this optimization, green hydrogen energy prices have become open to competition with hydrogen energy obtained from fossil sources. The purpose of the optimization is defined to minimize overall system cost under the constraint of a specific production quota or to maximize hydrogen output subject to a defined leveled hydrogen cost restriction. This new system, which undergoes optimization with the P2H system, provides green hydrogen production at a cost of $1.52/ kg- 2 $ / kg using wind energy over the grid in cases where the wind supply is insufficient (Lin et al., 2021).

According to Irena's 2020 untitled report, there are possible costs associated with electrolysis. Costs are projected to be reduced by 40% to 80% in the short and long term. There are 4 commercial variants of electrolysis. These commercial electrolysis systems are Alkaline, Proton Exchange Membrane, Anion Exchange Membrane and

Solid Oxide. Cost reduction studies are carried out for each system by adhering to its own technology. According to the results of the report, Irena has major cost studies. These include replacing thick membranes and diaphragms, replacing coatings consisting of expensive materials, redesigning the electrode system, designing new concepts for new PTL, increasing operational limits. The cost table, which is expected to the take place in 2050 with these studies, is given below. The cost and efficiency of four different electrolysis systems after the improvement studies were examined. The stack capital cost of PEM, Alkaline and AEM electrolysis system is smaller than USD 100/kW and system capital cost is USD 200/kW. Solide oxide stack capital cost is smaller than USD 200/kW and system capital cost is smaller than USD 300/kW.

Table 2. Target cost reduce of PEM

PEM	2020	2050
Electrical efficiency (stack)	47-66 kWh/Kg H_2	< 42 kWh/Kg H_2
Electrical efficiency (system)	50-83 kWh/Kg H_2	< 45 kWh/Kg H_2
Lifetime (stack)	50 000-80 000 hours	100 000-120 000 hours
Stack unit size	1 MW	10 MW
Capital costs (stack) minimum 1 MW	USD 400/kW	< USD 100/kW
Capital Costs (system) minimum 10 MW	700-1400 USD/kW	< 200 USD/kW

Table 3. Target cost reduce of Alkaline

ALKALINE	2020	2050
Electrical efficiency (stack)	47-66 kWh/Kg H_2	< 42 kWh/Kg H_2
Electrical efficiency (system)	50-78 kWh/Kg H_2	< 45 kWh/Kg H_2
Lifetime (stack)	60 000 hours	100 000 hours
Stack unit size	1 MW	10 MW
Capital costs (stack) minimum 1 MW	USD 270/kW	< USD 100/kW
Capital Costs (system) minimum 10 MW	USD 500-1 000/kW	< USD 200/kW

Table 4. Target cost reduce of AEM

AEM	2020	2050
Electrical efficiency (stack)	51.5-66 kWh/Kg H_2	< 42 kWh/Kg H_2
Electrical efficiency (system)	57-69 kWh/Kg H_2	< 45 kWh/Kg H_2
Lifetime (stack)	> 5 000 hours	100 000 hours
Stack unit size	2.5 kW	2 MW
Capital costs (stack) minimum 1 MW	Unknown	< USD 100/kW
Capital Costs (system) minimum 10 MW	Unknown	< USD 200/kW

Table 5. Target cost reduce of Solid Oxide

SOLID OXIDE	2020	2050
Electrical efficiency (stack)	35-50 kWh/Kg H_2	< 35 kWh/Kg H_2
Electrical efficiency (system)	40-50 kWh/Kg H_2	< 40 kWh/Kg H_2
Lifetime (stack)	< 20 000 hours	80 000 hours
Stack unit size	5 kW	200 kW
Capital costs (stack) minimum 1 MW	> USD 2 000/kW	< USD 200/kW
Capital Costs (system) minimum 10 MW	Unknown	< USD 300/kW

Another factor affecting costs during the production phase is plant size. Minutillo et al. (2021) showed that, a 20% Levelized cost of hydrogen reduction compared to the smallest (50 kg / day) of the plant with the highest hydrogen production capacity (200 kg / day). In their studies, they compared their costs using high, medium and low grid energy management. The results are given in the following table.

Table 6. Costs for High Grid energy management strategy

Electricity Mix: High Grid	Micro	Small	Medium
CAPEX (k€)			
PV modules	226.10	450.30	903.45
electrolyzer	129.80	259.60	520.30
compressor	233.88	393.07	671.25
refrigerator	91.35	182.72	182.72
Dispenser	65.00	130.00	130.00
Water system (pumping, purification)	1.00	1.99	3.99
TOTAL CAPEX (k€)	747.13	1417.68	2411.72
OPEX (k€)			
PV modules	3.57	7.11	14.27
electrolyzer	2.59	5.19	10.41
compressor	18.71	31.44	53.70
refrigerator	2.74	5.48	5.48
Dispenser	1.95	3.90	3.90
Water system (pumping, purification)	0.02	0.04	0.08
Annual water purchase	0.22	0.43	0.84
Annual electricity purchase	110.11	202.38	372.03
TOTAL OPEX (k€/year)	139.91	255.97	460.71
REPLEX (k€)			
PV modules	-	-	-
electrolyzer	52.51	105.02	210.49
compressor	233.88	393.07	671.25
refrigerator	91.35	182.72	182.72
Dispenser	65.00	130.00	130.00
Water system (pumping, purification)	1.00	1.99	3.99
TOTAL REPLEX (k€/year)	443.74	812.80	1198.45

Table 7. Costs for Low Grid energy management strategy

Electricity Mix: Low Grid	Micro	Small	Medium
CAPEX (k€)			
PV modules	678.30	1350.90	2711.30
electrolyzer	129.80	259.60	520.30
compressor	233.88	393.07	671.25
refrigerator	91.35	182.72	182.72
Dispenser	65.00	130.00	130.00
Water system (pumping, purification)	1.00	1.99	3.99
TOTAL CAPEX (k€)	1199.33	2318.28	4219.57
OPEX (k€)			
PV modules	10.71	21.34	42.84
electrolyzer	2.59	5.19	10.41
compressor	18.71	31.44	53.70
refrigerator	2.74	5.48	5.48
Dispenser	1.95	3.90	3.90
Water system (pumping, purification)	0.02	0.04	0.08
Annual water purchase	0.22	0.43	0.84
Annual electricity purchase	93.19	170.97	314.47
TOTAL OPEX (k€/year)	130.13	238.79	431.72
REPLEX (k€)			
PV modules	-	-	-
electrolyzer	52.51	105.02	210.49
compressor	233.88	393.07	671.25
refrigerator	91.35	182.72	182.72
Dispenser	65.00	130.00	130.00
Water system (pumping, purification)	1.00	1.99	3.99
TOTAL REPLEX (k€/year)	443.74	812.80	1198.45

3 Logistic

Green hydrogen can be produced in, large-scaled facilities. Since facilities produce energy from wind, sun, hydro and geothermal, location of the facilities is determined according to these criteria. Therefore, either hydrogen is produced at local facilities by transporting the electric energy produced by renewable sources or hydrogen is produced at the large-scaled facility and transported to the customers. Transporting the electricity is requires external investment which is not preferred most of the time. Transporting the hydrogen is more cost-effective way for logistic. There are two ways

to transport the green hydrogen. First way is setting network between hydrogen producer to customers and the second way is using transportation trucks. In research from Demir and Dincer (2018) for large power plants pipeline network is the most effective way to transport hydrogen, however, for small power plants H_2 delivery with tube trailers is the most suitable and cost-effective way to transport hydrogen. Pipeline transportation seems very suitable way to do since it is both practical and cost-effective. However according to the study from Kramer et al. (2006) stated that pipeline transportation does not provide coverage during early stages of hydrogen flow. Since pipeline transportation is not suitable, the most effective way is truck transportation. Truck transportation can be done by two ways. High-pressure gaseous truck transport and cryogenic liquid truck transport. Mostly, cryogenic liquid transportation is used in the gas market. Abe et al (1998), stated, using cryogenic liquid transportation for hydrogen is also useful for transportation overseas since easily loaded to the ships.

4 Taxes

Taxes are very important in trade world. In any action in trade, there are taxes. Amount of tax is very important to improve a specific area. For example, if taxes of corn are decreased while other foods remain unchanged, production and price of the corn would decrease. Similarly, if governments decrease the taxes of green hydrogen against while keeping carbon tax unchanged or increased, green hydrogen would become more common. In their study, Bruvoll and Larsen (2004) stated that, carbon taxes incentive to grow up renewable energy sector in Norway. If the renewable energies have lower taxation, they become more common in near future. In research from Cerniauskas et al. (2019) for comparable effective carbon taxing in Germany, hydrogen usage may be more common due to the costly competitive with traditional fossil fuels by half of the 2020s.

5 Conclusion

Due to the climate change, governments target to decarbonization until 2050. In this study, academic studies and reports have been examined. Cost of the green hydrogen production now and in the future are shown. According to the studies, up to %40 - % 80 reduction of cost is possible until 2050. These reductions have been explained into two parts; production and after production stages. In production improvements are depends on more efficient energy converting and better design of electrolyze systems. Also, improvements and the competition on the logistic sector will decrease the cost of logistic. Supporting green energy policies by states can play a major role in reducing green hydrogen costs and promoting its use. Especially in the industrial sector, which has the largest share of carbon emissions, the incentive to green hydrogen can be increased with the regulation of carbon emission taxes.

References

1. YEŞİL HİDROJEN RAPORU. (2020). WORLD ENERGY CONCUIL
2. Era of Hydrogen. ROSATOM NEWSLETTER. (2020, July). https://rosatomnewsletter.com/2020/07/25/era-of-hydrogen/.
3. Jovan, D. J., & Dolanc, G. (2020). Can Green Hydrogen Production Be Economically Viable under Current Market Conditions. Energies, 13(24), 6599. https://doi.org/10.3390/en13246599
4. Lin, H., Wu, Q., Chen, X., Yang, X., Guo, X., Lv, J., Lu, T., Song, S., & McElroy, M. (2021). Economic and technological feasibility of using power-to-hydrogen technology under higher wind penetration in China. Renewable Energy, 173, 569–580. https://doi.org/10.1016/j.renene.2021.04.015
5. GREEN HYDROGEN COST REDUCTION. (2020). IRENA.
6. Minutillo, M., Perna, A., Forcina, A., Di Micco, S., & Jannelli, E. (2021). Analyzing the levelized cost of hydrogen in refueling stations with on-site hydrogen production via water electrolysis in the Italian scenario. International Journal of Hydrogen Energy, 46(26), 13667–13677. https://doi.org/10.1016/j.ijhydene.2020.11.110
7. Demir, M. E., & Dincer, I. (2018b). Cost assessment and evaluation of various hydrogen delivery scenarios. International Journal of Hydrogen Energy, 43(22), 10420–10430. https://doi.org/10.1016/j.ijhydene.2017.08.002
8. Kramer, G. J., Austgen, D., & Huijsmans, J. (2006). WHEC 16. In Clean and Green Hydrogen. Lyon
9. ABE, A. (1998). Studies of the large-scale sea transportation of liquid hydrogen. International Journal of Hydrogen Energy, 23(2), 115–121. https://doi.org/10.1016/s0360-3199(97)00032-3
10. Bruvoll, A., & Larsen, B. M. (2004). Greenhouse gas emissions in Norway: do carbon taxes work? Energy Policy, 32(4), 493–505. https://doi.org/10.1016/s0301-4215(03)00151-4
11. Cerniauskas, S., Grube, T., Praktiknjo, A., Stolten, D., & Robinius, M. (2019). Future Hydrogen Markets for Transportation and Industry: The Impact of CO2 Taxes. Energies, 12(24), 4707. https://doi.org/10.3390/en12244707

Renewable Energy Impact on Damascus City Transportation Sector

Moaz Bilto[1], Doğancan Beşikçi[2], Tanay Sıdkı Uyar[3]

[1] Faculty of Engineering/ Mechanical/ Beykent University
[2] Faculty of Engineering/ Mechanical/ Marmara University
[3] Faculty of Engineering/ Beykent University

Beykent University faculty of engineering and architecture
Ayazağa, Hadım Koruyolu Cd. No:19, 34398 Sarıyer/İstanbul

mtbilto@gmail.com

Abstract. The city of Damascus ranks first among the Syrian governorates in terms of population inflation and random urban expansion, which lead to the air being saturated with polluting components that are higher than the standard of the World Health Organization and causes several health issues.

Several urban activity sections in Damascus contribute towards carbon emission, such as land use deforestation, agriculture, transportation, and power generation.

This paper seeks to provide an accurate calculation of power production, consumption, and greenhouse gases (GHG) emissions of the city of Damascus. This will provide a clear path for future research aiming towards improving the air quality of the city and enabling a smooth transition to renewables.

This research aims to analyze the energy situation is Damascus, and energy efficiency potential; focusing on the transportation sector and its effect because it accounts to almost 20% of Emission that the city produces.

We used the following method Integrated MARKAL-EFOM System (TIMES) to obtain city power demand over the next decade, which helped us to gather a detailed calculation of the city's residential and industrial Power usage, supply, and demand.

Result shows that Damascus city is almost completely dependent on traditional fuel sources to fuel the thermal and gas power plants that are supplying the city, with little to zero renewables sources, by looking at the situation now the best short-term solution is to work on improving the transportation sector by Integration of fuel cells, using hydrogen as a fuel source and many other green solutions.

Keywords: Fuel cells**,** Damascus, Greenhouse gases (GHG)

1 Introduction

There is no doubt the electric power sector, in all countries, contributes significantly to one's country's development, improving citizens lives, and raising welfare levels on a society standard. The energy sector as connected network work by converting conventional sources of energy such sources such as fossil fuels (Oil, natural gas) into electric power simply by burning them, such process results in many emissions mostly gases that are harmful to both our health and the environment.

As a Mediterranean country, Syria benefits from a vast, unlimited source of solar energy with good amounts of wind energy, which can be put into use for many applications. However, the adaptation of renewable energy resources by the public and private/governmental organization are still very modest. This is because of very simple reasons; availability and cheap prices of the conventional energy resources such as (petroleum and gas) which are subsidized by the government, high initial installation and manufacturing prices of any renewable system, and the availability of information is still not commonly known to people, the future energy and electricity supply and demand is going to expand rapidly in future because of many driving factors affecting its demand, such as increased population rate and many other.

this paper concentrates on analyzing Syria's future demands of energy focusing on Damascus transportation sector using the TIMES model. This type of research requires a lot of statistical data, we gathered our information from different governmental institutions, which are (CBS) Central Bureau for Statistic, (GPC) Governmental Planning Commission, (MOMR) Ministry of Oil and Minerals Resources and Ministry of Electricity, this sector plays a huge role in boosting the economic activities.

We also emphasized the use of modelling tools specifically (TIMES) model, that will be implemented for modelling the Damascus Syrian energy system, when implemented correctly it will aid in developing a stand-alone model for Damascus city, aiming to evaluate the assumptions and results concluded from this research, so the contributions of this article can be summarized as:

Introducing an understandable view (to the highest degree possible of accuracy) of Damascus current and future supply and demand regarding accurate number of electric power generation stations supplying the city, available capacity, and annual electricity generated and consumed regarding industrial and residential end-demands and introducing a renewable source to supply a hydrogen power plant, while focusing on the transportation sector and providing a path to integrate renewables such as Fuel-Cells, since most of the city emissions are caused by the transportation sector.

Chapter 2 Describes and analyzes the estimated available energy and energy statistics.

Chapter 3 Discusses Method used

Chapter 4 Overviews the transportation sector

Chapter 5 The energy transition

Chapter 6 Integrating fuel cells applications

2 Analyzing available data.

The energy sector is dominated mainly by fossil fuels, aside of renewable sources. Over the recent years, the Syrian Arab Republic's energy supply was using its own produced gas and oil. However, domestic oil production have declined during the time period 1996–2005 from about 600 000 to 400 000 barrels/day and almost altered at 200 000 barrels/day by mid-2015 [1], This situation has been surging because of the increase in consumption due to many factors like population growth, economic changes and the technological development achieved in all different consumption sectors which showed increased automation in industry, increased mobility and the vast penetration of electric equipment into household and service sector not to mention the little no change in the transportation sector not to mention that gas and oil production decreased in the last years due to damaged infrastructure and sanctions implemented on the country.

The Syrian fossil energy resources consists of mainly only sources which are Natural gas (NG) and Oil. The statistics on geological oil stocks are approximated to be around 24 billion barrel of oil equivalent (Bboe), on the other hand the statistics of natural gas (NG) is around 612 billion cubic meters (Bm^3), of which 371 Bm^3 are usable. [1]

The conflict going on imposed allot of damage to most of the internal energy infrastructure like such as leakages and destroyed parts of the network not forgetting the sanctions imposed on the country, yet we can still consider Syria a self-sufficient country regarding energy production, for example, in 2015 there was a total of 18 580 Mtoe ready to be transmitted and pumped into the network.

Before we focus on Damascus city, we will overview the system as a whole: [2]

- Oil fulfilled more than 50% of the total supply while hydro and gas represented 11% or 38% respectively.
- Hydropower contributes significantly to electricity generation in Syria. there are three large hydroelectric power stations on the Euphrates River under the control of the Ministry of irrigation. the installations are designed primarily for irrigation but produce important volumes of power, the installed capacity these plants are 1.5 GW.
- The wind potential is strong in places; annual mean daily wind speed in some regions of Damascus countryside (Golan heights) reaches 8 m/sec.
- The solar regime is good and extensive; the annual average long-term solar radiation on a horizontal plane is around 5 kWh/m2/day or 18 MWh/m2/Year. [3]
- Total Syrian power production cumulated to 37,283 GWh. In 2018
- Damascus electricity consumption in 2018 reaches a peak of 7446 GWh

The following tables show final energy consumption and energy balance across the network According to Ministry of electricity (MOE) [4],

2.1 Energy distribution, sources, and indicators

Table 1. Energy distribution for The Syrian Arab Republic 2015

	1990	2000	2010	2015	Year *	Average annual growth rate approx. (%)
Energy consumption**						
- Total	0.3	0.8	1.9	2.5		8.0%
- Solids						
- Liquids	0.26	0.45	0.67	0.88		6.5%
- Gases	0.04	0.31	0.32	0.55		14.9%
- Nuclear	-	-	-	-		-
- Hydro	0.02	0.02	0.04	0.04		4.7%
- Other Renewables	0.01	0.01	0.02	0.02		4.7%
Energy production						
- Total	0.93	1.5	1.15	1.32		1.4%
- Solids	-	-	-	-		
- Liquids	0.87	1.2	0.79	0.76		-0.6%
- Gases	0.04	0.3	0.3	0.5		14.4%
- Nuclear	-	-	-	-		
- Hydro	0.02	0.02	0.04	0.04		4.7%
- Other Renewables	0.01	0.01	0.02	0.02		4.7%
- Total	-0.6	-0.7	-0.11	-0.16		-10.7%

Table 2. Syrian energy sources and indicators

Energy production (Mtoe)	4.68	Electricity consumption (TWh)	15.01
Electricity-consumption/population (MWh/capita)	0.81	Net imports (Mtoe)	5.49
TPES/GDP (toe/thousand 2010 USD	0.59	TPES/GDP PPP (toe/thousand 2010 USD)	0.27
TPES (Mtoe)	9.98	TPES/population (toe/capita)	0.54
Carbon/population (t CO_2/capita)	1.42	Carbon/GDP-PPP (kg CO_2/2010 USD)	0.70
CO_2 emissions (Mt of CO_2)	26.24	CO_2/TPES (t CO_2/toe)	2.63

1.

Source: Syrian Arab republic 2015 report pub-IAEA**.**

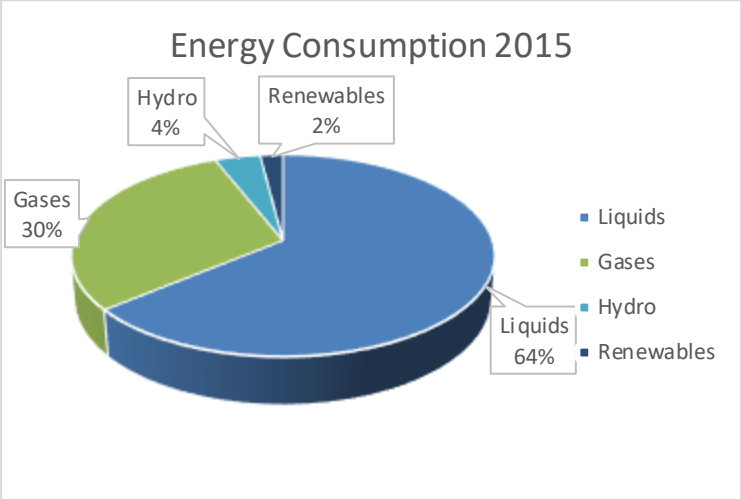

Fig. 1. shows Energy consumption

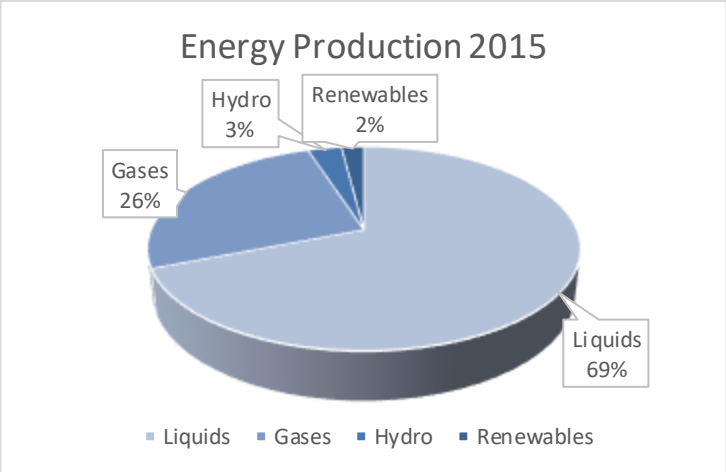

Fig. 2. Energy production

Here we can see that most of the consumption and production is dependent on liquids (Oil) and gas with little renewables integrated into the network.

Stations and power plants supplying the city.

Table 3. Shows the Thermal Power Plants Supplying the City In 2018.

Thermal Power plant	Generation Capacity (MW)	Total Production (GWh)	Self-consumption (GWh)	Net Production (GWh)	NCAP_FOM Mil$/Pj
Tishreen	320	1084.8	97.8	987.06	4.48
AL-ZARA	500	3103.8	232.19	2871.69	7
JANDAR	420	2728.8	88.2	2639.6	5.88
Total	-	-	-	6498.35	17.36

Table 4. Shows the Combined Gas Cycle Stations (Cgcp) Supplying the City In 2018.

CGCP Power plant	Generation Capacity (MW)	Total Production (GWh)	Self-consumption (GWh)	Net Production (GWh)	NCAP_FOM Mil$/Pj
NASIRIYAH	300	2413.5	56.7	2356.8	4.2
DER-ALI	705	2653	71.4	2581.6	9.87
Total	-	-	-	4938.4	14.07

We can observe that until now, Damascus did not make use of the available potential regarding renewable energy. For example, the yearly average Photovoltaic radiation is around 1800kWh/m^2 and the land surface areas 185 000km^2. This shows that the total available solar power is about 1500 times the total energy consumption in 2015, main reason of not making use of this free energy is the lack of infrastructure.

by the year 2030, the city demand for energy is estimated to sky rock to 1500MW/year. the available conventional energy is predicted to remain constant, therefore, it is imperative that energy consumption is reduced, rather than increasing energy generation, Simply to Reduce Emission levels not to mention that extra added need of about 80 MW of new generation capacity, while most of the powerplants listed above have almost max generation capacity installed.

Electricity consumption through all sectors and growth rate of the city

Table 5. Shows the city electricity consumption in 2018.

City	Residential (Mw)	Commercial (MW)	Industrial (MW)	Agricultural (MW)	City Services (MW)	Grand Total (MW)	Growth Rate (%)
Damascus	2382720	1787040	1935960	148920	1191360	7446000	5.70
Unit	-	-	-	-	-	-	-
Peta joules (Pj)	8.58	6.43	6.97	0.54	4.29	26.81	-

Table 6. Shows the growth rate as of 2018 until 2033.

Growth by year	Unit in Petajoules (Pj)
2018	26.81
2023	34.46
2028	42.71
2033	50.66

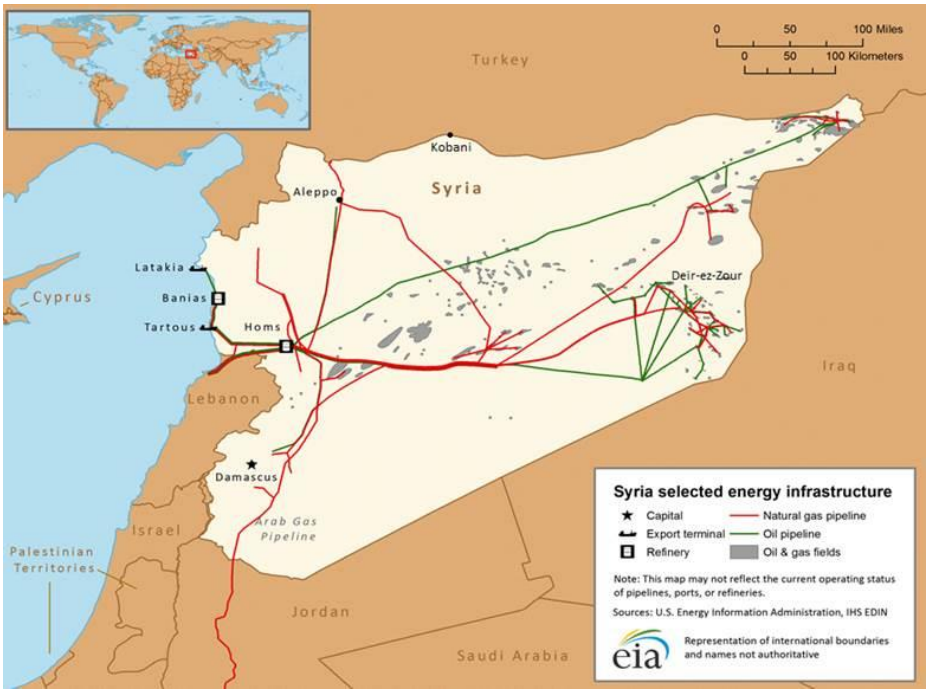

Fig. 3. Shows General infrastructure and the lies supplying the city

Source: U.S. Energy Information Administration, Oil & Gas Journal

Supply and Demand

Total generation of electricity in Syria was about 7,500 MW in 2011, of which 6,250 MW was available, this capacity was not sufficient to meet peak demand of 6566 MW in 2011, Specially for Damascus Which had a peak demand of 850MW in 2011 [5]

the demand for electricity in Damascus also increased on an average high rate of 7.5% per year, caused by the strong economic growth by 2011, at the same time, the power system experienced increasing difficulties in meeting the city's demand while rolling black out increased starting in mid-2014 because of the crisis. [5]

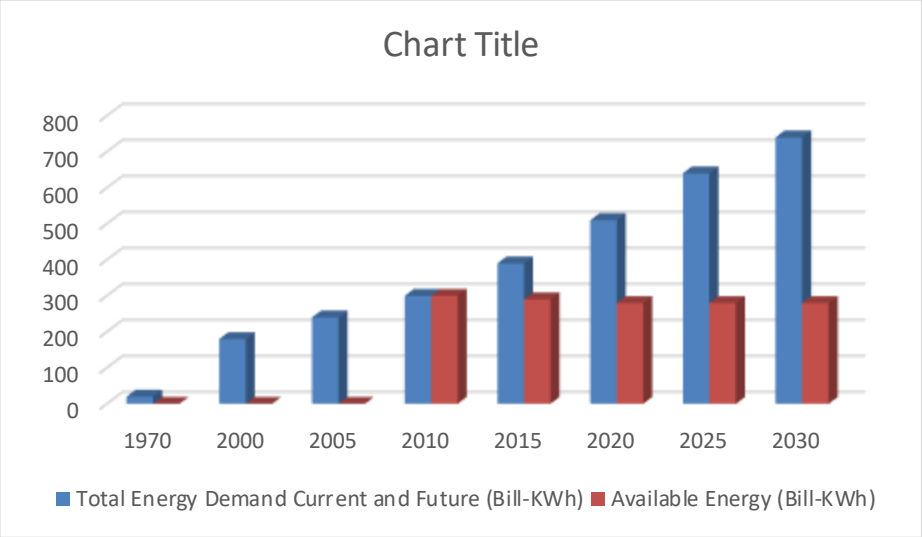

Fig. 4. Shows future and present supply and demand if no upgrades occurred on the network.

As shown demand of energy will exceed the available energy which it already did since mid-2015, so measures should be taken such as building solar farms which became cheap renewable solutions compared to building or improving any functional power plant. Therefore, it is obvious that that energy consumption should be reduced, rather than increasing energy generation. Another option would be to integrate renewable energy to meet the demands. However, from an environmental point of view, the renewable option seems effective on the long run.

3 Methodological approach

To analyze the upcoming development in the regarding energy and electricity demands gather its results so we can implement it to improve the transportation sector an integrated MARKAL-EFOM system (TIMES) [6] is used to calculate the final demand, for energy and electricity, We used Such model because it aims to capture the main characteristics of an energy system which are particularly useful for understanding the strategic choices that are required to decarbonize a city (zero emissions), the Damascus TIMES model is an entry level model, covering the entire Damascus city energy system and containing many variables covering existing technologies and processes.

This model is built up on a common basic structure the Reference Energy System, which basically represents the fundamental energy and materials flows by all different sector [7] (Commercial, Agricultural and Residential—RES, Industry— IND, Gas, Heat and Electricity—ELC, and Energy supply—SUP)

From the conducted literature reviews done on [8] and [9], we understand that:

The use of policy frameworks and legalization are the main building block for an accurate functional Reference Energy System

To enable the transition from electrics to renewable and sustainable systems possible we must create an accurate energy system.

This reference energy system can provide a path for fast building of the post-conflict city energy system.

After the energy system is obtained a plan to renew and improve AL-ZARA power plant is introduced by building a CSP in the southern part of the power plant naming it, extension of al-zara power plant, then power obtained from the CSP can be used to power a PEM hydrogen production plant.

We chose al-zara because of the Geographical location provided the empty areas around the power plant, and the solar power availability.

the next figures show the reference energy system.

collecting and analyzing all data and information from open sources mostly (governmental) combined with national statistical reports, studies, published articles from the following sources. [10] [11] [12] [13]

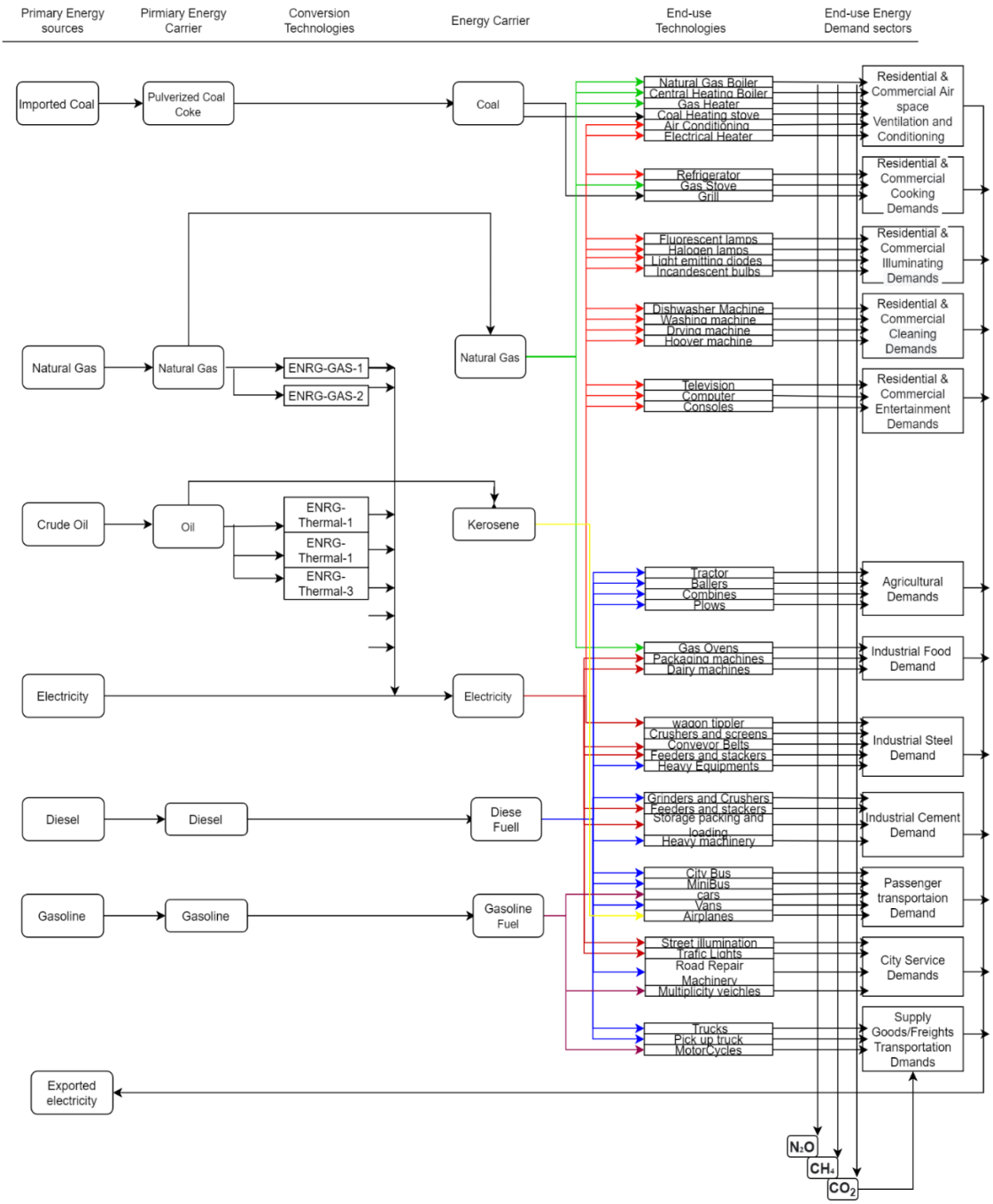

Fig. 5. Reference energy system

4 Transportation sector in the Damascus

According to the latest statistics - carried out on December 31, 2011 - the population of Damascus and its countryside reached (4590000) people, with the transportation movement increasing dramatically, which led to transportation crises and severe traffic jams, especially during peak hours and occasions, in addition to negative results Several, the most important of which are environmental pollution, the great waste of energy, the waste of time, the disruption of work, the weakening of production, the increase in daily traffic accidents, injury, and health and psychological damage.

From here, traffic issues and problems began to occupy an important aspect in the city of Damascus, as the traffic problems resulting from the severe congestion of vehicles in the main and secondary streets have not found a solution so far, even though cars and kilometers traveled are constantly increasing.

There is also no other mean of transportation (governmental) beside those minibuses and normal buses, there is no tram or metro network.

Table 7. Shows the numbers of registered cars in Damascus in 2014.

Type of transportations	Damascus
Car	351282
Bus	2515
Minibus	9232
Cargo truck	17440
Oil tanker	875
Pick-up truck	63400
Motorcycles	5665
Industrial machine	2330
Grand Total	452739

4.1 The impact of the transport and current traffic system on air quality in Damascus

Transportation is the main source of air pollution in Damascus, which if resolved air quality will improve at a high rate in the city.

Introducing the current used means of transportation which are mostly old minibuses, this leads to a decrease in the combustion efficiency of their engines, as old cars emit 20 times more pollutants than new-made cars, the low quality of fuel plays an important role in increasing the pollutant gases, especially sulfur dioxide, as the local fuel used contains a high percentage of sulfur, amounting to (0.15%) in gasoline and (6.7%) in diesel and reaching (5, 3%) in fuel.

Public transport means are small or large diesel buses that are primarily responsible for the release of respiratory plankton, at a rate of more than (30-50) times more than

the means operating on gasoline, and it is known that the largest number of transport modes, especially public transport, are large or small buses. It works on diesel, and the transport sector's consumption of diesel is about (38%) of the total quantities of diesel consumed in Damascus, and according to estimates, one third of the transportation modes in Syria are concentrated in Damascus. The presence of this number of cars and bad management leads to Traffic jams lead to traffic jams, which in turn lead to cars stopping at traffic lights for long periods. Studies have confirmed that (70-80%) of the air pollutants in the city of Damascus alone are due to the traffic system, transport and vehicles, and these pollutants include nitrogen gases and oxides., Sulfur dioxide, carbon monoxide, hydrocarbons, and lead (its concentration in some areas of Damascus reached 4-5 micrograms / m3, while the global permissible limit does not exceed 1 microgram / m3), in addition to the plankton containing Organic compounds and charcoal.

The following table shows a comparison between the annual averages of the concentration of plankton, sulfur dioxide and nitrogen dioxide for several cities in the world, with the standards permitted by the World Health Organization, where Damascus ranks first among them despite being the smallest.

Table 8. Compares Damascus with other big cities and per year.

City	Dust and macro plankton g/m^2	sulfur dioxide g/m^2	Nitrogen dioxide g/m^2
Standards permitted by the World Health Organization (WHO))	90	50	40
Damascus	418	96	122
Beijing	377	90	122
Mexico	279	74	130
Athens	178	34	64
Tokyo	49	18	68
Copenhagen	61	7	54
Berlin	50	18	26
Singapore	0	20	30

Table 9. Shows number of pollutants emitted per car

Pollutant Gram/Liter	Diesel Cars	Gasoline Cars	Avg Car emissions per year
Carbon Monoxide	29.5	249	297 kg / year
Hydrocarbons	1.8	9.63	39 kg / year
nitrogen oxides	7.2	9.85	10 kg / year
Sulfur Dioxide	4.15	0.37	2 kg / year
lead	-	0.37	1 kg / year
soot	1.9	-	28 kg / year
			Grand Total 377 kg / year of pollutants

4.2 Analyzing the situation

Statistics shows that growth rate in the city is 8 %, which makes it logical for us to adopt a new modern transportation system. For example, metro/tramway network can be help improve the congestion in the city which on the other hand will improve the air quality, Studying the various factors that contribute to air quality in Syria, the main component has been shown to be transportation, not to mention that the demand has increased dramatically in the last 10 years, Air quality in general in Syria is not even near the required standard set by World health organization (WHO) standard. The quality of air is relatively better during the summer months as compared to the winter when combined with transportation it even makes the situation worse.

5 The Damascus energy transition

The energy transition is awaiting all of us in the next decade and there is no doubt that we are going through a global climate crisis, taking that into consideration the main step towards decarbonizing a city is implementing renewables, knowing also how to store energy is an essential so our focus will be mostly on integrating Hydrogen as a source of renewable energy. we also work on Hydrogen production, distribution, usage, and storage [14]

We can implement few things to pave the road down for the transition.

Using less environmentally damaging (green) forms of private transport for example cycling for shirt distances, cars with substantially lower emission levels that damage the environment way less than conventional forms of transport (buses and minibuses).

Rationalizing proper energy use in the transportation sector. Making use of available renewable energy resources and in this paper focusing on Hydrogen.

5.1 Why Hydrogen

We like to call hydrogen as the dream fuel of the future since it holds many environmental and economic benefits, although lithium-ion batteries have a head-start in personal cars and some other small vehicles but, hydrogen fuel cell technology is not as far from some might think.

So why would we skip electric cars and trucks and go directly to hydrogen the answer is, Downtime. Charging electric vehicles takes time now such problem would not affect people with private means of transportation that much but for a government network like a fleet of buses this would not be the most efficient way to go but commercial fleet operators such as cargo and deliveries who drive around the city all day with a tight schedule showed that the inability to refuel in a matter of minutes will be detrimental for them to operate.

And this is where hydrogen fuel cell vehicles give us the answer. Fuel cell vehicles have a far greater range than electric vehicles (battery) [15], with fuel cell buses averaging on 300-450 km before needing to refuel and refueling time up to only 7 minutes. However, there are still several challenges to be overcome.

When hydrogen is produced from renewable energies, the process of producing and using it becomes part of the clean and natural cycle. to produce hydrogen in a green manner not through burning fossil fuels the most efficient method is through Electrolysis of water.

5.2 Case Scenario

Significant investment is a must in the current to ensure the viability of hydrogen fuel cell vehicles, not only to build refueling stations, but also to bring hydrogen costs down so it can compete with conventional fuels and to convince the public to use them and to eventually replace fossil fuels themselves, our case scenario is to invest in al -Zara power to expand it to produce hydrogen and step by step to transform into a clean energy power plan, to achieve that we must have a renewable source of energy for example solar, since as we can see in the Syrian Photovoltaic power potential the northern part of Damascus is the perfect spot for building
Concentrated solar power (CSP).

Suggested Location

Fig. 6. Shows the location of the project.

As shown above there is a $5Km^2$ at the southern part of the powerplant that can be used for this project called the extension of AL-ZARA Power plant, as I also provided before the Photovoltaic power is high at this area, so we take our idea a step further to build Solar powered Hydrogen Energy System

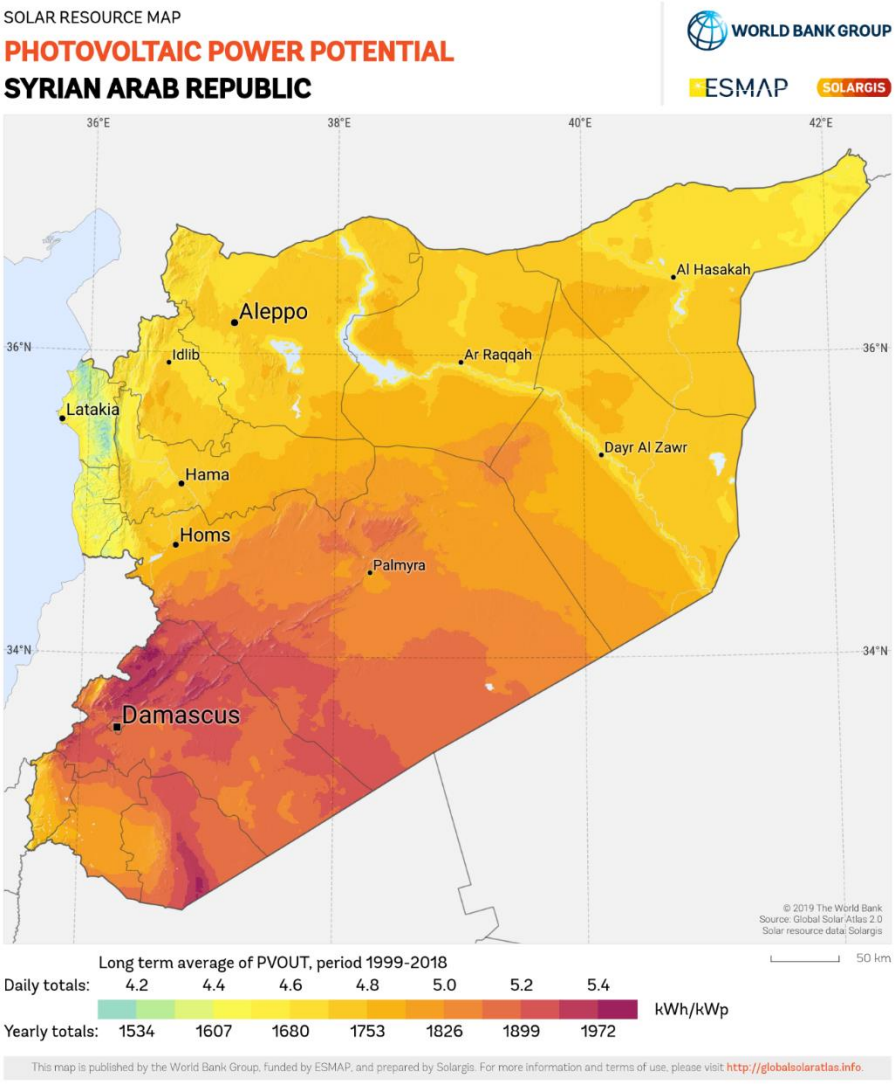

Fig. 7. Photovoltaic power potential in Syria

Solar irradiation

Monthly average direct normal irradiation for the selected area is shown in the following chart in kWh/m²

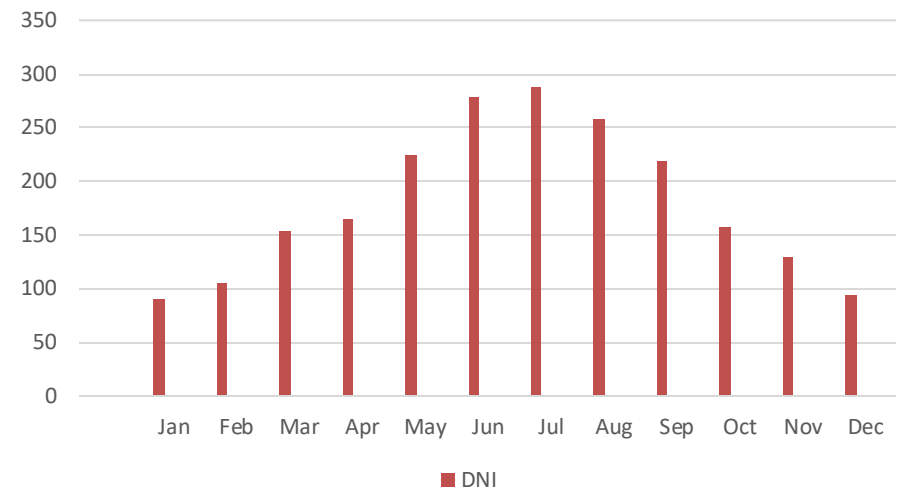

Fig. 8. Direct normal irradiation

Direct normal irradiation [Wh/m²]

	Jan	Feb	Mar	Apr	May	Jun	Jul	Aug	Sep	Oct	Nov	Dec
0 - 1												
1 - 2												
2 - 3												
3 - 4												
4 - 5					3	38	8					
5 - 6			5	48	238	379	313	139	53			
6 - 7	2	28	158	299	461	601	577	501	424	215	70	6
7 - 8	165	237	367	430	565	707	699	646	610	451	360	197
8 - 9	296	365	465	499	641	780	785	738	701	557	482	333
9 - 10	348	446	553	551	686	829	843	801	755	626	544	382
10 - 11	381	488	584	576	704	855	870	838	780	629	563	417
11 - 12	395	466	560	586	705	862	879	850	787	615	553	418
12 - 13	381	454	553	578	693	859	873	844	781	593	522	407
13 - 14	370	445	520	555	681	835	852	818	755	536	493	383
14 - 15	340	404	477	511	629	789	802	756	689	454	427	338
15 - 16	237	335	415	435	553	717	724	666	585	328	261	190
16 - 17	20	114	269	333	445	610	610	530	351	62	13	2
17 - 18			22	75	224	391	398	229	32			
18 - 19					6	27	37	1				
19 - 20												
20 - 21												
21 - 22												
22 - 23												
23 - 24												
Sum	2935	3782	4949	5476	7235	9279	9269	8356	7305	5066	4288	3074

Fig. 9. Average hourly profile

Source: Global Solar Atlas

Concentrated Solar power basic system design

CSP technology utilizes focused sunlight. CSP plants generate electric power by using mirrors to concentrate (focus) the sun's energy and convert it into high-temperature heat. That heat is then channeled through a conventional generator. The plants consist of two parts: one that collects solar energy and converts it to heat, and another that converts the heat energy to electricity. [16]

Power Towers–use large sun-tracking mirrors, called heliostats, to focus the sun's energy on a receiver located atop a tall tower. In the receiver, molten nitrate salts absorb the heat, which is then used to boil water to steam, which is sent to a conventional steam turbine-generator to produce electricity. [17]

Power tower will utilize the heliostats to focus sunlight onto a receiver at the top of a tower. A heat transfer fluid heated in the receiver up to around 600ºC is used to generate steam, which, in turn, is used in a conventional turbine-generator to produce electricity.

225-meter tower will be built that allows for a high concentration of heliostats, high tower will allow to produce the same amount of energy but with less amount, and the land around the new plant is farming land the mirrors are placed on metal individual poles pinned into the ground to minimize the loss of vegetation in the surrounding area

Since AL-ZARA power plant already have its own gas turbines the steam generated from this new CSP can be used to generate power to supply the Hydrogen electrolyze

Please note that the first paragraph of a section or subsection is not indented. The first paragraphs that follows a table, figure, equation etc. does not have an indent, either.

Subsequent paragraphs, however, are indented.

Fig. 10. Gema Solar Power Tower plant in Sevilla, Spain

System characteristics

A central receiver CSP is the most suitable type for our scenario not to mention also that it's the most efficient type of CSP, this works by using many heliostats that track the solar movement and reflect the sunlight onto a receiver at the top of the tower, heliostat design would be a radial stagger pattern because of the height of our receiver, a heat transfer fluid (HTF) will also be used to pass through the tower so its heated, the high temperature fluid is then fed towards the turbines in AL-ZARA plant to generate electricity.

Here we compare the 4 different types and show why Center receiver (tower) is the best option

Table 10. Comparison of most common CSP methods.

CSP Type	Operating Temp (°C)	Concentration Ratio	Thermal storage suitability	Annual Efficiency (%)	Installed Capacity
Parabolic Dish	120-1500	1000-3000	Difficult	25-30	5-25 KW
Central Receiver	300-1000	300-1000	Applicable	17-35	10-600 MW

Central receiver systems are considered to be the best cost-reduction electricity wise compared to parabolic dish technology, because they can achieve higher temperatures which results in a more efficient cycles or ultimately higher exergy cycles since our (CGCP) is using gas turbines at temperatures above 1000°C.

Area required.

A typical CSP plant requires 5 to 10 acres of land per MW of capacity. Since out plant is set to produce around

The CSP will be producing 160Mw, to calculate the required land size taking 8 acres of land per Mw we get:

$$160 \times 8 = 1280\,\text{acre} \approx 5km^2$$

Costs of the (CSP)

According to [18] Average installation cost for concentrated solar power (CSP) worldwide in 2019 (in U.S. dollars per kilowatt), Assuming our energy storage for the tower will be around 15 hours this would costs us 10 500 USD/KW.

$$160\ 000 \times 10\ 500 = 1.6\ bil\ \$$$

Access to water and Grid transition accessibility

The heliostats require small amounts of water to wash their surfaces with other feeding needs, since this is an extension project all water needs can be taken from AL-ZARA power plant pipes network, access to high voltage transmission grids is what

we look for and it is already available in Al-Zara power plant, new transmission could be needed to link the (CSP) with Hydrogen electrolyze plant

Hydrogen power plant

Our PEM electrolyzer is set to produce hydrogen from water electrolysis using electricity generated by the CSP so we are producing hydrogen from a renewable source.

To make the energy transition on a higher scale we plan to build one of the world's largest membrane electrolyzes in the world to produce carbon free hydrogen, we already presented a CSP that will be able to produce 160Mw, we can invest that power in a PEM power plant.

A total of 20 Mw in power can be produced a PEM plant that size can also produce around 8 tons of carbon free hydrogen according to [19]

Table 11. Capability of a 20Mw PEM plant

Plant power capacity (MW)	Hydrogen Production Capacity (Metric Tons)	Reduction of carbon intensity (Metric Tons)
20	8	27000

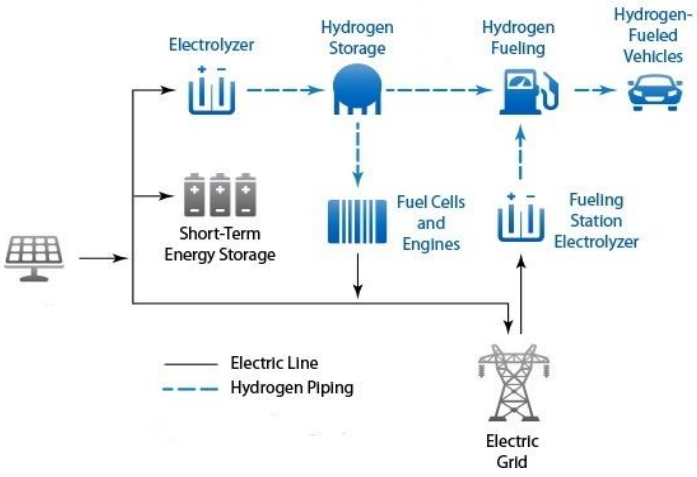

Fig. 11. process flow of the project.

Hydrogen Production

Since our goal is a carbon free Hydrogen society and aiming to produce Green hydrogen via water electrolysis since low to zero emissions will be emitted comparing it to producing hydrogen using fossil fuels, and providing that we already obtained the power needed to power the PEM electrolyze plant [20] we are aiming to produce around 8 tons of Liquid Hydrogen a day.

Table 12. Shows transportation method and its consumption

Transportation method	Amount	Avg consumption of Hydrogen per day
Car	1800	1~3
Bus	200	20~30
Truck	150	15~25

Hydrogen storage

Due to the nature of hydrogen molecules when it comes to storage and utilization there is two ways mobile applications such as compressed gas tankers or stationery in a liquid As a liquid in cryogenic storage or tanks (stored at -253°C). [21]

Since its not that easy to store hydrogen, it can be immediately transported after production to hydrogen fueling stations across the city so it can be used and utilized by hydrogen means of transportation.

6 Integrating fuel cells into the transportation network

Regarding transportation, the hybridization concept is applicable for cars, buses, and tramways. The Proton exchange membrane fuel cell (PEMFC)-battery-supercapacitor hybridization was applied for electric trams. [22]

Inside vehicles a fuel cell unit works by transforming hydrogen into electricity using air, with water as the only exhaust, we can categorize hydrogen fuel-cell vehicles as electric vehicle with the same power as conventional fuels vehicles but with a catch of zero-emissions.

We provided data before that shows we can have 1800 cars and 200 buses working on Hydrogen so the approach would be to create tram line or a bus line completely dependent on Hydrogen.

6.1 Stations and localization

(Damascus Directorate, 2007) suggested a line which includes 17 stations which connect most of the city commercial and habitation areas, our goal here is to improve and follow up the work that they started.

Fig. 12. Damascus green line

The line which included 17 stations can transport up to 840 000 passenger per day [23] if a metro/tram line was constructed, but for buses estimated starting capacity would be 14 000 passengers, the line is approximately 6,8 kilometers.

New fuel cell buses advantages and specifications are. [24]

- High traveling range and quick refueling times at the depot the main advantages provided by hydrogen fuel cell buses. New hydrogen fuel cell buses average 6 MPG (gas equivalent)
- Length: 12 meters
- Capacity: 35 seated, 33 standing
- Range: 650km per tank

This program would cost 460 million USD including the buses and transit hydrogen fueling station and depot/warehouses for maintenance.

Fueling

Rapid fueling can take place at any bus fueling depot designed with the addition of delivered hydrogen, utilizations around the world have showed that fuel cell electric buses can be fueled efficiently and safely in depot, hydrogen fuel allows zero emission transit, the infrastructure is also like CNG infrastructure.

Overview

Table 13. status and current conditions

Type	Status	Source
PEM electrolyzers power plant lifetime	40 000~60 00 working hours	Volta Chem 2015
Bus cost per unit (2016)	1,235,000 $	New Flyer
Maintenance cost	0.80 $ /km	NREL 2017
Bus range	430~560 km	NREL 2017

7 Possible Solutions pre transition

Traffic congestions can be addressed by reducing traffic signals, encouraging mass transit of citizens and employees such as a Metro Network working to establish floor garages and central markets and requiring modern buildings to allocate garages and regulate the entry of cars into crowded places, in addition to moving government departments to the suburbs, relieving population pressure on the city, and improving poor fuel specifications. The user, especially diesel by reducing the high sulfur percentage in it, and installing the transformer for all modern and old cars to convert harmful gases to health into harmless gases, as well as the use of environmentally friendly means of transport that work on electricity and gas, where proposals have been put forward to create a large and advanced transport system in the future that uses electric energy It relies on electric railway transportation (including the metro), in response to the increasing need for passenger movement and distribution in the city, and linking them with residential communities in the region, as the city of Damascus is currently totally relying on micro-buses as the only means of mass transport in it is not compatible with the importance of the city And their social, economic and environmental status, as well as work to get rid of cod cars In particular, the government and the government in particular, studying the flow of modern cars in a manner consistent with the ability to combat the pollution process resulting from it, maintain green areas, apply green tape requirements when constructing buildings and establishments, carry out an intensive afforestation campaign, and remove populated areas from highways, and citizens 'awareness must be made. Especially drivers for the importance of adhering to laws and not violating them, to maintain clean air and people's health, and to seek the help of the Ministry of Education through educational curricula and other ministries.

8 Results

In order create our base for a hydrogen powered transportation network we started from basics on how fuels are produced and consumed in the city until how our plan can be implemented.

- Calculations have proved how the city is completely dependent on conventional fossil fuels for energy.
- Power plants both gas and thermal that provide the city with power have been analyzed, consumption, production and costs were obtained and evaluated.
- Electricity consumption among all sectors in the city was calculated with the predicted growth rate as far as 2033.
- If no actions are taken the city will not be able to provide electricity regarding its future demands.

- A reference energy system was created, and results were obtained through TIMES model.
- After analyzing various factors that contribute to air quality in Syria, what mostly contributed to pollution was shown to be transport, especially since this has increased dramatically during the last few years.
- the highest values of pollutants can be found in the city of Damascus, due to irrigation with effluent from Damascus city for many decades and the absence of law to regulate the transportation system.
- Transportation sector was analyzed, and a plan was made to start the road for an emission free transportation network.
- We also concluded that hydrogen produced also depends/fluctuate on electricity produced daily.
- Proton Exchange Membrane (PEM) electrolyze was selected for electrolysis of water; Results are yet to be determined on how much can the electrolyze produce hydrogen in winter days.

Conclusion

Finally, it is important that steps are taken now rather than later to reduce the environmental damage and associated health implications. The later the preventive measures are implemented, the more will be the cost of improving the environment and the health of the Syrian nation.

Renewables are becoming widely spread now and it is time for us to adapt them.

The future for Damascus and its people is Green.

References

[1] T. A. E. C. o. t. S. A. Republic, "Country Nuclear Power Profiles," IAEA, 2017.

[2] R. c. f. r. e. a. e. efficiency, "Technological and Environmental Impact on Syria," RCREEE, Syria, 2009.

[3] PEEG, "Statistical reprot 2018," PEEG.GOV.SY, Damascus, 2018.

[4] M. o. electricity, "Annual report," 2015.

[5] t. W. Bank, "Syrian Arab Republic Electricity Sector Strategy Note Report No. 49923-SY," Sustainable Development Department (MNSSD), 2009.

[6] R. G. G. N. K. Loulou, " Documentation for the MARKAL Family of Models. ETSAP.," *(The MARKAL Family of Models)*, 2004.

[7] A. H. J. K. StefanP fenninger, "Energy systems modeling for twenty-first century energy challenges," *Renewable and Sustainable Energy Reviews*, vol. 33, pp. 74-86, 2014.

[8] F. P. S. L. M. S. C. C. Senatro Di Leo, "Energy systems modelling to support key strategic decisions in energy," *Renewable and Sustainable Energy Reviews*, 2014.

[9] AliAl-Mohamad, "Renewable energy resources in Syria," *Renewable Energy*, vol. 24, no. 3-4, p. 365, 2001.

[10] M. o. Electricity, "Annual statistical report," Public Establishment for Electricity Generation, Damascus, 2018.

[11] E. i. a. EIA, "Syria's energy sector," EIA, 2015.

[12] "Damascus Cash Crunch as Crude Below 10,000 b/d," *Middle East Economic Survey*, vol. 58, no. 18, 2015.

[13] E. Commission, "Trade in good with syria," 2015.

[14] M. P. D. M. Ankica Kovač, "Hydrogen in energy transition: A review," *International Journal of Hydrogen Energy*, vol. 46, no. 16, 2021.

[15] M. Connolly, "Hydrogen vehicles: the future of clean transport?," LEXOLOGY, United Kingdom, 2020.

[16] S. e. d. p. EIS, "Concentrating Solar Power (CSP) Technologies," EIS Information center.

[17] U. D. o. Energy, "Concentrating Solar Power technologies," U.S. Department of Energy, 2008.

[18] M. Jaganmohan, "Statista," june 2020. [Online].

[19] A. LIQUIDE, "Inauguration of the world's largest PEM electrolyzer," 2021.

[20] D. L. J. M. D. S. Marcelo Carmo, "A comprehensive review on PEM water electrolysis," *International journal of hydrogen energy*, vol. 38, no. 12, pp. 4901-4934, 2013.

[21] F. S. E. Center, "Hydrogen Basics- Storage".

[22] Q. Y. H. H. Y. L. M. &. C. W. Li, "A state machine strategy based on droop control for an energy management system of PEMFC-battery-supercapacitor hybrid tramway. International Journal of Hydrogen Energy," *International Journal of Hydrogen Energy*, no. 36, pp. 16148-16159, 2016.

[23] F. W. Samer Dakak1, "Designing Fast Transportation Network in Damascus," *Logistics, Informatics and Service*, vol. 7, no. 1, pp. 58-66, 2020.

[24] O. O. c. t. authority, "Hydrogen Fuel Cell Electric Bus," Orange county southern california, 2017.

A Regional Energy Optimization for Afyonkarahisar, Turkey

Utku Köker[1][0000-0001-7165-777X], Halil İbrahim Koruca[1][0000-0002-2448-1772],

Egemen Sulukan[2][0000-0003-1138-2465] and Tanay Sıdkı Uyar[3][0000-0002-0960-1203]

[1] Industrial Engineering Department, Süleyman Demirel University, Isparta, Turkey
[2] Mechanical Engineering Department, National Defence University, Turkish Naval Academy, Istanbul, Turkey
[3] Mechanical Engineering Department, Marmara University, Istanbul, Turkey

utku.koker@afad.gov.tr, halilkoruca@sdu.edu.tr,
esulukan@dho.edu.tr, tanayuyar@marmara.edu.tr

Abstract. In recent years the relationship between the energy security, society and sustainable development led to the improvements in energy planning interfaces. The dissemination of these interfaces finalized with increasing participation of societies in energy planning issues over the years. Even though national level analysis are studied since 1970s, regional level energy analysis are gaining popularity only in recent years. European Union (EU) powerfully supports open source programs with Horizon 2020 initiative especially in energy sector. "Open Source Energy Modelling System" (OSeMOSYS) which is a project under Horizon 2020 is used as the modelling platform in this paper. This paper describes an implementation of OSeMOSYS within Afyonkarahisar a small city in Internal Aegean Region of Turkey. Agricultural, industrial, residential, lighting and energy sectors are studied in a time span of 2016-2031 from optimization point of view in the study. A "zero electricity importer Afyonkarahisar" option is evaluated throughout the paper with a minimum of %40 and %60 renewable energy constraints. The economic and environmental outputs of two scenarios are studied comparatively in the results section. OSeMOSYS is found to be a powerful tool for regional energy modelling purposes which enables various scenario analysis with high accuracy.

Keywords: Energy Optimization, OSeMOSYS Optimization, Emissions, Energy Costs, Regional Energy Modeling.

1 Introduction

Numerous researches have resulted in new electrical energy generation methods from various renewable energy techniques to complex hydrogen processes. Even though the conventional gas turbine or lignite power plants still reigns in many re-

gions, renewable energy began to shake the old king in the western countries. Many futurists and experts announce the photovoltaic energy as the main energy of tomorrow [1,2] while some others claim [3,4] the nuclear energy will rise again with its emission friendly output profile. Neither one of these arguments fail to be true but this blurry overview tells so few on how to decide in real world problems in a portfolio of numerous power plant alternatives. Problem is the generation method and the selection of the right technology to construct when supply is expected to be surpassed by the annual demand. From this perspective, increase in energy supply methods and international regulations on emission quotas only make the decision makers' business more complicated than ever.

Selection of the most economical option in numerous power plant alternatives under the given criteria is the main issue in energy optimization. Applying various user defined constraints from storages to emission quotas and taxes also gained great importance in the last decades. As a total, energy optimization became a sophisticated study today including thousands of data and equations to be solved. Energy optimization tools are developed since 1970s starting with EFOM [5] to MARKAL in the 1980s [6] and TIMES [7] in the 1990s and 2000s. Since all these programs require licenses, both, students from academia and analysts come across with obstacles in reaching these powerful tools. Energy optimization programs can be grouped under two main titles namely commercial ones and open source models. TIMES, MARKAL and PLEXOS belong to group one while OSeMOSYS is a member of the second group. While commercial products offer so many advantages like well categorized and user friendly input data entry and output reporting options, the funding procedures are the main obstacle before the academicians and analysts. On the other hand, open source models has the advantage of using libraries of well-known compilers but lacks user friendly environment.

European Union and some other actors support the open source energy planning tools for a significant period of time via programs like Horizon initiative. Commercial licenses are costly but rather than the financial point of view, an "easily reachable and widely used optimization suit" was one of the most important goals of these mechanisms to provide a basis for cooperation and discussion on energy models.

Following its recognition in 2008, OSeMOSYS is used in many optimization studies in a wide spectrum of search areas. Multiple papers involved optimization works at national level such as Tunusia [8], Ethiopia [9], Chile [10], China [11], India [12], Saudi Arabia [13], Portugal [14] or Ghana [15] models while some studies focus on multinational level such as Drina River Model [16], Omo Basin [17] and South America Model Base (SAMBA) [18]. International models test the effects of creating direct connections of the energy grids of two or more countries. If the optimization model includes the combination of the countries due to solid geographical reasons, these models can be called regional optimization models. Basin or river models are also regional models from this point of view. On the other hand, regional models can be localized to a more local stage even to city level. Choco case in Columbia [19] is an example for this sub group.

This study is based on Afyonkarahisar province in Internal Aegean Region, Turkey. Even though the city is a net energy importer in 2016, two scenarios are devel-

oped in this paper namely %40 and %60 renewable energy scenarios both assuming zero electricity import from the main grid which means %100 electricity generation by its own assets. OSeMOSYS framework is chosen in the study for its open-source property which lets the analysts make custom modifications in the source code model. The full advantage of MOMANI interface is also used in the OSeMOSYS data entry process. %40 and %60 renewable energy scenarios are built to test if the city renewable supplies can meet the annual demand figures in 2016-31 at required ratios.

MARKAL and TIMES modelling dominated the Turkish energy optimization studies and as a result numerous papers are released at national scale at the last decade. OSeMOSYS tool is relatively ignored in national academic world in Turkey in the last 10 years. This paper aims to make a contribution by opening Afyonkarahisar province's two scenarios up for discussion with this new framework.

The following sections of the study are organized as follows. In the second part, a broad description of the OSeMOSYS framework is introduced. The implementation analysis is given in the third section. Fourth part includes the discussion of the results and the fifth section handles the conclusion.

2 OSeMOSYS Model

OSeMOSYS is an optimization model for energy modelling in the long term. It is an open source bottom-up framework built on modular block approach which consists of 7 main columns (Figure 1) namely, objective, costs, storage, capacity adequacy, energy balance, constraints and emissions [20]. These blocks represent a set of linear equations and inequalities. This structure is built upon the efforts of many institutions and specialists from Stanford to UCL [21].

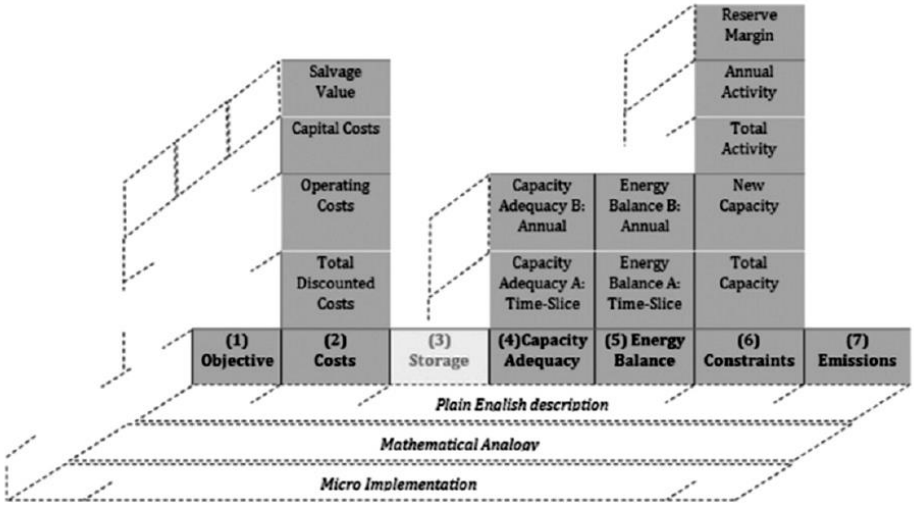

Fig. 1. OSeMOSYS block view [20]

Optimization suits like MARKAL, TIMES and MESSAGE are commercial products and require funds from the researchers/institutions. The open-source property of OSeMOSYS is a significant advantage from this point of view. Not for only financial perspective but the users all around the world modify the equation sets according to their needs and open new discussions which is a very important issue for a model to stay alive. Second advantage of the model is its relatively easier structure when compared to commercial alternatives. Past experiences show that learning curve of the university students is shorter with OSeMOSYS to build comprehensive models from real world [22-24].

The MOMANI interface was chosen during the implementation process to gain more control and visuality on the data entry phase.

2.1 OSeMOSYS Structure

Since 2008 lots of improvements were made at OSeMOSYS side. The first version of the model uses model and data files written in GNU Mathprog [25]. These files are entered as inputs to the solver "GNU Linear Programming Kit" (GLPK) to produce outputs. Students and specialists already equipped with operational research background can easily handle the model and data files of this version which accelerates the overall process of the framework.

The second version of the OSeMOSYS uses GAMS solver which replaces GLPK in the first version. Löffler et al [26] uses GAMS version in their Global Energy System Model (GENeSYS-MOD). On the other hand it should be noted that GAMS is not an open source kit and requires licenses.

The third version of the OSeMOSYS is written in Python environment to gain advantage of the available libraries provided by the community. Next to numerous benefits of the python functionalities, the data files in AMPL format also present some advantages in the compiling phase.

Except the three former OSeMOSYS versions there is also a fourth version named NEMO written on JULIA environment [27]. NEMO works in conjunction with LEAP software.

Objective function of the OSeMOSYS is so similar to TIMES expression which minimizes the net present value of the costs defined in the framework [28]

$$Zmin = \sum_y \sum_t \sum_r TotalDiscountedCost_{y,t,r} \quad 5$$

Costs are defined in the equation forms and levelized to the reference year (discounted to the reference year).

$$\forall_{y,t,r} TotalDiscountedCost_{y,t,r} = DiscountedOperatingCost_{y,t,r} + DiscountedSalvageValue_{y,t,r} + DiscountedCapitalInvestment_{y,t,r} + DiscountedTechnologyEmissionsPenalty_{y,t,r} \quad 2$$

$$\forall_{y,i,t,r} VariableOperatingCost_{y,i,t,r} = \sum_m RateofActivity_{y,i,t,m,r} * \text{VariableCost}_{y,t,m,r} \quad 3$$

$$\forall_{y,t,r} AnnualVarOperatingCost_{y,t,r} = \sum_{m} RateofActivity_{y,i,t,m,r} \quad 4$$

$$\forall_{y,t,r} AnnualFixedOperatingCost_{y,t,r} = \text{TotalCapacityAnnual}_{y,t,r}\text{FixedCost}_{y,t,r} \quad 5$$

$$\forall_{y,t,r} OperatingCost_{y,t,r} = \text{AnnualFixedOperatingCost}_{y,t,r} + \text{AnnualVarOperatingCost}_{y,t,r} \quad 6$$

$$\forall_{y,t,r} DiscountedOperatingCost_{y,t,r} = \frac{\text{OperatingCost}_{y,t,r}}{\left(1 + \text{DiscountRate}_{t,r}\right)^{(\text{y}-\text{StartYear}+0.5)}} \quad 7$$

$$\forall_{y,t,r} CapitalInvestment_{y,t,r} = \text{CapitalCost}_{y,t,r} * NewCapacity_{y,t,r} \quad 8$$

$$\forall_{y,t,r} DiscountedCapitalInvestment_{y,t,r} = \frac{\text{CapitalInvestment}_{y,t,r}}{\left(1 + \text{DiscountRate}_{t,r}\right)^{(\text{y}-\text{StartYear})}} \quad 9$$

$$\forall_{y,t,r} DiscountedSalvageValue_{y,t,r} = \frac{\text{SalvageValue}_{y,t,r}}{\left(1 + \text{DiscountRate}_{t,r}\right)^{(1+\text{card(Year)})}} \quad 10$$

$$\forall_{y,t,r} DiscountedTechnologyEmissionsPenalty_{y,t,r} = \frac{\text{AnnualTechnologyEmissionsPenalty}_{y,t,r}}{\left(1 + \text{DiscountRate}_{t,r}\right)^{(\text{y}-\text{StartYear}+0.5)}} \quad 11$$

So similar to TIMES optimization suit, OSeMOSYS can also handle more in-depth timeslices in the energy models. To provide a discussion base for Afyonkarahisar region, this paper focuses on the scenarios in "yearly manner" which means the timeslice option is chosen as a "yearly representative value" for the optimization parameters.

3 Implementation

Afyonkarahisar is a province in the Internal Aegean Region of Turkey with a population of 725568 [29] in 2019. A summary of the electrical energy consumption of the sectors (Lighting, Residential, Industry, Agriculture and Commercial) in Afyonkarahisar in 2016 is given in Table 1.

Table 1. Electricity Consumption in Afyonkarahisar in the reference year [30]

Year	Lighting	Residential	Industry	Agriculture	Commercial	Total
2016	52005,48	359914,47	470858,76	123516,80	608714,65	**1615010,15**

Existing electrical energy generation technologies in Afyonkarahisar are listed in Table 2 in megawatts.

Table 2. Installed Power Capacities of Afyonkarahisar in 2016

Technologies	Afyonkarahisar (MW)
Solar Power Plants (PP)	25,6
Wind PP	208.62
Hydro PP	3

Annual energy demand of Afyonkarahisar province is expected to jump to 11.48 PJ from 5.81PJ between 2016-2031 according to the projection of the Ministry of Energy and Natural Resources [31].

This paper focuses on the electrical energy production system of Afyonkarahisar taking the year 2016 as the reference year and 2016-2031 as the timespan. Year 2016 reference model is built on the OSeMOSYS environment using MOMANI interface for both of the scenarios consecutively. No electrical energy importation from main grid is permitted during the period to set the "self-sufficiency" policy.

Rather than 5 years of construction times, all investments are assumed to be completed annually in the models. Hydro energy, biomass, onshore wind, photovoltaic, geothermal, lignite, natural gas and combined cycle thermal power plants are the alternative technologies competing to enter the optimum plan. According to the cost minimization procedure one or more of these power plants are added as new investments in the optimum plan every year. Cost data are obtained from various source but mainly from IEA figures presented in Table 3 [32]. Photovoltaic and onshore wind power plants are assumed to be zero emission emitters and the emission values of the remaining technologies (natural gas, combine cycle natural gas, coal, geothermal and biogas power plants) are taken from various references [33-34]. Technology prices, costs, efficiencies, and availability factors are set to be steady in the timespan for comparison purposes. The fuel, operations &maintenance, and investment cost datasets are presented in Table 3.

Table 3. Installed Cost Figures per kWh for 2016

TECHNOLOGY	Investment Cost $/kW	Fixed Cost $/kWyr
Nat Gas PP	**950**	34
Nat Gas CC PP	**1100**	30,57
Geothermal PP	**4500**	100
Wind PP	**2500**	21,38
PV PP	**3500**	30,081
Biogas	**4500**	100
Coal PP	**3800**	37,82
Hydro PP	**2936**	14,13

4 Analysis of Scenario Results

Two scenarios are built on OSeMOSYS platform using MOMANI and GNU solver. Even though the MOMANI interface is very useful in the data entry process, the equations to maintain %40 and %60 renewable energy output flow are set manually on the model files of OSeMOSYS. The permission to edit the model files is an important flexibility of the framework. This property is thought to be greatly welcomed by the analysts having operations research background. MOMANI is not a necessity and researchers would like to edit the raw text files of the model and data files. However this option will need extra time in the modelling process which seems to be a major drawback.

The total annual demand of the city multiplied to 10.42 PJ from 5.28 PJ over the years. Wind and photovoltaic technology installed energy capacities of the city offered a strong stance for the analysts to demand high renewable energy sufficiency ratios. Without any fossil power plant reserve on hand, the city answered the whole energy demand with these two renewable energy sources and demanded new investments of power plants as the demand surpassed the available capacity at the beginning of the predetermined time span. Optimum plan included biomass and geothermal capacity investments at the beginning as these power plants have cost advantage against the other technologies. Combined cycle natural gas power plant investments are engaged after the two already given power plant types. The optimum plan sensitively kept the balance of the cost and % renewable energy ratio in the upcoming years of the whole time span with ignoring further investments on wind and photovoltaic potential as these assets are found to be more expensive to invest on. The complete electrical energy production of the province in the time span for 40% renewable energy scenario is shown in Figure 2 below.

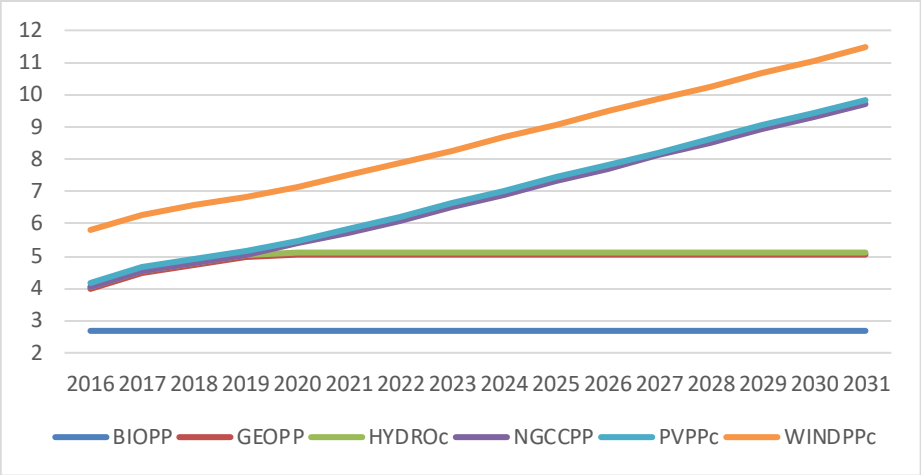

Fig. 2. Energy production by technology type in the time span (in PJ).

As the full potential of the biomass and geothermal energy are reached at the very beginning, these two technologies present a steady line in Figure 2 and natural gas energy supply increases over time. %60 renewable energy scenario gives almost identical results with only an exception of a small sized wind power plant investment in year 2031.

According to the two almost identical outputs, the CO_2 emission amount begins with slightly over 1.9 million tons and increases until 2019. By the end of this year until 2031, the pace of emission amount decreases as the energy need is closed with combined cycle power plants which are more environmentally friendly than biomass and geothermal power plants. The final emission amount reaches to 3.4 million tons by the year 2031. The emission amount over the years is graphed in Figure 3.

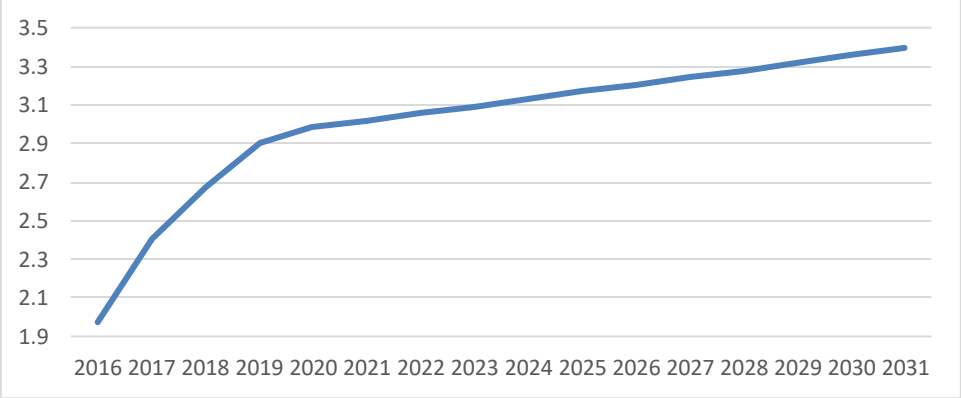

Fig. 3. CO_2 emission output of the 40% scenario (in mtons)

Even though some studies ignore investment costs in the optimization studies and use these costs in return on investment (ROI) calculations, this paper added these cost figures in the optimization process to evaluate their effects on the final outputs.

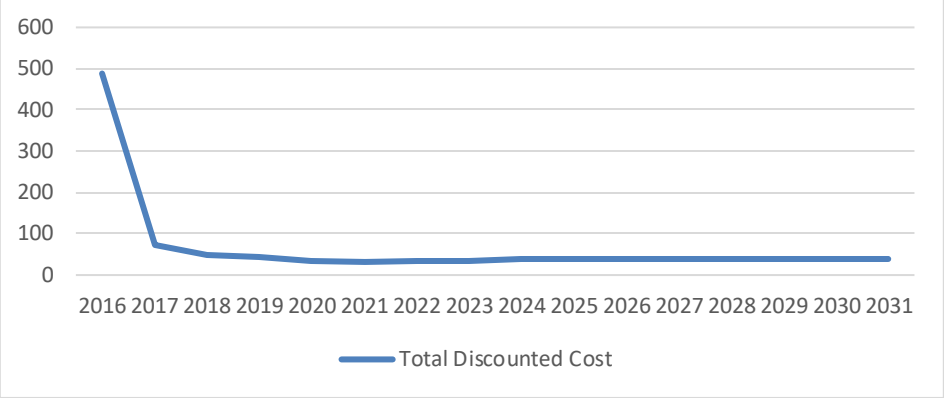

Fig. 4. Costs incurred over time (in Million USD)

Calculations show that the province invests heavily at the beginning of the project time scale since the city is not capable of electrical energy supply self-sufficiency and in the following years the cost amount slows to a relatively low medium. %40 and %60 scenarios both give the results shown in Figure 4.

5 Conclusion

This study introduced a regional analysis including an optimization method including user defined constraints on OSeMOSYS environment. Optimization process highlighted that the OSeMOSYS framework is easy to implement and modify according to the requirements of Afyonkarahisar energy model. Even though the output reporting phase is more time consuming, the framework proved to be a challenging alternative to commercial products.

Two scenarios, including at least %40 and %60 renewable energy are studied in this work for Afyonkarahisar province, Turkey. Scenario outputs are almost identical with only an exception of onshore wind power plant investment in %60 renewable energy scenario in year 2031.

A small city at Afyonkarahisar scale consumes a limited amount of electrical energy. Small amount of energy can be answered by limited renewable energy generators such as biomass and geothermal energy power plants since these assets are not constructed with high capacities like 1 GW or more. If a province has limited renewable energy potential and low annual energy consumption, the limited renewable energy potential can still be sufficient to answer the annual demand pattern in the time span. This is the case for Afyonkarahisar province. The province could answer the demand pattern with desired amounts of renewable energy even by not investing more on

photovoltaic and wind energy power plants. These two sources remain as reserve energy potential that can be activated for higher electrical energy demands in the future. It is certain that if the annual demand of the city increases due to new investments in industry etc the renewable energy amount needed to answer %60 renewable energy condition will require wind and solar reserves which will then initiate debates on the maximum potential of the renewable energy that can be utilized in the province.

This study underlines that the city can meet the %60 renewable energy targets if the decision makers needs to. The region can even meet higher targets in the short run however these more assertive ratios will eventually approach the city's maximum renewable limits in the long run and this policy will have to be evaluated.

This paper presents a regional analysis prepared on OSeMOSYS environment which will trigger more detailed works both in national and regional level in Turkey which will both be useful in the dissemination of the open source projects and the optimization methodology itself.

Acknowledgments

The findings in this paper result from a research project with project number FDK-2019-6839 and is supported by the Scientific Research Projects Coordination Unit of Süleyman Demirel University, Turkey.

References

1. Palz, Wolfgang. The Triumph of the Sun: The Energy of the New Century. CRC Press, 2018.
2. Lovins, L. H. (2015). The Triumph of Solar in the Energy Race. *J Fundam Renewable Energy Appl*, *5*(187), 2.
3. Brook, B. W., & Bradshaw, C. J. (2015). Key role for nuclear energy in global biodiversity conservation. *Conservation Biology*, *29*(3), 702-712.
4. Xie, H., Yu, Y., Wang, W., & Liu, Y. (2017). The substitutability of non-fossil energy, potential carbon emission reduction and energy shadow prices in China. *Energy Policy*, *107*, 63-71.
5. Jiminez, I. (1989, August). Electric power system planning in the framework of the overall energy system. In Proceedings of the 24th Intersociety Energy Conversion Engineering Conference (pp. 2943-2948). IEEE.
6. Loulou, R., Goldstein, G., & Noble, K. (2004). Documentation for the MARKAL Family of Models. *Energy Technology Systems Analysis Programme*, 65-73.
7. Loulou, R., Remme, U., Kanudia, A., Lehtila, A., & Goldstein, G. (2005). Documentation for the times model part ii. *Energy Technology Systems Analysis Programme*
8. Dhakouani, A., Gardumi, F., Znouda, E., Bouden, C., & Howells, M. (2017). Long-term optimisation model of the Tunisian power system. *Energy*, *141*, 550-562.
9. Jalkenäs, F., & Mizgalewicz, M. (2017). Modelling resources to supply Ethiopia with renewable electricity by 2030. KTH Royal Institute of Technology, 2017.
10. Abadie, B. (2020). Power investment outlook for Chile to 2040. KTH Royal Institute of Technology, 2020.
11. Caulcrick, O. O. (2018). The Electricity Model for China–Insights and Implications of Energy Policies. KTH Royal Institute of Technology, 2018.
12. Garlaschelli, M. (2018). Exploring decarbonisation pathways for India'selectricity system using OSeMOSYS. KTH Royal Institute of Technology, 2018.
13. Groissböck, M., & Pickl, M. J. (2016). An analysis of the power market in Saudi Arabia: Retrospective cost and environmental optimization. *Applied energy*, *165*, 548-558.
14. Anjo, J., Neves, D., Silva, C., Shivakumar, A., & Howells, M. (2018). Modeling the long-term impact of demand response in energy planning: The Portuguese electric system case study. *Energy*, *165*, 456-468.
15. Ahmed, A., & Gong, J. (2017). Assessment of the Electricity Generation Mix in Ghana: the Potential of Renewable Energy.
16. Fejzic, E. (2020). Renewable energy outlook for the Drina River Basin countries. KTH Royal Institute of Technology, 2020.
17. Sundin, C. (2017). Exploring the water-energy nexus in the Omo river basin: A first step toward the development of an integrated hydrological-OSeMOSYS energy model.
18. Moura, G., Howells, M., & Legey, L. (2015). Samba the open source south american model base: A brazilian perspective on long term power. *KTH-dESA Working Paper Series*.
19. Tomei, J., Cronin, J., Arias, H. D. A., Machado, S. C., Palacios, M. F. M., Ortiz, Y. M. T., ... & Anandarajah, G. (2020). Forgotten spaces: How reliability, affordability and engagement shape the outcomes of last-mile electrification in Chocó, Colombia. *Energy Research & Social Science*, *59*, 101302.
20. Howells, M., Rogner, H., Strachan, N., Heaps, C., Huntington, H., Kypreos, S., ... & Roehrl, A. (2011). OSeMOSYS: the open source energy modeling system: an introduction to its ethos, structure and development. *Energy Policy*, *39*(10), 5850-5870.

21. Gardumi, F., Shivakumar, A., Morrison, R., Taliotis, C., Broad, O., Beltramo, A., ... & Alfstad, T. (2018). From the development of an open-source energy modelling tool to its application and the creation of communities of practice: The example of OSeMOSYS. Energy strategy reviews, 20, 209-228.
22. Pappis, I. (2016). Electrified Africa–Associated investments and costs. KTH Royal Institute of Technology, 2016.
23. Henke, H. (2017). The open source energy model base for the European union (OSEMBE). KTH Royal Institute of Technology, 2017.
24. Moksnes, N. (2016). UN Sustainable development goals from a Climate Land Energy and Water perspective for Kenya. KTH Royal Institute of Technology, 2016.
25. OSEMOSYS GitHub Repository. https://github.com/OSeMOSYS/OSeMOSYS, last accessed 2021/03/05.
26. Löffler, K., Hainsch, K., Burandt, T., Oei, P. Y., Kemfert, C., & Von Hirschhausen, C. (2017). Designing a model for the global energy system—GENeSYS-MOD: an application of the open-source energy modeling system (OSeMOSYS). *Energies*, *10*(10), 1468.
27. NEMO GitHub Repository. https://github.com/sei-international/NemoMod.jl, last accessed 2021/03/05.
28. Moksnes, N., Welsch, M., Gardumi, F., Shivakumar, A., Broad, O., Howells, M., ... & Sridharan, V. (2015). 2015 OSeMOSYS User Manual. *Royal Institute of Technology, Stockholm, Sweden2015*.
29. Turkish Statistical Institute, 2019 Population of Afyonkarahisar, http://www.tuik.gov.tr/, last accessed 2020/03/20.
30. Energy Market Regulatory Authority (EMRA), Turkish Electricity Market Sector Report 2016 http://www.enerji.gov.tr/File/?path=ROOT%2F1%2FDocuments%2FSekt%C3%B6r%20Raporu%2FEUAS-Sektor_Raporu2016.pdf, last accessed 2020/03/10.
31. Ministry of Energy and Natural Resources (MENR), Electrical Energy Demand Projection Report, http://www.enerji.gov.tr/File/?path=ROOT%2F1%2FDocuments%2FE%C4%B0GM%20Ana%20Rapor%2FT%C3%BCrkiye%20Elektrik%20Enerjisi%20Talep%20Projeksiyonu%20Raporu.pdf, last accessed 2018/03/10.
32. International Energy Agency, Nuclear Energy Agency (2015). Projected Costs of Generating Electricity 2015 Edition.
33. United States Environmental Protection Agency, Direct Emissions from Stationary Combustion Sources, January 2016.
34. Official Site of Zorlu Enerji, https://www.zorluenerji.com.tr/fileuploads/kizildere/teknik-olmayan-ozet-tr.pdf, last accessed 2020/03/20.

An On-board Energy and Environmental Analysis within the Framework of Green Deal

Alperen Sarı[1][0000-0001-9417-3241], Egemen Sulukan[2][0000-0003-1138-2465], Doğuş Özkan[2][0000-0002-3044-4310], Tanay Sıdkı Uyar[3][0000-0002-0960-1203], Levent Erişkin[4][0000-0002-9128-2167]

[1] Marmara University, Mechanical Engineering Department, 34722 Istanbul, Turkey
[2] National Defence University, Mechanical Engineering Department, 34942 Istanbul, Turkey
[3] Beykent University, Department of Mechanical Engineering, 34398 Istanbul, Turkey
[4] National Defence University, Industrial Engineering Department, 34942 Istanbul, Turkey

alperensari@gmail.com, esulukan@dho.edu.tr, dozkan@dho.edu.tr, tanayuyar@beykent.edu.tr

Abstract. After the industrial revolution, advances in science, industry and technology cause relative abundance and the development of economies. Trade and transportation sectors are also developing in line with the development of economies. However, in order for the prosperity and abundance brought about by industrialization to be sustainable, the environment must be protected. Within the scope of environmental protection, many international measures are taken that concern every sector and investments are made to reduce greenhouse gas emissions, increase energy efficiency and develop alternative energy generation technologies. Decision support tools have been used significantly in all sectors in the last quarter century in order to help decision-makers and to produce alternatives to changing situations. Maritime trade and ships, one of the most important milestones of the transportation industry for centuries, constitute an important part of the greenhouse gas emitted worldwide. In this study, it is aimed to reduce carbon emissions from sea transportation and ships. In this context, energy analysis of a chemical tanker ship within the framework of the Reference Energy System concept has been performed. The calculations made with the LEAP Decision Support Tool in line with the decisions taken by the European Union and were analyzed in detail.

Keywords: Energy Modelling, Reference Energy System, LEAP, Maritime Sector, Greenhouse Gas Emissions.

1 Introduction

The figures on world trade show that seas have been important in international trade throughout history and that the cargoes transported by sea are constantly increasing [1]. The globalization of the world economy, the cross-border production and consumption relations as well as the advantages offered by sea transport played a role in this increase. These advantages can be counted as cheaper sea routes compared to air,

land and railways, less pollution to the environment, lower energy consumption, and the ability to transport large quantities of products such as raw materials at once and safely.

As shown in Fig. 1, the change in global production and the change in sea trade are directly proportional. When we examine the recent period, it is seen that the world maritime trade was behind the expectations with development of 2.7% in 2018. This rate was 4.1% in 2017 as a result of the fastest development of the last five years. Maritime trade is highly affected by political and economic developments at the global level. Tensions such as the spread of national trade restrictions, geopolitical conditions and sanctions, environmental regulations, the Strait of Hormuz as a strategic maritime point, as well as trade wars between China and America, can be counted as the main factors in the decline of this growth momentum. With the addition of the covid-19 epidemic to the stagnant economy experienced in recent years, it seems that there was a great decline in the economy and maritime trade worldwide in 2019 and 2020. It is expected in the report published by UNCTAD that 2021 will achieve a breakthrough with a recovery [2].

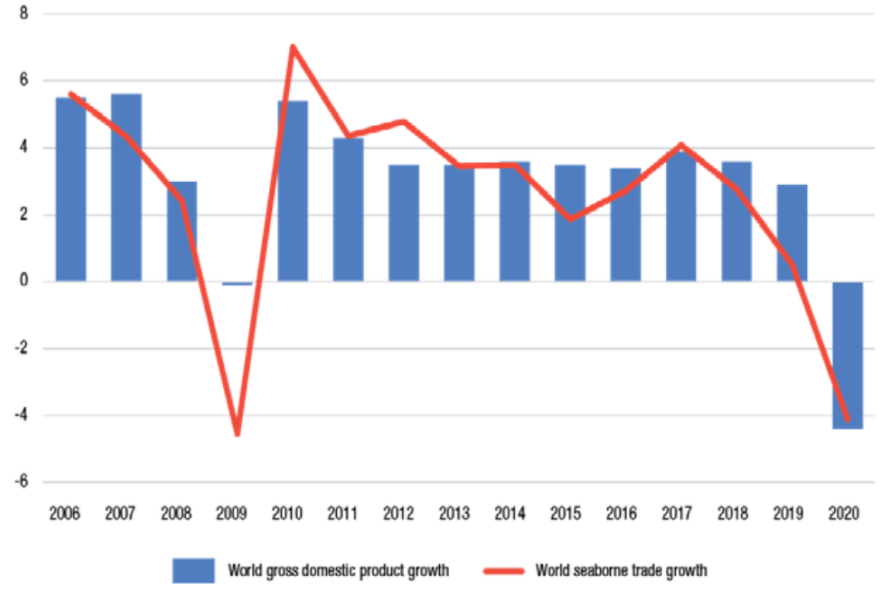

Fig. 1. Development of international maritime trade and global output, 2006–2020 (Annual percentage change) [2]

Another development affecting maritime transport is the new emission requirements and the accompanying cost increases.

1.1 Greenhouse Gas Emissions in Maritime Sector

When the global greenhouse gas emissions are examined, the transportation sector constitutes approximately one-fourth of the total greenhouse gas emissions as shown

in Fig. 2, while the greenhouse gas emission from the maritime sector accounts for 3 percent of this [3].

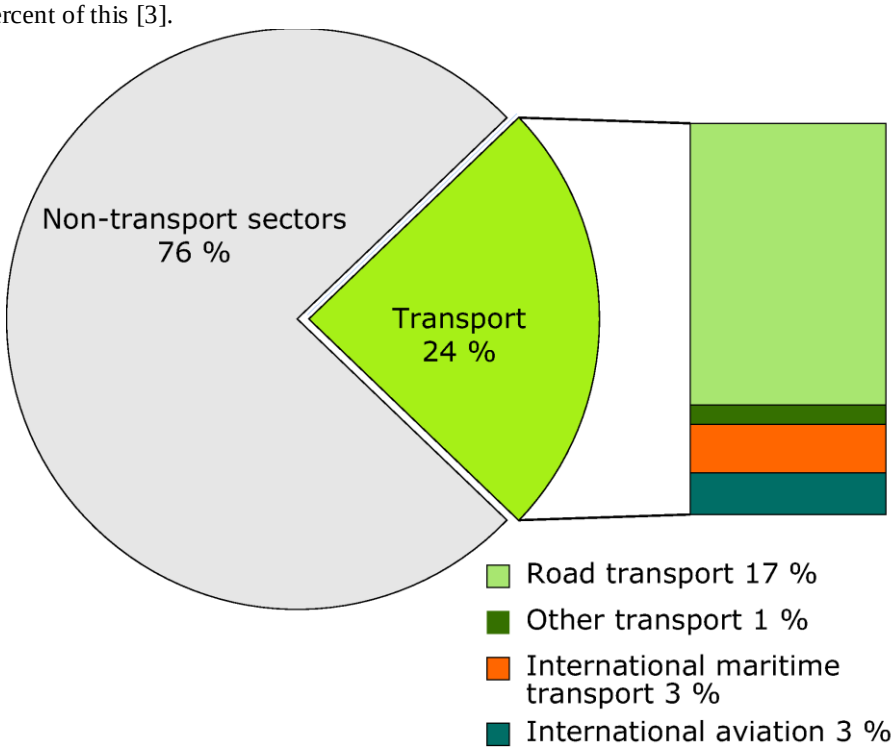

Fig. 2. Transport sector contribution to total GHG emissions, 2009 (EEA-32) [3].

Although there is an overall decrease in some pollutants from road transport (not carbon dioxide), pollutants from aviation and maritime continue to increase. Global aviation and shipping together are expected to account for almost 40% of global carbon dioxide emissions by 2050 if further emission reduction measures are not taken [4]. Maritime activities also lead to significant greenhouse gas emissions and air, noise and water pollution. If action is not taken, carbon dioxide emissions from global maritime activities alone could account for 17% of all carbon dioxide emissions by 2050 [4].

IMO has taken an important step to reduce the emissions from ships with the decision taken in 2016 to reduce the negative impacts of ships on the environment. The IMO Marine Environment Protection Committee aims to reduce greenhouse gas emissions from ships by 50 percent by 2050, carbon intensity by 40 percent by 2030 and by more than 80 percent by 2050 [5]. In the long run, emissions are aimed to be eliminated completely.

1.2 EU Green Deal

The European Union is the richest and largest economy in the world. Therefore, it has an important place in world trade. It is a fact that maritime transport, which is the world's largest trade area, is of great importance for the EU economy. Considering that roughly 90% of the EU's foreign trade and more than 42% of trade between its 27 members is by water, the EU certainly acknowledges the strategic, political and economic importance of shipping to the EU economy and prosperity [6]. Maritime transport and ports have an important place in European trade and economy, with both the transportation of consumed goods and the provision of raw materials for production.

Considering carbon emission restrictions, shipping is one of the few industries today that does not have binding measures to reduce carbon emissions. In addition, no payment is made due to carbon emission pollution. However, maritime in Europe cause high emissions of carbon emissions. According to Transport & Environment, Europe's leading clean transport campaign group, If Maritime was a country, it would be the 8th country emitting the most emissions in Europe (Stambler, 2020).

When the regulations within the European Union are examined, although the carbon emissions from ships have been monitored within the scope of the EU MRV since 2015, it does not have a restrictive feature to reduce carbon emissions. EU MRV was created to monitor and report marine CO2 emissions and other relevant information (European Union, 2015). In line with the information to be obtained here, it is planned to create a roadmap to reduce the amount of carbon emissions from the maritime sector.

The European Union (EU), known for its sensitivity to environmental and social sustainability issues, especially the fight against climate change, reduction of greenhouse gas emissions, use of renewable energy since the 1990s, took these sensitivities one step further in November 2019, It has presented a package of initiatives, a commitment to take decisive and ambitious steps in environmental and sustainability issues: the European Green Deal. The Green Deal is the EU's new growth strategy that includes the basic objectives of zeroing net greenhouse gas emissions by 2050, decoupling economic growth and leaving no one and no region behind. In other words, the Consensus will create jobs and improve the quality of life while reducing emissions.EU Green Deal has emerged with the goal of making Europe, including the maritime sector, the first continent in the world to reduce all carbon emissions to zero.

Within the framework of the EU Green Deal, it updated its 2030 and 2050 emission reduction targets for all sectors, including maritime. In this context, with the European Green Deal announced by the European Union (EU) Commission in December 2019, the EU plans to reduce its carbon emissions by 55 percent by 2030 and reach the zero carbon emission target by 2050.

2 Materials and Methods

In this study, it is aimed to perform energy and emission analysis and modeling of a chemical tanker ship using a decision support tool with the reference energy system (RES) concept within the framework of the EU Green Deal 2030 and 2050 targets.

2.1 RES Concept, Decision Support Tools and LEAP

The reference energy system concept is the most basic diagram showing the energy conversion of a simple or complex system from source to demand. As shown in Figure 1, after entering a primary energy source into a system, it turns into final energy resources in conversion and process technologies and meets the demands of that system by using it in demand technologies. Decision support tools are programs that are used to analyze the current state of a system and the changes that may occur in the future from the perspective of energy, economy, environment and engineering with the RES concept. Decision support tools are especially used by decision-makers in recent times because they ensure that the possible consequences are foreseen and the negative effects that may be experienced are minimized when making decisions on a house, building, city, region, country, the continent or global scale.

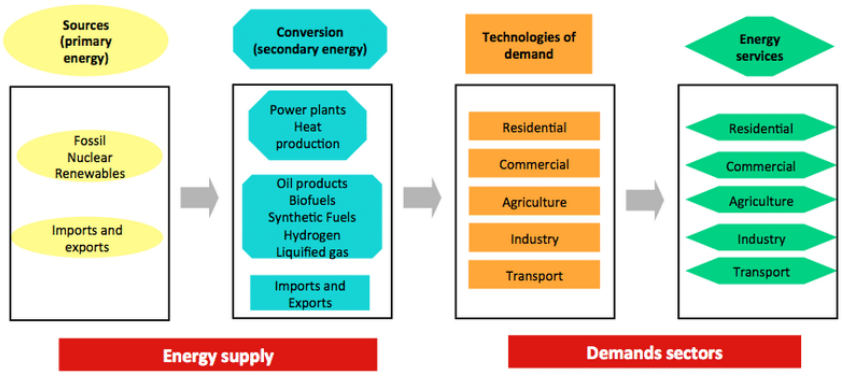

Fig. 3. Reference Energy System Diagram [9]

There are dozens of decision support tools that are widely used around the world and supported by institutes, corporate firms, non-governmental organizations or international organizations [10]. Commonly used decision support models are shown in table 1.

Table 1. Modeling tools [11]

Nu	Name	Developer	Platform	Methodology
1	ENPEP-BALANCE	Argonne National Lab	Windows	Simulation
2	EnergyPLAN	Aalborg University, Denmark	Windows	Simulation/ Optimization
3	FlexTool	IRENA	Excel/GLPK (Windows)	Optimization
4	GEMIS	IINAS	Windows	Accounting
5	HOMER Pro	HOMER Energy LLC	Windows	Accounting/ Optimization
6	LEAP	SEI	Windows	Accounting/ Simulation/ Optimization
7	MESSAGE	IAEA and IIASA	Windows	Optimization
8	RETScreen	NRCAN	Excel or Windows	Accounting
9	TIMES/MARKAL	ETSAP	Windows	Optimization
10	WEAP	SEI	Windows	Accounting/ Simulation

The Low Emissions Analysis Platform (LEAP) is a decision support modeling tool designed to estimate the energy consumption, CO2 emissions and cost of a given energy system in both real-world and hypothetical scenarios [12]. The LEAP modeling tool, which can analyze the economic and environmental aspects of energy demand and transformations in a particular region or economy, was developed by the Stockholm Environment Institute [11]. In order to make an analysis, the alternative scenarios to be developed by first creating under the basic scenario current account are analyzed with reference to this situation [13]. LEAP is a user-friendly, simple, technically rich and flexible modeling tool that enables comprehensive analysis [14]. LEAP is used extensively in many organizations at the local, academic, national and international levels to shape the future of energy, to show its environmental impact, and to establish new energy policies by identifying possible future challenges.

In this study, a chemical tanker ship was analyzed from an energy, engineering and environmental perspective, using the reference energy system concept and the LEAP decision support modeling tool within the scope of the EU Green Deal.

2.2 Reference Energy system of a Ship

A ship has an energy complex structure. The primary energy source used in the ship is imported and transformed into the final energy form required by demand technologies through the conversion and process technologies within the ship. A ship's primary energy source is HFO and MDO. In this study, we made analyzes to reduce the carbon emission of a chemical tanker ship, which is seen in figure 4, belonging to the transal shipping company, within the framework of the EU Green Deal. In this context, RES shown in figure 5 was created and defined to the LEAP energy model.

Fig. 4. The reference energy system of a chemical tanker ship.

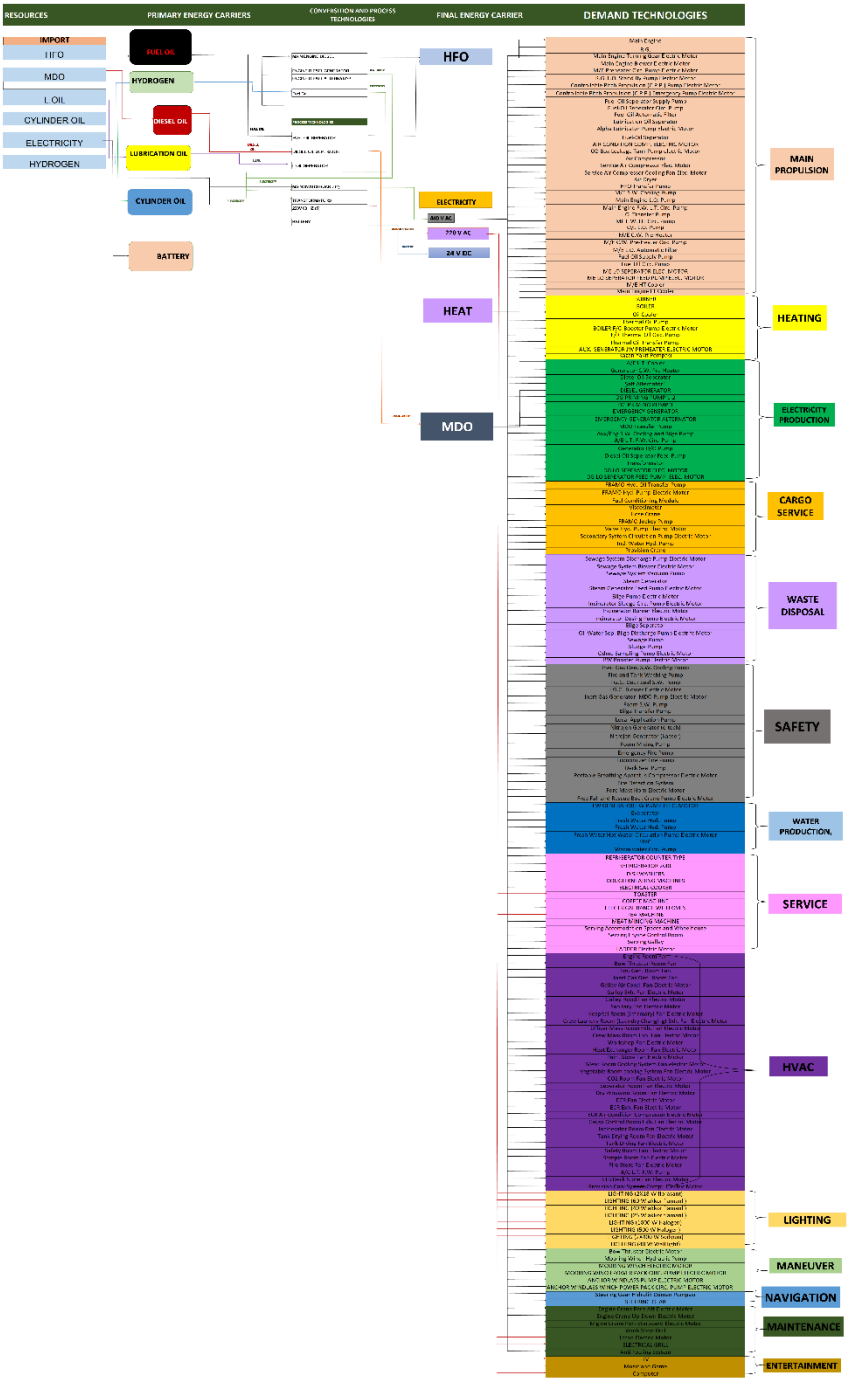

Fig. 5. The reference energy system of a chemical tanker ship.

3 Energy System Analysis of a Chemical Tanker Ship Via LEAP

In the LEAP system, the basic parameters should be determined first. In the basic parameters, information such as the year in which the current situation analysis will be performed, the year and time period when the analysis will end are entered in the basic scenario.

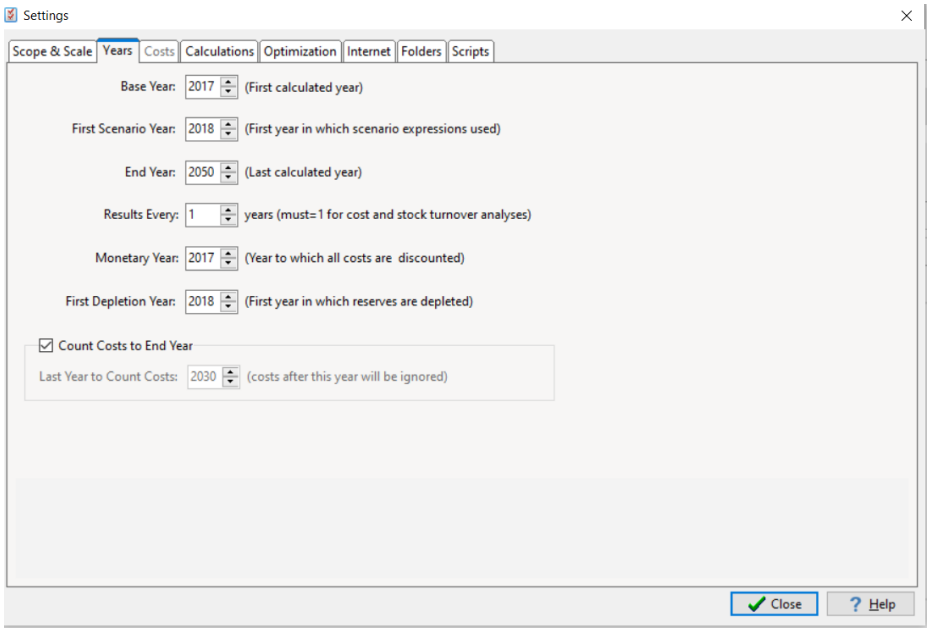

Fig. 6. LEAP basic parameters

For use in our analysis, 2017 was determined as the reference year by taking bunkering, cruise, port, device operating hours and technical documentation information of the Diamond-T ship from Transal Shipping. We planned to make our analyzes annually and set the end date of the analysis as 2050 within the scope of the EU Green Deal. After the basic parameters shown in fig. 6 such as analysis start year, analysis period, analysis end year were entered into LEAP, the demands and technologies under the demands in RES were defined to LEAP. Then, energy balance analysis was performed by entering the determined parameter values such as efficiency, availability, capacity, historical production, activity level, energy intensity into LEAP. Later, environmental factors were selected using the LEAP library and emission analyzes were made. Against our basic scenario, Business As Usual (BAU), EU Green Consensus 2030 targets and EU Green Consensus 2050 targets scenarios were created and analyzed against the reference scenario.

3.1 Energy Balance Analysis of a Diamond-T

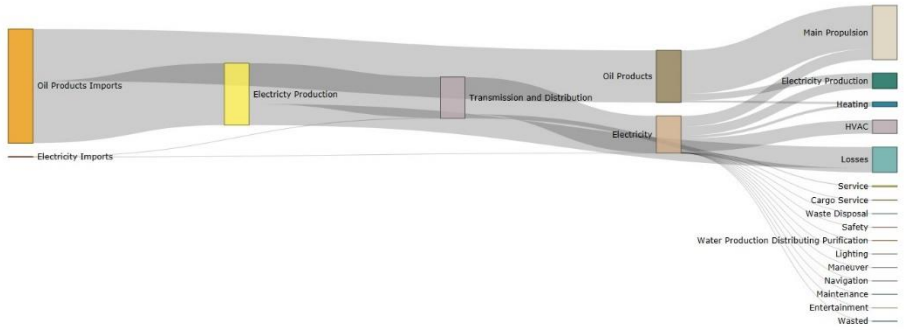

Fig. 7. Representation of energy balance analysis with Sankey Diagram

Table 2. Energy balance for area chemical tanker ship

Scenario: Business As Usual, Year: 2017, Units: Million Gigajoule	Electricity	Oil Products	Total
Production	-	-	-
Imports	1.032	219.333	220.365
Exports	-	-	-
Total Primary Supply	1.032	219.333	220.365
Main Propulsion	78.294	-119.224	-40.930
Transmission and Distribution	-7.933	-	-7.933
Total Transformation	70.361	-119.224	-48.863
Main Propulsion	20.649	83.748	104.396
Electricity Production	17.173	12.470	29.643
Cargo Service	0.480	-	0.480
Heating	5.138	3.892	9.030
Waste Disposal	0.013	-	0.013
Safety	0.107	-	0.107
Water Production Distributing Purification	0.040	-	0.040
Service	1.667	-	1.667
HVAC	25.883	-	25.883
Lighting	0.123	-	0.123
Maneuver	0.010	-	0.010
Navigation	0.098	-	0.098
Maintenance	0.010	-	0.010
Entertainment	0.003	-	0.003
Total Demand	71.393	100.109	171.503

The entire energy requirement of the chemical tanker ship we analyzed is met by fossil resources. The main energy requirement of the ship is met by HFO and MDO and these fuels are imported. As can be seen in Figure 7, while the main propulsion system uses the majority of the energy need of the ship, energy losses are in the second place. The energy demand and total energy demand of each demand for the chemical tanker ship are shown in table 2. Accordingly, 220,365 million gigajoules of energy is imported to meet the energy demand of 171,503 million gigajoules. Approximately 22% of imported energy is lost during energy conversion and transmission.

4 Scenarios and Results

After creating the baseline scenario using 2017 data, all scenarios were developed accordingly, assuming that the demand for maritime transport will increase by 3% annually, depending on the developing economy and increased production. In this study, a total of 3 scenario analyzes were made. The main purpose of these analyzes is to calculate how much emissions from ships should be reduced within the framework of the EU Green Consensus 2030 and 2050 targets. The BAU scenario has been analyzed in order to show the total emission amount to be emitted by a ship if no other measures are taken other than these scenarios.

4.1 Results of BAU Scenario

In BAU scenario; without taking any measures, a situation analysis was carried out between 2017-2050, considering that the demand for the maritime sector will increase by 3 percent every year.

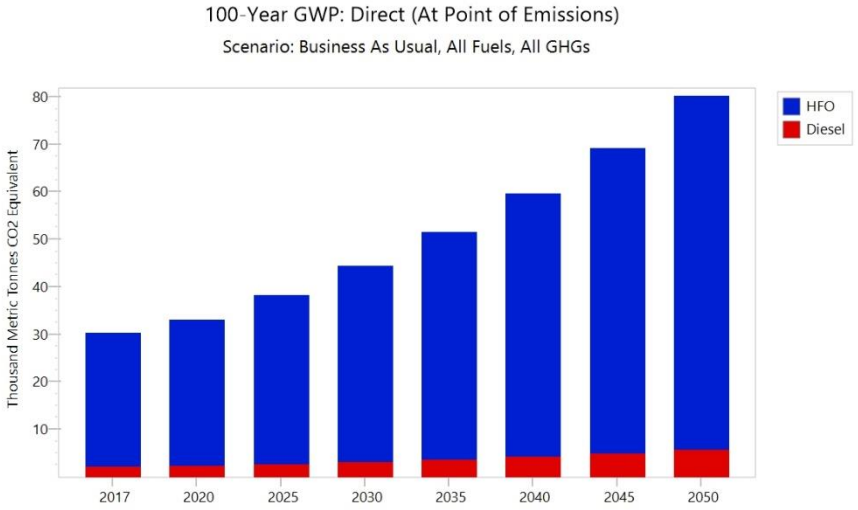

Fig. 8. BAU Scenario emission analysis

Table 3. BAU Scenario emission amounts (Units: Thousand Metric Tonnes CO2 Equivalent)

Branch	2017	2020	2025	2030	2035	2040	2045	2050
HFO	28.009	30.606	35.481	41.132	47.683	55.278	64.083	74.289
Diesel	2.205	2.409	2.793	3.238	3.753	4.351	5.044	5.847
Total	30.214	33.015	38.274	44.370	51.437	59.629	69.127	80.137

In the BAU scenario, a chemical tanker ship emitted 30.214 thousand metric tons of CO2 equivalent in 2017, while the emitted CO2 emission in 2030 increased to 44.370 thousand metric tons of CO2 equivalent, and in 2050 80.137 thousand metric tons of CO2 equivalent emission. Table 3 and Figure 8 show that, if no measures are taken, the amount of CO2 emissions emitted from a ship will increase by 1.5 times in 2030 and 2.5 times in 2050 compared to 2017.

4.2 Results of EU Green Deal 2030 Scenario

In this scenario, an analysis has been made in line with the EU's goal of reducing the carbon emission rate by 55% compared to the 1990 level in 2030, which is set within the scope of the Green Agreement. Accordingly, since 2017 is the reference year at our disposal, a 55% reduction in the amount of carbon emissions in 2030 compared to 2017 was analyzed in the analysis.

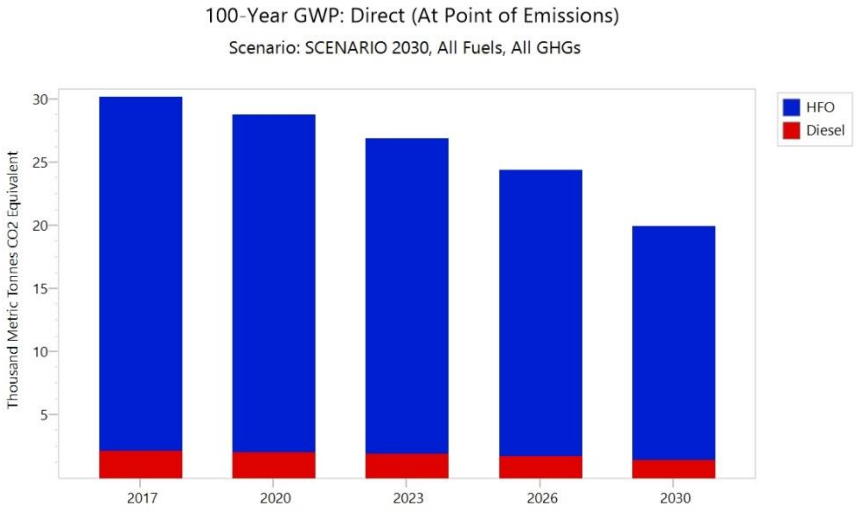

Fig. 9. EU Green Deal 2030 Scenario emission analysis

In this analysis, which is made considering that the demand for maritime will increase by 3% every year, it is seen in fig. 9 and table 4 that the amount of CO2 emission from a chemical tanker ship within the scope of the EU Green Deal targets in 2030 should decrease to 19.966 thousand metric tons of CO2 equivalent.

Table 4. EU Green Deal 2030 Scenario emission amounts (Units: Thousand Metric Tonnes CO2 Equivalent)

Branch	2017	2020	2023	2026	2030
HFO	28.009	26.722	24.955	22.630	18.509
Diesel	2.205	2.103	1.964	1.781	1.457
Total	30.214	28.825	26.919	24.411	19.966

4.3 Results of EU Green Deal 2050 Scenario

In this scenario, in addition to the EU Green Deal 2030 targets, the 2050 targets are also included in the analysis. In this context, the chemical tanker ship is aimed to emit zero carbon in 2050.

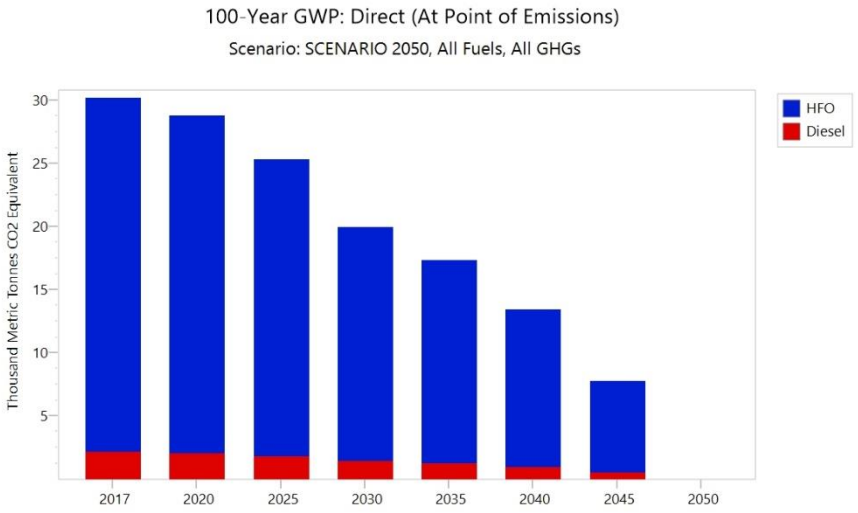

Fig. 10. EU Green Deal 2050 Scenario emission analysis

In order for a chemical tanker ship to reach its zero carbon emission target by 2050; After achieving the EU Green Deal 2030 targets, the amount of CO2 emissions should be reduced to 13.417 thousand metric tons of CO2 equivalent emission in 2040 and to the level of 7.777 thousand metric tons of CO2 in 2045.

Table 5. EU Green Deal 2050 Scenario emission amounts (Units: Thousand Metric Tonnes CO2 Equivalent)

Branch	2017	2020	2025	2030	2035	2040	2045	2050
HFO	28.009	26.722	23.472	18.509	16.093	12.438	7.209	-
Diesel	2.205	2.103	1.848	1.457	1.267	0.979	0.567	-
Total	30.214	28.825	25.320	19.966	17.360	13.417	7.777	-

The emission amounts of a chemical tanker ship emitting 30,214 thousand metric tons of CO2 equivalent in 2017 until it reaches zero emissions by 2050 are shown in figure 10 and table 5.

5 Conclusion

The maritime sector still stands out as one of the sectors where the least steps have been taken towards reducing the amount of CO2 emissions. The European Union wants to lead the maritime sector and to be the first continent in the international arena by taking the maritime sector into the scope of the sectors that will make zero carbon emission with its Green Deal goals.

In this context, firstly, efforts should be made to achieve the Green Deal 2030 targets. In addition to conducting research and development studies to enable the use of clean and sustainable alternative fuels until 2030, it is considered that success can be achieved by taking measures to increase efficiency in operational, technical and shipbuilding stages. In the operational sense, the use of scrubbers is increasingly widespread to increase technical efficiency, while using methods of selecting short ship routes and using wind and currents to increase efficiency. In the shipbuilding sector, it is aimed to reduce CO2 emissions by increasing efficiency with methods such as reducing body friction and design optimization.

It is considered that the use of clean and sustainable alternative fuels will be the definitive solution for achieving the EU Green Deal 2050 targets. For this reason, although the use of hydrogen as the most suitable fuel comes to the fore today, there is currently no sustainable and clean energy source to meet all the energy needs of a ship.

References

[1] Thomas, T. A., Atkins, W. A. : Transportation, http://www.waterencyclopedia.com/St-Ts/Transportation.html.,last accessed 2021/03/30.

[2] United Nations Conference on Trade and Development (UNCTAD), Review of Maritime Transport 2020, United Nations Publications, Geneva, 2020.

[3] European Environment Agency, Transport sector contribution to total GHG emissions, 2009 (EEA-32), https://www.eea.europa.eu/data-and-maps/figures/transport-sector-contribution-to-total, last accessed 2021/03/30.

[4] Cames, M., Graichen, J., Siemons, A., Cook, V., Emission reduction targets for international aviation and shipping., Policy Department A: Economic and Scientific Policy, European Parliament, B-1047 Brussels, 2015.

[5] IMO, Marine Environment Protection Committee (MEPC), 72nd session, 2018.

[6] Damen, M., Fact Sheets on the European Union, https://www.europarl.europa.eu/factsheets/en/sheet/160/the-european-union-and-its-trade-partners., last accessed 2021/04/30.

[7] Stambler, M., EU Green Deal takes bold steps toward cutting shipping emissions, wartsila.com/insights/article/eu-green-deal-takes-bold-steps-toward-cutting-shipping-emissions., last accessed 2021/04/30.

[8] European Union, REGULATION (EU) 2015/757 OF THE EUROPEAN PARLIAMENT AND OF THE COUNCIL of 29 April 2015 on the monitoring, reporting and verification of carbon dioxide emissions from maritime transport, and amending Directive 2009/16/EC, Official Journal of the European Union, pp. 55-76, 2015.

[9] Babonneau, F., Haurie, A., Energy technology environment model with smart grid and robust nodal electricity prices., Annals of Operations Research, 274, 1, pp. 101-117, 2019.

[10] Sulukan, E., Sarı, A., Özkan, D., Uyar, T. S., A Decision-Making Tool Based Analysis of Onboard Electricity Storage., In: 14th International Renewable Energy Storage Conference 2020 (IRES 2020), 2020.

[11] Heaps, C., LEAP: The Low Emissions Analysis Platform. [Software version: 2020.1.33], Stockholm Environment Institute. Somerville, MA, USA., 2021. https://leap.sei.org.

[12] Emodi, N. V., Emodi, C. C., Murthy, G. P., & Emodi, A. S. A., Energy policy for low carbon development in Nigeria: A LEAP model application, Renewable and Sustainable Energy Reviews, 68, pp. 247-261, 2017.

[13] Sulukan, E., Uyar, T. S., Beşikci, D., Özkan, D., Sarı, A., Energy System Analysis, Simulation and Modelling Practices in Turkey., In Accelerating the Transition to a 100% Renewable Energy Era , Cham, Springer, 2020, pp. 485-506.

[14] Sulukan, E., Özkan, D., & Sarı, A., Reference energy system analysis of a generic ship, Journal of Clean Energy Technologies, 6, 5, pp. 371-376, 2018.

An Energy System Simulation of Turkey with A Carbon-Neutral Scenario

Emre Leblebicioğlu[1][0000-0001-9974-3645], Egemen Sulukan[2][0000-0003-1138-2465], Tanay Sıdkı Uyar[3][0000-0002-0960-1203]

[1]*Marmara University, Department of Mechanical Engineering, Istanbul, Turkey,*

[2]*National Defence University, Turkish Naval Academy, Department of Mechanical Engineering, Istanbul, Turkey*

[3]*Beykent University, Department of Mechanical Engineering, Istanbul, Turkey*

leblebicioglu.emre@gmail.com

esulukan@dho.edu.tr

tanayuyar@beykent.edu.tr

Abstract. Decreasing the usage of fossil fuels in electricity production is a tough challenge for countries. The world is still depended on fossil fuels to generate electricity. Increasing the share of renewable energy systems in electricity production is significant in many aspects such as lower CO2 emissions, grid flexibility, decentralizing, etc. Nowadays, many countries shape their energy policies and strategies to use more renewable and indigenous resources. Turkey is one of these countries and has ambitions goals to use more domestic sources to produce electricity. Turkey generally aims to reduce the usage of imported energy sources in electricity generation. Thus this paper investigates the share of a 75% renewable energy system (RES) or carbon-neutral simulation in electricity production via the EnergyPLAN model. An energy system analysis was conducted in a 75% renewable scenario in 2053. The main target of this scenario is to perform a 75% renewable energy system in electricity production. A reference year is 2018 and the results of the 75% RES scenario were compared with a reference scenario. The main focus of this study is to investigate aspects of carbon emissions, RES share, and costs between the scenarios for the years 2018 and 2053.

Keywords: EnergyPLAN, Energy System Simulation, Renewable Energy System

1 Introduction

Since the industrial revolution, energy trends have been transformed from one source to another. A story of energy started with a flame in humans' early ages and reached today as green energy sources. Nowadays, there is a profound change in the energy industry from fossil fuels to renewable energy sources, and this change is also known as the clean energy transition. Many countries have ambitious energy policies to decrease their carbon footprints and accelerate the clean energy transition because of climate change's adverse effects.

The Paris Agreement's long-term temperature goal is to keep the increase in global average temperature to well below 2 °C above pre-industrial levels; and to pursue efforts to limit the increase to 1.5 °C, recognizing that this would substantially reduce the risks and impacts of climate change [2]. Countries are shaping their existing energy systems with a high rate of renewables. Such that renewable energy broke a new record in 2019, and installed power capacity rose more than 200 GW [1].

Renewable energy systems lead the clean energy generation and zero carbon emission implementations. A total of 181 GW of renewable power was added in 2018, and installed renewable power capacity reached 2378 GW, according to REN 21 Global Status Report [1] by the end of September in 2019, the installed power capacity of Turkey reached 90720 MW and the distribution of this installed power by resources is as follows 31,4% hydraulic, 29,0 % natural gas, 22,4 % coal, 8,0% wind, 6,0% solar, 1,5% geothermal and 1,7% other sources [2]. Furthermore, Turkey's total renewable power capacity is 44588 MW, almost half of the total power capacity of Turkey [2]. Turkey's long-term energy plan is based on increasing renewable capacity and energy efficiency in the power production sector.

The energy shifting from fossil fuels to renewables brings many challenges at the national and regional level. Furthermore, estimating future energy demand is another challenge to set an energy policy and plan. Due to the importance of energy policies, the simulating and planning of national energy systems are getting more critical than ever before.

The world has no choice but clean and sustainable energy solutions. Hence, renewables in energy generation should be increased, and renewable sources should lead to electricity and heat production at the national level.

2 Background

2.1 Energy Overview of Turkey

Turkey supplies its energy demand with various sources such as lignite, hard coal, imported coal, natural gas, petrol and renewable resources. Turkey's energy production is based on fossil fuels, mainly coal and natural gas. Moreover, Turkey's energy demand is growing day by day, and this brings some concerns, such as rising fuel dependence. Thus, Turkey set some energy policies which are considered to provide energy independence for the country.

Energy consumption of Turkey.

Turkey is a growing country, and its energy consumption is rising every year due to industrialization and population growth. Turkey's primary energy consumption increased by 2,2% to 304 TWh in 2018, and its electricity generation went up by 2,5 % to 304,8 TWh. Furthermore, according to the base scenario, electricity consumption is expected to increase by 4,3 % annually and reach 375,8 TWh in 2023 [3].

Energy generation of Turkey and resources.

Turkey generates electricity by different energy sources such as fossil fuels and renewable sources. At the end of 2018, Turkey supplied its energy demand by 37,8 % coal, 30,3% natural gas, 19,7% hydropower, 6,5% wind, 2,6% solar, 2,4% geothermal and 1,3% from other sources [2].

The installed power capacity of Turkey reached 88.551 MW by the end of 2018. This capacity consists of 31% hydropower, 29,5% natural gas, 22,2% coal, 7,9% wind, 1,4% geothermal, 5,7% solar and 1,4% other sources [3].

2.2 Renewable Energy Potential of Turkey

Renewable energy sources provide countries both energy independence and a cleaner environment. Hence the renewable source potential is significant for the growing countries like Turkey. Turkey is located between Europe and Asia, and it is like a bridge between two continents. Along with its strategic location, Turkey has immense renewable energy potential, especially for solar and wind energy, due to its geographical location.

Even though the energy density per square meter of solar and wind is high, the installed solar and wind power capacity is not as high as their potential. Renewable power production is growing in Turkey through new energy policies and investments.

The renewable installed capacity of Turkey in 2018 is 42.215 MW, including solar, wind, hydro, geothermal, biomass. Hydropower and wind energy lead to total energy production in Turkey [4].

Table 1: Renewable Energy Potential of Turkey by Resources [16-20].

Sources	Theoretical Potential	Feasible Potential
Solar	6150 TWh/year	305 TWh/year
Wind	88000 MWe	45000 MWe
Hydropower	433000 MW	127381 MW
Wave	-	10 TWh/year
Geothermal	38000 MW	4500 MW
Biomass	389,79 TWh/year	197,71 TWh/year

3 Methodology

3.1 EnergyPLAN Energy System Simulation Tool

EnergyPLAN is an input/output hourly simulation tool, which is used for energy system analysis at national or regional level. EnergyPLAN computer model was developed by Aalborg University, Denmark. This model is based on hourly values during a year period and carries out technical simulations and market-economic simulations.

The fundamental purpose of this model is to assist the design of regional and national energy system strategies and policies.

The model has inputs and outputs. Inputs of this model are renewable energy sources, demands, costs, installed power plant capacities and a number of optional different simulation strategies. Outputs are energy balances, fuel consumption, total costs, import/exports and annual productions [5].

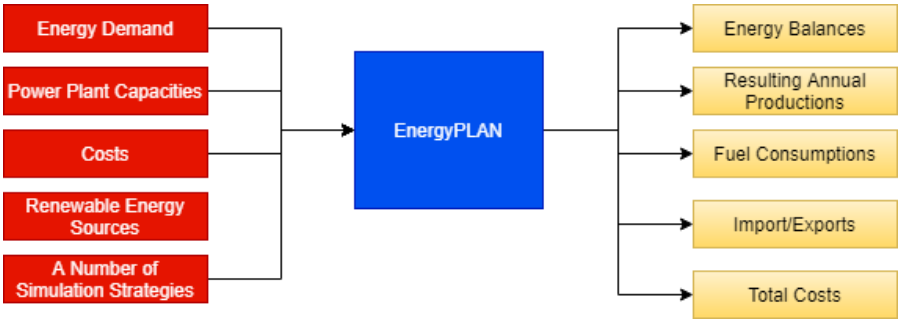

Figure 1: EnergyPLAN Input and Output [5].

4 Energy Scenarios

4.1 Reference Energy System Scenario of Turkey (RES)

Creating a reference energy system scenario is the first step of an energy system simulation. The reference scenario identifies the existing energy systems and energy demand into the EnergyPLAN model. For the reference scenario, a reference year should be determined. In this study, 2018 was chosen as the reference year. Because, 2018 is the last year in which the approved data can be found. After creating the reference scenario, alternative scenarios such as a 100% renewable energy system are implemented according to the reference scenario.

The reference energy model. The reference energy model shows differences between future energy system scenarios and the existing energy system. All actual data in 2018 was inserted into the software to build the reference energy model. The fundamental goal of this model is to compare results with other scenarios created for 2023 and 2053. Moreover, the total electricity demand in 2018 is 304,2 TWh/year. Table 2, which is given below, shows Turkey's installed electricity capacity by sources in 2018.

Table 2: Installed Electricity Capacity by Sources in 2018 [6].

Power Plants	Installed Capacity (MW)	Annual Electricity Production (TWh/year)
Geothermal	1260	6,92
Coal	19557	111,802
Fuel Oil+Nafta+LNG	709	1,43
Natural Gas	25647	90,085
Dammed Hydro	20505	40,88
Onshore Wind	6950	19,85
Solar PV	5063	5,73
River Hydro	7749	18,83
Biomass+Waste	946	2,31
Imported Electricity	1200	6,35
Total	**88386**	**304,19**

Model validation. A reference energy scenario was created for the year 2018. The existing energy system in Turkey was identified into the EnergyPLAN software, and results were compared with actual data for the model validation.

This scenario was created by actual energy demand and supply data. All data were taken from energy balance tables [7] and EPIAS-Transparency Platform [8]. After establishing the reference EnergyPLAN model, this model's outputs were compared with EPIAS electricity generation and production data, as shown in Table 3 below.

Table 3: Model Validation between EPIAS Data and EnergyPLAN Model Output

Demand and Supply	EPIAS Data (TWh)	EnergyPLAN Model Output (TWh)	Difference (%)
Demand	304,2	304,2	-0,01
Wind	19,85	19,9	-0,25
Solar	5,76	5,84	-1,37
Hydro-Dams	41,01	41,06	-0,12
Geothermal	6,92	6,92	0,02
Hydro-Rivers	18,88	19,86	0,1
Thermal Power	203,7	205,53	-0,89

As shown in Table 3, differences between EnergyPLAN output and EPIAS data are acceptable, which means all technical data, such as the annual hourly supply and the demand data, were identified to the software correctly. Then, renewable energy and indigenous scenarios can be built on this reference scenario.

The reference energy scenario shows that the RES share is 31,6%, and the amount of yearly electricity production by renewables is 96,20 TWh/year.

Fuel consumption and CO2 emissions. Turkey's existing energy system is mostly depended on fossil fuels, especially coal. Turkey imports a significant amount of natural gas and coal every year to use for power generation and heating. Table 4, given below, shows the amount of annual fuel consumption by sources and CO2 emissions. The amount of renewable electricity production can also be seen in this table.

Table 4: General Outputs of the Reference Scenario

The Share of RES	
RES Share of Electricity Production	31,6%
RES Electricity Production	96,20 TWh/year
Annual Fuel Consumption (TWh/year)	
Fuel Consumption (total)	467,31
Natural Gas Consumption (total)	96,61
Biomass Consumption	5,08
Coal Consumption	363,31
Annual CO_2 Emissions	
CO_2 Emission (Mt)	144,587

The RES share, fuel consumption, costs and CO2 emissions are the main parameters for comparing scenarios with scenarios. In the reference scenario, 467,31 TWh/year equivalent fuel was consumed, and 144,587 Mt CO2 was released to the atmosphere. Furthermore, the RES share of this scenario is only 31,6%, and 96,20 TWh electricity was generated by renewable sources in 2018.

Cost of the reference energy scenario. The cost of energy systems is another critical parameter that needs to be analyzed. The estimated costs of Turkey's existing energy system were calculated and identified in the software. The annual fixed operation-maintenance and installed costs of power plants in 2018 were calculated, using the average costs between 2010 and 2018 [9].

Table 5: Costs of Power Plants (2018) [9, 10].

Type	Installed Power Unit Costs (USD/kW)	Fixed O&M Cost (USD/kW)	Fixed O&M Cost (%)
Onshore Wind	1740	26,22	2
Solar	2366	15,19	1,15
Hydropower	3045	41,63	1,5
Geothermal	5268	113,29	4,22
Biomass	5800	125,19	3
Coal	3661	40,41	1,1
Natural Gas	954	12,15	1,27

The unit costs of power plants are shown in Table 5. These values were entered in the EnergyPLAN software and calculated the total cost of all power plants in 2018, as 221770 MUSD.

Commodity prices were also inserted into the EnergyPLAN software to calculate the variable costs. Table 6 shows the commodity prices in 2018 by sources.

Table 6: Commodity prices by sources [11-13].

Commodities	Prices-2018 ($/MWh)
Natural Gas	45,00
Biomass	40,00
Coal	20,00

EnergyPLAN calculates the variable cost of the scenarios by using fuel consumption data and fuel prices, along with other parameters of the variable costs. Table 7 shows the final cost overview of the reference scenario.

Table 7: Costs of the Reference Energy Scenario

Costs	Amount (MUSD)
Variable Cost	12604
Fixed Operation Cost	4803
Annual Investment Cost	6367
Total Annual Cost	23774

The given costs in Table 7 were calculated using the unit costs and installed power plants by sources. Total cost represents the cost of the existing Turkish energy system in 2018. By 2023, power capacity expansions will be carried out in 5 years since 2018. Using the estimated capacity expansions from 2018 to 2023, the total installation cost to perform the 50% RES scenario was calculated.

4.2 75% Renewable Energy System Scenario (75% RES)

By the power capacity's expansion of Turkey, RES share in electricity production was increased to 75%, and the rest of the capacity consists of nuclear power plants. The nuclear power plants and renewable energy systems were used together in this scenario to achieve a carbon-neutral electricity generation system. All power capacity extensions were carried out under considerations of technical and policy limitations. Along with Turkey's technical energy potential, long-term government strategies were also considered, just like the 50% RES scenario for 2023.

The electricity demand of 2053 was determined as 681 TWh/year. This value was calculated by considering the demand growth between 2000 and 2023. This growth model was also implemented between 2023 and 2053. Furthermore, long-term energy strategies, political and economic limitations were considered.

This scenario is based on the high renewable energy penetration and carbon-free energy system, which is why only nuclear energy was taken into account as a non-renewable source. The high-RES share in the power generation brings different challenges. Diverse technologies and strategies, such as the adjustment of minimum grid stabilization and storage technologies, were performed in this scenario to deal with these challenges.

An energy system overview of the 75% RES scenario. Various types of power plants were used for this scenario. Unlike the 50% RES scenario, offshore wind farm, tidal, and wave power plants were integrated into the country's energy system. Pumped-hydro storage systems were also used to provide grid stability in this scenario. Installed power plant capacities can be seen in Table 8 below.

Table 2: Installed Power Capacities and Annual Electricity Productions of the 75% RES Scenario by Sources

Power Plants	Installed Capacity (MW)	Annual Electricity Production (TWh/year)
Nuclear	19200	168,65
Geothermal	4500	31,61
Dammed Hydro	55000	128,78
Onshore Wind	25000	44,72
Offshore Wind	15000	72,63
Solar PV	55828	106,19
River Hydro	25481	117,04
Biomass	14635	7,67
Wave Power	3300	9,45
Natural Gas	18410	9,55
Exported Electricity	1800 (Transmission line Capacity)	11,21
Electricity Demand	-	681
Total	**236354**	**707,5**

As shown in Table 8, hydropower plants lead to total renewable power capacity and the annual renewable electricity production by 80481 and 246,13 TWh/year, respectively. Although the installed power capacities of biomass and natural gas power plants are high, their annual electricity generation is low. Because the minimum grid stabilization share was taken as zero in the EnergyPLAN software, this adjustment provided the higher usage of variable renewable electricity in the electricity production. However, rising the share of variable renewable electricity production causes some challenges, such as the critical excess of electricity. The critical excess electricity in a country energy system network should be either exported or stored.

In this scenario, both methods were applied, and as a part of excess electricity was exported, the rest was stored by the pumped-hydro storage systems.

Energy storage. A pumped-hydro storage system was calculated according to hourly electricity productions. The total charge capacity of the pumped hydro storage was determined as 8380 MW, and the total discharge capacity was 8380 MW. Moreover, the total storage capacity is 50 GWh.

Table 3: Pumped-Hydro Storage Capacity

Type	Capacities	Efficiencies
Charge	8380 MW	0,8
Discharge	8380 MW	0,9
Storage	50 GWh	

Only one type of storage system was considered for this scenario. Storage systems are significant to store excess electricity from variable renewable electricity, and this electricity can be pumped into the grid during peak electricity demand. It provides grid stability, energy security and higher renewable energy system integration into electricity production.

Fuel consumption. Table 10 shows the RES share, annual fuel consumption, and CO2 emissions share. The share of 75% RES represents 523,41 TWh/year electricity production. Moreover, the total fuel consumption of nuclear, biomass and natural gas is 270,01 TWh/year, which is relatively lower than the fuel consumption of the reference scenario. The consumption of natural gas and biomass is low since the minimum grid stabilization share is adjusted as zero, which means the share of natural gas and biomass power plants in electricity production was kept low.

Table 4: General Outputs of the 75% RES Scenario

The Share of RES	
RES Share of Electricity Production	75%
RES Electricity Production	520,24 TWh/year
Annual Fuel Consumption (TWh/year)	
Fuel Consumption (total)	269,81
Natural Gas Consumption (total)	3,87
Biomass Consumption	25,21
Nuclear Fuel Consumption	240,93
Annual CO_2 Emissions	
CO_2 Emission	0,898 Mt

Difference between the reference scenario and the 75% RES scenario.

Table 11 illustrates the installed power capacity comparisons between the reference energy and 75% RES scenarios. This table briefly shows how much capacity expansion is needed to perform 75% renewable electricity share. As a growing trend in the energy sector, offshore wind power capacity was set 15 GW for this scenario. On the other hand, other installed renewable power capacity was significantly increased by considering feasible potentials.

Table 5: Installed Capacity Differences between the Reference Energy and 75% RES Scenario

Sources	Reference Year 2018	75% Renewable Energy Scenario for 2053	Difference (%)
Solar PV	5064	55828	1002,45
Offshore Wind	0	15000	
Onshore Wind	6950	25000	259,71
Geothermal	1260	4500	257,14
River Hydropower	7749	25481	228,83
Dammed Hydropower	20505	55000	168,23
Biomass	946	14400	1422,20
Indigenous Coal	10213	0	
Natural Gas	25647	18115	-29,37
Nuclear	0	19200	

Nuclear energy. As mentioned before that Turkey has three nuclear power plants projects, which have 14400 MW as a total installed capacity. For 2053, it was assumed that these three power plants were entirely operated, and in addition to this, one more nuclear power plant was added to this scenario. Then the total power capacity was reached 19200 MW.

Natural gas and biomass. Natural gas and biomass power plants are other critical issues that should be evaluated. Due to the high share of renewable, central power plant capacity had to be increased in this scenario. However, these power plants were used less in electricity production during a year by adjusting the minimum stabilization share as zero. Then EnergyPLAN gives priority to the variable renewable electricity to generate electricity. However, natural gas and biomass power plants were still needed for this scenario because of not enough electricity generation to supply-demand during peak times.

The cost analysis of the 75% RES scenario. The 75% RES Scenario's cost analysis was carried out according to 2050 cost projections. Capital costs were determined by using 2050 projections data and listed below.

Table 6: Unit Costs of Power Plants [15].

2053			
Power Plants	**Capital Cost (M$/MW)**	**Life-time (Year)**	**Fixed O&M Cost (%)**
Dammed-Hydropower	3,1365	60	1,25
Large CHP Power Plants (Biomass+Natural Gas)	1,476	30	2,48
Nuclear	4,6248	60	1,6
Geothermal	4,4403	30	2,2
Onshore Wind	0,82	30	3,4
Offshore Wind	2,1	30	1,88
Solar	0,323	30	1,32
River-Hydro	6,9126	60	1,5
Tidal	2,337	20	4,9
Wave	2,829	20	5,8
Pumped-Hydro Storage	0,738	50	1,5
Pumped Storage Capacity	9225 (M$/GWh)	50	1,5

Data for fixed operations and maintenance costs represents the percentage of capital costs. Technical lifetime is another critical parameter for the cost analysis. Because annual total costs, which consist of capital, fixed and variable O&M costs, are calculated using the technical lifetime of power plants.

Table 7: Investment and Fixed O&M Costs of the 75% RES Scenario

Power Plants	Capacity (MW)	Investment Costs (MUSD/Unit)	Technical Lifetime (Years)	Fixed O&M Costs (%)
Nuclear	19200	4,62	60	1,6
Large Power Plants	33045	1,476	30	2,48
Geothermal	4500	4,44	30	2,2
Dammed-Hydropower	55000	3,1365	60	1,25
Hydro Storage Capacity	50 GWh	9,225	50	1,5
Pumped Capacity (Charge)	8380	0,738	50	1,5
Turbine Capacity (Discharge)	8380	0,738	50	1,5
Onshore Wind Farms	25000	0,82	30	3,4
Offshore Wind Farms	15000	2,1	30	1,88
Solar Power Plants (PV)	55828	0,323	40	1,32
River-Hydropower	25481	6,9126	60	1,5
Wave Power Plants	3300	2,829	20	5,8

As seen in Table 13, cost parameters such as investment and fixed O&M costs were specified in the EnergyPLAN software. Investment costs of power plants are calculated by multiplying the installed capacity costs by the unit costs. Furthermore, fixed O&M costs are percentages of total investment costs, shown in Table 13. Technical lifetime is used to determine annual total costs as known that each type of power plants has an operational lifetime. Hence, annual investment costs are calculated by dividing total investment costs by the technical lifetime. The total and annual costs of the 75% RES scenario are shown in Table 14 below.

Table 8: Total and Annual Costs of the 75% RES Scenario

Power Plants	Total Investment Costs (MUSD)	Annual Investment Costs (MUSD)	Annual Fixed O&M Costs (MUSD)
Nuclear	88704	1478	1419
Large Power Plants	48774	1626	1210
Geothermal	19980	666	440
Dammed-Hydropower	172508	2875	2156
Hydro Storage Capacity (GWh)	461	9	7
Pumped Capacity (Charge)	6184	124	93
Turbine Capacity (Discharge)	6184	124	93
Onshore Wind Farms	20500	683	697
Offshore Wind Farms	31500	1050	592
Solar Power Plants (PV)	18032	451	238
River-Hydropower	176140	2936	2642
Wave Power Plants	9336	467	541
Total Costs of Power Plants	**598304**	**12489**	**10128**

Variable O&M cost is another cost parameter, mostly depended on commodity prices. The amount of fuel usage in electricity production affects variable costs. That is why keeping fuel depletion low decreases the total cost.

There are mainly three fuel types (nuclear fuel, natural gas and biomass) used for the 75% RES scenario. The annual fuel expense for total electricity generation can be calculated using fuel consumption data in 2053, shown in Table 15. Commodity prices in both 2050 and 2018 are shown below.

Table 9: Commodity Prices in 2018 and 2050 [11-14].

Commodities	Prices-2018 ($/MWh)	Prices-2050 ($/MWh)	Prices-2018 ($/GJ)	Prices-2050 ($/GJ)
Natural Gas	45,00	30,00	12,50	8,33
Biomass	40,00	32,00	11,11	8,89
Nuclear Fuel	10,00	7,00	2,78	1,94
Coal	20,00	19,50	5,56	5,42

Prices of commodities were taken from ETSAP documentations and 2050 cost projections were used for this scenario. The clean energy transition is an expensive challenge. However, this transition reduces fuel consumption. Thus cost comparisons should also be made by considering the amount of fuel consumption and commodity prices, which make up a lion share of the variable O&M cost.

Table 10: Annual Costs of the 75% RES Scenario

Costs	2053
Variable Costs (MUSD)	3679
Fixed O&M Costs (%)	10128
Annual Investment Cost (MUSD)	12489
Annual Total Cost (MUSD)	26295
Average Investment Time (year)	27,22
Total Investment Cost (MUSD)	598304

Table 16 shows the annual and total investment costs of the 75% RES scenario for the year 2053. The total and annual total cost are 598,3 billion $ and 26,295 billion $, respectively for this scenario.

5 Conclusion

This study aimed to show a roadmap to implement a carbon-neutral electricity system for Turkey. By considering the long-term energy strategy of Turkey, nuclear power and renewable sources were considered together in the 75 % RES scenario.

Furthermore, energy storage systems, which can be used to store excess electricity produced by wind and solar power plants, were integrated into the energy system of Turkey.

Nuclear power can be considered as a non-clean solution for the environment due to nuclear wastes. However, there is already a nuclear power plant under construction in Turkey and will be commissioned by 2023. Moreover, there are two more nuclear power plant projects. Hence, considering the nuclear power plants in this study is a realistic solution for Turkey due to political and energy strategies.

EnergyPLAN software provided the most realistic results and energy model of Turkey. More scenarios such as the 100% RES scenario can be created and examined by this software.

Technological development and declining energy system costs were also considered and analyzed. Renewable energy system cost is declining day by day and its efficiency is also growing. Therefore this situation provides acceleration in the clean energy transition. These parameters also played a significant role to be shaped the carbon-neutral scenario of Turkey.

This study showed that the carbon-free energy system of Turkey is possible until 2053. However, a considerable amount of investment, ambitious energy policies and a reliable technical infrastructure are needed to achieve this goal.

References

1. REN21. 2020. Renewables 2020 Global Status Report (Paris: REN21 Secretariat). ISBN 978-3-948393-00
2. Bluebook citation: Paris Agreement to the United Nations Framework Convention on Climate Change, Dec. 12, 2015, T.I.A.S. No. 16-1104.
3. Republic of Turkey Ministry of Energy and National Sources. (2018).” Info Bank-Electricity”. Retrieved from https://enerji.gov.tr/bilgi-merkezi-enerji-elektrik-en
4. IRENA (2019).Renewable capacity statistics 2020. International Renewable Energy Agency (IRENA), Abu Dhabi
5. Lund H. & Thellufsen J. Z. (September, 2019). “*EnergyPLAN Advanced Energy Systems Analysis Computer Model Documentation Version 15*”. Sustainable Energy Planning Research Group, Aalborg University, Denmark. Retrieved from https://www.energyplan.eu/wp-content/uploads/2020/09/documentation.pdf
6. EPIAS. (December, 2018). “Monthly Electricity Market Report”. Retrieved from https://www.epias.com.tr/en/spot-electricity-market/electricity-market-reports/electricity-market-monthly-reports/
7. Republic of Turkey Ministry of Energy and National Sources. 2018. “*Energy Balance Tables”*. Retrieved from https://enerji.gov.tr/enerji-isleri-genel-mudurlugu-denge-tablolari
8. EPIAS Transparency Platform. 2018. “*Final Daily Production Program”*. Retrieved from https://seffaflik.epias.com.tr/transparency/uretim/planlama/_kgup.xhtml
9. IRENA, International Renewable Energy Agency, Abu Dhabi. (2020). “*Renewable Power Generation Costs in 2019*”, ISBN 978-92-9260-244-4. Retrieved from https://www.irena.org/publications/2020/Jun/Renewable-Power-Costs-in-2019
10. U.S. Energy Information Administration (January, 2020). “*Cost and Performance Characteristics of New Generating Technologies, Annual Energy Outlook 2020*”. Retrieved from https://www.eia.gov/outlooks/aeo/_assumptions/pdf/table_8.2.pdf
11. IEA ETSAP - Technology Brief. April, 2010. “*IEA-ETSAP-Technology Data-Supply Technology Data-Gas Fired Power Plants”*. IEA ETSAP - Technology Brief. Retrieved from https://iea-etsap.org/E-TechDS/PDF/E02-gas_fired_power-GS-AD-gct_FINAL.pdf
12. IEA ETSAP - Technology Brief. May, 2010. “*IEA-ETSAP-Technology Data-Supply Technology Data-Biomass Fired Power Plants”*. IEA ETSAP - Technology Brief. Retrieved from https://iea-etsap.org/E-TechDS/PDF/E05-Biomass%20for%20HP-GS-AD-gct_FINAL.pdf
13. IEA ETSAP - Technology Brief. April, 2010. “*IEA-ETSAP-Technology Data-Supply Technology Data-Coal Fired Power Plants*”. IEA ETSAP - Technology Brief. Retrieved from https://iea-etsap.org/E-TechDS/PDF/E01-coal-fired-power-GS-AD-gct_FINAL.pdf

14. IEA ETSAP - Technology Brief. April, 2010. "*IEA-ETSAP-Technology Data-Supply Technology Data-Nuclear Fired Power Plants*". ETSAP. Retrieved from https://iea-etsap.org/E-TechDS/PDF/E03-Nuclear-Power-GS-AD-gct_FINAL.pdf
15. EnergyPLAN Modelling Team. (October, 2018). "*EnergyPLAN Cost Database Version 4.0*". Sustainable Energy Planning Research Group, Aalborg University. Retrieved from www.EnergyPLAN.eu/costdatabase/
16. Melikoğlu, M. (2016). "*The Role of Renewables and Nuclear Energy in Turkey's Vision 2023 Energy Targets: Economic and Technical Scrutiny*". Renewable and Sustainable Energy Reviews, 62, pp. 1-12.
17. Sulukan E. (2018). "An analysis of centennial wind power targets of Turkey". Turkish Journal of Electrical Engineering; Computer Science (2018) 26: 2726 – 2736
18. Sağlam M., Sulukan E. & Uyar T.S. (2010). "*Wave Energy and Technical Potential of Turkey*". Journal of Naval Science and Engineering 2010, Vol. 6, No.2, pp. 34-50.
19. Gürel, B., (2020). "*Türkiye'deki Güncel Biyokütle Potansiyelinin Belirlenmesi ve Yakılmasıyla Enerji Üretimi İyi Bir Alternatif Olan Biyokütle Atıklar İçin Sektörel Açıdan ve Toplam Yanma Enerji Değerlerinin Hesaplanması*". Mühendislik Bilimleri ve Tasarım Dergisi, 8(2), 407-416.
20. Adem Akpınar, Murat İ. Kömürcü, Hızır Önsoy, Kamil Kaygusuz, Status of geothermal energy amongst Turkey's energy sources, Renewable and Sustainable Energy Reviews, Volume 12, Issue 4, 2008, Pages 1148-1161, ISSN 1364-0321, https://doi.org/10.1016/j.rser.2006.10.016.

Renewable Energy Modelling in Bursa Answer-Time Programme

Merve Topçu [1], Doğancan Beşikçi[1], Tanay Sıdkı Uyar [1]
[1]Mechanical Engineering Department/Faculty of Engineering/University of Beykent
34398 Sarıyer-Istanbul/Turkey

mervedesin@outlook.com
dogancanbesikci@outlook.com
tanayuyar@beykent.edu.tr

Abstract. Energy consumption in the world is increasing day by day. The reason for this is

the increase in population and income, the rapid industrialization and urbanization process of the country, as well as industrial and technological developments in the world. Every point with energy consumption has energy efficiency potential. The low energy intensity calculated in a country or sector indicates the high energy efficiency. In this paper, Firstly the bioenergy waste potential of the province of Bursa is examined by detail. In the second step, the data in the ANSWER-TIMES program in the reference energy system modeling, where we enter the energy network of the province of Bursa.

Keywords: Answer-TIMES, biogas, organic waste

1 Introduction

New and different industrialization the return to dimensions in the World and in our country in a rapid way increase. Fossil energy production and usage costs are increasing day by day. In the coming times, renewable energy sources that can compete with these energy sources will also come to the fore. Biofuels from these sources using the metabolic outputs of organisms that have completed their life produced, biologically recyclable solid, liquid or gaseous fuel sources. Biofuels, especially the electricity generation and transportation sectors, are using intense fossil fuels. It can damage living spaces because of it. As a resource for reducing losses

One of the renewable energy sources shown is biogas. Biogas, organic substances in an anaerobic environment by different groups of bacteria which is released as an end product during decomposition and its composition forms organic substances. It is a flammable gas mixture that varies according to the compounds. A well-functioning biogas. The composition of the gas to be obtained from the reactor is 55-70% CH4, 30-45% CO2 and less. It consists of amount of H2S, H2O. Usually, 40% to 60% of organic matter. It is converted to biogas and the biogas produced in the last stage of this conversion is up to 90% purified. Direct vehicle by naming according to production sources in the European Union Biogas used as fuel can also be used by mixing it with natural gas. Of biogas although its flammability varies according to the percentage of methane in the gas mixture, it is approximately 36000kJ / m3.

Biogas, wastes used after production are much more valuable instead of polluting the environment and it turns into a fertilizer necessary in organic farming. This transformation is especially it positively affects environmental health in rural areas. Ambient organic wastes undergo a natural fermentation with temperature, depending on climatic conditions.

Undesired appearance, odor and it invites diseases that will threaten human health. Instead, this both the odor of agricultural and animal wastes as a result of biogas production from wastes.

It disappears to an unnoticeable extent, and it also causes human health and threatening disease factors lose their effectiveness to a large extent.

2 Material and Methods

This work; industrial and agricultural organic waste raw materials in the province of Bursa in the first stage potential analyzes and determination of biogas yields and the second phase, the energy system of Bursa province, were carried out in two stages.

3 Information About Bursa City

Bursa is located in the southern Marmara Region of Turkey and as of 2020, it is the fourth most populous city with a population of 3.101.833. Bursa province is famous as 'Green Bursa'. 45% of the city is made up of forests. Bursa has an advantageous outlook in terms of renewable energy. According to the manufacturing industry employment figures of Bursa province, construction is in the first place with 17.61%, the service sector is in the second place with 16.40%, textile is in the third place with 14.71%, and the automotive is in the fourth place with 9.35%. The Turkish Statistical Institute's Industry and Service Statistics (2009) indicates that the number of local enterprises in the manufacturing industry is 20.372, 5.9% of the enterprises operating in Turkey, and the number of employed people corresponds to 6.8% with 176.534 people. There are 30 of Turkey's largest 500 industrial establishments in Bursa. In this regard, Bursa is the fourth largest region after Kocaeli. Bursa is also rich in terms of power plants. Currently, there are 50 power plants in Bursa, of which 50,15 of the power plants is natural gas and 12 is hydro power plant.

4 Material and Methods

Creating this Reference Energy System, energy carriers, technologies and demands determined from the city that have. First, the factories and demands in Bursa are found and sorted as sectoral to be able to determine technologies. Determining technologies, according to founded factories and demands, production and consumption steps are listed as machinery. Then, Distribution of energy consumption according to consumer type about respective city is founded from Energy Market Regulatory Authority Electricity Market Development Report 2018[9], Energy Market Regulatory Authority Petroleum Market Development Report 2018[14] and Energy Market Regulatory Authority LPG Market Development Report 2018[15](for transportation demand) Energy Market Regulatory Authority Natural Gas Market Development Report 2018[14]. The data of related demands are selected then the Fractions founded from the Report of Energy Efficiency in the World and in Turkey, The Chamber of Mechanical Engineering [16] . After that, Turkey growth rate founded according to 2019 year and assumed that the growth rate will be same in next years.[17] Assumed that the yields are %100. Using to all this data energy usage are founded and convert to petajoule and it implemented for Answer-TIMES.

5 Bursa Reference Energy System

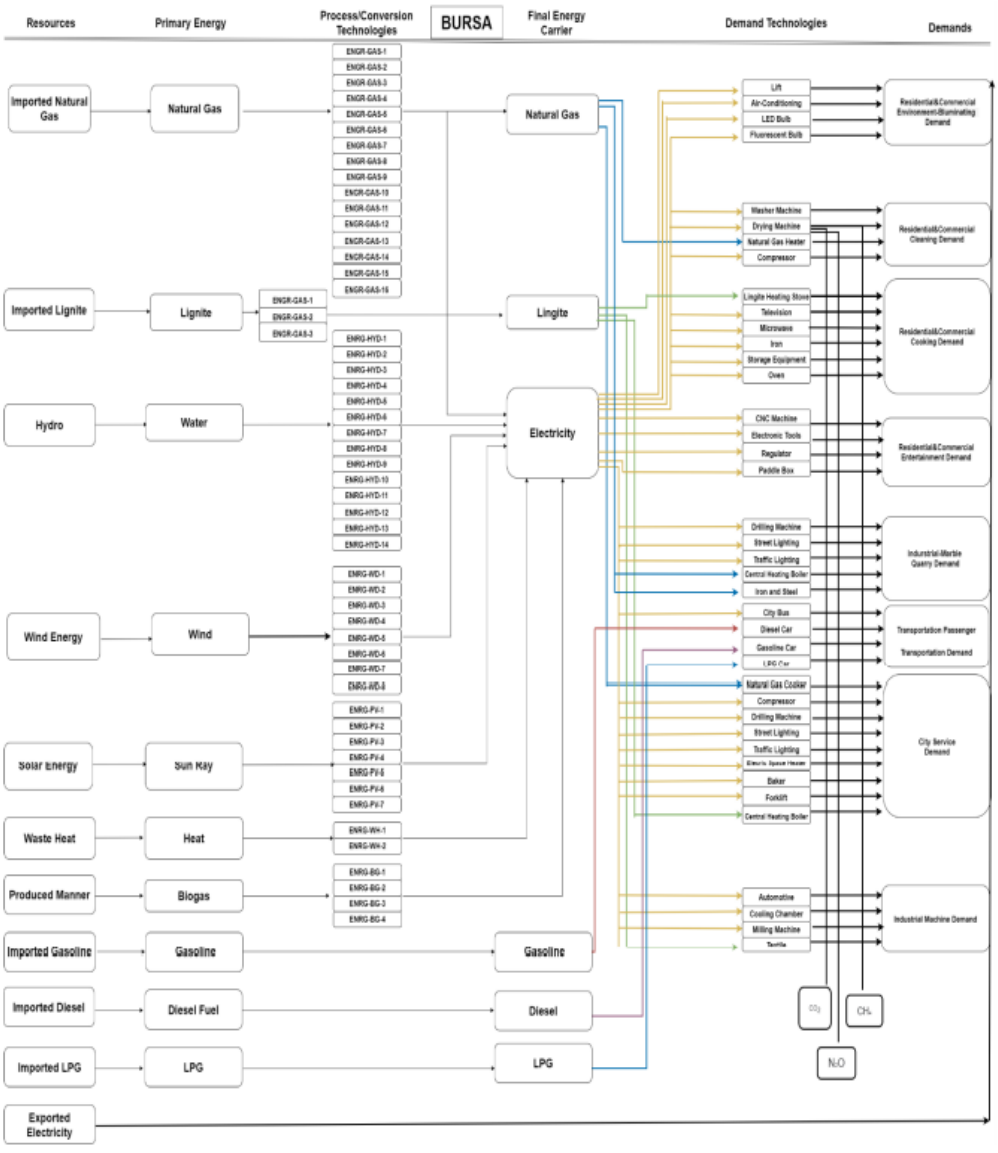

6 Conclusion

In this study, we discovered the potential of this model, which is a city reference energy system created for the city of Bursa, to further improve electricity generation and consumption. Data from EPDK and city municipality.

We have seen that energy production from renewable energy in Bursa will grow day by day in parallel with Turkey. In addition, sectoral demands will increase depending on technology and developments.

References

1. Peavy, H.S., D.R. Rowe, G. Tchobanoglous. 1985. Environmental Engineering, Mc Graw Hill Book Company, New York.
2. Toklu, E., M.S. Güney, M. Isik, O. Comaklı, K. Kaygusuz. 2010. Energy production, consumption, policies and recent developments in Turkey. Renewable and Sustainable Energy Reviews, 14: 1172–1186
3. Ulusoy, Y., A.H. Ulukardesler, H. Unal, K. Alibas. 2009. Analysis of Biogas Production in Turkey Utilising Three Different Materials and Two Scenarios, African Journal of Agricultural Research, 4(10): 996-1003.
4. Weiland P. 2010. Biogas production: current state and perspectives. Applied Microbiology and Biotechnology, 85:849-860.
5. Nayar, J. (2009). *Green Living By Design.* New York: Filipacchi Publishing
6. White, A.J., D.W. Kirk, J.W. Graydon. 2011. Analysis of small-scale biogas utilization systems on Ontario cattle farms. Renewable Energy, 36:1019-1025.
7. T.S. Uyar, D. Beşikci, E. Sulukan, An urban techno-economic hydrogen penetration scenario analysis for Burdur, Turkey, Int. J. Hydrogen Energy. 45 (2020) 26545–26558. https://doi.org/10.1016/j.ijhydene.2019.05.144.
8. S. Bakırcı, S.P. Razavi, E. Sulukan, T.S. Uyar, A Model Based Analysis on End-Use Energy Efficiency for Çanakkale , Turkey, (2019).
9. PortalAdmin_Uploads_Content_Menu_e987d11675660 (electricity), (n.d.).
10. A. Projesi, HİDROELEKTİRİK ENERJİ POTANSİYELİ Turgut GÖREZ * AHMET ALKAN * Dokuz Eylül Üniversitesi Mühendislik Fakültesi İnşaat Mühendisliği Bölümü Tınaztepe-Buca / İzmir, in: Chamb. Electr. Eng., EMO, Izmir/Turkey, 2018. https://www.emo.org.tr/ekler/7267ca39f652c0d_ek.pdf.
11. E. Plani, İzmir 2016, (2016).
12. enerji atlasi, (n.d.). https://www.enerjiatlasi.com/elektrik-uretimi/.
13. _PortalAdmin_Uploads_Content_Menu_1840fdf716780, (n.d.).
14. _PortalAdmin_Uploads_Content_Menu_b364380b64829, (n.d.).
15. ENEVerimliliği, (2008).
16. H. Kurallar, T. Ver Kaynaklar, U. Hesaplar, Yıllık Gayr saf Yurt İç Hasıla , 2019, (2021) 2019–2021.

Design And Analysis of Passive Buildings Using the Software Energy Plus and Open Studio

Simay Erdem [1], Tanay Sıdkı Uyar [1]
[1]Mechanical Engineering Department/Faculty of Engineering/University of Beykent
34398 Sarıyer-Istanbul/Turkey

simayerdem@outlook.com, tanayuyar@beykent.edu.tr

Abstract. Being the major energy consumer of electricity and natural gas, buildings consume more than 70% of electricity and 30% of natural gas. On the way to passive buildings and zero energy buildings, investigation and improvement of energy efficiency of the buildings will result in significant reductions in energy demands and CO_2 emissions; make cost savings and improve thermal comfort as well. Key steps of a successful green, energy efficient passive building can be summarized as whole building design, site design, building envelope design, lighting and day lighting design and HVAC system design.

Energy Plus software is mainly developed to simulate the performance of the buildings in the view of the above listed points. The design of a building or the analysis of an existing building with the software will show how efficient the building is or will be, and also helps finding the best efficient choice of the whole building system. Thesis focuses on the effect of changes in building envelope properties. In Turkey, topic of passive buildings has recently started to be studied. Therefore, this thesis aims to present efficient technologies providing energy savings in buildings, to present passive building concept and alternative energy simulation software.

Simulation was made for the existing building and the newly designed building.A reduction about 36% is achieved only with envelope material changes (36% reduction means 13 points out of 19 in LEED certification system).

Keywords: Passive Buildings, Energy Saving, Passive Design.

1 Introduction

The aim of this preliminary chapter is to introduce the need of designing and analyzing energy saving buildings while presenting the objectives of the study and methodology applied.

Sheltering is the very basic need of human beings since first ages. People built houses to be protected from rain, harsh climatic conditions, and wild animals. In addition to the fundamental requirements, modern world buildings are expected to provide total indoor environmental satisfaction with acceptable levels of energy use.

Compared to any industry or enterprise, buildings' consumption of energy; the use of natural sources and production of CO_2 (carbondioxide) causing pollution are considerably more [1]. US Department of Energy reports that, the buildings are responsible about 50% of all energy consumption and 30% on average of GHG emissions annually [2]. Chairman of Building Technologies Program adds: "73% of electricity and 34% of natural gas are consumed by the buildings, totaling energy bills about 418$ billion" [3]. Similarly, in Europe, 40% of final energy usage and 36% of CO_2 emissions are caused by buildings remarks Mlecnik [4]. Since buildings are and will be used for all times, the need of reducing the energy consumed by the buildings becomes very important. Not only will the actions provide energy savings; but also they would diminish CO_2 emissions and provide better indoor environments for humans.

Design of the building greatly affects the total energy use. Since the direct impact is present during buildings' lifetime, both efficient building systems and its management and building characteristics are important for proper design [1].

The interface between interior and exterior environments is defined as the envelope of the building. A great portion of buildings' energy is used to correspond with heat losses (or gains) through building envelope. Achieving the necessary insulation values are critical to satisfy proper internal temperatures for thermal comfort in the building. In addition, water heating, lighting and other building processes consume energy. Besides, buildings' interactions with each other and surroundings; also HVAC system parameters and efficiencies affect the total energy use. Mlecnik, et al. presents low energy building labels all over the world as: Certified Passive Houses, LEED Buildings, Green Buildings and Sustainable Buildings [4]. Similarly, Nayar, J. presents another definition; Net Zero Energy building, such that, energy efficient construction and appliances are combined with available commercial renewable energy systems. Producing energy for water heating with solar electricity for example, the idea is to set the computation result for a building energy use and production to zero [5].

According to American Society of Heating Refrigerating & Air Conditioning Engineers (ASHRAE), a zero energy building has to have zero net energy consumption and annual carbon emissions. Therefore, buildings should use minimum natural sources with high efficiency, minimize the emissions of GHG and air quality related gases, minimize the waste and create a "green" environment while considering indoor environmental quality requirements (thermal quality, air quality, lighting quality etc.) [6]. Considering all parameters that results in heat gains and losses, energy consuming

processes, quality requirements, interactions and system management affecting the design; studies presented in this thesis are defined as whole building design.

2 Objectives

The objectives of thesis study are to reduce the energy needs of a buildings and therefore create energy saving buildings, explaining building design parameters, green considerations and give guidelines; also present an alternative energy calculation tool via analysis and simulation.

The first objective is to create energy saving buildings by lowering the amount of energy needed, with better insulation, materials and components in compliance with green methods and higher HEX and HVAC efficiencies [7].

Secondly, design parameters that should be considered during a building design are explained throughout the thesis. These are envelope properties, building properties that affect the total energy need, indoor environmental quality considerations, green parameters and efficient HVAC system solutions.

Although energy savings focuses mainly on building envelope isolation, buildings embodied energy reduction should be considered as a green parameter. Yet, previous experience from literature will help for choosing green materials which are used for the attenuation of both embodied and operational energy need.

The last objective is to settle an understanding that energy simulations would show the daily behavior of building, total energy consumption at the very beginning of the project. American green rating system (LEED) require these calculations to be presented before the building project is signed. Therefore, the energy simulations become the most important part of a building project.

Architects, engineers and designers are guided and encouraged to create energy saving green buildings, use and develop green parameters and sustainable methods, creating applicable practices via simulations and satisfy both engineering and non-engineering needs [6].

3 Motivation

With the increasing energy demands of buildings energy savings become a major study topic in building design. The largest portion of energy is used to maintain the internal temperatures of buildings by means of heating and cooling; therefore the easiest way to reduce the need of this energy is minimizing energy losses and using energy more efficiently. It is stated that energy efficiency is the cheapest, cleanest, fastest energy source [2]. Beereport stated that building codes should be planned such that high insulation and air tightness levels, also passive strategies are to be applied which minimize the losses and provides efficient energy use [4].

In Turkey, a major portion of energy is imported. With the application of efficient thermal isolation, the resulting effect not only will be the energy reductions, but also

dependence on import energy will be diminished while consequently providing a better welfare to the nation [8].

A simple green design touch such as changing the orientation of a building to make it more efficient or provide more natural lighting and natural clean air to a space, making a better outdoor environment by putting a garden on a roof and doubling outside gardens on the site, is considered as a responsible design.

Planting low maintenance plants, heating from the floor surface rather than air volume heating of a space or painting sealants that are not harmful to the environment can also mean a lot for a building. The use of such very simple design methods can bring value to a poorly designed building. Not obliged to be more costly than a poor design, the great design is the one that does respond appropriately to the environment [5].

Green and Sustainability concept motivates in order to bring in healthy buildings with limited resources, less energy usage, and pollution with new technologies and science [9, 10].

Another motivation of this thesis study is to emphasize the methods for building design. Although it is not very common even the implementation of Turkish Standard TS 825 (Insulation Rules for Buildings) in Turkey, the proposed methods of software used are very practical and provides very detailed results. The application of green methods creates a willing for designers to include these efforts into their building parameters.

Finally, in addition to other green methods, energy producing elements such as solar collectors can be used for environment and hot water heating. With the help of more efficient HVAC system technologies, net zero energy buildings can be reached at the end of the design. Mlecnik et al. also explains the aim of European Commission as reaching net zero energy buildings, and diminishing CO_2 emissions and primary energy consumption to very low or zero [4].

4 Methodology

Zheng defines buildings as “energy gluttons”. He remarks that energy consumption of buildings will reduce significantly by improving building envelope and adds that the development of advanced building envelope systems would reduce the energy losses is a critical research frontier [11]. Case studies show the importance of building envelope design and material choice of envelope components. For example, a poor insulated wall, floor or roof can be held responsible of 40% of the total heat loss. Similarly, inappropriate windows and doors result in 30%; also draft and other undesired air movements accounts for 25% of total heat loss [11]. Therefore, improvements of building envelopes should be brought to top priority.

Insulation attempts to keep thermal energy where it is wanted. Here the definition of overall heat transfer coefficient appears. Overall heat transfer coefficient, also known as U – value, is a measure of the flow of heat by means of conduction, convection, and radiation through a material. Thus, lowering the U – value means the insula-

tion is better, consequently, the material transfers heat more slowly in and out of the building [12]. The methodology that is applied shall be lowering the U – value of building envelope materials, and the building itself as a result.

High energy consumptions of the building and the need of its reduction bring the attention to the calculations of U – value of the envelope, analysis of the building with all aspects.

As it is discussed, the most important design parameters are found at the building envelope elements, that consisting floor, walls, roof and glazing. While doing the whole building analysis, size and shape of building, orientation and relations to its environment should also be taken into account, including HVAC design results from the calculations of solar gains, internal loads from occupancy, lighting and equipment, with properly chosen fresh air requirements and design temperatures.

Three key steps; reducing the loads, applying systems with highest efficiencies and combining elements should be considered by designers. Lowering solar loads, lighting loads, providing daylight, and optimizing the building would reduce total load of a building. High efficiencies are aimed for energy, site, design elements and materials, thermal and air qualities as a rule of thumb. Parameters that will affect the overall building thermal definition and that can be analyzed create the synergy.

Other subjects that a designer should keep in mind during analysis are: scale of the building, environments and geographical constraints, green guidelines, regulations etc. [13]

The case study is done for a new office building with new building envelope materials. Building is assumed to be built similar to its present or existing version on the same location. First step will be analyzing the existing building with its existing properties, using the weather data provided by USDOE for Ankara, by using the software Open Studio and Energy Plus solver with the help of auxiliary programs or add-ins.

After the existing building analyses are completed, improvements for the new building will be done on the envelope and design parameters. Called the improved design (or re – design), size and shape of the building shall be kept as it is in general terms. Also considering internal IEQ concerns and green applications, total energy savings will be calculated and compared with the existing building. Additionally, the results would show daily internal temperature variations on an hourly basis which shows a better picture of lifetime temperature profile. Details are presented in the analysis chapter.

TS 825 analysis will also be performed and the capabilities and advantages of Energy Plus simulations shall be presented and compared with TS 825.

Lastly, building parameters, design considerations, green methods and green parameters will be given as guidelines. Building envelope structures, effects of green materials, indoor environmental quality considerations, green methods and applications and HVAC system suggestions will be summarized.

5 Analysis Steps

Analysis is performed using the software Energy Plus as the thermal solver, and two auxiliaries Open Studio and Google Sketchup. Open Studio is used as a user interface and all definitions, also it understands thermal properties of any component. Meanwhile, Google Sketchup is a drawing tool used to draw building geometry.

Analysis requires an Open Studio model and the user starts to develop its own requirements inside that model. The model contains building details, envelope details, materials database, load definitions, schedules, HVAC systems and so on.

Building parameters such as location (latitude, longitude), orientation is entered at the very beginning. Building envelope details (walls, roofs, floor, fenestration etc.) are drawn with Google Sketchup and building geometry is constructed. Thermally, it is sufficient to use a single layer interface between indoor and outdoor, or indoor spaces. Later on, material layers will be defined for each building envelope element.

Assigning space relations is important in order to define boundary conditions. A space component can be exposed to outdoor conditions, sun and wind, or ground; but an internal space may be adjacent to another internal space, that is, exposed to indoor conditions.

Material properties can be defined manually in the software. Thermal properties of the materials, as well as thickness is necessary in order to create an envelope component composed of material layers.

Loads and schedules are to be defined in order to simulate building's behavior throughout the desired time period. Internal loads (occupancy, lighting, equipment etc.) that differ as per building shall be inputted by the user; although solar loads and conduction loads are calculated by the program itself regarding the location, orientation and time of day, also outdoor weather properties.

After all input data is entered, last step is to run a whole year simulation using the available weather data file.

5.1 Analysis of the Existing Building

Inputs, Properties and Explanations for Existing Building Analysis. This section is devoted to studies of the results of building analysis before for the existing building.

	Value
Program Version and Build	EnergyPlus-64 7.0.0.036, 12.05.2012 14:15
Weather	OS:RUNPERIOD 1
Latitude [deg]	40.12
Longitude [deg]	32.98
Elevation [m]	949.00
Time Zone	2.00
North Axis Angle [deg]	90.00
Rotation for Appendix G [deg]	0.00
Hours Simulated [hrs]	8760.00

Table 1. Energy Plus Analysis General Properties.

Space	Length [m]	Width [m]	Height [m]
Office – 1	34	16	4.5
Office – 2	49	16	4.5
Office – 3	34	16	4.5
Office – 4	49	16	4.5
Hall – 1	34	49	9
Hall – 2	49	49	9

Table 2. Building Dimensions.

	Area [m^2]
Total Building Area	5395.00
Net Conditioned Building Area	5395.00
Unconditioned Building Area	0.00

Table 3. Building Area.

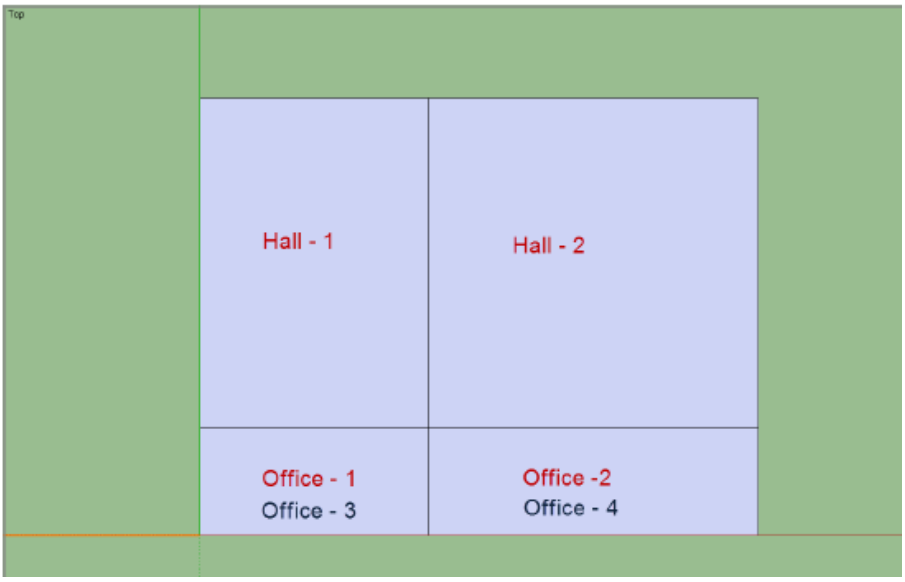

Figure1. Building Space Diagram.

After building is drawn, 6 spaces are created with desired dimensions. All space properties can be defined separately, or construction sets can be employed.
Fenestration and door details are drawn on the envelope with dimensions given in Table 4. Building total window and wall areas and window to ratios are given in Table 5.
The surface type rendering view shows the roof as red, and walls are yellow. Fenestration and doors will be shown as blue and brown, respectively in the Figures 2.
Properties of the envelope components, walls, roof, floor and fenestration are presented as envelope layer details given in Figure 3 and Figure 4.

Item	Length [m]	Height [m]
Windows	3.5	1.1
Door – 1	3	3
Door – 2	4	4
Door – 3	4	4

Table 4. Fenestration Dimensions.

	Total	North (315 to 45 deg)	East (45 to 135 deg)	South (135 to 225 deg)	West (225 to 315 deg)
Gross Wall Area [m^2]	2664.00	585.00	747.00	585.00	747.00
Window Opening Area [m^2]	88.55	0.00	0.00	0.00	88.55
Window-Wall Ratio [%]	3.32	0.00	0.00	0.00	11.85

Table 5. Window-Wall Ratio (General).

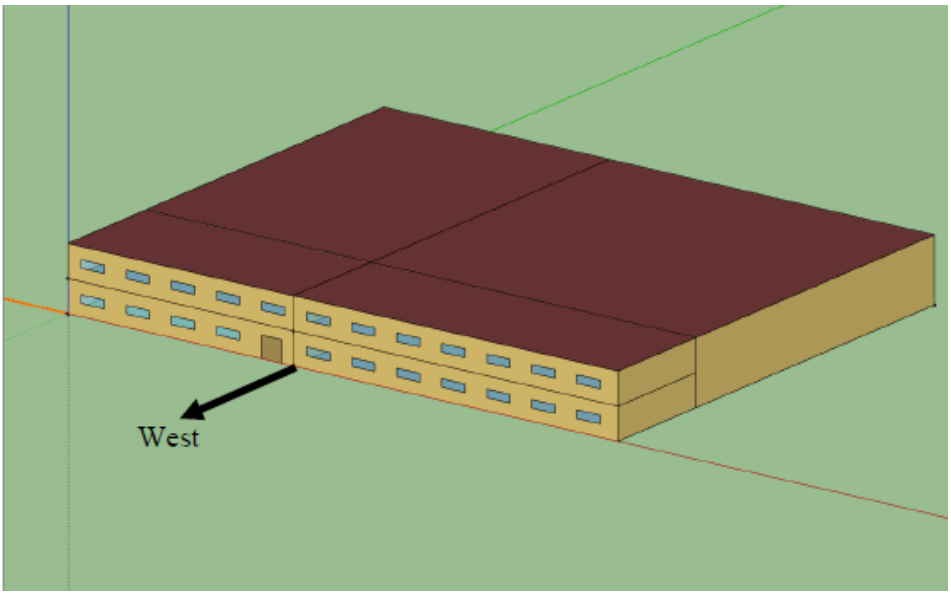

Figure 2. General View of Analysis Building (Isometric View Front Side).

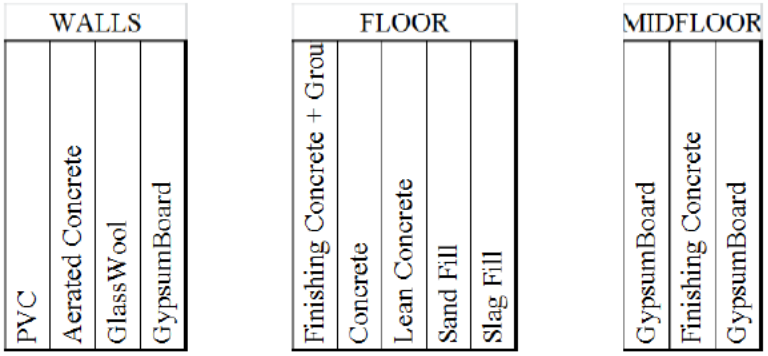

Figure 3. Walls and Floor Material Layers.

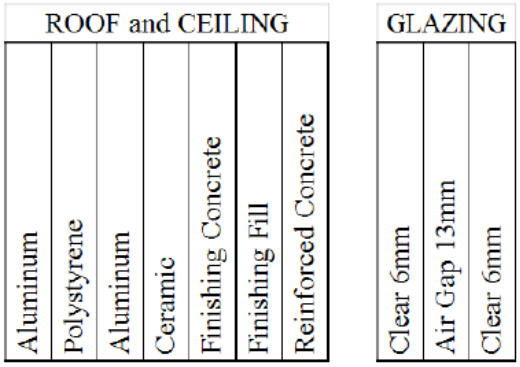

Figure 4. Roof-Ceiling and Glazing Material Layers.

	Total	North (315 to 45 deg)	East (45 to 135 deg)	South (135 to 225 deg)	West (225 to 315 deg)
Gross Wall Area [m^2]	2664.00	585.00	747.00	585.00	747.00
Window Opening Area [m^2]	88.55	0.00	0.00	0.00	88.55
Window-Wall Ratio [%]	3.32	0.00	0.00	0.00	11.85

Table 6. Window-Wall Ratio (General).

Therefore, envelope overall heat transfer coefficients for existing building envelope are presented in Table 1, Table 2 and Table 3.

The building is divided into two thermal zones as halls and offices. Loads for occupancy, lighting and equipment are calculated and presented in the Table 7. Regarding thermal zones, Table 8 presents the zone summary.

	Occupancy	**Lighting**	**Equipment Load**
Offices	0.095 people/m^2	12.08 W/m^2	56.81 W/m^2
Hall – 1	0.140 people/m^2	12.08 W/m^2	48.33 W/m^2
Hall – 2	0.103 people/m^2	12.08 W/m^2	19.07 W/m^2

Table 7. Occupancy, Lighting and Equipment Load Distributions.

	Area [m^2]	Conditioned (Y/N)	Volume [m^3]	Gross Wall Area [m^2]
OS:THERMALZONE 4	1328.00	Yes	11952.00	1035.00
OS:THERMALZONE 3	4067.00	Yes	36603.00	1629.00
Total	5395.00		48555.00	2664.00
Conditioned Total	5395.00		48555.00	2664.00
Unconditioned Total	0.00		0.00	0.00
	Window Glass Area [m^2]	Lighting [W/m^2]	People [m^2/person]	Plug and Process [W/m^2]
OS:THERMALZONE 4	88.55	12.0800	2.96	124.7100
OS:THERMALZONE 3	0.00	12.0800	2.96	124.7100
Total	88.55	12.0800	2.96	124.7100
Conditioned Total	88.55	12.0800	2.96	124.7100
Unconditioned Total	0.00			

Table 8. Zone Summary.

Weather data file is available for Ankara as TUR_Ankara_171280_IWEC.epw in USDOE website.In the analysis weather file for Ankara is used and the annual simulations are made for ideal air loads regarding weather file by Energy Plus. Ideal air loads means that performance of the HVAC system is idealized such that the thermostat values are perfectly supplied by the HVAC system.

Existing Building Analysis Results.

Existing building analysis results are presented in the following tables.

	Total Energy [GJ]	Energy Per Total Building Area [MJ/m^2]	Energy Per Conditioned Building Area [MJ/m^2]
Total Site Energy	39798.69	7376.96	7376.96
Net Site Energy	39798.69	7376.96	7376.96
Total Source Energy	122656.36	22735.19	22735.19
Net Source Energy	122656.36	22735.19	22735.19

Table 9. Site and Source Energy.

	Calculated Design Load [W]	User Design Load [W]	Calculated Design Air Flow [m^3/s]	User Design Air Flow [m^3/s]
OS:THERMALZONE 4	727331.47	727331.47	73.642	73.642
OS:THERMALZONE 3	2180358.78	2180358.78	220.755	220.755
	Design Day Name	**Date/Time Of Peak**	**Temperature at Peak [°C]**	**Humidity Ratio at Peak [kgWater/kgAir]**
OS:THERMALZONE 4	ANKARA| ANN CLG .4% CONDNS DB=>MWB	8/21 15:00:00	33.00	0.00781
OS:THERMALZONE 3	ANKARA ANN CLG .4% CONDNS DB=>MWB	8/21 15:00:00	33.00	0.00781

Table 10. Zone Cooling (Cooling Design Days).

	Calculated Design Load [W]	User Design Load [W]	Calculated Design Air Flow [m^3/s]	User Design Air Flow [m^3/s]
OS:THERMALZONE 4	359116.57	359116.57	15.651	15.651
OS:THERMALZONE 3	1154654.00	1154654.00	50.322	50.322
	Design Day Name	**Date/Time Of Peak**	**Temperature at Peak [°C]**	**Humidity Ratio at Peak [kgWater/kgAir]**
OS:THERMALZONE 4	ANKARA ANN CLG 2% CONDNS DP=>MDB	8/21 07:00:00	7.99	0.00746
OS:THERMALZONE 3	ANKARA ANN CLG 2% CONDNS DP=>MDB	8/21 07:00:00	7.99	0.00746

Table 11. Zone Heating (Heating Design Day).

5.2 Analysis of New Design Building

Inputs, Properties and Explanations for New Building Analysis. This section is intended to analyze the improved building regarding the items described in the chapter "whole building design".

Improved analysis is done for the same building at the same location. Building shape, orientation and fenerstation openings are kept as it is. Loads and schedules have not been changed. Building envelope parameters are improved and thermal analysis is repeated. Differences are tabulated in the following section. Building envelope components are improved as presented in Figures 5 and Figure 6.

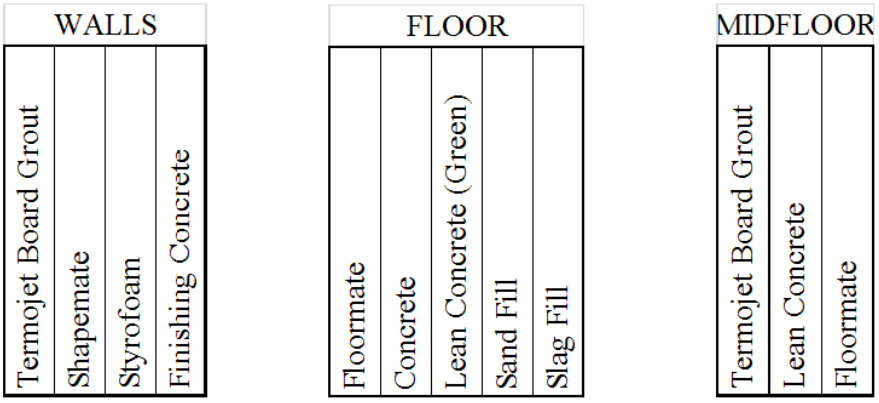

Figure 5. Walls and Floor Material Layers (New).

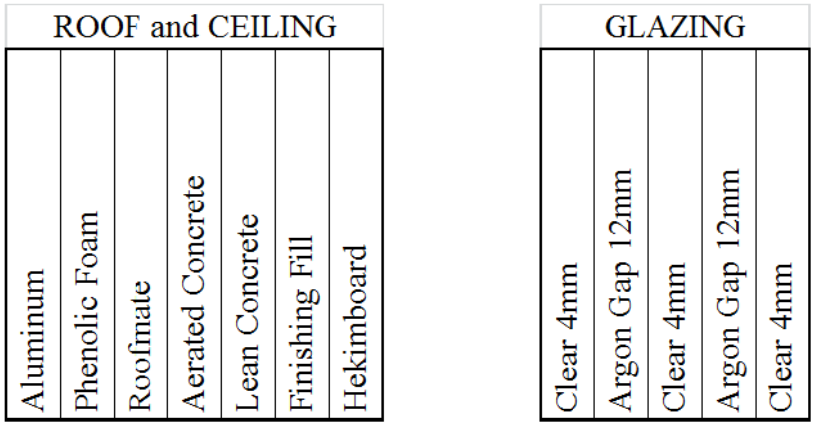

Figure 6. Roof-Ceiling and Glazing Materials (New).

	Construction	Reflectance	U-Factor with Film [W/m^{2}K]	U-Factor no Film [W/m^{2}K]
OS:SURFACE 10	0000_GREEN_DIS	0.30	0.147	0.151
OS:SURFACE 7	0000_GREEN_FLOOR	0.30	0.360	0.395
OS:SURFACE 36	0000_GREEN_ROOF	0.30	0.261	0.275
	Azimuth [deg]	**Tilt [deg]**	**Cardinal Direction**	
OS:SURFACE 10	0.00	90.00	N	
OS:SURFACE 7	90.00	180.00		
OS:SURFACE 36	90.00	0.00		

Table 12. Opaque Exterior New Building.

	Construction	Glass Area [m^2]	Area of One Opening [m^2]	Glass U-Factor [W/m^{2}K]	Glass SHGC
OS:SUBSURFACE 6	0000_GREEN_WINDOW	3.85	3.85	1.628	0.685
	Parent Surface	**Shade Control**	**Glass Visible Transmittance**	**Azimuth [deg]**	**Cardinal Direction**
OS:SUBSURFACE 6	OS:SURFACE 17	No	0.738	270.00	W

Table 13. Fenestation Details New Building.

New Building Analysis Results. New building analysis results are presented in the following tables. Existing building analysis are performed. Simulation done for 24 hours and 365 days by inputting building envelope properties, loads, schedules, thermostat values (with idealized HVAC system approach) and provided weather data has resulted in an energy consumption of 7376.96 MJ/m2 for the existing building.

The second simulation is applied to see the difference if the envelope components are chosen to be high performance and green. Changing the materials used in walls, roof and floor, and also selecting of triple glazed windows reduced the energy consumption to 4689.25 MJ/m2.

A reduction about 36% is achieved only with envelope material changes (36% reduction means 13 points out of 19 in LEED certification system).

	Total Energy [GJ]	Energy Per Total Building Area [MJ/m^2]	Energy Per Conditioned Building Area [MJ/m^2]
Total Site Energy	25298.49	4689.25	4689.25
Net Site Energy	25298.49	4689.25	4689.25
Total Source Energy	51891.10	9618.37	9618.37
Net Source Energy	51891.10	9618.37	9618.37

Table 14. Site and Source Energy New Building.

	Calculated Design Load [W]	User Design Load [W]	Calculated Design Air Flow [m^3/s]	User Design Air Flow [m^3/s]
OS:THERMALZONE 1	663781.70	663781.70	65.695	65.695
OS:THERMALZONE 2	238599.81	238599.81	24.176	24.176
	Design Day Name	**Date/Time Of Peak**	**Temperature at Peak [°C]**	**Humidity Ratio at Peak [kgWater/kgAir]**
OS:THERMALZONE 1	ANKARA ANN CLG .4% CONDNS DB=>MWB	8/21 07:00:00	18.99	0.00781
OS:THERMALZONE 2	ANKARA ANN CLG .4% CONDNS DB=>MWB	8/21 17:00:00	30.84	0.00781

Table 15. Zone Cooling New Building.

	Calculated Design Load [W]	User Design Load [W]	Calculated Design Air Flow [m^3/s]	User Design Air Flow [m^3/s]
OS:THERMALZONE 1	56464.43	56464.43	2.711	17.183
OS:THERMALZONE 2	25588.63	25588.63	1.229	5.611
	Design Day Name	**Date/Time Of Peak**	**Temperature at Peak [°C]**	**Humidity Ratio at Peak [kgWater/kgAir]**
OS:THERMALZONE 1	ANKARA ANN HTG 99.6% CONDNS DB	1/21 24:00:00	-15.70	0.00107
OS:THERMALZONE 2	ANKARA ANN HTG 99.6% CONDNS DB	1/21 24:00:00	-15.70	0.00107

Table 16. Zone Heating New Building.

6 Conclusion

This study presented an alternative year-round energy performance simulation software, Energy Plus, its auxiliaries Open Studio and Google Sketchup; analyzed the case study building energy performance with existing properties and new properties.

Whole building design concept with its components are presented, green methods and guidelines of are summarized in the thesis study. Whole building design concept covers and explains the following topics: Site design that includes location, size, shape and orientation of a building; envelope design with envelope properties of

roofs, walls, floor and fenestration, also thermal and moisture control; indoor environmental quality considerations; efficient HVAC system suggestions; green methods, applications accompanied with tips and guidelines. Lastly, most widely-known green building rating systems are presented.

In the context of this study, design, methods and material guidelines are introduced to reduce energy needs of buildings and to bring in the passive building design concept. Building and system parameters to enhance building energy efficiency and energy savings together with passive building principles are summarized. Moreover, whole building energy analysis methods and simulation steps are explained; year-round simulation is performed for a sample building; as a result, energy savings about 36% is achieved.

References

1. Sözer, H. (2010). Improving energy efficiency through the design of the building envelope. *Building and Environment,* (45), 2581-2593.

2. U.S. Congress, Office of Technology Assessment, *Building Energy Efficiency*, OTA-E-518 (Washington, DC: U.S. Government Printing Office, May 1992).

3. Chalk, S., (2009). Statement to Committee on Science and Technology U.S House of Representatives

4. Mlecnik, E., Visscher, H. & Van Hal, A. (2010). Barriers and opportunities for labels for highly energy-efficient houses. Energy Policy, (38), 4592-4603.

5. Nayar, J. (2009). *Green Living By Design.* New York: Filipacchi Publishing

6. ASHRAE. (2010). *Green Guide, The Design, Construction and Operation of Sustainable Buildings*. USA: Mixed Sources.

7. Thormark, C. (2006). The effect of material choice on total energy need and recycling potential of a building. *Building and Environment,* (41), 1019-1026.

8. Fixa, Isı Yalıtım Sistemi from www.fixa.com.tr, Last accessed on: 28.08.2011

9. Kutzmark, T., Geis, D. (2004). "Developing Sustainable Communities: The Future is Now", Center of Excellence for Sustainable Development.

10. Hui, C.S.M., (2001). "Low Energy Building Design in High Density Urban Cities", Renewable Energy, No.24, Pergamon, Elsevier Science Ltd.

11. Zheng, G., Jing, Y. & Huang, H. (2010). Application of improved grey relational projection method to evaluate sustainable building envelope performance. *Applied Energy, 87* 710-720.

12. Bynum, R.T, (2001). *Insulation Handbook.* New York: McGraw-Hill.

13. Keeler, M. & Burke, B. (2009). *Fundamentals of Integrated Design for Sustainable Buildings*. Hoboken, N.J: John Wiley & Sons.

14. Wang, W.M., Radu, Z., Hugues, R. (2005) Applying multi-objective genetic algorithms in green building. *Build Environment,* 40:1512–1525

15. The Whole Building Design Guide, from www.wbdg.org, last accessed on 26.05.2012

16. ASHRAE. (2009). *ASHRAE Handbook – Fundamentals*. Atlanta: American Society of Heating, Refrigerating and Air-Conditioning Engineers, Inc.

17. Grondzik, W.T. (2001). The mechanical engineer's role in sustainable design: Indoor environmental quality issues in sustainable design. HTML presentation from www.polaris.net~gzik/ieq/ieq.htm, last accessed on 19.05.2011

18. Liu, Y., Joseph, C.L., Tsang, C.L. (2008) Energy performance of building envelopes in different climate zones in China. *Applied Energy*, 85:800–817

19. ASHRAE. (2010). *AISI/ASHRAE/IES Standard 90.1-2010, Energy Standard for Buildings Except Low-Rise Residential Buildings*. Atlanta: American Society of Heating, Refrigerating and Air-Conditioning Engineers, Inc

20. Givoni, B. (1994). *Passive and Low Energy Cooling of Buildings*. New York: Van Nostrand Reinhold.

Photovoltaic Energy Forecasting via Artificial Neural Networks and Support Vector Machine Approaches

Özge Baltacı[1][0000-0001-5025-1180], Zeki Kıral[2][0000-0002-9154-0509] and Yüksel Çağrı Gürses[3][0000-0002-8986-9858]

[1] Department of Mechatronics Engineering, The Graduate School of Natural and Applied Sciences, Dokuz Eylul University, Tinaztepe, Buca, Izmir, Turkey
[2] Department of Mechanical Engineering, Dokuz Eylul University, Tinaztepe, Buca, Izmir, Turkey
[3] Department of Intelligent Transportation Systems and Technologies, Graduate School of Natural and Applied Sciences, Bandirma 17 Eylul University, Bandirma, Balikesir, Turkey

ozge.baltaci@ogr.deu.edu.tr, zeki.kiral@deu.edu, yc.gurses@zenaenerji.com

Abstract. In recent decades, many Renewable Energy Systems particularly photovoltaics (PVs) is becoming important source for power generation and have been installed all over the world. However, frequently varying output of PV because of weather data including irradiation and temperature, soiling, cloud cover etc. make it an intermittent and unreliable source when connected to grid. For this reason, output forecasting plays an important role in the energy generation and implementation of solar power systems. Until recently, conventional and empirical solutions have been applied in traditional way to predict the solar energy. However, when the results of these approaches are examined, insufficient accuracy and other limitations are detected in the predictions obtained by traditional methods. To overcome these limitations, to deal with uncertainties and to handle the shortcomings of these traditional methods Artificial Intelligence based techniques come up with their strong and certain effectiveness. Artificial Neural Network (ANN) and Support Vector Machine (SVM) approaches are both artificial intelligence forecasting methods which maximize the accuracy of results of the real-world applications and gain the upper hand about execution speed and time. This study aims to compare the forecasting capabilities of ANN (using different learning functions for each ANN) and SVM approaches by providing the 2,5 year-historical data from the solar PV plant located in Simav, Kütahya as input. Predictions of the higher accuracy can be achieved by SVM using PV measures with weather data including irradiance and temperature. Results showed that the SVM model performed better than ANN model.

Keywords: PV power plant, Artificial Neural Network, Support Vector Machine.

1 Introduction

Energy is fundamental to life and plays an indispensable and substantial role in modern society. Sustainable energy provides many benefits to the environment and life. The most important of these is that sustainable energy technologies are clean energy sources with less negative environmental impact than traditional energy technologies. Among the different forms of clean energy, solar energy is a vast, inexhaustible, and clean resource for the entire universe as it is not only sustainable but is also renewable [1]. According to the International Energy Agency (IEA), solar radiation hitting the Earth's surface in 90 minutes is enough to meet the energy needs of the whole world for a year. The IEA predicts that by 2050, as much as 11% of global electricity generation will be provided by solar energy.

In recent decades, many photovoltaic cells have been installed all over the world. However, there are still issues including different parameters such as solar elevation angle, haze effect and cloud cover etc. that will cause fluctuations in the output. For this reason, output forecasting becomes important for the generation and implementation of solar power systems. In [2] Zendehboudi et al. states that conventional and empirical solutions have been applied in traditional way to forecast the solar energy, but they have demonstrated insufficient accuracy as well as other important limitations. Artificial intelligence-based techniques have addressed these issues effectively and overcome the mentioned limitations with its potential to deal with the uncertainties and other shortcomings of the traditional methods to real world applications. Artificial Neural Network (ANN) is one of artificial intelligence forecasting methods that is widely used in many investigations. However, in some cases the prediction results of ANNs are incorrect. In addition to it, ANNs consume too much time for a large network. Moreover, there is no proven method for selecting the numbers and sizes of hidden layers as well as activation functions to develop a high precision model [3]. The Support Vector Machine (SVM) approach, another artificial intelligence prediction model, has been proven to have better accuracy and speed in solving nonlinear problems and is successful in situations where ANNs are inadequate.

2 SVM Modeling Approach

A SVM is a machine learning algorithm based on statistical learning theory and the principle of structural risk minimization, which was presented firstly by Cortes and Vapnik in 1995 [4]. The network structure of an SVM is given in a tree structure (see Fig.1). SVMs have been successfully implemented for various purposes so far, such as image retrieval [5], fault diagnosis [6], text detection [7], and regression problems [8].

The main idea of SVM approach (see Fig. 2) is transforming the nonlinear input data to an area with high dimensional properties to find a hyper-plane via nonlinear mapping. For classification, pattern recognition and analysis of regression, SVMs are mostly implemented and usually outperformed other methodologies such as traditional statistical models that have been developed earlier [9][10].

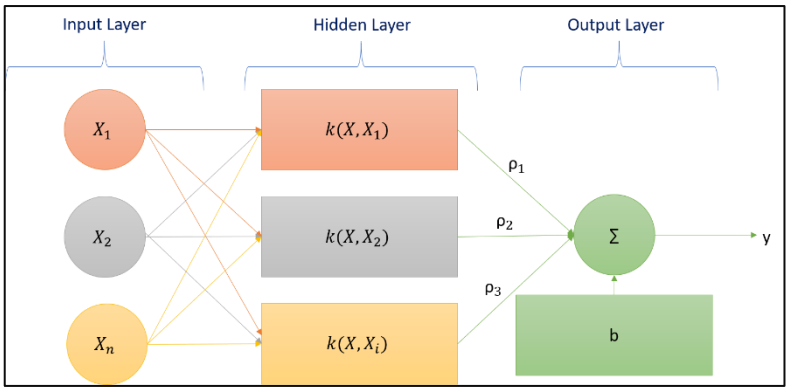

Fig. 1.The Network Structure of SVM (Taken from A. Zendehboudi et al. / Journal of Cleaner Production 199 (2018) 272e285, and re-drawn.)

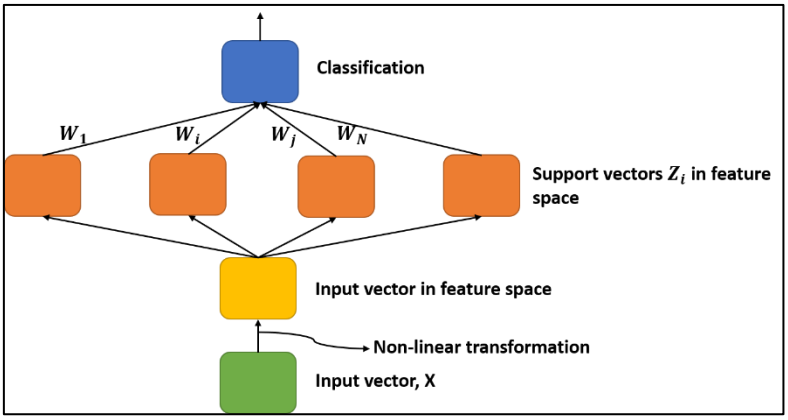

Fig. 2.The Classification by SVM (Taken from 4. Cortes, C., Vapnik, V., 1995. Support vector network. Mach. Learn. 20, 273-297, and re-drawn.)

The Support Vector Regression (SVR), on the other hand, is the SVM utilization for function approximation and regression. A training dataset of input-output pairs is considered as Z={X_i, Y_i | i=1,2,3,…,n} where $X\_i \in R\^q$, q is the dimensional input vector, $Y\_(i\ ) \in R$ is the corresponding target value and n refers to the training data size. The regression model can be constructed, as shown:

$$Y=W\^T\ Q(X)+b \tag{1}$$

where W: weight vector, b: bias term, $Q(X)$: representative of a nonlinear mapping function which maps X into higher dimensional feature space.

Generally, the characteristics of the SVM method can be briefly stated as:

1. Considerably precise and robust,
2. Able to model complex nonlinear decision boundaries,

3. Less prone to overfitting in comparison with other models,
4. Exhibit a compact description of the learned model,
5. Potential of implementation in pattern recognition, regression, and classification.

2.1 Development of SVM in Solar Energy

In recent years, SVM modeling approaches have been implemented extensively in the fields of solar energy and can range from single to hybrid and complex models. Zendehboudi et al., stated in [2] that SVMs have been frequently implemented and got wide acceptance since 2009. Their article contained a list of 75 publications. 47 of them were found for the time period between 2015 and 2017 (see Fig.3).

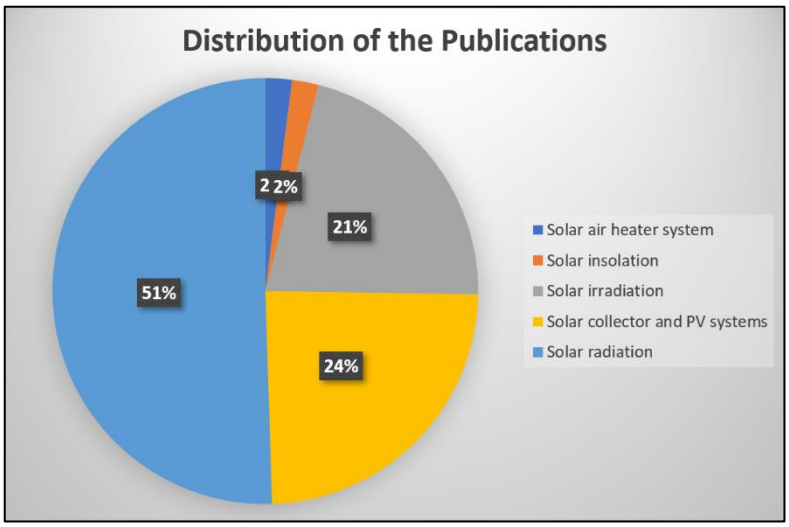

Fig. 3. Distribution of the Publications Investigated (Taken from A. Zendehboudi et al. / Journal of Cleaner Production 199 (2018) 272e285, and redrawn.)

In [11] Wu and Liu developed five SVM models with various input attributes to estimate monthly mean daily solar radiation by considering 13 years' meteorological data for twenty-four stations all over China. Studies have demonstrated that machine-learning approaches outperformed traditional statistical methods. The authors concluded that the SVM methodology may be a promising alternative to the traditional approach for forecasting solar radiation at any location for which air temperatures are available.

SVM has been successfully used to address many forecasting problems. In [12] a SVM was used to estimate daily solar radiation based on the duration of exposure to sunshine in China. Generally, the SVM models presented good performance and significantly outperformed the empirical models. However, the developed SVM model was preferred due to its greater accuracy and simplicity.

The other SVM model developed and compared with empirical models. The results showed that SVM models achieved 14%-26% greater accuracy [13].

Another application of SVM and ANN models for forecasting solar radiation in Saudi Arabia was investigated by [14]. According to Root Mean Square Error (RMSE), the coefficient of correlation and the magnitude of relative error as well as the speed of computation for the algorithms, the SVM approach was considerably more accurate during computation and rapid in forecasting radiation.

Kazem et al. aimed to design and implement SVM for the management of energy generation based on experimental work [15]. The experiments achieved a value which indicates the predicting model is remarkably close to the regression line and a well data fitting to the statistical model. Besides, the proposed model achieved less Mean Square Error (MSE) in comparison with other related work.

3 Artificial Neural Networks

According to [16], in its history, the artificial neural networks (ANN) have gone through three landmarks. The first in 1943 with the work of McCulloch and Pitts, who were the first to address the subject and to develop the initial concept of artificial neurons. Later, in 1960, the Perceptron network won space for Rosenblatt's work, but was soon discredited because of its limitations in dealing with problems that are not linearly separable, the disadvantage of the single layer perceptron network highlighted by Minsky in his work. After this drawback, just a few researchers were developed in the area until the 1980s. However, in that decade, the development of the backpropagation algorithm has rekindled researchers' interest. After that, advances in the areas, such as economics, health, computing, engineering, among others. The artificial neural networks, have their basic structure and functioning based on the human brain. Their aim is to emulate the brain's ability to solve problems.

In [17], Haykin defines these networks as follows: "A neural network is a massively parallel distributed processor made up of simple processing units, which has a natural propensity for storing experimental knowledge and making it available for use". These networks have been applied in several tasks, such as pattern classification, function approximation, prediction of parameters, systems optimization, among others. A simple classification between types of architectures is to divide them into two categories, defined in relation to the form of connection between the neurons of the network. The difference between these categories is that the one of them encompasses networks that do not have feedback connections between their neuron, while the other deals only with networks that have such connections. These categories are feedforward and recurrent networks.

4 Experimental Study

In this article the aim is to predict future solar energy data from historical data, hence the model will be implemented with regression techniques from supervised learning.

4.1 Dataset

As mentioned in the study of Pradhan and Panda, even though the main input to the PV system is the solar radiation, still there are other factors like temperature, angle of tilt, soiling and shading which affects the efficiency of the PV module [19]. In this study, an experiment has been conducted to analyze the effect of irradiance and temperature on the power output of the Tekfen's PV module by using the dataset collected from Simav (39.131037∘N, 29.181358∘E), Kütahya.

The dataset is used as historical data to predict the future solar energy that will be produced by a determined photovoltaic system. The data from the different inverters are put together in the same dataset, as all the inverters are from the same PV module and they have similar range of power values.

The total dataset consists of a matrix of 1013 rows and 19 columns, the first column is the month and day, the second one the total energy generated, and the rest of the columns are the different inverters (see Fig.4). The rows are the daily data, as it is almost three years, there are 1013 points of solar energy data. The solar energy data is in kWh. As the maximum values in each location are different, the data has been normalized to values from 0 to 1, to improve the efficiency on the models.

PV plant name:904_SIMAV_1	Period:Month	Unit:Energy Yield (kWh)							
Generated On	904_SIMAV_1	Inverter1.1	Inverter1.2	Inverter1.3	Inverter2.1	Inverter2.2	Inverter2.3	Inverter2.4	Inverter2.5
2021-04-01	2505.48	148.38	144.64	139.03	151.94	149.67	145.74	144.59	139.90
2021-04-02	2534.79	150.49	149.54	149.51	150.58	149.21	149.53	149.92	149.42
2021-04-03	5159.45	303.68	302.30	298.64	303.00	301.99	303.29	303.37	303.77
2021-04-04	2772.96	163.02	160.46	155.39	162.24	161.40	162.44	162.31	162.43
2021-04-05	507.52	29.79	28.84	135.34	30.00	29.66	29.96	30.19	29.40
2021-04-06	1979.90	117.77	116.42	115.29	117.21	116.41	116.87	116.99	116.24
2021-04-07	5170.74	305.87	304.39	304.78	306.23	304.34	304.33	304.30	303.66
2021-04-08	1613.42	95.99	93.57	91.28	95.74	94.69	94.90	94.68	94.21
2021-04-09	1656.18	103.08	101.86	100.80	99.29	96.33	93.50	93.30	88.80
2021-04-10	5015.20	296.52	295.00	292.07	296.09	295.23	295.55	295.40	295.52
2021-04-11	4750.33	278.75	275.66	269.39	278.38	277.90	278.78	277.79	278.57
2021-04-12	4042.43	243.55	242.11	245.44	242.95	240.42	239.55	239.39	237.95
2021-04-13	4987.92	293.10	290.78	284.07	291.18	290.71	292.54	291.97	292.06
2021-04-14	4911.34	289.01	286.99	282.05	288.29	287.00	288.02	287.57	288.05
2021-04-15	3172.84	185.74	183.58	177.30	184.53	184.50	185.76	185.30	185.84

Fig. 4. A small sample data taken from Simav PV Monitoring Program

For the machine learning algorithms, it is needed two types of data: training data and testing data. In this case, the dataset has been divided into 75% training data and 25% testing data. The algorithms will be first trained with the training data, i.e., it is provided a series of predictors (input) and the known results (output), and the model will work with this data to find a relation between the predictors and the results.

Once the relation is obtained, if it is not enough accurate, the model can be retrained until the correct results are obtained. After that, the algorithms are tested with the testing data. In this step, it is only provided to the algorithm the input data, to test if the model can correctly make predictions. Once the predictions are done, as the real output data of the test data is on the data set, the predicted data and real data is compared to see which model is better.

The results of every model will be discussed comparing the MSE of the model performance in the training phase, as well as the RMSE of the predicted data vs. real data in the testing phase.

4.2 Experimental Results

PV Model / Effect of the Irradiance and the Temperature on the Energy Output). Habbati et al. mentioned the necessity of irradiance and temperature for solar PV [20]. The PV module is the interface which converts light into electricity. Modeling this device, necessarily requires taking weather data (irradiance and temperature) as input variables. The output can be current, voltage, power or other. Any change in the entries immediately implies changes in outputs.

A standardized model is always helpful in predicting the performance of solar PV of different capacity under any environmental condition. The maximum power generated by the solar PV module can be written as

$$PV = \eta A[I - 0.05\,(t - 0.25)] \tag{2}$$

where total conversion efficiency is represented by 'η'. This 'A' is for the entire solar PV array, total area covered by the solar PV array represented by $A(\mathrm{m}^2)$. Solar irradiance falling on the array is represented by $I\,(\mathrm{KW/m}^2)$ and 't' represents the total ambient temperature of PV array in (°C).

When all parameters are constant, the higher the irradiance, the greater the output current, and as a result, the greater the power generated.

As the Sun's position changes throughout the day irradiance also keeps changing with it. It is found that maximum irradiance is around 10:00 to 12:00 pm and slowly it goes on decreasing. Keeping factors like temperature and spectral content constant both short circuit current and open circuit voltage increases with increase in the intensity of radiation. As the number of photons striking the module increases photon generated current also increases.

Results. In this study, the energy values taken from the Simav power plant were brought together with the temperature and radiation values at the date the values were recorded. The results obtained in this way were then compared with the results produced by running the same algorithms with energy values alone.

The ANN models have been tested with the different training algorithms; Levenberg-Marquardt (LM), Bayesian Regularization (BR) and Scaled Conjugated Gradient (SCG). Comparative graphs of predicted and real data are presented in Table 1, regression graphs of training, test and validation values are presented in Table 2, and RMSE values of the performance of the models are presented in Table 3.

Table 11. Comparative graphs of Predicted vs Real Data

Artificial Intelligence Method:ANN		
	ANN-1 **PV Data with Temp. and Irradiance**	**ANN-2** **PV Data**
BR	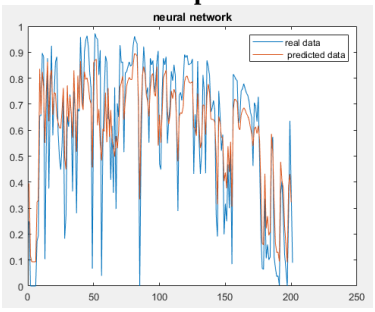	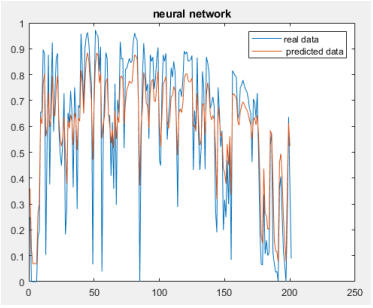
LM	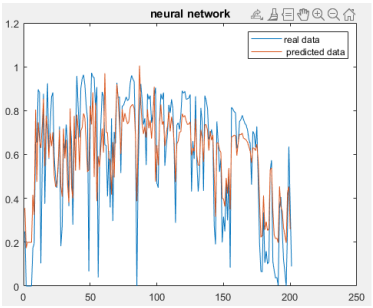	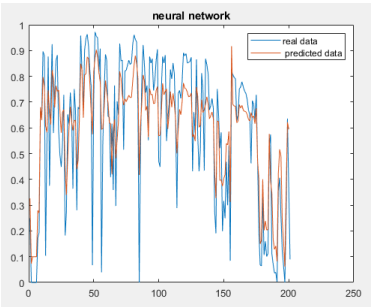
SCG	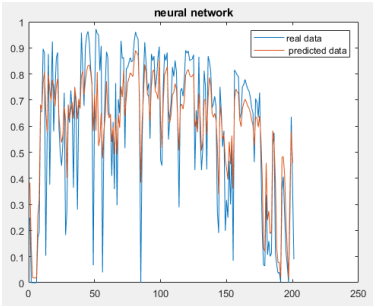	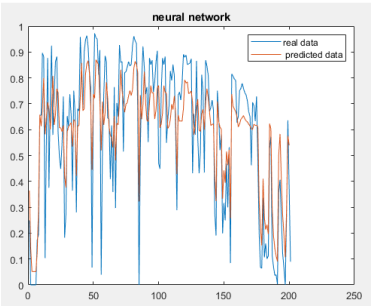

Table 2. Regression graphs of training/test/validation data

Artificial Intelligence Method:ANN		
	ANN-1 **PV Data with Temp. and Irradiance**	**ANN-2** **PV Data**
BR	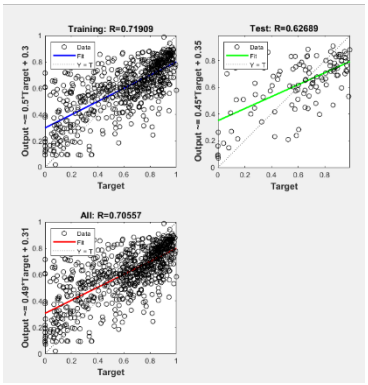	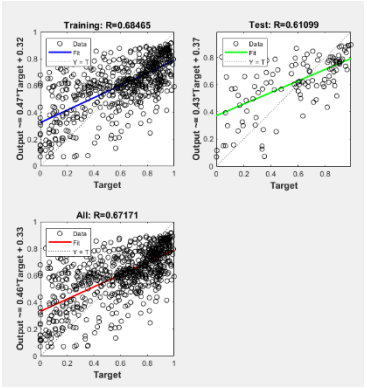
LM	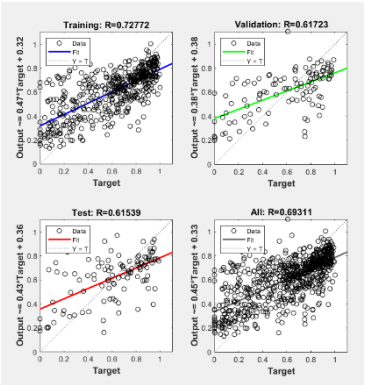	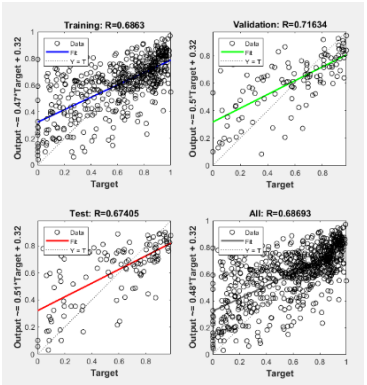
SCG	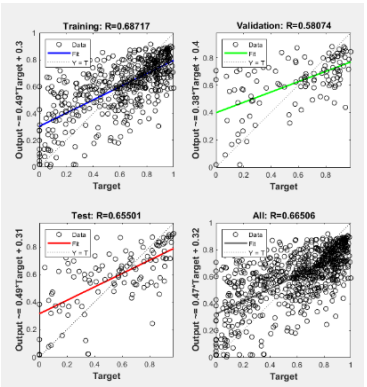	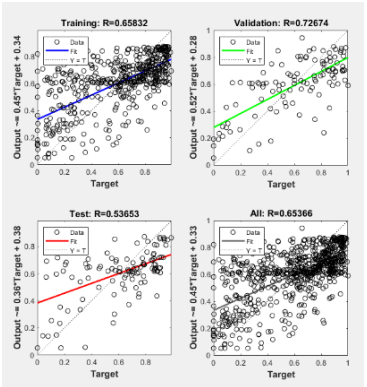

Table 3. RMSE of Model Performance, ANN

Artificial Intelligence Method:ANN				
	ANN-1 PV Data with Temp. and Irradiance		ANN-2 PV Data	
	Model	Real vs Predicted	Model	Real vs Predicted
BR	0.0427	0.1300	0.0474	0.1374
LM	0.0465	0.1562	0.0462	0.1623
SCG	0.0504	0.1203	0.0484	0.1342

With SVM it has been compared two different SVM models, the first one, using a linear kernel and the second one, using a gaussian kernel shown in Table 4 and Table 5:

Table 4. Comparative graphs of Predicted vs Real Data

Artificial Intelligence Method:SVM		
	SVM-1 PV Data with Temp. and Irradiance	**SVM-2 PV Data**
Linear kernel	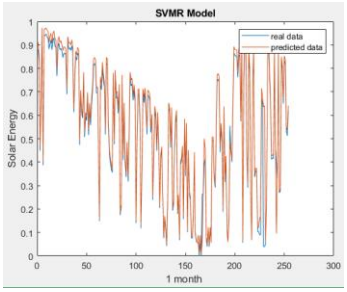	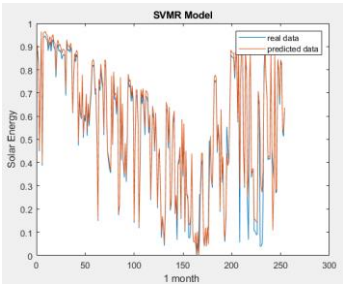
Gaussian kernel	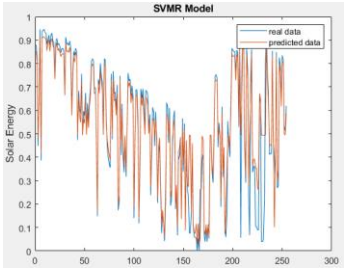	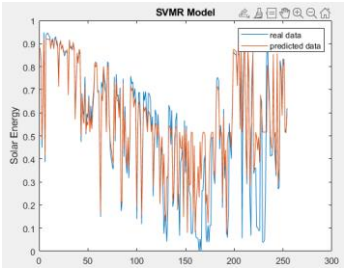

Table 5. RMSE of Model Performance, SVM

Artificial Intelligence Method:SVM				
	SVM-1 PV Data with Temp. and Irradiance		SVM-2 PV Data	
	Model	**Real vs Predicted**	**Model**	**Real vs Predicted**
Linear kernel	0.0230	0.0618	0.0408	0.0625
Gaussian kernel	0.0221	0.0623	0.1180	0.1331

Machine learning has the potential to provide a more accurate and efficient solution in forecasting the energy output as it can be observed from the model RMSE values. While the accuracy rate of the model is 96% in ANN, this rate has increased to 98% in SVM. In our research, we demonstrated such feasibility and made a performance comparison between ANN and SVM techniques. The results showed that SVM algorithm with linear kernel function had an average accuracy up to 94%. Contrary to this, the ANN method yielded ~87% accuracy with the Bayesian Regularization training function. Both methods showed excellent genus level performance, but SVM showed slightly better accuracy for energy estimation.

5 Conclusion

This paper aimed to perform a comparison study of prediction data system of PV/I&T output power by using ANN and SVM techniques. Many factors are affecting the performance of PV panels, such as the strength of sunlight, dust on the panel, humidity, wind speed, ambient temperature, and rainfall. We have only used temperature and radiation values here.

One of the main characteristics of SVR is that it attempts to minimize the generalized error bound to achieve generalized performance. The result showed that the SVR is better than ANN in predicting energy output. The performance of the SVRs approaches when compared with the results provided by ANN obtained interesting improvements in the prediction system. Both techniques are relatively good in terms of root mean square error. However, estimated results by SVR produce remarkably smaller estimation errors compared to ANN. From the results it can be concluded that SVR method can predict PV energy with higher estimation accuracy and shorter computation time.

6 Acknowledgement

The research dataset leading to these results has received from Tekfen Holding's Simav PV, Kütahya. The authors would like to acknowledge to Tekfen Holding for their support.

References

1. Ramedani, Z., Omid, M., Keyhani, A., Khoshnevisan, B., Saboohi, H.: A comparative study between fuzzy linear regression and support vector regression for global solar radiation prediction in Iran. Solar Energy 109, 135–143 (2014).
2. Zendehboudi A., Baseer M.A., Saidur R.: Application of Support Vector Machine Models for Forecasting Solar And Wind Energy Resources: A review. Journal of Cleaner Production 199, 272-285 (2018).
3. Zendehboudi, A.: Implementation of GA-LSSVM modelling approach for estimating the performance of solid desiccant wheels. Energy Convers. Manag. 127, 245-255 (2016).
4. Cortes, C., Vapnik, V.: Support vector network. Mach. Learn. 20, 273-297 (1995).
5. Tao, D., Tang, X., Li, X., Wu, X.: Asymmetric bagging and random subspacing for support vector machines-based relevance feedback in image retrieval. IEEE Trans. Pattern Anal. Mach. Intell. 28, 1088-1099 (2006).
6. Tian, Y., Fu, M.Y., Wu, F.: Steel plate's fault diagnosis on the basis of support vector machines. Neurocomputing 151, 296-303 (2015).
7. Francis, L.M., Sreenath, N,: TEDLESS – Text detection using least-square SVM from natural scene. Computer and Information Sciences (2015). http://dx.doi.org/10.1016/j.jksuci. 2017.09.001.
8. Hemmati-Sarapardeh, A., Shokrollahi, A., Tatar, A., Gharagheizi, F., Mohammadi, A.H., Naseri, A.: Reservoir oil viscosity determination using a rigorous approach. Fuel 116, 39-48 (2014).
9. Huang, C., Davis, L.S., Townshend, J.R.G.: An assessment of support vector machines for land cover classification. Int. J. Rem. Sens. 23, 725-749 (2002).
10. Sung, A.H., Mukkamala, S.: Identifying important features for intrusion detection using support vector machines and neural networks. In: Proceedings of the 2003 Symposium on Applications and the Internet. IEEE, Orlando, FL, USA (2003).
11. Wu, W., Liu, H.B.: Assessment of monthly solar radiation estimates using support vector machines and air temperatures. Int. J. Climatol. 32, 274-285 (2012).
12. Chen, J.L., Li, G.S., Wu, S.J.: Assessing the potential of support vector machine for estimating daily solar radiation using sunshine duration. Energy Convers. Manag. 75, 311-318 (2013).
13. Chen, J.L., Li, G.S.: Evaluation of support vector machine for estimation of solar radiation from measured meteorological variables. Theor. Appl. Climatol. 115, 627-638 (2014).
14. Ramli, M.A.M., Twaha, S., Al-Turki, Y.A.: Investigating the performance of support vector machine and artificial neural networks in predicting solar radiation on a tilted surface: Saudi Arabia case study. Energy Convers. Manag. 105, 442-452 (2015).
15. Kazem, H.A., Yousif, J., Chaichan, M.: Modelling of Daily Solar Energy System Prediction using Support Vector Machine for Oman. International Journal of Applied Engineering Research 11. 10166-10172 (2016).
16. Lopes, S.M.A.: A Photovoltaic Power Forecasting Method using Artificial Neural Networks. Sao Paulo University, Sao Carlos School of Engineering, Electrical Engineering Course (2018).
17. Simon H.: Neural networks: a comprehensive foundation. Delhi: Pearson Education, 1999. ISBN: 81-788-300-0.
18. Habbati B., Ramdani Y., Moulay F.: A detailed modeling of photovoltaic module using MATLAB.

19. Pradhan, A., Panda, B.: Experimental Analysis of Factors Affecting the Power Output of the PV Module. International Journal of Electrical and Computer Engineering (IJECE). Vol. 7, No. 6, pp. 3190-3197 (2017).
20. Habbati B., Ramdani Y., Moulay F.: A detailed modeling of photovoltaic module using MATLAB.

Energy, Exergy and Environmental Analysis and Multiobjective Optimization of a Solar Renewable Energy Multi-Generation System Considering the Summer Daytime Climatic Conditions of Mediterranean Region in Turkey

Mert Colakoglu[1][0000-0002-8333-3024] and Ahmet Durmayaz[2][0000-0002-6884-8791]

[1,2] Istanbul Technical University, Energy Institute, 34469, Istanbul, Turkey

mertcolakoglu@gmail.com, durmayaz@itu.edu.tr

Abstrat. In this study, a novel concentrated solar thermal energy driven renewable energy system for multi-generation products is proposed and analyzed. Analysis is performed for the summer daytime climatic conditions of both the selected cities of Antalya, Hatay and Kahramanmaras and Mediterranean region in Turkey. A heliostat field and solar tower-based intercooling-regenerative open Brayton cycle is used as the primary power cycle. Two organic Rankine cycles are coupled to utilize the waste heat of the intercooling and the exhaust of the topping cycle. To produce multi-generation products of power, cooling, green hydrogen, fresh water, industrial process heating and domestic hot water, the proposed plant is incorporated with an electrolyzer, a multi-effect desalination system, an absorption chiller cycle, an industrial process heater and a domestic hot water chamber. Study is performed with energy, exergy and environmental analyses to examine the system performance. A detailed parametric analysis is carried out to investigate the effects of variation of some important design parameters on the performance indicators of energy efficiency, exergy efficiency, exergetic quality factor (EQF) and emission savings for the proposed plant considering the climatic conditions of the selected cities. Multiobjective optimization of the proposed plant is conducted to determine the optimum operating conditions of the plant. The proposed MG system has energy and exergy efficiencies and exergetic quality factor of 49.37%, 39.63% and 57.12%, respectively, while it saves 266.1 kg CO_2 emissions per hour. The optimized system operates at the highest performance in Kahramanmaras among analyzed cities.

Keywords: Multi-generation, Multiobjective Optimization, Energy Analysis, Exergy Analysis, Environmental Analysis, Solar Energy.

1 Introduction

Renewable energy sources have been considered as one of the most viable solutions to meet the ever increasing energy demand in an environmentally benign way, and solar energy has been one of the focus areas [1]. Multi-generation (MG) systems have become a point of attention due to their ability to utilize the source of energy at a higher overall system efficiency, and to produce different utilities such as power, cooling, heating, fresh water, hydrogen, domestic hot water etc., compared to other energy conversion systems [2]. Mediterranean region of Turkey is one of the warmest regions in Turkey and has been affected from the climate change severely. Hence, power, cooling and fresh water have become critical utilities due to increased temperatures and water scarcity issues, especially in summer times [3-5]. On the other hand, being at the southernmost part of Turkey, this region has a good potential for utilization of solar energy, and a solar-driven MG system would contribute to meet significant amount of demand of utilities in the region. The role of green hydrogen as an energy carrier has been increasingly recognized recently, which has a potential to store excess energy for later use in a sustainable way and decarbonize several sectors [6].

Siddiqui and Dincer [7] proposed a MG system based on a solar tower with a Rankine cycle (RC) and an organic Rankine cycle (ORC) as power cycles, together with a reverse osmosis (RO) desalination system and an electrolyzer (EL) to produce power, green hydrogen and fresh water and thermodynamically investigated the system for the climatic conditions of Jubail, S.Arabia. They concluded 23.2% energy and 6.2% exergy efficiencies. Montenon et al. [8] investigated a trigeneration system based on a linear Fresnel reflector (LFR) solar system for power, heating and cooling as utilities, and analyzed the performance of the system for use in Italy, Cyprus, Jordan and Egypt. They utilized a RC in Jordan case, and an ORC for other countries for power generation. They concluded power, heating and cooling outputs between 1.2 kW - 10 kW, 23 kW - 48.3 kW and 17.1 kW and 35 kW, respectively. Khalid et al. [9] performed energy and exergy analyses of a hybrid MG system composed of biomass-driven gas turbine cycle (GTC) and solar tower driven RC, in addition to a bottoming GTC and an additional RC, with an absorption chiller cycle (ACC) and a heater. The MG products are power, cooling, hot water and heated air, and they concluded 66.5% energy and 39.7% exergy efficiencies, respectively.

Yilmaz et al. [10] developed a solar-tower based MG system driven by a solar tower-based intercooling-regenerative open Brayton cycle (IR-STBC) as the power cycle, in addition to an ACC, a high-temperature EL, a dryer and a hydrogen compression-liquefaction system for the production of power, cooling, heating, drying and liquid hydrogen. They reported 60.14% energy and 58.37% exergy efficiencies, respectively. Koc et al. [11] analyzed a novel hybrid MG system driven by a biomass-based GTC and a solar parabolic dish collector (PDC)-based ORC and a Kalina cycle (KC) as the power cycles, and an ACC, an EL and a hydrogen compression-liquefaction system to produce power, heating, cooling, liquid hydrogen and hot water. They achieved 58.53% energy and 54.18% exergy efficiencies, respectively. Sezer et al. [12] proposed a hybrid MG system based on wind and solar energy, where

solar energy is harvested by using a heliostat-field and concentrated solar power (CSP) and concentrated photovoltaics (CPV) receivers and utilized a RC as the main power cycle. Their system can produce power, heating, cooling, fresh water, hydrogen and oxygen with energy and exergy efficiencies of 61.3% and 47.8%, respectively.

Ozlu and Dincer [13] investigated a novel solar-based MG system composed of a KC as the power cycle, a four-stage ACC and an EL to produce power, cooling, green hydrogen and domestic hot water. They reported energy and exergy efficiencies of 57% and 36% with 1398 t CO_2 emission savings. Luqman et al. [14] analyzed a solar energy-based MG system with a parabolic through collector (PTC) that drives an ORC, an ACC, a multi-stage flash (MSF) system and a RO to produce power, cooling, fresh water. They showed that the proposed system has 34.54% energy and 14.55% exergy efficiencies, respectively. Hogerwaard et al. [15] introduced a MG system based on a solar-driven IR-STBC as the topping and an ORC as the bottoming power cycles, with an ARC, and a flash desalination and a heater for production of power, fresh hot water, cooling and heating. They reported 28% and 27% energy and exergy efficiencies, respectively.

Colakoglu and Durmayaz [16] developed a novel MG system based on solar tower with an IR-STBC as the topping cycle and an ORC and a KC as bottoming power cycles, with an ACC, an EL and two domestic hot water heaters (DHWH) to produce power, cooling, green hydrogen, domestic hot water and swimming pool heating (SPH). They concluded 55.57% energy and 39.45% exergy efficiencies, with an achievement of 45.65 kg CO_2/h emission savings. Demir and Dincer [17] developed a novel solar tower-based MG system driven by a simple STBC with two phase change materials (PCM) a thermo-electric generator (TEG), a multi-effect desalination (MED), and an EL for production of power, green hydrogen, fresh water and heating. They concluded 42.5% energy and 40.5% exergy efficiencies, respectively. El-Emam and Dincer [18] developed and assessed a MG system based on a solar tower with RC as the power cycle, a RO, an ACC, an EL and a heater to produce power, green hydrogen, cooling, domestic hot water and fresh water in Aswan city of Egypt. They found energy efficiency values from 75% to 89% and exergy efficiency values from 39% to 51% considering the analyzed range.

Literature review showed that no study investigated a solar-based MG system considering the different climatic conditions and critical utilities of the Mediterranean region cities of Turkey. Moreover, a MG system based on a IR-STBC coupled to two ORCs as the bottoming cycles, which has a significant potential to effectively harness the waste heats of intercooling and exhaust sections, have never been analyzed. Hence, in order to fulfill the research gap in these fields, this novel study focuses on the following main objectives:

- Proposing a novel solar-tower based MG system with an IR-STBC and two ORCs as the power cycles, in addition to a MED, an EL, a ACC, a DHWH and an industrial process heater (IPH) to produce power, fresh water, green hydrogen, cooling, domestic hot water and industrial process heating with 100% renewable energy.

- Analyzing the system performance comparatively considering the different daytime climatic conditions of the selected cities in the Mediterranean region of Turkey.
- Performing a comprehensive energy, exergy and environmental-based parametric analysis and multiobjective (MO) optimization to assess the performance of the proposed MG system.

2 System Description

The proposed MG system consists of an IR-STBC based on a heliostat field-solar tower setting as the topping power cycle and two ORCs to utilize the waste heat of IR-STBC as the bottoming power cycles, an ACC, a MED, an EL, a DHWC and a IPH. MG products of the proposed plant are power, cooling, fresh water, green hydrogen, domestic hot water and industrial process heating. The proposed novel MG system is illustrated in Fig. 1.

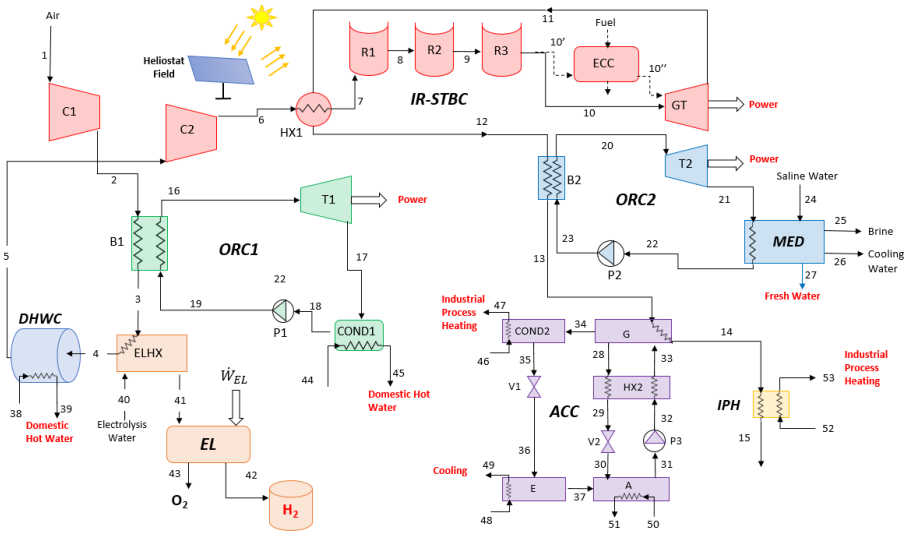

Fig. 1. Schematic illustration of the proposed multi-generation system.

3 Assumptions and Analysis

In this section, assumptions of the thermodynamic model of the proposed MG system, and energy, exergy and environmental analyses are presented. Main assumptions are as follows:

- System operates at steady-state conditions.
- Reference temperature, pressure and average hourly direct normal solar irradiation (DNI) are taken as 28°C, 1 bar and 800 W/m^2 considering the

summer daytime climatic conditions of the Mediterranean region of Turkey [19,20].
- Heat losses in solar field, tower and electrolyzer are considered, other components are adiabatic.
- Pressure losses in turbines, compressors and pumps, are taken into account with isentropic efficiencies, pressure drops in other devices are negligible.

3.1 Energy and Exergy Analysis

General rate of mass, energy, exergy and concentration balance equations for a steady-flow control volume are utilized as

$$\sum_{in} \dot{m}_{in} = \sum_{out} \dot{m}_{out} \tag{6a}$$

$$\dot{Q} - \dot{W} + \sum_{in} (\dot{m}\, h)_{in} - \sum_{out} (\dot{m}\, h)_{out} = 0 \tag{1b}$$

$$\left(1 - \frac{T_0}{T}\right) \dot{Q} - \dot{W} + \sum_{in} (\dot{m}\, ex)_{in} - \sum_{out} (\dot{m}\, ex)_{out} - \dot{E}x_D = 0 \tag{1c}$$

$$\sum_{in} (\dot{m}\, x)_{in} = \sum_{out} (\dot{m}\, x)_{out} \tag{1d}$$

Performance indicators based on energy and exergy analyses are defined as

$$\eta_{en} = \frac{\dot{W}_{net,MG} + \dot{Q}_{cool} + \dot{m}_{fresh} h_{fresh} + \dot{m}_{H_2} LHV_{H_2} + \dot{Q}_{DHW} + \dot{Q}_{IPH}}{\sum_{j=1}^{n} \dot{Q}_{solar,in,j}} \tag{2a}$$

$$\eta_{ex} = \frac{\dot{W}_{net,MG} + \dot{E}x_{cool} + \dot{E}x_{fresh} + \dot{E}x_{H_2} + \dot{E}x_{DHW} + \dot{E}x_{IPH}}{\sum_{j=1}^{n} \dot{E}x_{solar,in,j}} \tag{2b}$$

$$EQF = \frac{\dot{W}_{net,MG} + \dot{E}x_{cool} + \dot{E}x_{fresh} + \dot{E}x_{H_2} + \dot{E}x_{DHW} + \dot{E}x_{IPH}}{\dot{W}_{net,MG} + \dot{Q}_{cool} + \dot{m}_{fresh} h_{fresh} + \dot{m}_{H_2} LHV_{H_2} + \dot{Q}_{DHW} + \dot{Q}_{IPH}} \tag{2c}$$

where η_{en}, η_{ex} and EQF represent energy efficiency, exergy efficiency and exergetic quality factor of the proposed MG system, respectively, as defined by Ref. [16], and utilized as the thermodynamic performance indicators in the parametric analysis and MO optimization.

3.2 Environmental Analysis

Environmental analysis is performed considering the CO_2 emission savings of the proposed solar-based MG system compared to a counterpart natural gas-fired reference system to produce the same utilities. Emission savings are calculated by considering the power and non-power (thermal) utilities produced by the proposed system as

$$\Delta \dot{m}_{CO_2} = \left(\frac{\dot{W}_{gross,MG}}{\eta_{CCPP}} + \frac{\dot{Q}_G + \dot{Q}_{ELHX} + \dot{Q}_{MED} + \dot{Q}_{DHWC} + \dot{Q}_{IPH}}{\eta_B} \right) e_{CO_2} \tag{3}$$

Where η_{CCPP}, η_B and e_{CO_2} represents thermal efficiency of a natural gas-fired combined cycle power plant and state-of-art boiler efficiency as a reference, and CO_2 emission factor of natural gas.

3.3 Multiobjective Optimization

In order to maximize the overall performance of the proposed MG system, a multi-criteria MO optimization is performed in this study. Selected design variables are total pressure ratio of IR-STBC, r_{STBC}, pressure ratio of ORC1, r_{ORC1}, pressure ratio of ORC2, r_{ORC2}, intercooling temperature, T_5, and top brine temperature of MED, T_{Br}. Considered range for the design variables and their references are presented in Table 1.

Table 1. Selected design parameters, considered range and corresponding references.

Design variable	Range	Reference
r_{STBC}	5 – 11	[21]
r_{ORC1}	2 – 5	[15]
r_{ORC2}	10 – 20	[16]
T_5 (K)	303 – 333	[16]
T_{Br} (°C)	52 – 72	[22]

For ORC1 and ORC2, considered working fluids are isobutane and R123, and condenser pressures are 6 bar and 1.8 bar, respectively. Multiobjective function, MOF is defined by weighting and summing up each objective function into an overall objective function to perform simultaneous optimization as

$$Maximize\ (MOF = \alpha_1\,\eta_{en} + \alpha_2\,\eta_{ex} + \alpha_3\,EQF) \tag{4}$$

where α_1, α_2 and α_3 are weight coefficients and considered equal as 1/3 in this study.

4 Results and Discussion

Optimum values of the design variables and performance indicators as the results of MO optimization are presented in Table 2 together with that of the base case values for the climatic conditions of the Mediterranean region of Turkey. It shows that design variables are optimized at a different value than the base case value within the given range. Furthermore, MO optimized case results with 1.8% and 2.1% higher energy and exergy efficiencies, and slightly higher EQF than the base case values. Ultimately, emission savings value of MO optimized case is 3.2% higher than that of the base case.

Table 2. Results of MO optimization compared to performance indicators in the base case.

Parameters	Base case	MO optimum
r_{STBC}	6.0	6.444
r_{ORC1}	2.5	4.981
r_{ORC2}	12.0	19.94
T_5 (K)	318.2	303.2
T_{Br} (°C)	70.0	71.88
η_{en}	0.4851	0.4937
η_{ex}	0.388	0.3963
EQF	0.5703	0.5712
$\Delta\dot{m}_{CO_2}$(kg CO_2/h)	257.8	266.1

Resulting input and output values of the MO optimized MG system are presented in Table 3 for the climatic conditions of the Mediterranean region of Turkey. It shows that the net power output of the MO optimized system is 4.8% higher than that of the base case with only 2.8% increase in rate of solar energy input. Moreover, total exergy rate of the MG products is 4.8% higher than the base case value, with only 1.3% increase in exergy destruction rate. Hence, it is concluded that the MO optimized system design uses the energy source more efficiently compared to the base case design.

Table 3. Input and output values of MO optimized MG system.

Input/output	Base case	MO case
$\dot{W}_{net,MG}$ (kW)	501.6	525.7
$\dot{m}_{H_2}$ (kg/h)	1.152	1.198
$\dot{m}_{fw}$ (kg/s)	0.401	0.3387
$\dot{m}_{DHW}$ (kg/s)	1.222	1.469
$\dot{Q}_{cool}$ (kW)	44.38	44.38
$\dot{Q}_{IPH}$ (kW)	137.1	137.1
$\dot{E}_{prod,MG}$ (kW)	987.2	1033.0
$\dot{E}x_{prod,MG}$ (kW)	563.0	589.9
$\dot{E}x_D$ (kW)	880.3	891.5
$\dot{Q}_{solar,in}$ (kW)	2035.0	2092.0
$\dot{E}x_{solar,in}$ (kW)	1451.0	1488.0

In this study, a comprehensive parametric analysis is also performed in order to assess the effects of variation of design variables on the performance indicators and outputs of the proposed MG system. Effect of summer daytime climatic conditions of different cities in the Mediterranean region of Turkey are also investigated within this parametric analysis by considering the inputs presented in Table 4. For average hourly

DNI and ambient temperature, average hourly peak DNI in July and average daytime temperature on 1st July, 2018 values of the cities are taken as reference, respectively [19,20].

Table 4. Summer daytime climatic conditions of the selected cities in the Mediterranean region of Turkey.

City	DNI (W/m^2)	T (°C)
Antalya	773	27.4
Hatay	813	27.8
Kahramanmaras	913	29.4

Effect of r_{STBC} on η_{ex} and $\dot{W}_{net,MG}$ in the climatic conditions of three different cities are illustrated in Fig. 2.

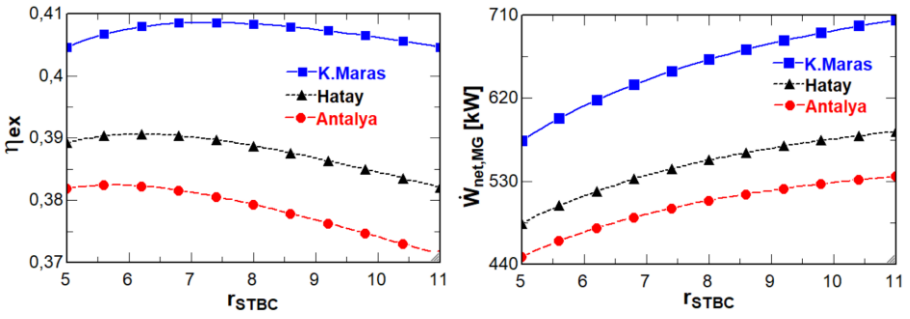

(a) (b)

Fig. 2. Effect of r_{STBC} on η_{ex} and $\dot{W}_{net,MG}$ for three different cities.

Fig. 2a shows that the proposed system has the highest η_{ex} in Kahramanmaras, and the lowest in Antalya, due to higher average hourly DNI values enable higher receiver outlet temperature, which increases the exergy efficiency of the overall MG system. η_{ex} reaches its maximum value at a different value of r_{STBC} for three cities, and it is observed that optimum value of r_{STBC} increases from Antalya at 5.75 to Hatay at 6.2 and to Kahramanmaras at 7.4.

Fig. 2b indicates that the proposed system is able to produce the largest power output in Kahramanmaras and the least in Antalya. The net power output increases as r_{STBC} increases from 5 to 11. The highest power output that can be reached within the specified range and the selected cities is 710 kW in Kahramanmaras.

Effect of r_{ORC2} on $\Delta\dot{m}_{CO_2}$ and $\dot{E}x_D$ with three different values of r_{ORC1} at the base case climatic conditions in the Mediterranean region are illustrated in Fig. 3. Fig. 3a shows that $\Delta\dot{m}_{CO_2}$ increases with increasing r_{ORC2} from 10 to 20. Moreover, it is observed that r_{ORC1} has a positive effect on $\Delta\dot{m}_{CO_2}$. The highest emission savings rate is

reached when r_{ORC2} = 20 and r_{ORC1} = 4, resulting with 258.7 kg CO_2/h emission savings.

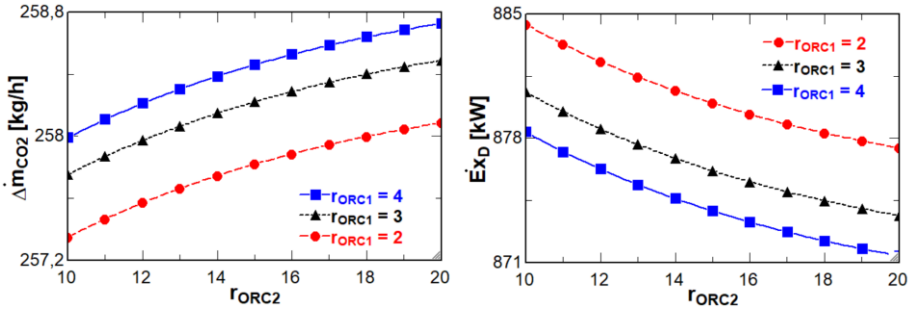

(a) (b)

Fig. 3. Effect of r_{ORC2} on $\Delta\dot{m}_{CO_2}$ and $\dot{E}x_D$ for three different r_{ORC1} values.

Fig. 3b reveals that $\dot{E}x_D$ decreases with increasing r_{ORC2}. Also, increase in r_{ORC1} has a positive effect on decreasing $\dot{E}x_D$. The lowest level of $\dot{E}x_D$ is attained at r_{ORC2} = 20 and r_{ORC1} = 4, resulting with 871 kW exergy destruction rate.

Resulting performance indicators of the MO optimized MG system in different climatic conditions of three cities are presented in Table 5. It shows that the proposed system operates at the highest overall performance in Kahramanmaras and the lowest in Antalya, mainly effected by the average hourly DNI values of the cities.

Table 5. Performance indicators of the proposed MG system in different climatic conditions of three cities.

Performance Indicator	Antalya	Hatay	Kahramanmaras
η_{en}	0.4955	0.4934	0.4914
η_{ex}	0.3905	0.3989	0.4164
EQF	0.5608	0.5763	0.6086
$\Delta\dot{m}_{CO_2}$(kg CO_2/h)	256.0	271.0	308.4

5 Conclusion

In this study, a novel solar tower driven renewable energy based MG system is proposed and analyzed in terms of energy, exergy and environmental viewpoints for the daytime climatic conditions of the Mediterranean region of Turkey. Main conclusions of this study are summarized as follows:

- The proposed MG system can produce 525.7 kW power, 1.198 kg/h green hydrogen, 0.3387 kg/s fresh water, 44.38 kW cooling, 137.1 kW industrial process heating and 1.469 kg/s domestic hot water.

- Energy efficiency, exergy efficiency and exergetic quality factor of the MG system are 49.37%, 39.63% and 57.12%, respectively.
- Solar-driven renewable MG system can save 266.1 kg CO_2 emissions per hour.
- The optimized system operates at the highest performance in Kahramanmaras and the lowest performance in Antalya among analyzed cities.

References

1. Ozlu, S., Dincer, I.: Performance assessment of a new solar energy-based multigeneration system. Energy 112, 164–178 (2016). https://doi.org/10.1016/j.energy.2016.06.040.
2. Ozturk, M., Dincer, I.: Thermodynamic assessment of an integrated solar power tower and coal gasification system for multi-generation purposes. Energy Conversion and Management 76, 1061–1072 (2013). https://doi.org/10.1016/j.enconman.2013.08.061.
3. Altin, T.B., Barak, B.: Trends and changes in tropical and summer days at the Adana Sub-Region of the Mediterranean Region, Southern Turkey. Atmospheric Research 196, 182–199 (2017). https://doi.org/10.1016/j.atmosres.2017.06.017.
4. Sánchez, A.S., Subiela, V.J.: Analysis of the water, energy, environmental and socioeconomic reality in selected Mediterranean countries (Cyprus, Turkey, Egypt, Jordan and Morocco). Desalination 203(1–3), 62–74 (2007). https://doi.org/10.1016/j.desal.2006.02.017.
5. Hamut H.S., Dincer I., Rosen M.A.: Assessment of Desalination Technologies Integrated with Renewable Energy Sources in Turkey. In: Dincer I., Midilli A., Kucuk H. (eds.) Progress in Exergy, Energy, and the Environment. Springer, Cham. (2014). https://doi.org/10.1007/978-3-319-04681-5_24.
6. Sorgulu, F., Dincer, I.: Thermodynamic analyses of a solar-based combined cycle integrated with electrolyzer for hydrogen production. International Journal of Hydrogen Energy 43(2), 1047–1059 (2018). https://doi.org/10.1016/j.ijhydene.2017.09.126.
7. Siddiqui, O., Dincer, I.: Examination of a new solar-based integrated system for desalination, electricity generation and hydrogen production. Solar Energy 163, 224–234 (2018). https://doi.org/10.1016/j.solener.2018.01.077.
8. Montenon, A.C., Paredes, F., Giaconia, A., Fylaktos, N., DiBono, S., Papanicolas, C.N., Montagnino, F.M.: Solar multi-generation in the Mediterranean area, the experience of the sts-med project. In: Proceedings of 2016 EuroSun Conference. pp. 1–9. International Solar Energy Society Selection (2016). http://dx.doi.org/10.18086/eurosun.2016.05.06.
9. Khalid, F., Dincer, I., Rosen, M.A.: Energy and exergy analyses of a solar-biomass integrated cycle for multigeneration. Solar Energy 112, 290–299 (2015). https://doi.org/10.1016/j.solener.2014.11.027.
10. Yilmaz, F., Ozturk, M., Selbas, R.: Development and performance analysis of a new solar tower and high temperature steam electrolyzer hybrid integrated plant. International Journal of Hydrogen Energy 45, 5668–5686 (2020). https://doi.org/10.1016/j.ijhydene.2019.03.061.
11. Koc, M., Tukenmez, N., Ozturk, M.: Development and thermodynamic assessment of a novel solar and biomass energy based integrated plant for liquid hydrogen production. International Journal of Hydrogen Energy 45(60), 34587–34607 (2020). https://doi.org/10.1016/j.ijhydene.2020.03.038.
12. Sezer, N., Bicer, Y., Koc, M.: Design and analysis of an integrated concentrated solar and wind energy system with storage. International Journal of Energy Research 43, 3263–3283 (2019). https://doi.org/10.1002/er.4456.

13. Ozlu, S., Dincer, I.: Analysis and evaluation of a new solar energy-based multigeneration system. International Journal of Energy Research 40, 1339–1354 (2016). https://doi.org/10.1002/er.3516.
14. Luqman, M., Ghiat, I., Maroof, M., Lahlou, F.Z., Bicer, Y., Al-Ansari, T.: Application of the concept of a renewable energy based-polygeneration system for sustainable thermal desalination process—A thermodynamics perspective. International Journal of Energy Research 44, 12344–12362 (2020). https://doi.org/10.1002/er.5161.
15. Hogerwaard, J., Dincer, I., Naterer, G.F.: Solar energy based integrated system for power generation, refrigeration and desalination. Applied Thermal Engineering 121, 1059–1069 (2017). https://doi.org/10.1016/j.applthermaleng.2017.03.116.
16. Colakoglu, M., Durmayaz, A.: Energy, exergy and environmental-based design and multi-objective optimization of a novel solar-driven multi-generation system. Energy Conversion and Management 227, 113603 (2021). https://doi.org/10.1016/j.enconman.2020.113603.
17. Demir, M.E., Dincer, I.: Development of a hybrid solar thermal system with TEG and PEM electrolyzer for hydrogen and power production. International Journal of Hydrogen Energy 42,30044–30056 (2017). https://doi.org/10.1016/j.ijhydene.2017.09.001.
18. El-Emam, R.S., Dincer, I.: Development and assessment of a novel solar heliostat-based multigeneration system. International Journal of Hydrogen Energy 43(5), 2610–2620 (2018). https://doi.org/10.1016/j.ijhydene.2017.12.026.
19. Global Solar Atlas, https://globalsolaratlas.info/detail?c=36.22932,36.123734,11&s=36.229477,36.123962&m=site, last accessed 2021/04/25.
20. World Weather Online, https://www.worldweatheronline.com/, last accessed 2021/04/25.
21. Peng, S., Hong, H., Hongguang, J., Wang, Z.: An integrated solar thermal power system using intercooled gas turbine and Kalina cycle. Energy 44(1), 732–740 (2012). https://doi.org/10.1016/j.energy.2012.04.063.
22. Safari, F., Dincer, I.: Development and analysis of a novel biomass-based integrated system for multigeneration with hydrogen production. International Journal of Hydrogen Energy 44(7), 3511–3526 (2019). https://doi.org/10.1016/j.ijhydene.2018.12.101.

Use of Waste Heat Emitted from A Fuel Cell in Thermoelectric Modules

Busra Yilgin[1[0000-0002-7799-8556]], Anil Can Turkmen[1,2[0000-0002-3916-2854]], Fatma Burcu Keles[1[000-0001-5168-0542]], Ismet Tikiz[1[0000-0003-4477-799X]], and Cenk Celik[1[000-0002-2918-3695]]

[1] Kocaeli University, 41380 Kocaeli, Turkey
[2] ACT Scientific Ltd., 34776 Istanbul, Turkey
busra_ylgn@hotmail.com

Abstract. In this study, the use of thermoelectric modules in harvesting the heat generated during the operation of a fuel cell and converting it back into electrical energy was investigated. The general operating range of low-temperature fuel cells is 55 °C – 85 °C with a 5°C interval. These temperatures are accepted as the lower and upper limit and the electricity generation performance of the thermoelectric module at these temperatures has been investigated. A small-scale structure with 11 p-n junctions is used as a thermoelectric module. It was concluded that as the temperature of the fuel cell increases, the electrical power obtained from the thermoelectric module will increase and this will have a positive effect on the system efficiency.

Keywords: Fuel Cell, Thermoelectric, Energy Harvesting

1 Introduction

In recent years, energy consumption has been increasing due to factors such as population growth, development of industrialization, and people's desire to live in comfort. Due to the environmental pollution of fossil energy resources, and the decrease in their reserves interest in alternative energy sources is gaining momentum. However, it is also very important to be able to use energy efficiently. Ensuring efficient use of energy, especially the use of waste heat is very important. Many systems radiate heat to their environment while operating. Thermoelectric materials can be utilized to capture this heat and convert it into electricity.

Thermoelectric modules are electronic devices consisting of semiconductor materials, one surface of which is cooling while the temperature of other surface heat according to the direction of direct current (DC). These tools are used for cooling or electricity generation.

The first studies on thermoelectricity were carried out by German physicist Thomas Seebeck in 1821. In this study, the electric current was circulated in a closed circuit containing metals, and the response of the needle for two different temperature values was observed. However, Seebeck did not realize the basis of the study and assumed

that continuing heat generation creates an effect of equal value with the electric current circulating in the circuit [1].

In 1834, the Peltier effect has been found by the French physicist Jean Charles Athanase Peltier. Peltier by passing a current through the interface of two different conductive materials found that heat was observed or expelled. After this discovery William Thomson (Lord Kelvin) examined these two effects within the framework of thermodynamics laws and defined them as follows; two different conductors are both heated and when the current flows over them, heat is either absorbed throughout the whole structure or is given out of the system [2].

Today the diversity of the energy production methods has gained importance, and thermodynamic energy has been used in studies for the recovery of waste heat. In 2017, Kunt designed a liquid-cooled thermoelectric generator system to be used for waste heat recovery in the exhaust systems of internal combustion engines. Also, in this study, the effect of the change of refrigerant flow rate on waste heat recovery performance at constant exhaust temperature was investigated experimentally. He observed that; the obtained electrical power directly proportional with the increase of the temperature difference between the thermoelectric generator surfaces, the increase in the amount of refrigerant flow rate, and Pmax value. At TH=350 °C, the increase in the amount of refrigerant increased the power by 26% and the voltage by 13%. At TH=300 °C, the increase in the amount of refrigerant increased the power by 23% and the voltage by 11% [3].

In their study Maral et. al., 2017 investigated the capacity of Peltier materials to be used in the cooling of electric vehicle batteries and established an experimental setup for measuring the thermal power of the battery unit. As a result of the experiments, they observed with Peltier, the batteries can be cooled effectively and the battery can be kept between -20 °C and 60 °C, which is a safe temperature range [4].

This study, it is aimed to obtain electricity from the waste thermal power in a fuel cell with thermoelectric modules.

2 Methodology

This study, it is aimed to reduce the energy deficit by converting the heat energy released to nature without being used as electrical energy. For this purpose, the mathematical model of the designed setup created by the principles of heat transfer laws was analyzed in a commercial finite element software. The current, voltage, and power values obtained as a result of these analyzes were recorded depending on certain boundary conditions.

Thermoelectric modules (TEM) are the thermo-elements formed by n and p-type semiconductors connected in series electrically and in parallel thermally. In this study, three thermoelectric modules are connected parallel to each other in terms of heat transfer. Both sides of n and p-type semiconductor materials were chosen as copper. Also, isotropic thermal conductivity 1.46 W/m.°C, isotropic resistivity 1.64e-5 ohm.m, isotropic Seebeck coefficient 0.000187 W/m.°C has been defined by the software. The model design of the thermoelectric module is shown in Figure 1.

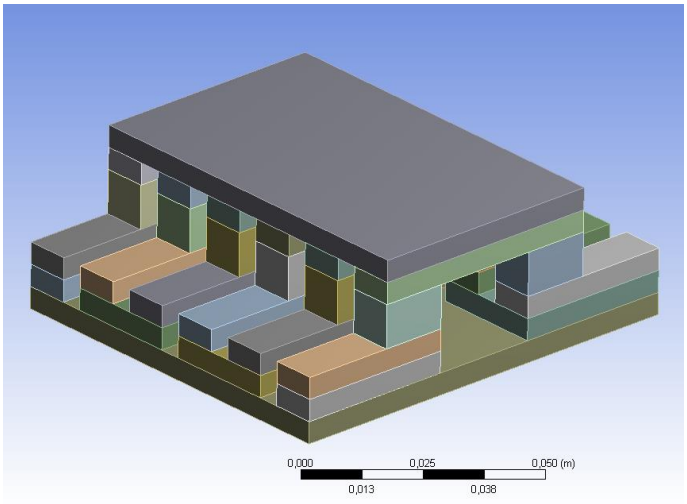

Fig. 1. Modeling thermoelectric modules' geometry

After that, the modeling thermoelectric modules, model meshed and it has been found 12,000 mesh elements. The finite element mesh structure in thermoelectric modules is shown in Figure 2.

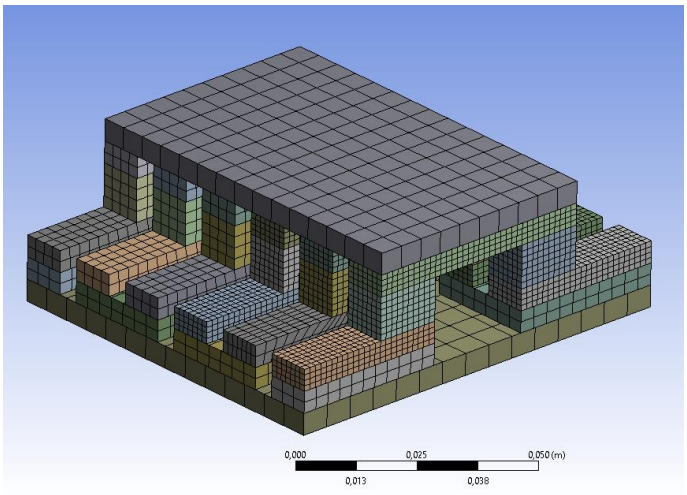

Fig. 2. Finite element mesh structure in thermoelectric modules

Also, since hot and cold heat sources are needed to produce thermoelectric energy, the required hot surface temperature was selected as 85, 80, 75, 70, 65, 60, and 55 °C, which are the efficient operating temperature range of a fuel cell, and the cold surface was selected as 22 °C. The convection coefficient is 1000 W/m^2. °C, potential values

are determined as Vmin = 0 mV, Vmax = 80 mV. Boundary conditions of thermoelectric modules are shown in Figure 3.

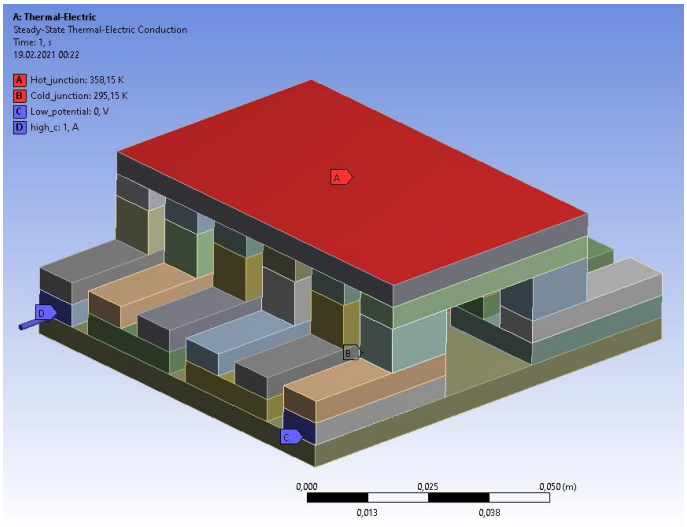

Fig. 3. Boundary conditions in thermoelectric modules

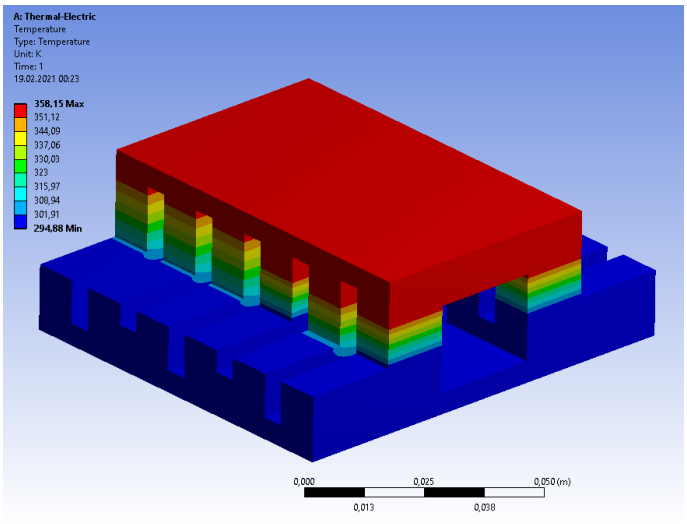

Fig. 4. Temperature results in thermoelectric modules

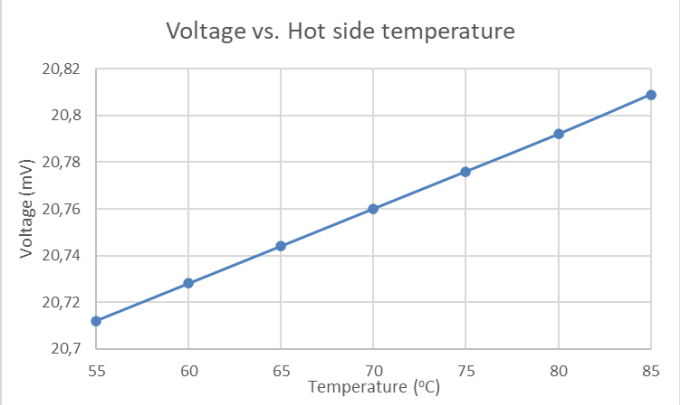

Fig. 5. Voltage vs temperature

3 Conclusion

In this study, the electrical power that can be produced by a thermoelectric material included in the system was determined by using the heat emitted by a fuel cell in the optimum operating temperature range. The results of the thermoelectric module with a hot surface of 85 °C are shown in Figure-4, also a current value of 1 A, a power value of 20,809 mW was obtained. As the operating temperature of the fuel cell increases, the electrical power generated from the thermoelectric module increases accordingly, which is shown in Figure 5. The study is valid for a thermoelectric module produced with the serial connection of 11 p-n junctions, it is predicted that the total electrical energy produced will increase when this number is increased. This study, which was carried out to increase the system efficiency of fuel cells and to provide an energy harvesting method, energy generation system from heat, is promising in terms of its results.

References

1. Dikmen, E. “Fixing of Factors What Affects Thermoelectric Coolers’ working criteria and fields of use in the industry”, Master Thesis Suleyman Demirel University, 2002.
2. Ozgun, H. “Termoelektrik Jeneratörlerin Çok Düşük Sıcaklıklarda Teorik ve Deneysel Karakterizasyonu”, Master Thesis, Istanbul Technical University, 2009.
3. Kunt M. A. “A design of a liquid cooling thermoelectric generator system for the exhaust system of internal combustion engines and experimental study on the effect of refrigerant fluid quantity on recovery”, Pamukkale University Journal of Engineering Sciences 2019, 25(1), 7-12.
4. Maral Y., Polat F., Aktaş M. “Determination of leaf spring fatigue life for vehicle suspension system”, Journal of Advanced Technology Sciences 2018, 7(3).

Design of the Off-Grid PV Electricity Generation System for Residential Lighting and Income Generating Activities of Gediya Community, Sumaila Local Government, Kano State, Nigeria

Nuraini Sunusi Ma'aji[1], Tanay Sıdkı Uyar[2]

[1, 2] Energy System Engineering Department, Cyprus International University, Nicosia, Northern Republic of Cyprus
[2]Department of Mechanical Engineering, Beykent University, İstanbul Turkey
maajinuraini@gmail.com

Abstract. This study aims to address the suffering of the Gediya Community to use available renewable energy sources. In this paper, off-grid solar PV was designed for the lighting and commercial activities of the Gediya Community. This will help to reduce anthropogenic emissions and accelerate the European Union green transition and energy access partnership with Africa. In return, job opportunities, climate mitigation and adaptation potentials will be influenced positively. In addition to the existing literature on PV solar systems, numerous innovation tools were considered and the cost implication of the project was also provided to bridge the gap of the current studies in the literature. For this goal, HOMER software was used to design, simulate and optimize the proposed mini-grid Standalone PV system for Gediya community. The results show that a total of 11,115,243 kWh/yr can be produced at total net cost of $4,813,922.00 and save 1,978,1440kg/yr of carbon dioxide emissions with the proposed off-grid system.

Keywords: Electricity, Gediya, Homer, Off-Grid.

1 Introduction

Electricity production from conventional fossil fuels is becoming expensive day after day since the source is limited. Moreover, it causes undesirable environmental and health issues. In most of the rural areas, including Gediya ward Sumaila Local Government, Kano State, the supply of electricity is mainly through power plants that use petrol as an energy source. This results in significant emissions of pollutants and other greenhouse gases, causing an unfriendly environment and health effects for the people living in that area. Renewable energy source developments set records for their low cost in the past decade, especially for the remote communities with access to the power grid [1].

Most of the sufferings are for the remote village that has no-access to the electricity grid and the scale of such a structure is the driving force behind this research work.

Solar power mini-grids are efficient and reliable solutions for the small scale uses of electricity where the large percentage of energy is used for lighting and other commercial uses [2]. With a substantial expansion of cost effective renewables energy power sources, the future energy systems might look totally different from that of the present energy situation [3]. Nigeria is among the 31% of sub-Saharan populace that face a severe challenge on generation, transmission and distribution of electricity [4]. The electricity production capacity in Nigeria is still fluctuating between 3200MW and 4000MW of electricity with total populace of above 230 million. In 2004, World Bank reported that rural electrification systems are typically inefficient unless there is adequate economic success in rural communities. This economic success can be summarized as being able to afford appliances such as Televisions, refrigerators and enhanced lighting [4].

In the design of solar off-grid PV power systems, certain number of the available literature includes backup storage and very few has considered the use of storage. Modeling of a PV with battery storage system should include an optimization based on hourly usage and charge status [5]. The proposed Off-grid PV with storage system in this study clears the gap and pave the way for the communities that are not yet connected to the national grid [6]. Rural areas can no longer wait for national power grid connection projects that are very expensive and take longer to execute [8]. Isolated mini-grids which are cheaper and faster to install, will therefore be the appropriate technology to supply rural communities without electricity accessed. In addition, these kinds of off-grid systems will create new business projections for both European and African companies. Besides, practical applications of these kind of projects will accelerate the achievement of the Paris Agreement goals of African region which is also in line with the European Green Deal commitment and external aspects of clmate neutrality [7][8].

This project aims for the design, simulation and optimization of mini-grid standalone PV solar power system for Gediya Community. The project provides sufficient electricity for lighting applications and commercial activities of the Gediy community.

2 Methodology

2.1 Study Area

For reliable and optimum design, it is very important to take into consideration of environmental conditions. The location of the project in this paper is given as precisely as possible in fig 1. This research is conducted at Gediya Town in Sumaila Local Government Area, Kano State, Nigeria. Gediya is located in a southeastern part of sumaila local government with the coordinates of 11° 20' 08.33" North and 08° 53' 52.64" East. Presently, the community is using petrol for electricity generation and it is mainly for irrigation activities.

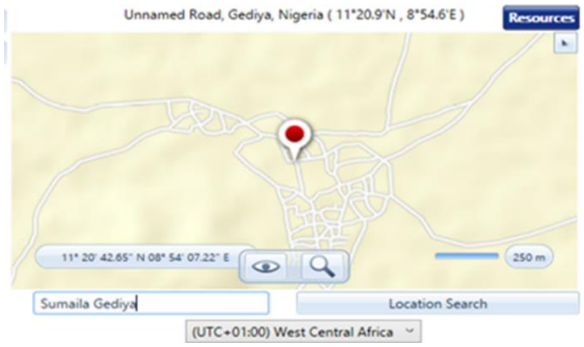

Fig. 1. GEDIYA Community Location (HOMER Software).

Solar Data Analysis. Solar Data for the daily radiation of Gediya town is obtained from HOMER software which uses the information from NASA satellite for Sumaila Gediya. Then the data is exported electronically through HOMER program by entering the corresponding Sumaila latitude and longitude (11° 20' 08.33" North, 08° 53' 52.64" East) detail. Gediya town has a yearly average solar power density assessment of 5.25kWh/m2/day as shown in Fig. 2 below.

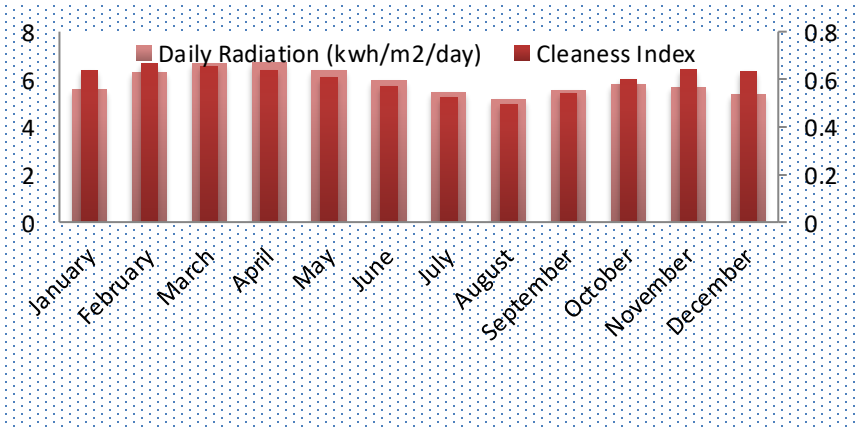

Fig. 2. Average solar daily radiation profile for Gediya Ward

Load Data Analysis. In this study load demand is estimated based on the data available in the existing literature and also typical rural area load demand is considered. In comparison to urban areas, electricity consumption in a remote rural village is not high. Domestic usage (for radios, ceiling fans, compact fluorescent lamps), agricultural activities (Irrigation pump), other community activities (school, and hospital), and rural commercial or small-scale industrial activities are all included as shown in Table 1 below. After calculating the total load a group diversity factor is applied and the total load current of all the outgoing breakers gives the required size for the LV Pane [9].

Table 1: Gediya community estimated load demand[10][11]

S/N	Load	Nos.	Power (w)	hr/day	watt-hr/day
Community					
1	light bulb (CLC)	5	8.3	7	293.1
2	Radio	1	10	5	50
3	Fan	1	30	12	360
4	Socket	2	100	2	400
	Total				1103.9
A	No. of houses	150			**165,590**
Commercial					
1	Shops	10	1500	12	180,000
2	Irrigation pump	50	1491.2	8	596,480
3	Water pump	20	2000	5	200,000
5	Welding	5	6000	8	240,000
B	**Total**				**1,048,480**
Industrial load	Rice, Cassava and Maze Processing				**1,323,420**
C					
Hospital	LED light	20	15	12	3600
	Ceiling fan	6	70	8	3360
	Refrigerator	3	600	12	21600
D	**Total**				**28,560**
School	LED light bulb	30	15	8	3,600
	Ceiling fan	15	70	8	8,400
	Computer	20	200	2	8,000
	Television	1	200	8	1,600
E	**Total**				**21,600**
F	**Total Power**				**2,587,650**

Total power connected= **2587650Wh/d or 2587.65kWh/d**
Base on the assumption that if 80% of the total power connected is likely to be working at the same time, the total power demand can be calculated as shown in equation 1 below.

Total power demand= Total power connected x 80% diversity factor (1)

Total power demand= 2,070.12kWh/d or 86,255W

The total load current (Id) can be obtained from the equation 2 below

$$Id = (Total\ Power\ demand\ (w))/(\sqrt{3}\ x\ 415\ x\ Pf) \quad (2)$$

Using 0.8 as the power factor

$$Id = 86{,}255 / (\sqrt{3}\ x\ 415\ x 0.8) \quad (3)$$

Id = 150A

In summary 200A low voltage panel was chosen for this design.

2.2 Model System Descriptions

Two systems are going to be compared in this study. The one will be working with a fossil fuel source only. And the other one will be working with solar energy. Proposed systems consist of a diesel auto-generation unit, solar photovoltaic modules, an inverter, and the battery charge controller. Batteries store electricity that is generated by solar photovoltaic panels. This storage is needed because of the load requirement during the night ours or winter period where the energy from the sun is not sufficient. Input variables in HOMER are electrical load data, component specifications, photovoltaic cost data of solar energy sources and system. Homer software applies models with techno-economic viability calculated, to see whether or not the load demand and economic feasibility are satisfied. Some parameters within the lifetime of the project such as the model of components, costs, performance, lifespan, etc. supplied into the HOMER as needed for the simulation.

System Schematics. System Assembly of diesel and renewable-based models is shown in Fig. 3 and 4. The first model is made of diesel auto-generation set as the source of energy while the second model consists of only one renewable energy source and a system converter, which is responsible for converting the current from DC to AC, with a power battery device, for storing the power generated by these energy sources for later use. The proposed renewable system also consists of a solar PV renewables energy source, Lithium acid battery, and solar converter to generate Electricity for the usage of Gediya community.

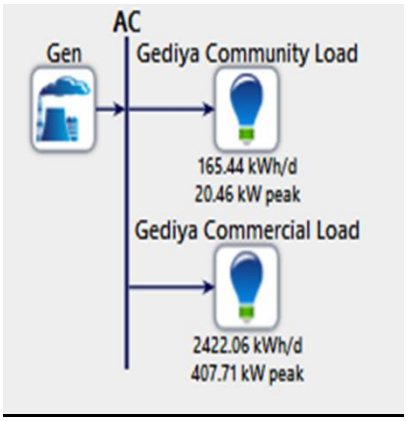

Fig. 3. Schematic Diagram of Model 1

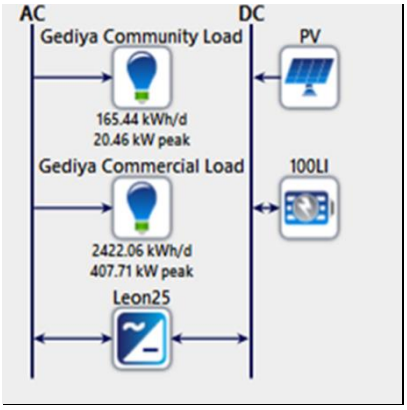

Fig. 4. Schematic Diagram of Model 2

The models consist of two different types of load and these are Gediya community and Commercial load. Community load is a typical community load requirement , for lighting, refrigeration, etc. On the other hand, commercial loads are defined as agricultural hospital equipment, market, and other uses of electricity such as grinding machines.

Simulation Parameters. HOMER software is cable of providing off-grid PV optimization models for various renewable energy sources. In this study, the combinations of a solar PV array, battery bank, and DC-AC converter is involved. Henceforth, the best sizing and selection of the required items is the key to the optimum possible PV off-grid design [7][12].

Table 2: Component Description for modeling (Source: Homer Pro Software).

ITEMS	DESCRIPTION		COST
1. Battery	Model	Generic 100kWh Li-Ion	$2.25M
	Kwh	4575/ battery	
	Bus Voltage (V)	600	
	Capacity (Ah)	167	
	Batteries/String	21	
	Min. State of Charge (%)	20	
	Maximum discharge current (A)	500	
2.Power Converter	Model	Leonics MTP-413F 25kW	$789,077
	Capacity (KW)	25	
	Life Time (yrs)	15	
	Efficiency (%)	90	
	Rectifier Efficiency (%)	70	
	Relative Capacity (%)	100	
3. PV panel	Model	Generic flat plate	$1.78M
	Size (KW)	150	
	Maximum output (KW)	6,198	
4. Auto size Gen set	Fuel	Diesel	$16.5M

2.3 Innovation tools

In this paper, some innovation tools were used for Gediya solar PV mini-grid design to enable transformative developments. The four innovation tools are called enabling technologies, business models, market design, and system operation. Details for each innovation tool are provided in the following sections.

Enabling technologies. To address the electricity challenge of Gediya Community, Lithium ion battery storage infrastructure which is an emerging technology and demand-side management is being considered to store the power [2].

Business models. The proposed project is plan to be community ownership where by the power system is own by the general community and given chance to all the people living in that community to have access and share the benefit of the system. The system will be based on pay as you go system where every user will pay the bill of the power they consume through mobile payment technology that is simple and manageable in the remote areas [13].

Market design. Electricity markets were set up to ensure that customers get reliable power at a low cost [14]. In this project new market models are scheduled in order to reform the agricultural and economic framework of Gediya community. This enhanc-

es the business opportunities for the small businesses to extend the variety of services available to the people living in the area of study. There will be strong regulatory compliance of the people living in the area [2].

System Operation. The system operation will facilitate the proper functioning and operational evolution of the Gediya community electricity sales and distribution network at the same point through organized relationship between the power system generation and the com-munity users. The system operation was considered to be based on the community ownership.

3 Result and Discussions

To decide the best configuration from the possible configurations in each model, various simulation cases are conducted to test and compare different types of models. In terms of architecture and costs, all possible configurations are identified. The technical and economic information was provided along with other variations of the optimized configurations obtained for the models.
The system simulations are performed to compare and evaluate the best possible combination between the two different types of models selected and examine the suitable configuration between them. The two possible configurations are selected, based on their architectures and associated costs. The optimized configurations for the two models, as well as other combinations, were described in technical and economic detail in the preceding sections.

3.1 Model 1

Figure 5 present the optimization result of model 1 that uses diesel generators as the only source of energy for the generation of electricity in Gediya community. This configuration has a total NPC of $16,498,465.76 and a COE of $0.7212.

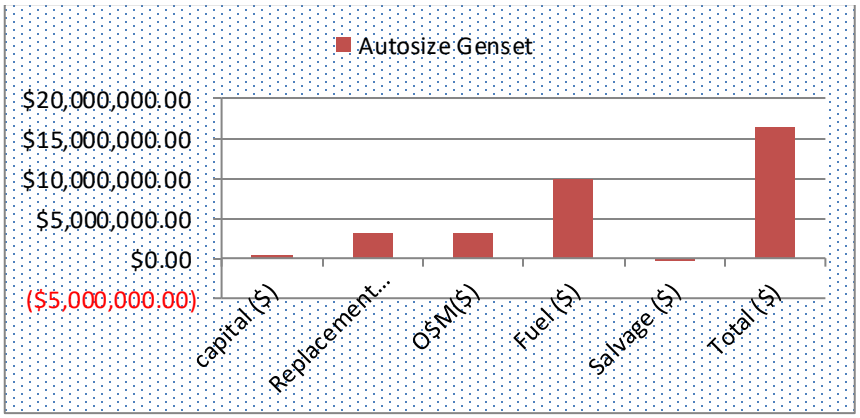

Fig.5. Model one optimization result

3.2 Model 2

Model 2 uses only renewable energy as the source of generating electricity. The optimized result is presented in Fig. 6. It has a higher NPC and initial capital with a lower Levelized Cost of Energy (COE) of $0.2105 compared to $ 0.7212 for the gasoline system. In turn, the cost of operations and maintenance, as well as the cost of fuel, are cut. Despite the rapid rise in the initial cost, the off-grid PV system has a lower NPC due to lower operating costs.

Fig. 6 illustrates the cost summary of the system chosen by presenting capital, operating, replacement, salvage of solar PV panel, battery, and the Inverter. The total cost of the system is $4,813,922.01 and the Levelized Cost of energy is $0.2105 as obtained from the homer software simulation results.

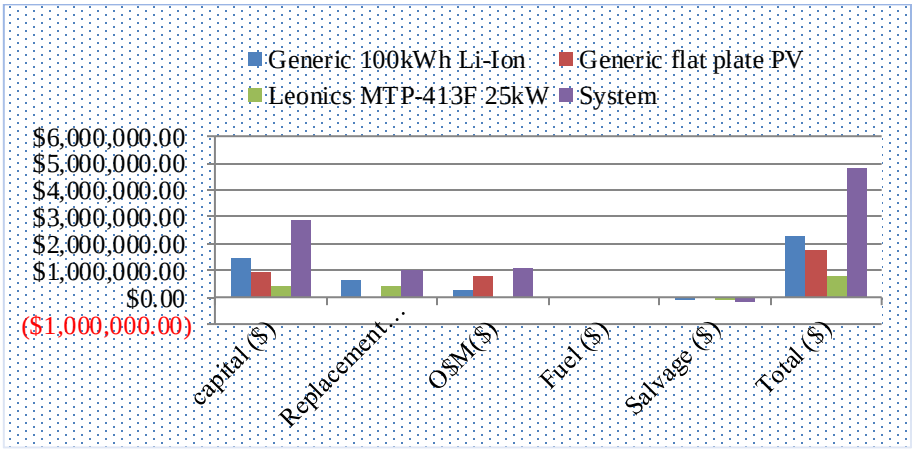

Fig. 6. Cost Summary of proposed Gediya Solar mini off-grid System.

3.3 Electricity Consumption and Production Comparison

The results of electricity consumption and production are given in the tables below which are based on the simulation results obtained from the models proposed. Similarly, in a Renewable based system, it was discovered that solar PV components contribute 100% to the total electricity generation. As compared to a diesel-only system, there is a substantial increase in excess capacity. This surplus energy generation would be sufficient to meet potential load demand as well as fluctuations in the current peak load period.

Table 3. Production and consumption Summary

Component	Model 1	Model 2
Excess Electricity (kwh/yr)	715,614	9,230,396
Unmet Electric Load	0	624
Capacity Shortage	0	1,764
Production (kwh/yr)	2,485,318	11,115,243
Consumption (kwh/yr)	1,769,704	1,769,080

3.4 Techno-Economics Comparison

Table 4 demonstrates the operational performance and techno-economic results by comparing the renewable-based model 2 and the diesel base system as model 1. For both, the diesel and renewable-based systems, it defines the techno-economic operation as well as system parameters.

Table 4. Economic analysis comparison

Components	Model 1	Model 2
Present worth ($)	$16,498,465	$11,684,540
Annual worth ($/yr.)	903,851	$343,638
Return on investment (%)	40.9	43.8
Internal rate of return (%)	45.2	52.4
Simple payback (yr.)	2.17	1.29
Discounted payback (yr.)	2.45	1.79

3.5 GHG Emission Results

Based on the simulation results obtained for greenhouse gas emission from two different models, there is an increased pollution and greenhouse gas compounds, from the diesel-based systems leading to a negative impact on the atmosphere. Besides that, the GHG emissions are marginal as compared to the proposed renewable-based model 1. Solar PV has a low negative impact on emissions and is becoming more environmentally friendly. Thus, the renewable-based model will save 1,978,1440kg/yr of carbon dioxide emission per year as shown in Table 5.

Table 5. GHG reduction summary

Pollutant	Emission Reduction (kg/yr)
Carbon Dioxide	1,978,140
Carbon Monoxide	12,469
Unburned Hydrocarbons	544
Particulate Matter	75.6
Sulfur Dioxide	4,844
Nitrogen Oxides	11,713

4 Conclusion

The main objective of this project was to design, the off-grid solar photovoltaic system generating system for the Gediya Community. Two different types of models were designed and simulated for the suitable sizing of the off-grid solar PV system. The simulation results were obtained on the basis of economic viability and technical feasibility. The solar-based model can meet the energy demand at the low simple payback of 1.29 years. The homer software was successfully applied to the design and the results show that model 2 is more environmentally friendly because it consists of 100% renewable energy. This project will be used for residential application (lighting, radio, and refrigeration) agricultural activities (water irrigation), and community usage (town hall meetings, clinics, schools, maize, cassava, and rice processing). However, if this project actualized, will provide many jobs opportunity to the youth in this area and solve the electricity access problem.

References

[1] IRENA, *Global Renewables Outlook: Energy transformation 2050*. 2020.

[2] IRENA, *Innovation Outlook Mini-Grids*. 2016.

[3] IRENA, *Scenarios for*, no. September. 2020.

[4] A. Ieg and I. Evaluation, *The welfare impact of Rural Electrification: A Reassessment of the Cost and Benefits*, vol. 02, no. c. 2009.

[5] IRENA, "Reaching zero with renewables: Eliminating CO2 emissions from industry and transport in line with the 1.5^0C climate goal," p. 216, 2020, [Online]. Available: https://www.irena.org/publications/2020/Sep/Reaching-Zero-with-Renewables.

[6] A. V. Anayochukwu, "Simulation of photovoltaic/diesel hybrid power generation system with energy storage and supervisory control," *Int. J. Renew. Energy Res.*, vol. 3, no. 3, pp. 605–614, 2013, doi: 10.20508/ijrer.32506.

[7] S. R. Tito, T. T. Lie, and T. N. Anderson, "Optimal sizing of a wind-photovoltaic-battery hybrid renewable energy system considering socio-demographic factors," *Sol. Energy*, vol. 136, pp. 525–532, 2016, doi: 10.1016/j.solener.2016.07.036.

[8] A. Iqbal and M. T. Iqbal, "Design and Analysis of a Stand-Alone PV System for a Rural House in Pakistan," *Int. J. Photoenergy*, vol. 2019, pp. 1–8, 2019, doi: 10.1155/2019/4967148.

[9] C. O. Okoye and B. C. Oranekwu-Okoye, "Economic feasibility of solar PV system for rural electrification in Sub-Sahara Africa," *Renew. Sustain. Energy Rev.*, vol. 82, no. October 2017, pp. 2537–2547, 2018, doi: 10.1016/j.rser.2017.09.054.

[10] R. Sen and S. C. Bhattacharyya, "Off-grid electricity generation with renewable energy technologies inIndia: An application of HOMER," *Renew. Energy*, vol. 62, pp. 388–398, 2014, doi: 10.1016/j.renene.2013.07.028.

[11] A. Gupta, R. P. Saini, and M. P. Sharma, "Design of an optimal hybrid energy system model for remote rural area power generation," *2007 Int. Conf. Electr. Eng. ICEE*, 2007, doi: 10.1109/ICEE.2007.4287310.

[12] A. M. Abdilahi, A. H. Mohd Yatim, M. W. Mustafa, O. T. Khalaf, A. F. Shumran, and F. Mohamed Nor, "Feasibility study of renewable energy-based microgrid system in Somaliland's urban centers," *Renew. Sustain. Energy Rev.*, vol. 40, pp. 1048–1059, 2014, doi: 10.1016/j.rser.2014.07.150.

[13] D. J. Teece, "Business models, business strategy and innovation," *Long Range Plann.*, vol. 43, no. 2–3, pp. 172–194, 2010, doi: 10.1016/j.lrp.2009.07.003.

[14] P. Cramton, "Electricity market design," *Oxford Rev. Econ. Policy*, vol. 33, no. 4, pp. 589–612, 2017, doi: 10.1093/oxrep/grx041.

Exergoeconomic Analysis and Multi Objective Optimization of a Solar Combined System (ORC - Ejector Refrigeration System)

Rania Hammemi[1], Mouna Elakhdar[1] and Ezzedine Nehdi[1]

[1] Research Unit Energetic & Environment – ENIT BP 37 Belvédère 1002, Tunis, Tunisia

raniahammemi75@yahoo.com

Abstract. The demand for power consumption has increased during the past few decades, where fossil fuels dominated current energy systems. Therefore, finding novel solutions became a pressing challenge for many researchers. In fact, using low-grade renewable energy sources such as geothermal, solar and waste heat in industrial applications has acquired greater interest. In this work, solar energy is used in a combined ejector refrigeration system with an organic Rankine cycle (ORC) to produce a cooling effect and generate electrical power. This study presents an energetic, exergetic and exergoeconomic analysis of the system. The simulation results of the parabolic trough collector are used in the system evaluation. This work focuses on the design optimization and performance assessment of the system. A genetic algorithm is applied to permit multi-objective optimization, and optimal values are obtained for the design parameters. Two objective functions are considered, exergy efficiency and the total product unit cost, with the aim of maximizing the exergy efficiency and minimizing the total product unit cost. The results demonstrate that the optimal design point should be selected from the Pareto optimal solution front. The programming language used is MATLAB.

Keywords: Solar Combined System, Exergoeconomic Analysis, Multi-Objective Optimization.

1 Introduction

In order to contribute to the valorization of solar energy and the development of energy systems, we are interested in the study of the combined system, ORC – ejector refrigeration cycle to investigate the opportunity of such a system. Several researchers have studied the use of solar energy in combined cycles. Dai et al [1] presented a new combined ORC/ejection system operating with R123 as refrigerant. A modification of this cycle was introduced by Wang et al [2] to improve its performance and achieve better results, [3].

This study is carried out in two parts. In the first part, we have developed a thermodynamic, exergetic and exergoeconomic analysis of the system based on the prin-

ciples of conservation of mass, momentum and energy. A mathematical model of the parabolic trough concentrator allowing the control of the outlet temperature of the heat transfer fluid is established in the previous work [4]. The simulation results of the parabolic trough solar receiver, which are calculated hour by hour from sunrise to sunset, are introduced in the simulation of the combined system (ORC - Ejector Refrigeration System). In the second part, we have presented the procedure of multi objective optimization of the system using MATLAB.

2 Overview of the system

The proposed system consists of the ejector refrigeration, ORC, and HTF cycles. HTF enters at state 14 the solar parabolic trough, where it receives the concentrated heat from solar radiation and gets heated to state 16. In fact, the solar parabolic trough heat collector consists of a tubular stainless steel absorber inside a glass envelope. The absorber tube receives the solar radiation reflected by the parabolic mirrors. The thermal energy, in the form of heat, is transferred to the HTF as it circulates through the absorber tube. The high-temperature HTF enters the steam generator and transfers heat to the working fluid in the ORC and the ejector cooling cycle and leaves the generator at state 14. The working fluid in the ORC enters the steam generator at state 1 and gains heat. It leaves the steam generator at state 2 with high pressure and temperature conditions. Then, it enters the turbine, where it expands generating electrical power. The steam extracted from the turbine at state 3, called primary fluid, is admitted at the entrance of the ejector's driving nozzle which converts its enthalpy into kinetic energy. When it arrives in the ejector, the primary fluid drives by friction the secondary fluid coming from the evaporator at state 9. The two flows then enter into the secondary nozzle where, after mixing, they are compressed in the diffuser. A new pressure, between the turbine extraction pressure and the evaporation pressure, is established (state 4). The exit flow from the ejector is mixed with the second stream from the exhaust of the turbine (state 13) and the mixed stream is delivered to the preheater at state 10. This stream exits the preheater at state 12 and enters the condenser, where it condenses to liquid (state 5). The liquid refrigerant is divided into two streams, where the first stream at state 6 is pumped by pump 1 to a higher pressure at state 11 and enters the preheater. Then, it exits the preheater at state 1 and enters the steam generator and the ORC is complete. The second stream at state 7 enters the expansion valve, where it expands and leaves to the evaporator at lower pressure and temperature at state 8. The refrigerant evaporates in the evaporator and exit at state 9, where it enters the ejector and the ejector cycle is complete. A schematic diagram and the cycle pressure-enthalpy of the proposed system are presented in Fig.1.

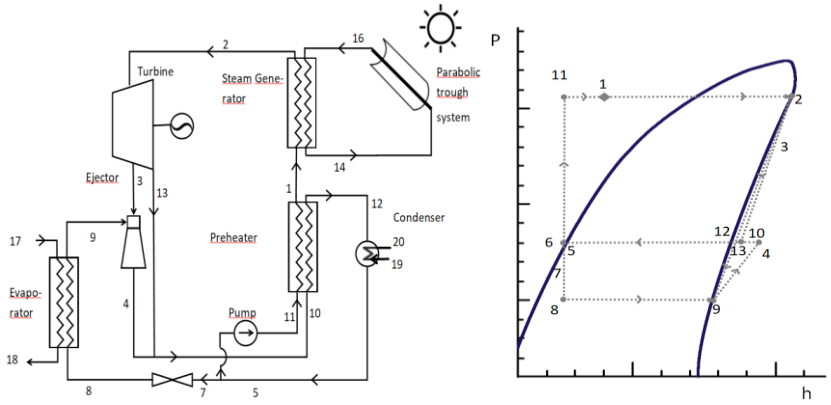

Fig. 1. (a) Schematic of the system, (b) The lg p-h diagram of the system

3 Energy Analysis

Thermodynamic analysis was developed to study the behavior of the combined system using the conservation of mass and energy equations. The thermodynamic equations for each component of the cycle are given in Table 1:

Table 1. Energy balances for the system components

Component	Equation
Evaporator	$\dot{Q}_e = \dot{m}_9(h_9 - h_8)$
Condenser	$\dot{Q}_{cond} = \dot{m}_5(h_{12} - h_5)$
Expansion valve	$h_8 = h_7$
Ejector	$\dot{m}_3 h_3 + \dot{m}_9 h_9 = \dot{m}_4 h_4$
Pump	$\dot{W}_{pump} = \dot{m}_2(h_{11} - h_6)$
Turbine	$\dot{W}_{Turb} = \dot{m}_2(h_2 - h_3) + \dot{m}_{13}(h_3 - h_{13})$
Preheater	$\dot{Q}_{Pre} = \dot{m}_{11}(h_1 - h_{11})$
Steam generator	$\dot{Q}_{ger} = \dot{m}_2(h_2 - h_1)$
COP	$COP = \dfrac{\dot{Q}_e + \dot{W}_{Net}}{\dot{Q}_{ger}}$
	$\dot{W}_{Net} = \dot{W}_{Turb} - \dot{W}_{pump}$

To predict the entrainment ratio and the pressure at the ejector outlet, the constant cross-sectional mixing model in the transition regime (RT) of the ejector was developed by Elakhdar et al [4]. The RT gives the optimal performance of the ejector [5,6].

4 Exergy Analysis

Exergy is the maximum theoretical work delivered by the system in relation to its conditions to the environment equilibrium [7]. Neglecting the nuclear, electrical, magnetic and other less predominant effects, the rate of system total exergy ($\dot{E}_{total}$) constitutes of the chemical, physical, potential and kinetic exergy rates ($\dot{E}_{ch}, \dot{E}_{ph}, \dot{E}_{pt}, \dot{E}_{kn}$).

$$\dot{E}_{total} = \dot{E}_{ch} + \dot{E}_{ph} + \dot{E}_{pt} + \dot{E}_{kn} \quad (1)$$

Exergy analysis is an extension of energy analysis; it takes into account the quality of a given quantity of energy.

The physical exergy is further considered, and all other forms are neglected in this study. It was calculated according to Equation (2)

$$\dot{E}_{ph} = \dot{m}[(h_i - h_0) - T_0(s_i - s_0)] \quad (2)$$

Here, h, T and s; denote the enthalpy, temperature, and entropy, respectively. Moreover, the subscripts 0 and i denote a given and reference state, respectively.

The exergy analysis is conducted in the form of "exergy of fuel/exergy of product". For each component of the system [7]:

$$\dot{E}_{F,k} = \dot{E}_{P,k} + \dot{E}_{D,k} \quad (3)$$

Where, $\dot{E}_{F,k}$, $\dot{E}_{P,k}$ and $\dot{E}_{D,k}$ are the rates of exergy fuel, exergy product and exergy destruction, respectively.

The exergy efficiency (ε_k) is defined as the ratio

$$\varepsilon_k = \frac{\dot{E}_{P,k}}{\dot{E}_{F,k}} \quad (4)$$

Overall system exergy efficiency ε_{tot}

$$\varepsilon_{tot} = \frac{\dot{E}_{P,tot}}{\dot{E}_{F,tot}} \quad (5)$$

Table 2. Exergy balances for the system component

Component	Exergy of product ($\dot{E}_{P,k}$)	Exergy of fuel ($\dot{E}_{F,k}$)
Evaporator	$\dot{E}_{P,e} = \dot{E}_{18} - \dot{E}_{17}$	$\dot{E}_{F,e} = \dot{E}_{8} - \dot{E}_{9}$
Condenser	$\dot{E}_{P,cond} = \dot{E}_{20} - \dot{E}_{19}$	$\dot{E}_{F,cond} = \dot{E}_{12} - \dot{E}_{5}$
Expansion valve	$\dot{E}_{P,ev} = \dot{E}_{8}$	$\dot{E}_{F,ev} = \dot{E}_{7}$
Ejector	$\dot{E}_{P,ejec} = \dot{m}_9 * (e_4 - e_9)$	$\dot{E}_{F,ejec} = \dot{m}_3 * (e_3 - e_4)$

Pump	$\dot{E}_{P,pump} = \dot{E}_{11} - \dot{E}_6$	$\dot{E}_{F,pump} = \dot{W}_P$
Turbine	$\dot{E}_{P,turb} = \dot{W}_{Turb}$	$\dot{E}_{F,turb} = \dot{E}_2 - \dot{E}_{13} - \dot{E}_3$
Preheater	$\dot{E}_{P,pre} = \dot{E}_1 - \dot{E}_{11}$	$\dot{E}_{F,pre} = \dot{E}_{10} - \dot{E}_{12}$
Steam generator	$\dot{E}_{P,ger} = \dot{E}_2 - \dot{E}_1$	$\dot{E}_{F,ger} = \dot{E}_{16} - \dot{E}_{14}$
Mixer	$\dot{E}_{P,mix} = \dot{m}_{13} * (e_{10} - e_{13})$	$\dot{E}_{F,mix} = \dot{m}_4 * (e_4 - e_{10})$
Total system	$\dot{E}_{P,tot} = \dot{E}_{P,e} + \dot{W}_{Net}$	$\dot{E}_{F,tot} = \dot{E}_{F,ger}$

5 Economic Analysis

In order to evaluate and cost-optimize an energy conversion system, an economic analysis is required. The total revenue requirement (TRR) method is used, [7]
The levelized TRR is the addition of carrying charges (CC_L) and the expenses of fuel and operation and maintenance costs (FC_L) and (OMC_L), respectively.

$$TRR_L = CC_L + FC_L + OMC_L \tag{6}$$

The value of the levelized carrying charges CCL is calculated as:

$$CC_L = \text{TCI} * \text{CRF} \tag{7}$$

Where CRF is the capital recovery factor, which is given by:

$$CRF = \frac{i_{eff}(i_{eff}+1)^n}{(i_{eff}+1)^n - 1} \tag{8}$$

In this equation, the effective interest rate is i_{eff} and it is assumed to be equal to 12% in this work, while the number of years is the lifetime n and it is equal to 15 years.
The levelized value of annual fuel cost (FC_L) and operating and maintenance cost (OMC_L) can be obtained by:

$$FC_L = FC_0 * CELF = FC_0 * \frac{k_{FC}(1-{k_{FC}}^n)}{1-k_{FC}} * CRF \tag{9}$$

And

$$OMC_L = OMC_0 * CELF = OMC_0 * \frac{k_{OMC}(1-{k_{OMC}}^n)}{1-k_{OMC}} * CRF \tag{10}$$

With $k_{FC} = \frac{1+r_{FC}}{1+i_{eff}}$ and $k_{OMC} = \frac{1+r_{OMC}}{1+i_{eff}}$ where r_{FC} is the average inflation rate of the fuel cost and r_{OMC} is the average inflation rate of the operating and maintenance cost.

FC_0 is the first-year fuel cost, OMC_0 is the first-year operating and maintenance cost. The cost rate associated with the investment and the operation and maintenance cost ($\dot{Z}$), which will be used as input for the exergoeconomic analysis. ($\dot{Z}$) is either the components' or total system cost rate, as shown in Equations (11) and (12).

$$\dot{Z}_k = \dot{Z}_k^{CI} + \dot{Z}_k^{OM} = \frac{CC_L}{\tau}\frac{PEC_k}{\sum PEC_k} + \frac{OMC_L}{\tau}\frac{PEC_k}{\sum PEC_k} \quad (11)$$

$$\dot{Z}_{tot} = \sum \dot{Z}_k \quad (12)$$

Where; τ is the total annual time (7000h) of system operation at full load. PEC_k denotes the purchased equipment cost of the kth component, which is estimated from cost estimating charts [7,11], shown in table 3.

Table 3. Purchased Equipment Cost of each component

Component	Estimation of PEC (US$2019)
Evaporator	$PEC_{evap} = 5786 * (\frac{A_{evap}}{10})^{0.6}$
Condenser	$PEC_{cond} = 5786 * (\frac{A_{cond}}{10})^{0.6}$
Expansion valve	$PEC_{ev} = 220 * \dot{m}_7$
Ejector	$PEC_{ejec} = 11600 * (\frac{\dot{w}_f * r_p}{100})^{0.6}$
Pump	$PEC_{pump} = 13500 * (\frac{\dot{W}_{pump}}{10})^{0.37}$
Turbine	$PEC_{turb} = 173571 * (\frac{\dot{W}_{turb}}{1000})^{0.5}$
Preheater	$PEC_{preh} = 5786 * (\frac{A_{preh}}{10})^{0.6}$
Steam generator	$PEC_{ger} = 5786 * (\frac{A_{ger}}{10})^{0.6}$

6 Exergoeconomic Analysis

Exergoeconomic analysis is unique combination of exergy and economic analysis. It is a powerful method to identify and evaluate the economical effectiveness of the system. This analysis is based on the cost balance equations and auxiliary equations (if required) for the system components [7].

For each component of the system,

$$\dot{C}_{P,k} = \dot{C}_{F,k} + \dot{Z}_k \tag{13}$$

$$c_P \dot{E}_{P,k} = c_F \dot{E}_{F,k} + \dot{Z}_k \tag{14}$$

Where the average component cost of fuel $c_F = \frac{\dot{C}_{F,k}}{\dot{E}_{F,k}}$ and product $c_P = \frac{\dot{C}_{P,k}}{\dot{E}_{P,k}}$, and the exergy destruction cost rates within the component,

$$\dot{C}_{D,k} = c_F \dot{E}_{D,k} \tag{15}$$

For the total system,

$$\dot{C}_{P,tot} = \dot{C}_{F,tot} + \dot{Z}_{tot} - \dot{C}_{L,tot} \tag{16}$$

$$c_{P,tot} \dot{E}_{P,tot} = c_{F,tot} \dot{E}_{F,tot} + \dot{Z}_{tot} - \dot{C}_{L,tot} \tag{17}$$

Where $\dot{C}_{L,tot}$ is the cost of exergy losses from the system to the environment.

The detailed cost balance equation with the corresponding auxiliary equations is shown in Table 4. The exergoeconomic balance equations for the system components is shown in Table 5.

Table 4. Cost balance equations for the system component

Component	Cost Balance	Auxiliary equations
Evaporator	$\dot{C}_9 + \dot{C}_{18} = \dot{C}_8 + \dot{C}_{17} + \dot{Z}_e$	$c_{17} = 0$ $c_8 = c_9$
Condenser	$\dot{C}_{20} + \dot{C}_5 = \dot{C}_{19} + \dot{C}_{12} + \dot{Z}_{cond}$	$c_{19} = 0$ $c_{12} = c_5$
Expansion valve	$\dot{C}_8 = \dot{C}_7 + \dot{Z}_{ev}$	$c_7 = c_5$ $c_5 = c_{11}$
Ejector	$\dot{m}_9(c_{4,9}e_4 - c_9e_9)$ $= \dot{m}_3 c_3(e_3 - e_4) + \dot{Z}_{ej}$ $c_{4,9} = c_4 + \frac{\dot{m}_3}{\dot{m}_9}(c_4 - c_3)$	—
Pump	$\dot{C}_{11} = \dot{C}_6 + c_{w,pump} * \dot{W}_{pump} + \dot{Z}_{pump}$	$c_{w,pump} = c_{w,Turb}$
Turbine	$\dot{C}_3 + \dot{C}_{13} + \dot{W}_{Turb} * c_{w,Turb} = \dot{C}_2 + \dot{Z}_{turb}$	$c_2 = c_3$ $c_2 = c_{13}$
Preheater	$\dot{C}_{12} + \dot{C}_1 = \dot{C}_{11} + \dot{C}_{10} + \dot{Z}_{preh}$	$c_{12} = c_{10}$

Steam generator	$\dot{C}_{14} + \dot{C}_2 = \dot{C}_{16} + \dot{C}_1 + \dot{Z}_{ger}$	$c_{16} = c_{14}$
		$c_{16} = \frac{\dot{Z}_{solarcollector}}{\dot{E}_{F,ger}}$
Mixer	$\dot{C}_{10} = \dot{C}_{13} + \dot{C}_4$	—

Table 5. Exergoeconomic balance equations for the system components

Component	Generated product rate ($\dot{C}_{P,k}$)	Fuel supplied rate ($\dot{C}_{F,k}$)
Evaporator	$\dot{C}_{P,e} = \dot{C}_{18} - \dot{C}_{17}$	$\dot{C}_{F,e} = \dot{C}_8 - \dot{C}_9$
Condenser	$\dot{C}_{P,cond} = \dot{C}_{20} - \dot{C}_{19}$	$\dot{C}_{F,cond} = \dot{C}_{12} - \dot{C}_5$
Expansion valve	$\dot{C}_{P,ev} = \dot{C}_8$	$\dot{C}_{F,ev} = \dot{C}_7$
Ejector	$\dot{C}_{P,ejec} = \dot{m}_9(c_{4,9}e_4 - c_9 e_9)$	$\dot{C}_{F,ejec} = \dot{m}_3 c_3 (e_3 - e_4)$
Pump	$\dot{C}_{P,pump} = \dot{C}_{11} - \dot{C}_6$	$\dot{C}_{F,pump} = \dot{W}_{pump} * c_{w,pump}$
Turbine	$\dot{C}_{P,turb} = \dot{W}_{Turb} * c_{w,Turb}$	$\dot{C}_{F,turb} = \dot{C}_2 - \dot{C}_{13} - \dot{C}_3$
Preheater	$\dot{C}_{P,pre} = \dot{C}_1 - \dot{C}_{11}$	$\dot{C}_{F,pre} = \dot{C}_{10} - \dot{C}_{12}$
Steam generator	$\dot{C}_{P,ger} = \dot{C}_2 - \dot{C}_1$	$\dot{C}_{F,ger} = \dot{C}_{16} - \dot{C}_{14}$
Total system	$\dot{C}_{P,tot} = \dot{C}_{P,e} + \dot{C}_{Wnet}$	$\dot{C}_{F,tot} = \dot{C}_{F,ger}$

7 Multi objective optimization

In thermal design systems, engineering problems often include several conflicting objectives that must be satisfied simultaneously. Therefore, a multi-objective optimization method based on a genetic algorithm is an appropriate and practical tool to determine the optimal solution and optimal design parameters for the system. A genetic algorithm, which was presented and developed for the first time by Holland [8], is a natural biological evolution method to detect an optimal solution.

To achieve an optimized solution in the present work, gamultiobj multi-objective optimization using a genetic algorithm is employed, based on the MATLAB software optimization toolbox. The tuning parameters selected for the genetic algorithm optimization procedure applied in the present study are listed in Table 6.

7.1 Objective functions

Two important objective functions are defined for the multi-objective optimization of the overall system. The first is the exergy efficiency which must be maximized and the second is the total product unit cost which must be minimized. They are defined as follows:

Exergy efficiency (objective function I)

$$\varepsilon_{tot} = \frac{\dot{E}_{P,e} + \dot{W}_{Net}}{\dot{E}_{F,ger}} \tag{18}$$

The total product unit cost (objective function II)

$$TUPC = \frac{\dot{C}_{P,tot} + \dot{C}_{Loss,tot}}{\dot{E}_{P,tot}} = \frac{\dot{C}_{P,evaporator} + \dot{W}_{Net} * c_{w,turbine} + \dot{C}_{20}}{\dot{E}_{P,tot}} \tag{19}$$

7.2 Decision variables

The evaporator temperature, Extraction ratio, Turbine isentropic efficiency, Ejector entrainment ratio, Turbine Expansion ratio, Evaporator cooling capacity, Evaporator coefficient, Condenser coefficient, Preheater coefficient and Steam generator coefficient are considered as decision variables in this work. The ranges of the mentioned decision variables are summarized in Table 7.

Table 6. Tuning parameters in the genetic algorithm optimization program.

Tuning parameters	Value
Population size	50
Maximum number of generation	150
Selection function	Tournament
Tournament size	2
Probability of crossover	85%
Mutation function	Adaptive feasible
Crossover function	Intermediate

Table 7. List of decision variables' range for the system optimization

Parameters	Range
Evaporator temperature	[-2°C; 7°C]
The ratio of extraction	[0.2 ; 0.5]
The isentropic efficiency of the Turbine	[0.76 ; 0.86]
Ejector entrainment ratio	[0.2; 0.3]
Evaporator cooling capacity (kW)	[15; 50]
Turbine Expansion ratio	[1.5; 2.5]
Evaporator coefficient	[0.8; 1]
Condenser coefficient	[0.9; 1.2]
Preheater coefficient	[1; 1.2]
Steam generator coefficient	[1; 1.2]

8 Results and Discussion

8.1 Energy, Exergy and Exergoeconomic results of the base case

MATLAB computer program was developed for the simulation of the cogeneration system. The NIST and REFPROP programs are used to determine and calculate the refrigerant thermodynamic properties [9]. The simulation results of the parabolic trough solar collector are calculated on an hourly basis from sunrise to sunset. The hourly variation of the temperature of the HTF and the global irradiance, estimated for June 21, are given in Figure 2.

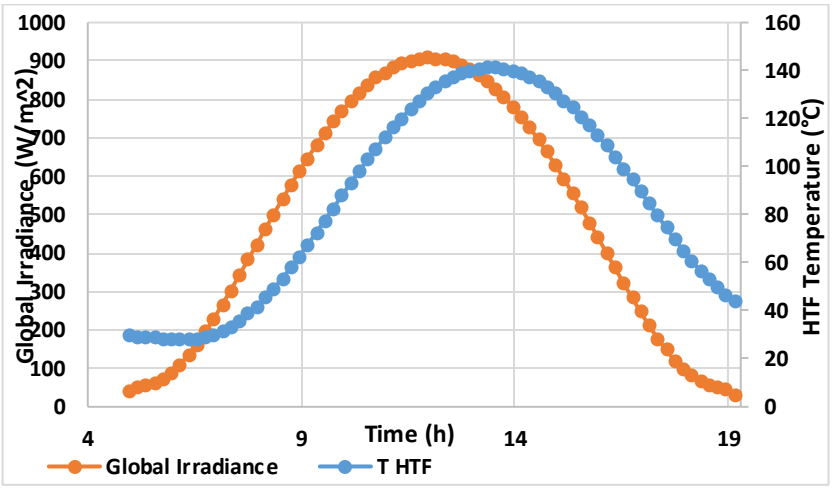

Fig. 2. Hourly variation of the temperature of the HTF and the global irradiance, in 21 June

The hourly variation of the temperature of the HTF depends on the global irradiance. The HTF recovers thermal energy, in form of heat and transfers it; therefore, it can be used in the system. The highest temperature of the HTF, generated is obtained between 01:00 and 03:00 pm, which is 141.25°C.

The operating conditions used to simulate the cycle are presented in Table 8. The computer program is used to calculate the cycle thermodynamic, exergetic and exergoeconomic characteristics at all state points.

Table 8. Operating conditions for the base case

Parameters	Value
Working fluid	R601a
Temperature of the evaporator, Tevap (C°)	2 °C
Difference in temperature, ΔT (C°)	10
Heat Transfer Fluid (Water) temperature (C°)	141.25
Extraction ratio, Rext	0.3
Turbine expansion ratio, ER = p2/p3	2
Ejector geometry ratio, Φ	8
Cooling capacity, Qevap (kW)	45
Turbine isentropic efficiency, (%)	80
Pump Isentropic efficiency, (%)	80

The energy performance of the investigated cycle in terms of COP, net power output, entrainment ratio, and heat power of the steam generator are presented in Table 9. The cooling capacity was fixed at a constant value of 45 kW. The simulation results of the Combined system were estimated for the longest day of the year; 21 June at 13.55 pm. The hourly variation of the temperature of the HTF in the PTC is used to visualize the performance of the combined system, as shown in figure 3 and figure 4.

Table 9. Performance of the Combined system

Performance	Value
Net power output (kW)	146
Evaporator cooling capacity Qevap (kW)	45
Heat power Qger (kW)	1135
Entrainment ratio U	0.19
Coefficient of performance COP	0.17

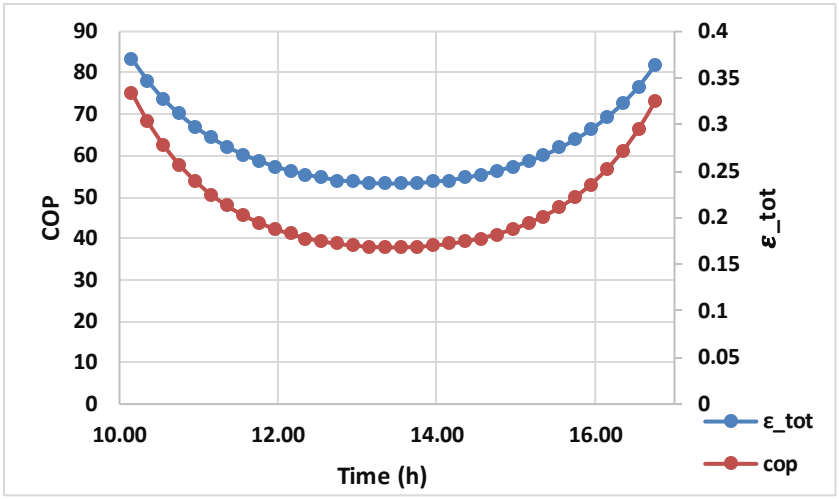

Fig. 3. Hourly variation of the coefficient of performance and total exergy efficiency

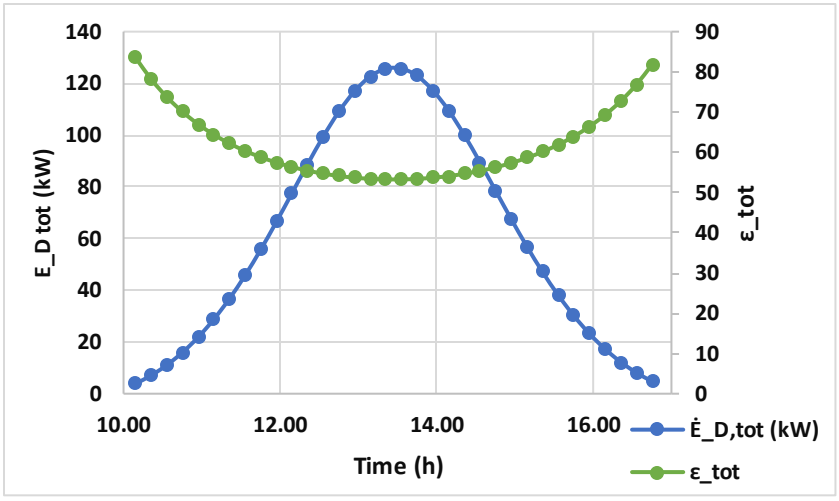

Fig. 4. Hourly variation of the Total exergy destruction and total exergy efficiency

Through the figure 3, the coefficient of performance and the total exergy efficiency varies during the day. They reaches the minimum value in the middle of the day.

The total exergy destruction rate and the total exergy efficiency varies during the day. It is clear that the highest total exergy destruction rate occurs between 01:00 and 03:00 pm, when the system is giving the highest net power output. It is inversely proportional with the exergetic efficiency of the system, as shown in the figure 4.

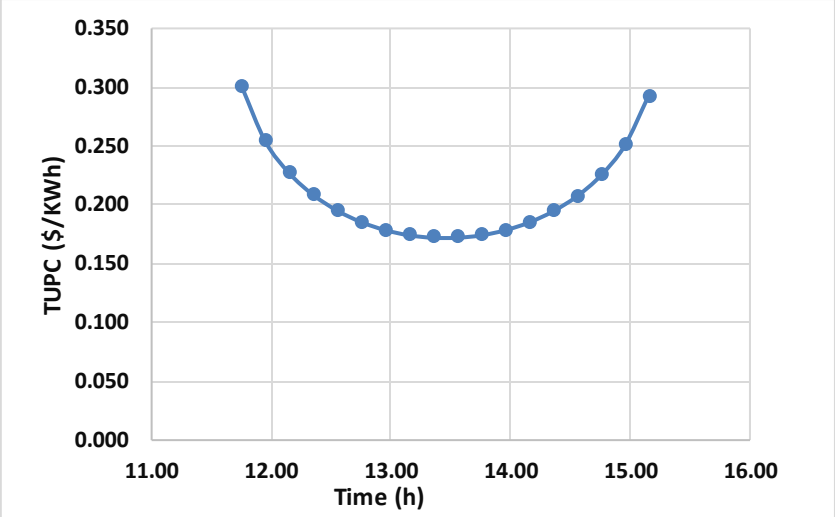

Fig. 5. Hourly variation of the total product unit cost

Through Figure 5, representing the hourly variation of the total unit cost of the product, it can be seen that the total system cost rate is the highest at the beginning and the end of the day and lowest between 1:00 and 2:00 pm.

8.2 Optimal case

The obtained simulation results in MATLAB are shown in figure 6. The Pareto frontier solution for the combined system considering the objective functions as the exergy efficiency and the total product unit cost is shown in figure 7. The highest exergy efficiency (68.3%) is obtained at design point B where the product unit cost is the highest (0.210 $/Kwh). Figure 14 also indicates that the lowest value of product unit cost (0.134 $/Kwh) is obtained at point A where the exergy efficiency is the lowest (64.81%).

Therefore, the point A or B is defined as the optimal point when the total product unit cost or the exergy efficiency is considered as a unique objective function, respectively. For selecting the final optimum point in the present work, we have performed with the aid of the equilibrium point. In this method as a first step an equilibrium point (ideal point) is determined. Equilibrium point is introduced as a point in which both objective functions have their optimum values simultaneously. The closest point, on the Pareto frontier, to the equilibrium point is considered as the final optimum point as shown in Fig.7 [10]. The exergy efficiency and total product unit cost at this point are obtained as 66.85% and 0.156 $/Kwh, respectively. The values of selected optimal solution is shown in table 10.

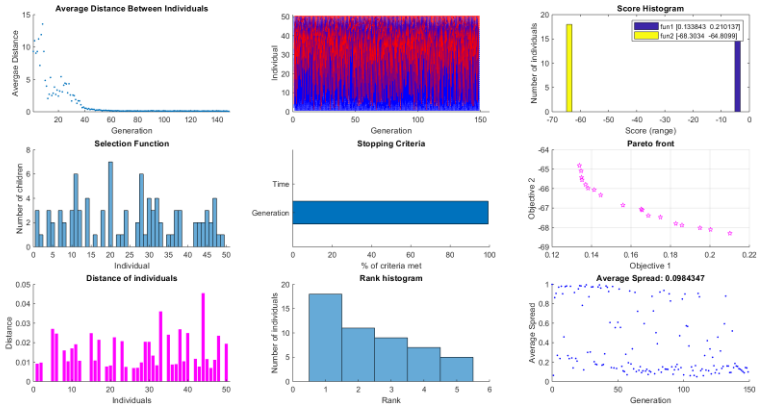

Fig. 6. MATLAB simulation results

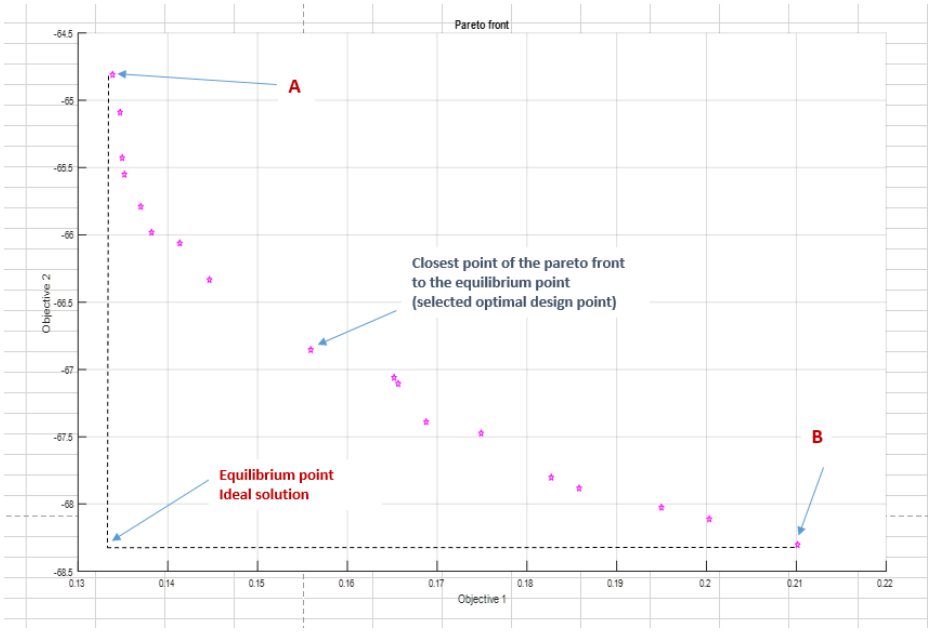

Fig. 7. The distribution of the Pareto optimal solutions for exergy efficiency and total product unit cost of the system

Table 10. Selected optimal solution

Design parameters	Value
Evaporator temperature	0.05
Extraction ratio	0.2
Turbine isentropic efficiency	0.86
Entrainment ratio	0.24
Cooling capacity, Qevap	40.83
Turbine Expansion ratio	2.44
Evaporator coefficient	0.98
Condenser coefficient	1.17
Preheater coefficient	1.14
Steam generator coefficient	1.19

9 Conclusion

In the present work, we have studied the implementation of solar energy in a ejector refrigeration system combined with an Organic Rankine cycle for the simultaneous production of cold and electricity. In such systems, the intensity of solar radiation influences the amount of cold and power produced. The model presented in this work allows, for known operating parameters and cooling power, to evaluate the system from an energetic, exergetic and exergoeconomic point of view. The hourly variation of the heat transfer fluid temperature of the parabolic trough concentrator was used in the simulation of the combined system to evaluate the performance using R601a refrigerant as working fluid. A multi-objective optimization is conducted to obtain the optimal design parameters of the system.

Nomenclature

$\dot{C}$ Cost rate [$/h]
c Cost rate per unit of exergy [$/kWh]
COP Coefficient of Performance [-]
$\dot{E}$ Exergy rate [kW]
e Specific exergy [$kJ.kg^{-1}$]
h Specific enthalpy [$kJ.kg^{-1}$]
s Entropy [$kJ.kg^{-1}.K^{-1}$]
$\dot{m}$ Mass flow rate [$kg.s^{-1}$]
p pressure [bar]
$\dot{Q}$ Heat rate [kW]
T temperature [°C]
$\dot{W}$ Power [kW]
U entrainment ratio [-]
TUPC Total product unit cost [$/kWh]

Greek symbols
ε Exergy efficiency [%]
Φ Ejector geometry ratio [-]

Abbreviations
ORC Organic Rankine Cycle
HTF Heat Transfer Fluid
cond condenser
e evaporator
ejec ejector
ger steam generator
turb turbine
pre preheater
ev expansion valve
mix mixer

Subs- and superscripts
0 reference state (for exergy analysis)
D exergy destruction
F exergy of fuel
k kth component
L exergy losses, levelized
P exergy of product
tot overall system

References

1. Dai, Y., Wang, J., & Gao, L. (2009). Exergy analysis, parametric analysis and optimization for a novel combined power and ejector refrigeration cycle. Applied Thermal Engineering, 29(10), 1983– 1990.
2. Wang, J., Dai, Y., & Sun, Z. (2009). A theoretical study on a novel combined power and ejector refrigeration cycle. International Journal of Refrigeration, 32(6), 1186–1194.
3. Bellos, E., & Tzivanidis, C. (2018). Investigation of a hybrid ORC driven by waste heat and solar energy. Energy Conversion and Management, 156, 427–439.
4. Elakhdar, M., Landoulsi, H., Tashtoush, B., Nehdi, E., & Kairouani, L. (2019). A combined thermal system of ejector refrigeration and Organic Rankine cycles for power generation using a solar parabolic trough. Energy Conversion and Management, 199, 111947.
5. Elakhdar, M., Nehdi, E., Kairouani, L., & Tounsi, N. (2011). Simulation of an ejector used in refrigeration systems. International Journal of Refrigeration, 34(7), 1657–1667.
6. Nahdi, E., Champoussin, J. C., Hostache, G., & Chéron, J. (1993). Les paramètres géométriques optima d'un éjecto-compresseur frigorifique. International Journal of Refrigeration, 16(1), 67–72.
7. A., Bejan, G., Tsatsaronis, M. Moran, 1996.Thermal design and optimization. John Wiley & Sons 9
8. Holland JH. Adaptation in natural and artificial systems: an introductory analysis with applications to biology, control, and artificial intelligence. U Michigan Press; 1975.
9. Lemmon E, McLinden M, Huber M. NIST standard reference database 23: reference fluid thermodynamic and transport properties-REFPROP, version 9.0. Gaithersburg, USA: National Institute of Standards and Technology, Standard Reference Data Program; 2010.
10. Sadeghi, M., Mahmoudi, S. M. S., & Khoshbakhti Saray, R. (2015). Exergoeconomic analysis and multi-objective optimization of an ejector refrigeration cycle powered by an internal combustion (HCCI) engine. Energy Conversion and Management, 96, 403–417.
11. A GUIDE TO CHEMICAL ENGINEERING PROCESS DESIGN AND ECONOMICS, GAEL D. ULRICH University of New Hampshire.

Design of A Hybrid Solar Collector and The Numerical Analysis of Air Performance

Levent Akbulut[1], Özgür Erol[2]

[1] Baskent University, Ankara, Turkey
[2] Baglıca Campus, Dumlupinar Boulevard, No:20, Etimesgut, Ankara

Abstract. In this study, modeling and numerical analysis of a photovoltaic (PVT) flat air solar collector using solar energy, which is one of the leading renewable energy sources, has been carried out. Numerical analysis of air solar collector, photovoltaic (PV) panel, photovoltaic thermal (PVT) panel and PVT systems with various fins was done with Ansys program. It has been investigated to increase the electricity generation efficiency of the PVT panel by reducing the surface temperature with air cooling. As a result of this analysis, the most efficient system among five different systems in terms of both heat and electrical energy efficiency was determined as the crow's feet fin photovoltaic thermal (PVT) system. In this system, an increase of 7.88% was achieved in the power value obtained, while an increase of 19.85% was achieved in the heat efficiency value obtained. The hot air obtained from the fin structured photovoltaic (PVT) panels has been used in various fields such as vegetable and fruit drying. In addition, the electricity obtained from the photovoltaic cell is provided to operate the system or to be used outside the system.

Keywords: Photovoltaic thermal systems, Solar energy, Thermal energy efficiency.

1 Introduction

Energy is very important for economic and social development in today's world. Energy makes a great contribution to the improvement in the quality of life of all countries in the world. Renewable energy is the energy obtained from the existing energy flow in continuous natural processes. Renewable energy sources are provided from natural resources and are sustainable energies. Today, about 80 percent of global energy comes from fossil fuels. Therefore, renewable energy sources are effective in reducing dependence on fossil fuels such as coal, oil, and natural gas. Renewable energy sources can be classified as solar, wind, biomass, geothermal, hydraulic, hydrogen energy. Solar energy, which provides technological and economic advantages, has a great place among renewable energy sources [1-2]. Therefore, solar energy has become the most popular option among renewable energy sources. The energy production characteristics of the data to be obtained from solar energy change signifi-

cantly over time, such as hours and days. The variety of these characteristics and the quality estimation depend on the region and surface structure. Solar energy is the reaction that takes place with the conversion of hydrogen on the sun's surface into helium. While the intensity of solar energy is approximately 1370 W/m² outside the atmosphere, it is 0-1100 W/m² on earth. The technology systems produced to obtain solar energy directly collect the sun's rays and provide heat and electricity production with these rays. These technological systems can be classified as Photovoltaic (PV) and Photovoltaic thermal (PVT) systems. Photovoltaic (PV) systems convert solar energy into electrical energy and these systems can be placed on roofs of buildings, various areas, and cars. Photovoltaic thermal systems (PVT) are attracting increasing attention as they meet both electricity and hot water or air needs. At the same time, these photovoltaic systems can be transformed into more efficient systems in terms of energy efficiency by adding fin structures. Both heat and electrical efficiency in air solar collector, photovoltaic (PV) panel, photovoltaic thermal (PVT) system and various fin structures will be examined and compared with the Ansys program. With this comparison, the most beneficial system will be selected in terms of both heat and electrical efficiency.

2. Modeling and Design

Modeling and design of air solar collector, photovoltaic thermal (PVT) system, flat and crow's feet fin (PVT) systems will be determined and compared in terms of thermal energy efficiency. The heat to be obtained for these systems will be calculated with Eqs. (1) and (2):

$$Q = \dot{m} \times C_p \times \Delta T \quad (1)$$

$$\Delta T = (\text{air outlet temperature} - \text{air inlet temperature}) \quad (2)$$

$\dot{m} = 0{,}028$ kg/s, $C_p = 1046$ J/kg℃, $T_{in} = 43{,}03$ ℃, A= 2,160 m^2 and I= 518W/m^2 are taken from Kalaiarasi et al. [3]. The heat efficiency is calculated from Eq. (1):

$$\eta_Q = \frac{Q}{I \times A} \times 100 \quad (3)$$

Temperature-dependent power value in photovoltaic (PV), photovoltaic thermal (PVT) and fin structured photovoltaic thermal (PVT) systems that produce electrical energy will be obtained by Eq. (4):

$$W_E = \{\frac{100 - [\,(\text{average panel temperature} - 25℃) \times 0{,}427\%\,]}{100}\} \times 500\ W \quad (4)$$

The constant 0.427% in the equation [4] is taken from the panel properties table.

1. Case: The modeling of the air solar collector was kept the same as the measurements in Kalaiarasi et al. [3] for verification. Radiation, inlet air temperature, air flow rate and surface area will be examined with the same values in five different cases.

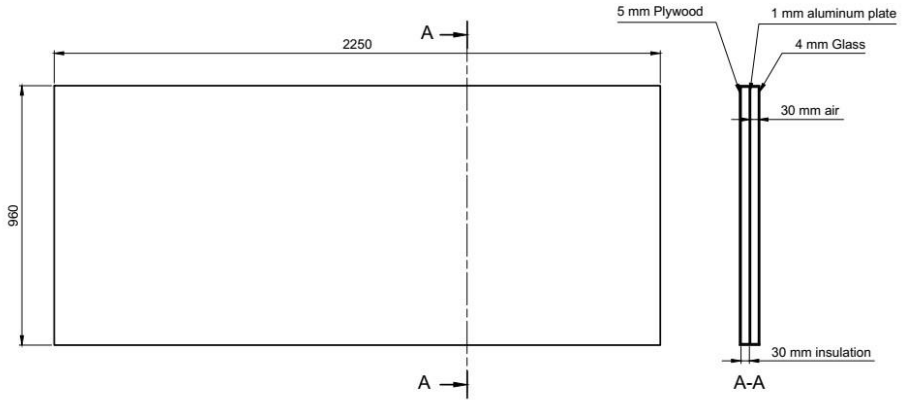

Figure 1 Technical drawing of air solar collector

2. Case: Photovoltaic (PV) panel is selected and designed in accordance with the collector surface area. Mitsubishi D6M35E4A photovoltaic model is selected as the panel [4] and its thickness is 0.3 mm.

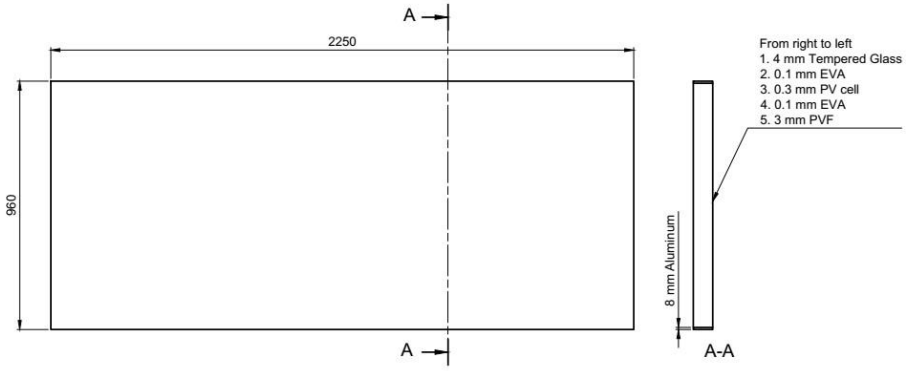

Figure 2 Photovoltaic (PV) system technical drawing

3. Case: In the photovoltaic thermal system: 4 mm thick glass layer at the top and 0.1 mm thick Ethylene Vinyl Acetate (EVA) film is used above and below the (PV) panel. At the bottom, a 1 mm thick aluminum layer is designed.

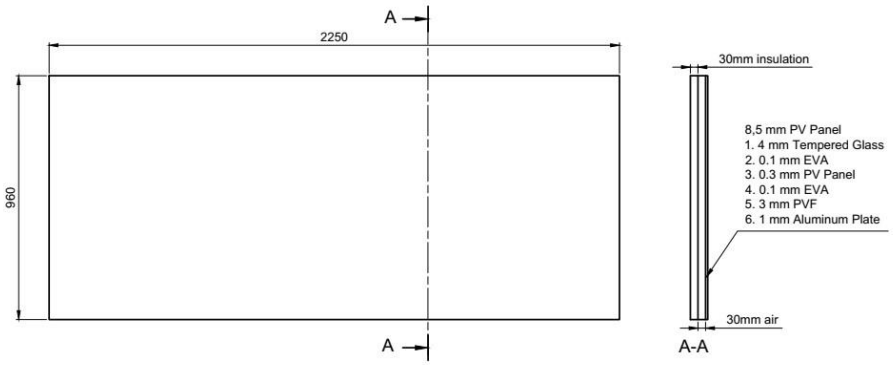

Figure 3 photovoltaic thermal (PVT) system, technical drawing

4. Case: In the photovoltaic thermal PVT system with flat fin structure, flat fins of 150 mm width and 15 mm height are designed between the panel and the plate. With these fins, it is aimed to reduce the panel surface temperature by distributing the air flow compared to the PVT system.

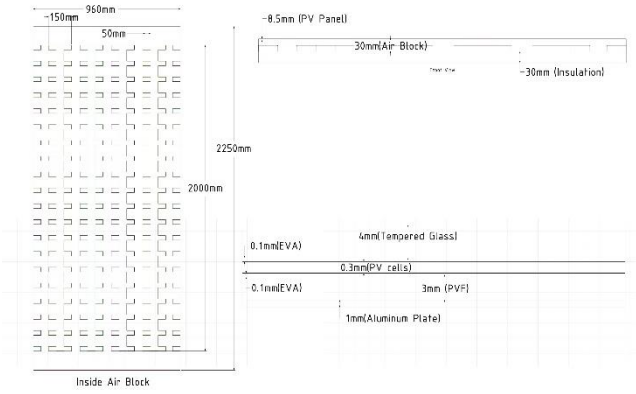

Figure 4 Flat-fin photovoltaic thermal (PVT) system technical drawing

5. Case: In the crow's feet fin structure PVT system, the fins are designed from copper material to create an obstacle at an angle of 45° to the flow direction. In this design, the structure of the fin structures in Ata and Acır [5] were examined and a

different modeling was carried out. These fins are designed with a height of 30 mm and at certain intervals.

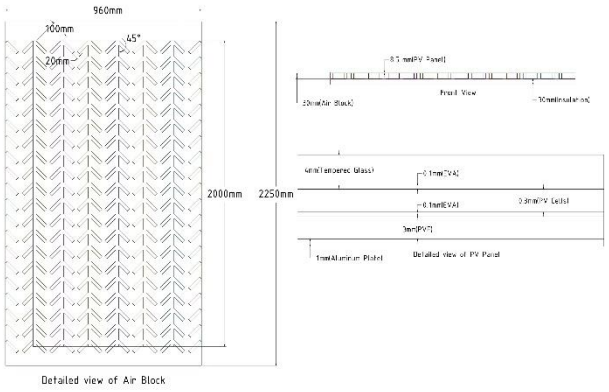

Figure 5 Technical drawing of crow's-feet fin photovoltaic thermal (PVT) system

3 Verification

Results were validated using the Ansys program in line with the modeling taken from Kalaiarasi et al. [3]. First of all, the outlet temperature of the air solar collector was determined as 44.7 °C with the Ansys program and the heat obtained was calculated with the equation (1). In India, on June 2, at 10:00, the percentage of heat energy efficiency was found to be 18.45% from equation (3), according to the radiation value falling on the plate at an angle of 12°.

When compared with the study done by Kalaiarasi et al. [3], a difference of 1.55% was observed. This difference may be caused by unknown reasons such as material type and structure therefore can be neglected.

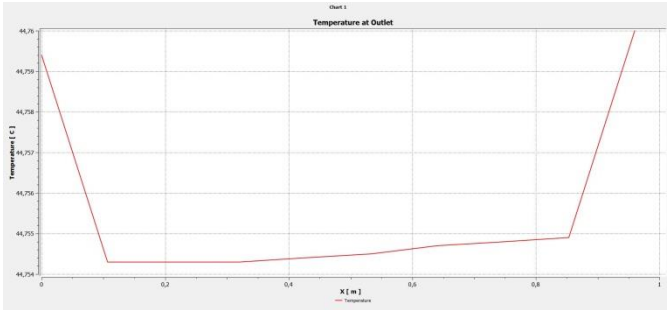

Figure 6 Air solar collector air temperature graph

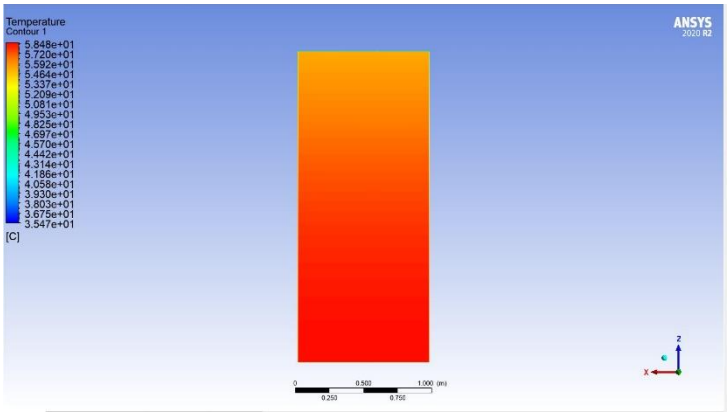

Figure 7 Air solar collector temperature analysis image

4 Results

2. Case: fotovoltaik (PV) paneli Ansys programı ile panel sıcaklık analizi sağlanıp panelin ortalama sıcaklık değeri 74,97 °C bulunmuştur. Ortalama panel sıcaklığı (4) numaralı denkleme taşınır ise sıcaklığa bağlı PV güç değeri 393,31 Watt olarak bulunmuştur.

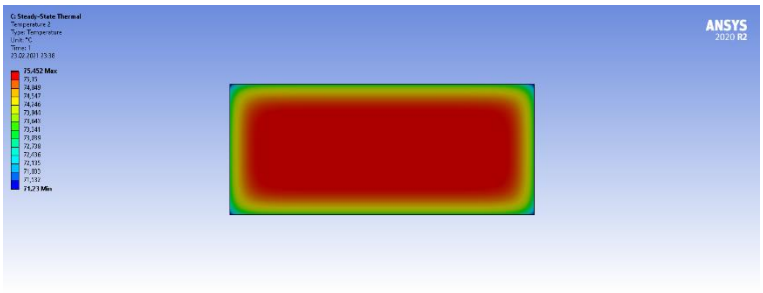

Figure 8 Photovoltaic (PV) panel temperature analysis image

3. Case: In the photovoltaic thermal (PVT) system, with the Ansys program, the air outlet temperature was found to be 50.91°C, and the average panel temperature was 63.9°C. The heat energy gained is 30.87%. The temperature-dependent power value was found to be 416.94 Watts.

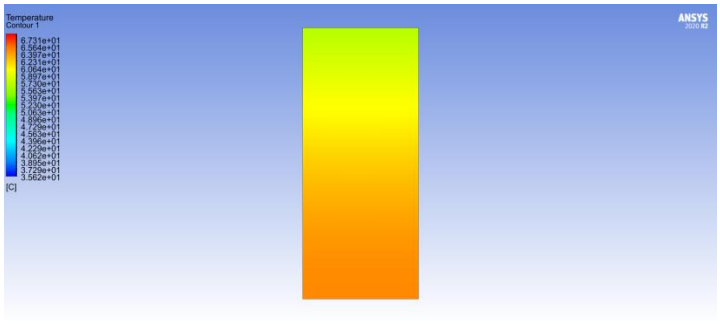

Figure 9 Photovoltaic thermal (PVT) panel temperature analysis image

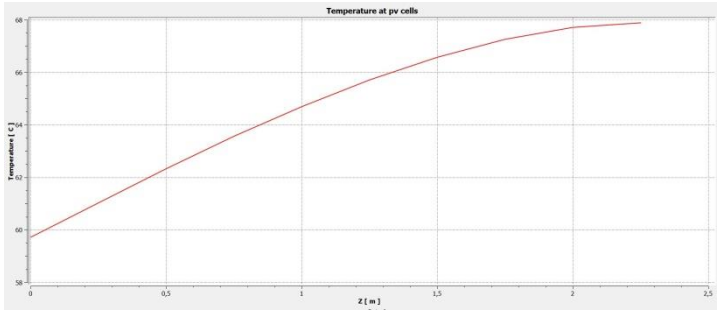

Figure 10 Photovoltaic thermal (PVT) panel temperature graph

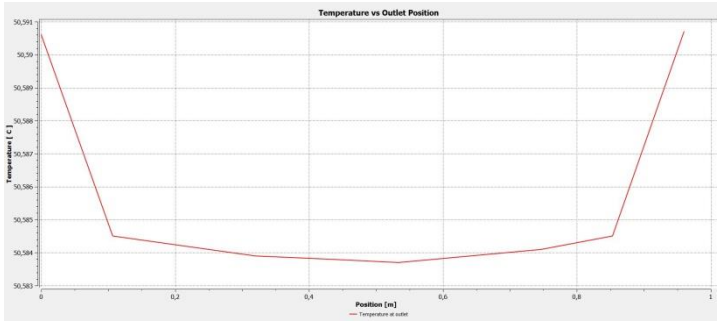

Figure 11 Photovoltaic thermal (PVT) panel air flow temperature graph

4. Case: In the flat fin (PVT) system, the air outlet temperature was found to be 1.75 ℃ and the average panel temperature was 61.85 ℃. The heat energy obtained was found to be 32.573%. The temperature-dependent power value is calculated as 421.32 Watts.

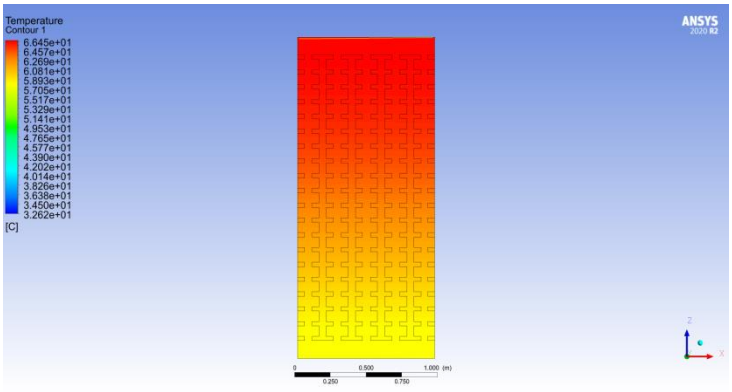

Figure 12 Flat fin photovoltaic thermal (PVT) panel temperature analysis image

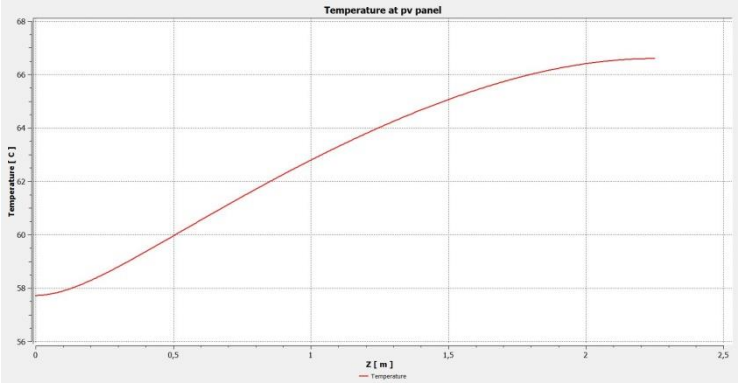

Figure 13 Flat fin photovoltaic thermal (PVT) panel temperature graph

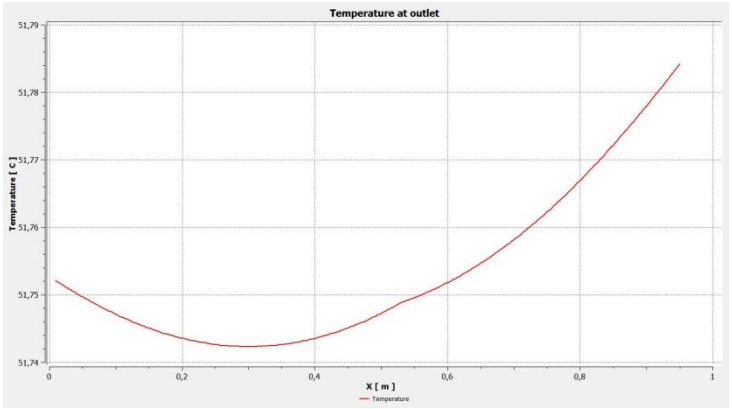

Figure 14 Flat fin photovoltaic thermal (PVT) air flow temperature graph

5. Case: The air outlet temperature was found to be 54.36 °C while the average panel temperature was 60.7 °C in the crow's feet fin (PVT) system. The heat energy efficiency was found to be 37.8%. The temperature-dependent power value was calculated as 423.8 Watts.

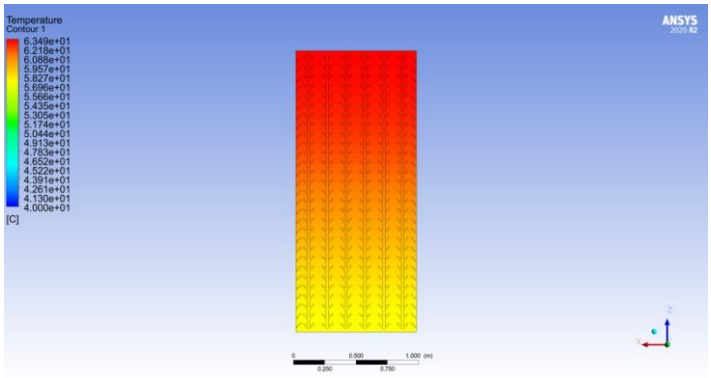

Figure 15 Photovoltaic thermal (PVT) temperature analysis image with crow's feet fins

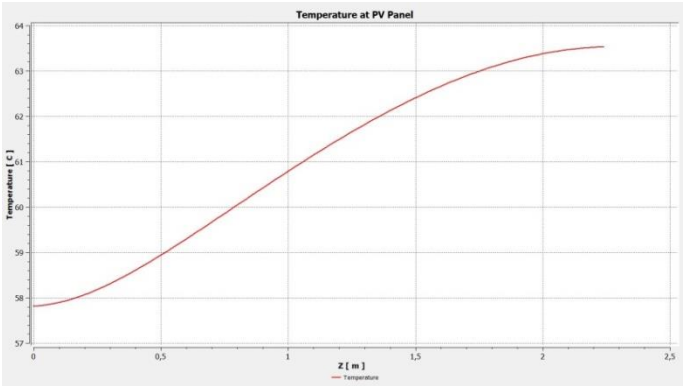

Figure 16 Photovoltaic thermal (PVT) panel temperature graph with crow's feet fins

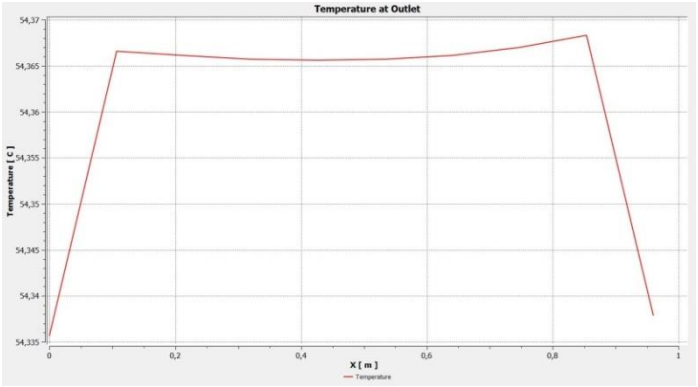

Figure 17 Photovoltaic thermal (PVT) air flow temperature graph with crow's feet fins

Table 1 The values of 5 cases as a result of numerical analysis

Values	Air solar collector	Photovoltaic (PV)	Photovoltaic thermal (PVT)	PVT with flat fins	PVT with crow's feet fins
Air outlet temperature	44,7 ℃	-	50,91 ℃	51,65 ℃	54,36 ℃
Average panel temperature	-	74,97 ℃	63,9 ℃	61,8 ℃	60,7 ℃
Heat efficiency	% 18,45	-	% 30,8	% 32,5	%37,8
Power value	-	393,3 Watt	416,9 Watt	421,32 Watt	423,8 Watt

The heat efficiency and temperature-dependent power value obtained as a result of the numerical analysis of the system in five different situations were compared and the crow's feet fin photovoltaic thermal (PVT) system was determined as the most efficient system. This system shows an increase of 19.85% in the heat energy efficiency compared to the flat air solar collector. When a comparison is made according to the power value obtained in the PV system, the power value from the PV panel is 393.3, while the power value from the crow's feet fin system is 423.8 watts. When this increase is calculated as a percentage using the following equation, an increase of 7.88% is obtained:

$$\frac{(423{,}8 - 393{,}3)}{393{,}3} \times 100 = \%7{,}88$$

.

Reference

1. http://www.solar-academy.com/menuis/Yenilenebilir-Enerji-Kaynaklarinin-Turkiye-Acisindan-Onemi.005039.pdf
2. Antoni G.Corrigendumto“Transportationina100%renewableenergysystem”,Spain,(2018)
3. Kalaiarasi, G., Velraj, R., Vanjeswaran, M. N., & Pandian, N. G. (2020). Experimental analysis and comparison of flat plate solar air heater with and without integrated sensible heat storage. *Renewable Energy*, *150*, 255-265.
4. https://www.mitsubishielectricsolar.com/images/uploads/documents/specs/NSP_350W_355W_360W_lo_res.pdf
5. Ata, İ., & Acır, A. (2020). Hava Akışkanlı Güneş Kollektöründe Isı Transferi İyileştirmesine Etki Eden Parametrelerin Taguchi Metodu ile Optimizasyonu. *Politeknik Dergisi*, 23(2): 527-535.

11th INTERNATIONAL 100% RENEWABLE ENERGY CONFERENCE

IRENEC 2021 PROCEEDINGS

20-23 MAY 2021

RENEWABLE ENERGY ASSOCIATION

EUROSOLAR Turkey